The Role of YeaZ in the VBNC state of *Vibrio parahaemolyticus* NCTC 10884

Shih-Hsun Chen, M.Sc (National Taiwan Ocean University)

A thesis submitted for the Degree of Doctor of Philosophy

School of Molecular and Biomedical Science

Faculty of Sciences,

The University of Adelaide

Adelaide, South Australia, Australia

10 July 2012

Presentation of Figures and Tables

All figures and tables referenced in this thesis are placed at the end of relevant chapters. This has been done to minimize the impact of large numbers of figures and tables on document flow and as an aid to interpretation of results and discussion sections of each chapter.

Table of Contents

Chapter 1: Literature review 1

1.1 The Genus *Vibrio* 1

1.2 Ecology of Vibrio Species 1

1.2.1 The Effect of Seasonal Temperature and Salinity in Vibrios 2

1.2.2 Vibrios in Aquatic Wildlife and Zooplankton 4

1.2.3 Bacteriophages and Vibrios 5

1.3 Pathogenesis of *Vibrio parahaemolyticus* 6

1.4 The Viable But Non-Culturable State 8

1.4.1 Induction of the VBNC State 10

1.4.2 Characterization of VBNC State Cells 12

1.4.3 Virulence of Cells in the VBNC State 14

1.4.4 Gene Expression in the VBNC State 15

1.4.5 Antibiotic Resistance of VBNC Cells 16

1.5 Resuscitation from the VBNC State 17

1.5.1 Resuscitation following a Temperature Upshift 17

1.5.2 Resuscitation Promoting Factors 17

1.5.3 Biological Mediators of the VBNC State 18

1.5.4 Autoinducers and the VBNC State 19

1.6 The YjeE/YeaZ/YgjD Signal Transduction Network 20

1.7 YeaZ Protein-Protein Interactions 21

1.7.1 YeaZ 21

1.7.2 Structure of YeaZ 21

1.7.3 YgjD 22

1.7.4 YjeE 24

1.8 Summary 25

1.9 Hypothesis and Aims 25

1.9.1 Overall Aims and Hypothesis 25

1.9.2 Specific Hypothesis 26

1.9.3 Specific Aims 26

Chapter 2: Materials and Methods.....43
2.1 Chemicals and Reagents 43
2.2 Buffers and Solutions.....43
2.3 Bacteria and Yeast Strains 43
2.4 Growth Media 43
2.5 DNA and Protein Molecular Weight Markers 44
2.6 Plasmids used in this Study.....44
2.7 Oligonucleotide Primers.....44
2.8 Antibodies 44
2.9 Molecular Biology Techniques.....44
2.9.1 Preparation of Chromosomal DNA 44
2.9.2 Preparation of Plasmid DNA.....44
2.9.3 Polymerase Chain Reaction (PCR) 44
2.9.4 Restriction Enzyme Digestion.....45
2.9.5 Extraction of DNA from Agarose Gel.....45
2.9.6 DNA Ligation.....45
2.9.7 Transformation of Chemically Competent *E. coli* Cells 45
2.9.8 Electro-transformation of *V. parahaemolyticus* Cells.....46
2.9.9 DNA Sequencing.....46
2.9.10 Agarose Gel Electrophoresis 47
2.10 RNA Transcript Analysis.....47
2.10.1 RNA Isolation.....47
2.10.2 RNA Quantification.....48
2.10.3 RNA Quality Confirmation 48
2.10.4 Quantitative Reverse Transcription PCR 48
2.11 Protein Techniques.....48
2.11.1 Protein Quantification 48
2.11.2 SDS-PAGE 49
2.11.3 Western Blot Analysis.....49
2.11.4 Expression and Purification of His-tagged fusion Protein 50
2.11.5 Production of a YeaZ specific Polyclonal Antiserum 50
2.11.6 Co-immunoprecipation.....51

2.11.7 Immunofluoresence Microscopy 51
2.11.8 Extraction of Outer Membrane Protein 52
2.11.9 Trichloroacetic Acid (TCA) Precipitation 52
2.11.10 Formaldehyde Cross-linking 53
2.11.11 MALDI-TOF Mass Spectrometry 53
2.11.12 Bacterial Two-Hybrid Analysis 54
2.11.13 Yeast Two-Hybrid Analysis 55
2.11.14 Transmission Electron Microscopy (TEM) 56
2.12 Site-directed Mutagenesis by Overlap Extension PCR 56
Chapter 3: Factors affecting Resuscitation and Entry to the VBNC State 67
3.1 Introduction 67
3.2 Experimental Approach 68
3.3 Results 68
3.3.1 Effect of Initial Cell Concentration and NaCl Concentration on Culturability 68
3.3.2 Effect of Initial Cell Concentration and pH on Culturability 71
3.3.3 Effect of Cell Concentration and NaCl Concentration on Resuscitation 72
3.3.4 Effect of Cell Concentration and pH on Resuscitation 73
3.4 Discussion 74
Chapter 4: The role of YeaZ in the VBNC state 92
4.1 Introduction 92
4.2 Experimental Approach 93
4.3 Results 94
4.3.1 Characterization of *yeaZ*$_{Vp}$ Nucleotide and Amino Acid Sequence 94
4.3.2 Cloning the *yea*Z gene from *V. parahaemolyticus* strain NCTC 10884 94
4.3.3 Mutagenesis of *yeaZ*$_{Vp}$ 94
4.3.4 Construction of a *V. parahaemolyticus yeaZ*::*kan* Mutant 95
4.3.5 Complementation Analysis 96
4.3.6 Overexpression and Purification of YeaZ$_{Vp}$ 96
4.3.7 Generation of a Polyclonal Antiserum for YeaZ$_{Vp}$ 97
4.3.8 Characterisation of the *yeaZ*$_{Vp}$ Mutant 98
4.3.9 The Effect of YeaZ$_{Vp}$ Fusion Protein on Resuscitation 99
4.3.10 Cellular Location of YeaZ in *V. parahaemolyticus* NCTC 10884 99

4.3.11 $YeaZ_{Vp}$ Levels during VBNC Induction and Resuscitation 100
4.3.12 Transcriptional Analysis of VBNC State and Resuscitating Cells 101
4.3.13 TEM of *V. parahaemolyticus* NCTC 10884 Cells in the VBNC State 102
4.4 Discussion 103
Chapter 5: YeaZ Protein-Protein Interactions 132
5.1 Introduction 132
5.2 Aims and Approaches 133
5.3 Results 134
5.3.1 Characterization of the $YgjD_{Vp}$ and $YjeE_{Vp}$ Nucleotide and Amino Acid Sequences 134
5.3.2 Protein-protein Interactions in Bacterial Two-hybrid Analysis 135
5.3.3 Protein-protein Interactions in Yeast Two-hybrid Analysis 138
5.3.4 Protein-protein Interactions in Pull-down Analysis 141
5.3.5 Co-immunoprecipitation of $YeaZ_{Vp}$ Associated Proteins 144
5.3.6 $YeaZ_{Vp}$ Domains involved in Protein-Protein Interactions 144
5.4 Discussion 148
Chapter 6: Conclusions 179
6.1 Introduction 179
6.2 Conclusions 180
6.3 Significance and Future Work 182
Chapter 7: References 184
Appendices 200

List of Figures

Figure 1.1: Counts of *Vibrio* species from the east coast of North Carolina, USA. 27
Figure 1.2: Counts of *Vibrio* species(■) and estuarine bacteria (●) in sea sediments. 28
Figure 1.3: Counts of Vibrios and TVC within oysters from South Australia. 29
Figure 1.4: Counts of Vibrio and TVC within oyster grow seawater in South Australia.....30
Figure 1.5: Entry of *V. vulnificus* into the VBNC state. 31
Figure 1.6: Morphological characteristic of *V. alginolyicus* cells analysed by scanning electron microscopy. 32
Figure 1.7: Proposed interaction of regulatory factors involved in the VBNC state.....34
Figure 1.8: Time required for resuscitation of VBNC *V. vulnificus* cells. 35
Figure 1.9: Effect of purified RPF on stimulation of growth of washed *M. luteus* cells.....36
Figure 1.10: Alignment of Rpf amino acid sequences.....37
Figure 1.11: Dose-dependency of recombinant Rpf protein in *Salmonella* Oranienburg. 38
Figure 1.12: Alignment of YeaZ amino acid sequences.....39
Figure 1.13: Model of YjeE, YeaZ and YgjD essential signal transduction network. 40
Figure 1.14: Structure of YeaZ from *S.* Typhimurium. 41
Figure 1.15: The potential YeaZ biological dimer of *S.* Typhimurium. 42
Figure 3.1: Counts of *V. parahaemolyticus* cells incubated in ASW containing 2.5% NaCl at 4°C and 20°C.....78
Figure 3.2: Counts of *V. parahaemolyticus* cells incubated in ASW containing 5.0% NaCl at 4°C and 20°C.....79
Figure 3.3: Counts of *V. parahaemolyticus* cells incubated in ASW containing 10% NaCl at 4°C and 20°C.....80
Figure 3.4: Time to loss of culturability of *V. parahaemolyticus* cells suspended in ASW containing different levels of NaCl. 81
Figure 3.5: Plots of $\ln(N/N_0)$ *vs.* time at 4°C in ASW with different levels of NaCl. 82
Figure 3.6: Counts of *V. parahaemolyticus* incubated at 4°C and 20°C in ASW at pH 5.....84
Figure 3.7: Counts of *V. parahaemolyticus* incubated at 4°C and 20°C in ASW at pH 8.....85
Figure 3.8: Counts of *V. parahaemolyticus* incubated at 4°C and 20°C in ASW at pH 9.5.....86
Figure 3.9: Effect of pH on time to loss of culturability of *V. parahaemolyticus* cells in ASW adjusted to different pH. 87

Figure 3.10: Plot of ln(N/N_0) versus time at 4°C in ASW adjusted to different pH. 88
Figure 3.11: Counts of *V. parahaemolyticus* during resuscitation from the VBNC state from 4°C upshift to 20°C in ASW containing 2.5% NaCl and 5% NaCl 90
Figure 3.12: Counts of *V. parahaemolyticus* NCTC 10884 during resuscitation from the VBNC state from 4°C upshift to 20°C in ASW at pH 8. 91
Figure 4.1: DNA and amino acid sequence for $YeaZ_{Vp}$. 109
Figure 4.2: PCR amplification of the 1561bp fragment *yeaZ*$_{Vp}$.....110
Figure 4.3: Construction of plasmid pCTX100. 111
Figure 4.4: Construction of plasmid pCTX101. 112
Figure 4.5: PCR confirmation of the 1.9 kbp *yeaZ::kan* fragment of pCTX101. 113
Figure 4.6: Construction of plasmid pCTX102. 114
Figure 4.7: PCR confirmation of the 1.9 kbp fragment of the pCTX102. 115
Figure 4.8: PCR confirmation of the *V. parahaemolyticus yeaZ*$_{Vp}$ mutant. 116
Figure 4.9: Construction of plasmid pCTX103. 117
Figure 4.10: PCR amplification of the 3 kbp *yeaZ*$_{Vp}$ fragment.....118
Figure 4.11: Construction of pCTX104. 119
Figure 4.12: Construction of pCTX105. 120
Figure 4.13: Purification of $YeaZ_{Vp}$ protein. 121
Figure 4.14: Western blot analysis of $YeaZ_{Vp}$ proteins. 122
Figure 4.15: Effect of a *yeaZ* mutation on entry into the VBNC state. 123
Figure 4.16: Effect of exogenous $YeaZ_{Vp}$ protein on resuscitation from the VBNC state. 124
Figure 4.17: SDS-PAGE separation of proteins from *V. parahaemolyticus*. 125
Figure 4.18: Detection of cell surface associated $YeaZ_{Vp}$ by IF.....126
Figure 4.19: $YeaZ_{Vp}$ prepared from VBNC state cells and Resuscitated Cells. 127
Figure 4.20: Expression of the *rpoS* and *yeaZ* genes in different states. 128
Figure 4.21: TEM images of sections of wild type *V. parahaemolyticus* cells. 129
Figure 4.22: TEM images of sections of *V. parahaemolyticus yeaZ* mutant cells. 130
Figure 5.1: Nucleotide and deduced amino acid sequence for $YgjD_{Vp}$. 155
Figure 5.2: Nucleotide and deduced amino acid sequence for $YjeE_{Vp}$. 156
Figure 5.3: Construction of plasmid pCTX106. 157
Figure 5.4: Construction of plasmids pCTX107, pCTX108 and pCTX109. 158
Figure 5.5: $YeaZ_{Vp}$ interaction with $YeaZ_{Vp}$, $YgjD_{Vp}$ and $YjeE_{Vp}$. 159

Figure 5.6: Construction of plasmid pCTX110. 160
Figure 5.7: Construction of plasmids pCTX111 and pCTX112. 161
Figure 5.8: Protein interaction in yeast two-hybrid. 162
Figure 5.9: Construction of plasmid pCTX113. 163
Figure 5.10: Construction of plasmids pCTX114 and pCTX115. 164
Figure 5.11: Confirmation of pCTX114 and pCTX115. 165
Figure 5.12: Co-expression of $YeaZ_{Vp}$ with $YgjD_{Vp}$ or $YjeE_{Vp}$ in *E. coli* BL21DE3. 166
Figure 5.13: The His-tag pull down assay of $YeaZ_{Vp}$ complexes.....167
Figure 5.14: Western blot detection of cross-linked $YeaZ_{Vp}$ complexes. 168
Figure 5.15: Immuno-precipitation of $YeaZ_{Vp}$ associated protein.....169
Figure 5.16: YeaZ amino acid sequence alignments. 170
Figure 5.17: The structure of $YeaZ_{ST}$ and predicted structure of $YeaZ_{Vp}$. 171
Figure 5.18: Potential interaction domains and amino acids in $YeaZ_{ST}$ dimers. 172
Figure 5.19: Construction of plasmids pCTX116, pCTX117 and pCTX118. 173
Figure 5.20: Interaction of $YeaZ_{Vp}$ mutants with $YgjD_{Vp}$. 174
Figure 5.21: Interaction of I75A, L83A and F85A $YeaZ_{Vp}$ mutants with $YeaZ_{Vp}$. 175
Figure 5.22: Western blot analysis of interacting $YeaZ_{Vp}$ and $YgjD_{Vp}$ protein. 176
Figure 5.23: Western blot analysis of interacting $YeaZ_{Vp}$ mutants and $YeaZ_{Vp}$ wt proteins. 177

List of Tables

Table 1.1: Bacterial known to enter a VBNC state.....33
Table 2.1: Bacteria and Yeast strains used in this study.....58
Table 2.2: Composition of SD medium. 59
Table 2.3: Plasmids used in this study. 60
Table 2.4: Primer pairs used in this study.....63
Table 4.1: Effect of a *V. parahaemolyticus yeaZ* mutation on resuscitation from the VBNC state.....131
Table 5.1: Protein mass spectrometry sequencing results for potential $YeaZ_{Vp}$ associated proteins. 178

Abstract

Vibrio parahaemolyticus is an important food-borne pathogen known to enter a Viable But Non-Culturable (VBNC) state that increases the survival of *V. parahaemolyticus* during stress eg. starvation and low temperature. The purpose of this study was to better characterize the impact of environmental factors on loss of culturability associated with entry into a cold induced VBNC state by *V. parahaemolyticus* NCTC 10884 and undertake an analysis of the role of resuscitation promoting factors in the molecular mechanism that underpins this physiological phenomenon.

Entry to the VBNC state was examined for high (10^9 and 10^7 cells mL^{-1}) and low (10^5 and 10^3 cells mL^{-1}) concentration cell suspensions in artificial seawater (ASW) adjusted to different pH and salinity, with incubation at 4°C. Salinities (5 and 10% NaCl) and pH (5 and 9.5) considered suboptimal for growth resulted in short incubation periods required for entry to the VBNC state. Interestingly, the time to loss of culturability of all suspensions tested was found to be dependent on cell suspension concentration. Furthermore, low density cell suspensions, but not high density suspensions that had achieved complete loss of culturability, could not be resuscitated following a temperature upshift to 20°C. This novel result indicated that survival of VBNC state cells is likely to require maintenance nutrients from dead cells within the suspension.

To investigate the role of potential resuscitation factor proteins in establishment of the VBNC state and subsequent recovery, a *V. parahaemolyticus* NCTC 10884 $yeaZ_{Vp}$ mutant was constructed. Compared to the wild type parent, suspensions of the $yeaZ_{Vp}$ mutant took substantially longer to lose culturability under conditions required to achieve a VBNC state. Furthermore, this mutant was unable to be resuscitated from the VBNC state. Complementation with $yeaZ_{Vp}$ returned the mutant phenotype to a wild type phenotype. These results suggested that $YeaZ_{Vp}$ plays an integral role in establishment of the VBNC state and subsequent resuscitation for *V. parahaemolyticus* NCTC 10884.

To determine the patterns of expression and cellular distribution of $YeaZ_{Vp}$ in *V. parahaemolyticus* NCTC 10884, a recombinant, His-tagged $YeaZ_{Vp}$ protein (*ca.* 25 kDa) was over expressed from *E. coli* BL21DE3 and purified using affinity chromatography. Purified protein was used to raise a polyclonal antibody of $YeaZ_{Vp}$ protein in a rabbit. This specific

antiserum was used to detect presence of $YeaZ_{Vp}$ in the VBNC state cells and during resuscitation. Western analysis and immunofluorescence microscopy was used to demonstrate $YeaZ_{Vp}$ protein is located in the cytoplasm of cells as well as outer-membrane fractions of *V. parahaemolyticus* NCTC 10884.

As YeaZ has been shown to interact with proteins that are considered essential proteins involved in viability (YgjD and YjeE), interaction of the $YeaZ_{Vp}$ with these proteins in *V. parahaemolyticus* NCTC 10884 was examined. Protein-protein interactions were determined using bacterial and yeast two-hybrid analysis, pull down analysis and immunoprecipitation analysis. Two-hybrid analysis showed that $YeaZ_{Vp}$ was able to interact strongly with other $YeaZ_{Vp}$ monomers as well as $YgjD_{Vp}$, but only weakly with $YjeE_{Vp}$. These results confirmed previous work that showed that YeaZ homologs interact with YgjD, and form dimeric structures. His tag technologies were also used to demonstrate that $YeaZ_{Vp}$ natively interacts with $YjeE_{Vp}$ and $YgjD_{Vp}$ when pairs of these three proteins were expressed in *E. coli*. Furthermore, the ability of $YeaZ_{Vp}$ to form dimers was separately demonstrated following cross-linking of $YeaZ_{Vp}$ natively expressed in *E. coli*. Attempts to demonstrate this in *V. parahaemolyticus* NCTC 10884 were not successful. However, the immunoprecipitation of *V. parahaemolyticus* NCTC 10884 whole cell lysates with a $YeaZ_{Vp}$ specific antiserum indicated that $YeaZ_{Vp}$ is also associated with OmpU. This suggested that $YeaZ_{Vp}$ that decorates the cell surface of this organism may interact with OmpU.

To determine amino acid residues involved in interaction of $YeaZ_{Vp}$ monomer that lead to formation of dimeric forms, site-directed mutagenesis of $YeaZ_{Vp}$ was used together with two-hybrid analysis. The results showed that the YeaZ L83A and F85A substitutions significantly affected interactions between $YgjD_{Vp}$ and $YeaZ_{Vp}$. However, a YeaZI75A substitution only affected interaction between monomers of $YeaZ_{Vp}$. These results suggested that L83 and F85 residues of $YeaZ_{Vp}$ play important roles in the $YeaZ_{Vp}$ and $YgjD_{Vp}$ protein-protein interactions.

Declaration

This work contains no material which has been accepted for the award of any other degree or diploma in any university or other tertiary institution to Shih-Hsun Chen and, to the best of my knowledge and belief, contains no material previously published or written by another person, except where due reference has been made in the text.

I give consent to this copy of my thesis, when deposited in the University Library, being made available for loan and photocopying, subject to the provisions of the Copyright Act 1968.

I also give permission for the digital version of my thesis to be made available on the web, via the University's digital research repository, the Library catalogue, the Australasian Digital Theses Program (ADTP) and also through web search engines, unless permission has been granted by the University to restrict access for a period of time.

Shih-Hsun Chen

Date: Tuesday, July 10, 2012

Abbreviations

~	Approximately
°C	degrees Celsius
µF	Microfarad/s
µg	Microgram
µL	Microlitre
g	Relative centrifugal force
A_{600}	Absorbance at 600 nm
aa	Amino acid/s
Amp	Ampicillin
bp	Base pairs
ca.	Circa
CFU	Colony forming units
cm	Centimeters
Cm	Chloramphenicol
d	days
DNA	Deoxyribonucleic acid
EDTA	Ethylene-diamine-tetra-acetic-acid disodium salt
Erm	Erythromycin
$g\ L^{-1}$	Grams per litre
h	hour/s
HCl	Hydrochloric acid
HEPES	4-(2-hydroxyethyl)-1-piperazineethanesulfonic acid
HPK	Histidine kinase
IPTG	Isopropyl-β-D-thio-galactopyranoside
Kb	Kilobase/s
kDa	Kilodalton/s
kg	Kilogram/s
kV	Kilovolts/s
L	Litre/s

LB	Luria Bertani broth
M	Molar
mg	Milligram/s
min	Minute/s
mL	Millilitre/s
mM	Millimolar
MQ	MilliQ grade pure water
mRNA	Messenger RNA
ms	Milliseconds
nm	Nanometres
OD_{600}	Optical density of 600 nm
O/N	overnight
ONPG	O-nitrophenyl-β-D-galactopyranoside
ORF	Open reading frame
PAGE	Polyacrylamide gel electrophoresis
PBS	Phosphate buffered saline
PCR	Polymerase Chain Reaction
qRT-PCR	Quantitative reverse-transcription PCR
rRNA	Ribosomal ribonucleic acid
RNA	Ribonucleic acid
RNase	Ribonuclease
RR	Response regulator
RT	Room temperature
SDS	Sodium Dodecyl Sulphate
sec	Second/s
SOC	Super Optimum broth with Catabolite repression
spp	Species
TAE	Tris-acetate EDTA buffer
TTSS	Type three secretion system
TVC	Total viable count (= Total Plate Count)
vol	Volume/s

v/v	Volume per volume
w/v	Weight per volume
X-Gal	5-bromo-4-chloro-3-indolyl-β-D-galactopyranoside

Acknowledgements

I would like to thank my supervisor Dr. Connor Thomas. Thank you for giving me the opportunity to do my PhD with you and for teaching me so much in research. Under his patience, encouragement and guidance, I have grown and developed much as a scientist. I am grateful for his patience and understanding. I also like to thank my co-supervisor Dr. Renato Morona for advice and help on my research.

Thanks are also due to Dr. Keith Shearwin and Dr. Grant Booker for advice on bacterial two-hybrid analysis and Site-directed mutagenesis analysis. To Miss Lyn Waterhouse and Ruth Williams, Adelaide Microscopy Center, for their patient and advice to solve my problem in TEM experiment. To all my lab members Rethish, Caroline, Johnson, Ann and Mei Mei, thanks for your advice, support and friendship. I appreciate all the joy and fun with you guys in the lab. To all the people from other labs Jennifer, Rachelle, and Mei Zhi, thanks for the joy brought to us during the break time. I also like to thank all the people from Morona, Paton, McColl lab and Grant Booker, especially Dr. David Ogunniyi, Dr. Layla Mahid, Min Yan and Ethan Chen for their help, support and advice in my research. To other members in the school, including CUS stuffs, Sergei Volgin and Garry Penney, thank you for being there to help and provide advice.

Finally, I would like to thank my parents and my wife for all your encouragement, love and wonderful support to me in many ways. Especially to my wife, thank you to being here with me for all your love, support and encouragement over the years of study. I could not have done this without you, and I love you very much.

Chapter 1: Literature review

1.1 The Genus *Vibrio*

Vibrio species are Gram negative (G-ve) bacteria that belong to the family Vibrionaceae. This family also comprises the genera *Aeromonas*, *Photobacterium* and *Plesiomonas* (Demain et al., 1999). All *Vibrio* species are nonspore-forming rods, 1.4 to 2.6 µm in length and 0.5 to 0.8 µm (McLaughlin, 1995). There are 12 species of Vibrios that are pathogenic to humans, including *V. chlolerae*, *V. mimicus*, *V. parahaemolyticus*, *V. vulnificus*, *V. fluvialis*, *V. alginolyticus*, *V. cincinnatiensis*, *V. damsela*, *V. hollisae*, *V. furnissii*, *V. metshnikovii*, *V. carchariae.* All of these species are present in marine or estuarine environments and with the exception of except *V. cholerae* and *V. mimicus,* have a requirement for sodium chloride for growth. *V. metshnikovii*, *V. cholerae*, *V. parahaemolyticus* and *V. vulnificus* are the most important strains responsible for human disease. Infections acquired by consumption of contaminated shellfish result in gastroenteritis, but may lead to more serious symptoms such as septicaemia. Clinical symptoms include diarrhea, abdominal cramps, vomiting, headache, fever, and chills, during the incubation periods ranging from 4 to 96 h (Joseph et al., 1983).

1.2 Ecology of Vibrio Species

Vibrio species are considered to be ubiquitous within marine and estuarine systems. *V. parahaemolyticus* and *V. vulnificus* can easily be isolated in high numbers from bivalves, crustaceans, finfish, sediment, and plankton (DePaola et al., 1994; Kelly, 1982; O'Neill et al., 1992; Oliver *et al.*, 1982; Tamplin *et al.*, 1982). Counts of *V. parahaemolyticus* in shellfish can increase approximately 13 to 26 fold following harvest and storage for 24 h at 26°C (Kaufman et al., 2003). *V. parahaemolyticus* and *V. vulnificus* have been isolated from U.S. waters as far north as the Great Bay of Maine (*V. vulnificus*) (O'Neill et al., 1992), Alaska (*V. parahaemolyticus*) (McLaughlin et al., 2005), and Long Island, New York (*V. parahaemolyticus*) (Tepedino, 1982). Lower densities of *V. vulnificus* and *V. parahaemolyticus* were isolated from Pacific, Canadian, and North Atlantic waters, where water temperatures are generally lower year round; higher densities were found in mid-Atlantic, Chesapeake Bay, and Gulf of Mexico waters where water temperatures are warmer

year round (Cook & Bolster, 2007; DePaola et al., 1994; Motes et al., 1998; Wright et al., 1996).

1.2.1 The Effect of Seasonal Temperature and Salinity in Vibrios

The main factors involving the occurrence and distribution of Vibrios in environments are water temperature, salinity and nutrient. Tantillo et al. (2004) showed that the prevalence of Vibrios is related to temperature and salinity, and hypothesized that the increased density of *Vibrio* species in coastal environments is a result of higher temperatures in these environments (Tantillo et al., 2004).

It is now recognized that water temperature is the most important factor that determines the distribution and abundance of Vibrios. Cell densities remain low at temperatures below 20°C and the highest cell densities occur when the water temperature is about 20°C. Vibrios are less frequently isolated when the temperature of aquatic environments is below 10°C or exceeds 30°C (Tantillo et al., 2004). Remarkably, a direct relationship exists between detection of *Vibrio* species and the seasonal temperature. This phenomenon has been observed in several distinct geographic regions including the USA, Asia, Europe and more recently Australia (Arias et al., 1999; Hervio-Heath et al., 2002). Kelly et al. (1988) reported that *V. parahaemolyticu*s was found in Pacific Northwest coastal waters only during the summer months, when water temperatures were above 17°C and salinities were below 13 ppt (Kelly & Stroh, 1988).

Salinity is another ecological factor that influences bacterial growth rate. Kaspar et al. (1993) reported that *V. vulnificus* cell numbers increased at salinities between 5 and 25 ppt. However, at salinities of 30, 35, and 38 ppt., *V. vulnificus* cell numbers decreased by 58%, 88%, and 83%, respectively (Kaspar & Tamplin, 1993). Motes et al. (1998) also observed lower numbers of *V. vulnificus* at salinities above 28 ppt. that are typical of some Atlantic coastal sites in North and South Carolina. The negative effect of high salinity may explain why *V. vulnificus* cannot be isolated from oysters harvested from waters off these shores. High counts of *V. vulnificus* cells however, were found in oysters harvested from intermediate salinities between 5 and 25 ppt. (Motes et al., 1998).

In spite of the role of salinity, temperature may play the most important role on the prevalence and levels of the pathogenic Vibrios. The growth of *V. vulnificus* is favoured by

relatively high water temperatures. *In vitro* growth characteristics of environmental isolates of *V. vulnificus* demonstrated salinity optima of 1.0 to 2.0% NaCl and a temperature optimum of 37°C (Kelly, 1982). Kaspar & Tamplin indicated that *V. vulnificus* is favoured by the temperature range of 13 to 22°C (Kaspar & Tamplin, 1993). Wright et al. (1996) were able to culture *V. vulnificus* from estuarine waters of Chesapeake Bay collected during winter when water temperatures were below 8°C (Wright et al., 1996). However, *V. vulnificus* could not be recovered from waters from the Gulf of Mexico when temperatures were lower than 12.5°C (Simonson & Siebeling, 1986). In general, *V. vulnificus* was seldom isolated from surface water samples from the Gulf of Mexico during winter (January to March), when water temperatures are below 20°C (Kelly, 1982). These studies indicate that the peak season of recovery of *Vibrio* species is summer, and there is substantial seasonal variation in prevalence and levels of the organism. This is supported by studies that have demonstrated that during the summer months, counts of *V. vulnificus* in oysters harvested from the Gulf of Mexico and Mid Atlantic states, were higher than other seasons (Cook et al., 2002).

The seasonal variation in the distribution and levels of *V. vulnificus* in aquatic systems has also been reported for *V. parahaemolyticus*. For example, counts of *V. parahaemolyticus* in Gulf Coast oysters were shown to be high during summer months, but gradually declined in the colder months (Motes et al., 1998). DePaola et al. compared seasonal levels of *V. parahaemolyticus* in Pacific, Gulf, and Atlantic Coast waters and oyster samples. The results indicated a strong relationship exists between water temperature and *V. parahaemolyticus* levels. The Gulf Coast had the warmest mean water temperature (22°C) and highest mean counts of *V. parahaemolyticus* in oysters, while the Pacific coast water was the coldest (15°C) and was associated with lower levels of *V. parahaemolyticus* in oysters (DePaola et al., 1990). Pfeffer et al. (2003) demonstrated the same relationship between water temperature and levels of Vibrios. Figure 1.1 and Figure 1.2 indicate the seasonal decline in levels of Vibrio species in seawater and sea sediments during winter months in United States. The result shows a correlation between water temperature and culturability; the coldest water temperature (14°C) harboured the lowest levels of Vibrios (Pfeffer et al., 2003). Interestingly, the same effect of water temperature on counts of *V. parahaemolyticus* occurs for South Australian (SA) winter seawater temperatures in commercial oyster growing regions (Figure 1.3 and Figure 1.4), and Madigan et al. (2007) have reported a strong seasonal

trend in counts of *Vibrio* species associated with seawater and oysters grown in this region of Australia (Madigan et al., 2007).

1.2.2 Vibrios in Aquatic Wildlife and Zooplankton

Aquatic birds maybe a vector for *Vibrio* species, particularly during the winter months. Bisgaard et al. reported that *V. cholerae* could be isolated from aquatic birds at low levels and that non-O1 *V. cholerae* could be isolated from ducks (Bisgaard & Kristensen, 1975) and gulls during the winter, when *Vibrio* species were not found in the water column (Lee et al., 1982). Roberts et al. (1984) demonstrated that *V. parahaemolyticus*, non-O1 *V. cholerae* and other lactose-positive Vibrios were isolated from bird feces. *Vibrio* species have also been recovered from feces of six types of aquatic birds (gulls, pelicans, Canada geese, swans, egrets, cormorants) (Buck, 1990). Miyasaka et al. (2006) found higher proportions of *V. parahaemolyticus* positive samples compared to *V. vulnificus* positive samples in wild aquatic birds in Japan during the winter months. In all cases, the level of Vibrios was quite low in bird populations (Miyasaka et al., 2006).

Although counts of *V. vulnificus* and *V. parahaemolyticus* present in estuarine environments decline to almost undetectable levels during the colder winter months, these organisms nevertheless persist all year round. There are many ways in which *V. vulnificus* and *V. parahaemolyticus* can overwinter. One strategy for survival is association with chitinous zooplankton and shellfish. Vanoy et al. (1992) found *V. vulnificus* over-winters in a floc zone present at the sediment-water interface. This floc is resuspended into the water column in early spring following changes in climatic conditions, and the Vibrios colonize the surfaces of zooplankton that bloom during early spring. These zooplankton-associated Vibrios are ingested by oysters during their normal feeding process (Vanoy et al., 1992). DePaola et al. (1994) isolated *V. vulnificus* during the winter months from the intestines of estuarine fish from the Gulf of Mexico. The counts of *V. vulnificus* from these samples were higher than that of crabs, oysters, sediment or seawater (DePaola et al., 1994).

It is well-documented that *Vibrio* species make up an important part of the natural microflora of zooplankton, particularly zooplankton such as copepods (Carli et al., 1993; Huq et al., 1983). Huq et al. (1983) found higher densities of Vibrios associated with zooplankton than were present in the surrounding water column. Watkins et al. (1985) showed a positive

association with the amount of particulate matter in the water and specifically with its zooplankton content. Of several particulates added to the water, only chitin and net zooplankters[1] supported the growth of *V. parahaemolyticus* (Watkins & Cabelli, 1985). Heidelberg et al. (2002) found various groups of bacteria associated with zooplankton, that the higher densities of bacteria related to zooplankton during the winter months. Nevertheless, the majority of Vibrios identified were *V. cholerae, V. parahaemolyticus* and *V. vulnificus* (Heidelberg et al., 2002).

Strom et al. (2000) reported that *V. vulnificus* exports a number of degradative enzymes and toxins into the extracellular milieu. These extracellular proteins are thought to be particularly important for the organism's ability to survive in the estuarine environment and cause disease in infected hosts. For example, *V. vulnificus* secretes chitinase that is presumably useful for the bacterium to colonize and adhere to the chitin exoskeletons of zooplankton. In fact, this may be one way that *V. vulnificus* is collected by molluscs, that is, as a by-product of normal filter feeding. Similarly, Strom et al. (2000) have suggested metalloproteases and hemolysins, may be important for the organism to colonize and multiply in molluscan shellfish. Presumably, these act by breaking down tissue at the site of colonization to release necessary nutrients required for growth.

1.2.3 Bacteriophages and Vibrios

Bacteriophages are common in the marine environment, and those specific for pathogenic *Vibrio* species are no exception (Jiang & Paul, 1994; Baross et al., 1978). For example, Pelon et al. (1995) isolated 9 phage strains particular from *V. vulnificus*, with patterns of susceptibility varying with specific *V. vulnificus* strain (Pelon et al., 1995). Based on these results, the same researchers found that *in vitro* exposure to 1.0 mL of pooled bacteriophage reduced *V. vulnificus* levels by five $\log_{10}$ fold. Indeed a pool of 9 bacteriophage strains were shown to reduce *V. vulnficus* populations in estuarine water (Pelon et al., 1995). DePaola et al. (1997) identified phages that infected *V. vulnificus* isolates from estuarine waters, sediments, plankton, crustacea, and the intestines of finfish and molluscan shellfish harvested from the Gulf Coast. Apparently, molluscan shellfish contains more phage diversity and

[1] Small planktonic animals eg copepods.

abundance than other habitats. *V. vulnificus* phages, isolated from oysters, did not lyse other mesophilic bacteria. Furthermore, *V. vulnificus* phages and *V. vulnificus* were found in a variety of oyster tissues and fluids, although the lowest densities were detected in the hemolymph and mantle fluid. These observations indicate an interesting ecological relationship between *V. vulnificus* phages and molluscan shellfish (DePaola et al., 1997).

Koga et al. (1982) isolated 18 bacteriophages lytic for *V. parahaeomlyticus* that could be divided into 4 different morphological groups. However, these finding suggested that there was no correlation between the O and K serotype of *V. parahaeomlyticus* strains and host range of phages. Typically, these bacteriophages have different sensitivities to heat and organic solvents (Koga et al., 1982). Comeau et al. (2005) found 13 bacteriophages specific for *V. parhaemolyticus* to be consistently prevalent throughout the year in oysters compared to sediment and water column. However, 10 bacteriophages were not species specific and also infected more than one of *V. alginolyticus*, *V. natriegens* and *V. vulnificus* (Comeau et al., 2005). In a later study, the same investigators demonstrated that *V. parahameolyticus* phages infected between 4 and 13 *V. parahaemolyticus* strains with a unique host range pattern (Comeau et al., 2006). These phage showed the same relationship between host range and season (Comeau et al., 2005). Using these same 13 bacteriophages to control *V. parahaemolyticus* in the environment, the investigators succeeded in reductions of 74%, 62%, and 30% in sediment, oysters, and the water column respectively. Whether the use of bacteriophage, is a practical method to control *Vibrio* contamination in oysters is still not clear.

1.3 Pathogenesis of *Vibrio parahaemolyticus*

Most *Vibrio* species are pathogenic to humans, marine vertebrates or invertebrates. *V. parahaemolyticus* strains have two types of classifications. The species *V. parahaemolyticus,* has been typed according to serotype and the presence of genes associated with virulence. Eleven O (somatic) antigen types and 71 K (capsular) antigen types have been reported (Kaysner & DePaola, 2001). However, alternative classifications based on the presence of particular genes, some of which are required for pathogenicity, are also used. For example, *V. parahaemolyticus* strains are considered pathogenic if these carry

genes encoding the thermostable direct hemolysin (*tdh*), TDH-related hemolysin (*trh*) and thermolabile haemolysin (*tlh*) (Nishibuchi & Kaper, 1995).

Virulence factors that are known to play a role in the pathogenicity of *V. parahaemolyticus* include hemolysin(s) responsible for β-haemolysis, adherence factors, and the products of the *tdh*, *trh* and the *ure* genes. However, clinical isolates of *V. parahaemolyticus* are differentiated from non-pathogenic environmental isolates based on expression of β-haemolysis on Wagatsuma agar (a modified blood agar). Nearly all clinical isolates are haemolytic strains (or Kanagawa phenomenon (KP) positive) whereas only 1% to 2% of environmental strains have been reported to be KP-positive (Sakazaki, 1968). For this reason, the haemolysin expressed by KP positive isolates has been considered the most important marker of pathogenic strains (Takeda, 1983). The protein responsible for the KP is the thermostable direct hemolysin (TDH) and was named for its characteristics: TDH was not inactivated by heating at 100°C for 10 min, and the hemolytic activity is not enhanced by the addition of lecithin, suggesting it acts directly on erythrocyctes (Nishibuchi & Kaper, 1995). Nishibuchi et al. (1989) indicated that all KP-positive (clinical) *V. parahaemolyticus* strains carry two copies of the *tdh* gene, whereas clinical and environmental strains of *V. parahaemolyticus* that give weak hemolysis on Wagatsuma agar and are considered to be KP-intermediate, carry a single copy of the *tdh* gene (Nishibuchi et al., 1989). However, only 16% of KP-negative isolates, most of which are of environmental origin, carry a single copy of the *tdh* gene. The remainder of the KP-negative strains were *tdh* negative, suggesting that most KP-negative strains cannot produce the TDH protein (Nishibuchi & Kaper, 1995).

Honda et al. (1987) reported that some KP-negative strains of *V. parahaemolyticus* implicated in humans illness, produced a haemolysin that was similar to, but not identical TDH protein. This TDH related haemolysin (TRH) was first found in *V. parahaemolyticus* O3:K6 strains (Honda et al., 1987). In addition, Sarkar et al. (1987) found that this new hemolysin was associated with environmental *V. parahaemolyticus* strains, which was responsible for lethality in the mouse model when the animals were challenged by intraperitoneal infection of *V. parahaemolyticus* (Sarkar et al., 1987). The nucleotide sequence similarity of the *trh* and *tdh* genes is about 69% (Nishibuchi et al., 1989). In addition, some clinical strains, but not environmental strains, were reported to contain both the *tdh* and *trh* genes (Xu *et al.*, 1994a). Deletion of all or part of the *trh* gene results in loss

of hemolytic activity; although the mutants retained activity in cytoxity assays and were able to cause partial fluid accumulation in ligated rabbit small intestines (Xu et al., 1994b). These results indicate that TRH and TDH are virulence factors associated with the pathogenicity of *V. parahaemolyticus.*

In addition to TDH and TRH, a thermolabile haemolysin (TLH), also called lecithin-dependent haemolysin (LDH), has been identified in *V. parahaemolyticus* isolates (Taniguchi et al., 1985). Shinoda et al. (1991) indicated that the TLH haemolysin gene (*tlh*) comprises an ORF of 1254 bp. The *tlh* gene encodes a 418 amino acid (MW = 47.5 kDa) pre-protein that is cleaved to a 398 amino acid mature form (45.3 kDa) that has phospholipase A2/lysophospholipase activity (Shinoda et al., 1991). Furthermore, there was no homology between the nucleotide sequences of the *tdh* and *tlh* gene of *V. parahaemolyticus* (Taniguchi et al., 1986). The *tlh* gene has been found in the genomes of all *V. parahaemolyticus* isolates derived from clinical or environmental sources (Bej et al., 1999; McCarthy et al., 1999; Taniguchi et al., 1985). On the other hand, the role of the TLH haemolysin in the enterpathogenicity of *V. parahaemolyticus* is unclear (Shinoda et al., 1991).

Another thermostable haemolysin (δ-VPH), encoded by *V. parahaemolyticus* isolates has no nucleotide and amino acid sequences homology with the TDH/TRH and TLH genes and peptides of *V. parahaemolyticus*. The gene was present in all *V. parahaemolyticus* strains tested and in one strain of *V. damsel* (Taniguchi et al., 1990). A study by Fallarino et al. (2002) identified a new HlyA haemolysin from *V. cholerae* O1 that shared 71.5% similarity to the δ-VPH haemolysin of *V. parahaemolyticus.* This haemolysin was been termed *V. cholerae* δ thermostable haemolysin (Vc-δTH, encoded by the *dth* gene). Some haemolysins, for example, TDH of *V. parahaemolyticus* have been studied extensively and closely associated with virulence. However, the role of these haemolysins, especially the TLH and δ-VPH, are unknown and await the outcome of further research.

1.4 The Viable But Non-Culturable State

Many bacteria, including a variety of human pathogens, are known to enter a novel physiological state when subjected to harsh environmental conditions, whereby the bacteria cells remain viable, but are no longer culturable by standard bacteriological methods. This physiological state is termed the Viable But-Not Culturable state (VBNC). Since the

pioneering study by Xu et al. (1982), over 400 papers have described this particular phenomenon in a variety of bacteria. Most investigators believe that the VBNC state represents a survival strategy or response to environmental stresses. Nevertheless, it is clear that VBNC state cells are a medically important reservoir of pathogens in the environment (Del Mar Lleò et al., 2007). For example, the antibiotic-resistant VBNC state cells of *Haemophilus influenzae* contained in biofilms have the ability to trigger chronic ear infections (Ehrlich et al., 2002). Shleeva et al. (2004) demonstrated that the latent phase of *Mycobacterium tuberculosis* infections represents the VBNC state of this organism, that can remain dormant as a non-culturable organism, and later reactivate and cause disease in man and animals. In this instance, reactivation is due to the resuscitation of this pathogen from the VBNC state (Pai et al., 2000). Indeed, the VBNC state has been recognised in a range of other human pathogens including, *Campylobacter* species, *Escherichia coli* (containing EHEC strains), *Francisella tularensis*, *Helicobacter pylori*, *Legionella pneumophila*, *Listeria monocytogenes*, *M. tuberculosis*, *Pseudomonas aeruginosa*, *Salmonella* and *Shigella* species and the pathogenic *Vibrio* species (Table 1.1).

Many non-human pathogenic bacteria that have adapted the VBNC state as a way of survival are associated with infection of various animals such as fish (Biosca et al., 1996; Magariños et al., 1994), corals (Banin et al., 2000; Tomer et al., 2001) and sea urchins (Masuda et al., 2004). For example, Margariños et al. (1994) demonstrated that starvation induced *Pasteurella piscicida* to enter a VBNC state. These cells maintained infectivity and pathogenic potential for fish (Magariños et al., 1994). Biosca et al. (1994) reported that the *Vibrio vulnificus* biotype 2 could be induced to enter the VBNC state by exposure to low temperature (4°C). These VBNC cells recovered culturability on solid media by incubation at elevated temperatures (25°C). Culturable cells of this bacterium remained infective for either eel or mice (Biosca et al., 1996). Similarly, the coral pathogen *Vibrio shiloi* that causes bleaching was present during the summer in the tissues of all of host corals, *Oculina patagonica*. During the winter, when seawater temperatures dropped below 20°C, *V. shiloi* could not be detected in bleached corals by standard bacteriological methods although VBNC state cells of this organism were detected inside coral tissues (Tomer et al., 2001).

Various plant pathogenic bacteria are also known to enter a VBNC state (Del Campo et al., 2009; Grey & Steck, 2001; Ordax et al., 2009). For example, Grey et al. (2001) demonstrated that *Ralstonia solanacearum* entered into a VBNC state in response to cupric sulfate, suspension in a saline solution, or when placed in autoclaved soil. The resuscitated bacterial cells were able to infect plants. Interestingly, this was the first report of *R. solanacearum* entering the VBNC state and of resuscitation of any VBNC plant-pathogenic bacteria and provided evidence that the VBNC state may explain the persistent nature of some plant infections (Grey & Steck, 2001).

The presence of the VBNC state has been debated for several years (Barcina & Arana, 2009; Bogosian & Bourneuf, 2001; Nyström, 2001). Some of the disagreement centers on the phrase "viable but non-culturable", that is most commonly used to define this phenomenon (Barer, 1997; Colwell, 2000; Kell et al., 1998). However, the debate over whether the VBNC state truly exists has largely been put to rest, primarily as a result of numerous molecular studies reported in recent years (discussed below). A numbers of reviews presented in recent years have supported the concept of the VBNC state (Barcina & Arana, 2009; Colwell & Grimes, 2000; Edwards, 2000; McDougald et al., 1998; Oliver, 2005b; Rowan, 2004; Sardessai, 2005; Yamamoto, 2000), although several have argued against the concept (Nyström, 2005; Sinton, 2006). Other reviews have specifically examined the potential public health hazards associated with VBNC state food-borne pathogens (Oliver, 2005).

However, the VBNC state in *V. vulnificus* has been used as a model system to study this phenomenon. Indeed the VBNC state is now generally regarded as the G-ve equivalent of the dormancy achieved by sporulating, Gram positive (G+ve) bacteria cells. VBNC cells are now defined as those that maintain metabolic activity while being incapable of supporting cellar division on media that normally encourage the growth of the bacterium. Exposure to low temperature, low nutrient availability, high pressure and salinity are examples of environmental stresses which are consistently associated with induction of the VBNC state (Colwell et al., 1985).

1.4.1 Induction of the VBNC State

Various extrinsic factors known to induce the VBNC state include: nutrient starvation (Cook & Bolster, 2007), incubation outside the normal temperature range of growth (Maalej et al.,

2004; Valérie et al., 2002; Wong & Wang, 2004), increased or lower osmotic concentrations (Asakura et al., 2008; Wong & Liu, 2008), oxygen concentrations (Kana et al., 2008), commonly used food preservatives (Cunningham et al., 2009), heavy metals (Ghezzi & Steck, 1999) and exposure to white light (Gourmelon et al., 1994). The common response, is the ultimate inability to develop into colonies on routine culture media, even though the cells may remain viable for long periods of time.

1.4.1.1 Impact of Starvation and Temperature on Induction of the VBNC State

Mårdén et al. (1985) were the first to report cellular physiological and morphological changes of marine bacteria following starvation. Their results were discussed in terms of defining the mechanisms of initial cellular responses to nutrient deprivation (Mårdén et al., 1985). Furthermore, they showed that starvation combined with cold stress was particularly effective in induction of the VBNC state (Linder & Oliver, 1989). The VBNC state bacteria cells prepared in this way however, do not form colonies on high nutrient solid media even though cell suspensions still display detectable metabolic activity (Gauthier, 2000; Oliver, 2000).

Although VBNC cells cannot be directly cultured, these cells apparently maintain virulence for susceptible hosts. Oliver et al. (1995) reported that cells of *V. vulnificus* remain virulent, at least for some time, when present in the VBNC state and are capable of causing fatal infections following *in vivo* resuscitation. Nevertheless, virulence decreases dramatically as cells enter the VBNC state. This may explain the observed decrease in incidence of infections caused by this bacterium during winter months (Oliver & Bockian, 1995). Interestingly, there is some evidence to suggest that stress conditioning impacts the rate at which cells enter the VBNC state. For example, Bryan et al. (1999) reported that *V. vulnificus* initially entered the VBNC state when incubated at 6°C. However, when the culture was incubated at 15°C before a further temperature downshift, the cells remained culturable (Bryan et al., 1999). Oliver et al. (1991) also observed that if *V. vulnificus* cells were starved of nutrients for 24 h at room temperature and subsequently exposed to 5°C, they failed to enter a VBNC state. Conversely cells starved for the same period at 5°C were able to enter the VBNC state. Furthermore, cells starved for 1, 2, and 4 h prior to incubation at 5°C, also entered the VBNC state, but at a slower rate. These observations have been taken to

indicate that temperature and nutrient starvation are the key factors involved in induction of the VBNC state (Oliver et al., 1991).

1.4.1.2 Stress Responses as Inducers of the VBNC State

In addition to temperature and nutrient stress, there are other stressors known to induce the VBNC state. For example, Wong and Liu (2008) characterized the low salinity stress in *V. vulnificus.* The study was designed to investigate the response of *V. vulnificus* to lethal low salinity (0.04% NaCl) and its adaption to the sub-lethal salinity (0.12% NaCl with amino acids added). After 30 min of exposure to lethal low salinity, cells entered the VBNC state for a short period of time, followed by cell death. Food preservatives may also act as an inducer in the VBNC state induction. For example, Cunningham et al. (2009) showed that *Listeria monocytogenes* grown in the presence of potassium sorbate at pH 4.0 entered a VBNC state, but these cells became nonviable after 24 h contact with sorbate. By contrast, cells incubated under these conditions in the absence of potassium sorbate entered the VBNC state and maintained viability throughout the 24 h study period (Cunningham et al., 2009).

Heavy metals are also thought to act as a kind of VBNC state inducer. For example, addition of cupric sulfate assisted entry of *Xanthomonas campestris* cells into the VBNC state (Ghezzi & Steck, 1999).

1.4.2 Characterization of VBNC State Cells

Phenotypic characteristics used to determine whether a bacterial cell has entered the VBNC state or not include: reduction in cell size, macromolecular synthesis, nutrient transportation and respiration rate. Viable cell counts are typically determined using the substrate responsive assay of Kogure et al. (1979) in which intracellular hydrolysis of 5-cyano-2,3-ditolyl tetrazolium chloride (CTC) occurs in intact viable cells (Coallier et al., 1994). Alternatively, the presence of an intact cytoplasmic membrane can be determined using fluorescent dyes (Wong & Wang, 2004). Moreover, Porter et al. (1995) showed that VBNC state cells can be monitored using multi-parameter flow cytometry. Oliver (2005b) used a combination of phenotypic tests to show changes in viability and culturability as bacterial cells entered into the VBNC state at low temperature (Figure 1.5).

All studies of induction of the VBNC state however, are characterized by use of high density (usually $>10^6 - 10^{10}$ cells mL^{-1}) suspensions of bacteria (Abe et al., 2007; Du et al., 2007; Gonzalez-Escalona et al., 2006). There is limited information about the response of low density suspensions incubated under identical conditions. This issue is significant and of practical importance. Firstly, it is conceivable that VBNC cells present in high density suspensions are simply survivors that derive maintenance energy requirements from nutrients released from dead and lysed cells. If this scenario is correct, under resuscitation conditions, "VBNC cells" may derive sufficient maintenance energy from the remnants of dead cells to support viability in a manner similar to the reported kinetics of resuscitation. Secondly, the cell densities used to demonstrate the VBNC state rarely occur in nature. For example, it is unusual for *Vibrio parahaemolyticus* and *V. vulnificus* at levels $>10^6$ cells mL^{-1} to be present in seafood such as oysters. However it is not yet clear whether these bacteria enter a VBNC state when contaminated harvested oysters are stored at refrigeration temperatures, even though it is known that counts of these bacteria decrease rapidly in refrigerated, stored oysters (Cook & Ruple, 1989, 1992; Gooch et al., 2002). Nevertheless, this important oversight of the impact of cell density on ability to induce the VBNC state and recovery from that state requires further study.

The morphology of VBNC cells changes from rod to coccoid shapes and the cell size of VBNC state cells is smaller than that of actively growing cells (Du et al., 2007) (Figure 1.6). These morphological changes are similar to those observed when cells enter stationary phase in response to some nutritional stress (Hood et al., 1986). As might be expected, new cold shock and starvation proteins are expressed during the establishment of VBNC state. Johnson et al. (2002) found that VBNC state cells tend to clump together and suggested that exopolysaccharides from the outer-membrane are blebbed (Johnston & Brown, 2002). Blebbing is a kind of modification to the outer-membrane and involved in bacterial resistance mechanisms (Jones et al., 1989). However, biosynthesis apparently does not cease entirely in VBNC state cells (McGovern & Oliver., 1995; Morton & Oliver., 1994). Although rates of biosynthesis are low compared to actively metabolizing cells, levels of cellular ATP remain high compared to dead and moribund cells (Beumer et al., 1992; Federighi et al., 1998).

Changes in cell physiology and morphology also include alterations in membrane fatty acid composition responsible for membrane fluidity and these changes may lead to altered cell

viability. For example, Oliver et al. (1973) showed that incubation at low temperatures caused an increase in the amount of unsaturated fatty acids in the cell membrane of *V. vulnificus* (Oliver & Colwell, 1973). Indeed, Linder et al. (1989) reported that fatty acid content was decreased by 57%, but short-chain fatty acid content increased from 5.4% to 29.0% as cells were entering the VBNC state (Linder & Oliver, 1989). Wong et al. (2004) found changes in the activities of two enzymes and in the fatty acid profiles of *V. parahaemolyticus* by comparing the VBNC state and culturable state cells. During the induction of starvation conditions, an increase in saturated fatty acid and a decrease in mono-unsaturated fatty acid were observed. The enzyme superoxide dismutase became undetectable in VBNC state cells, while the cellular concentration of glucose-6-phosphate dehydrogenase did not change upon entry into the VBNC state. Therefore, the morphology changes seem to be regulated through fluctuation of chain length and saturated/unsaturated ratio of fatty acid (Wong et al., 2004).

Clearly analysis of the VBNC response has traditionally focused on physiological changes. However, the genetic and cellular mechanisms underpinning establishment and maintenance of the VBNC state are still unclear. A genetic approach is required to determine whether there are specific genes or regulatory pathways responsible for the development of the VBNC response. Figure 1.7 shows a possible model for the interaction of regulatory factors involved in the VBNC state (Rice et al., 2000).

1.4.3 Virulence of Cells in the VBNC State

The relationship between VBNC state and virulence is an important issue with significant implications for public health. Colwell et al. (1996) studied human volunteers given an inoculum of VBNC state cells of the attenuated vaccine strain (CVD 101) *V. cholera* O1 and showed that viable CVD 101 colonized the intestine of these volunteers. This suggested that the VBNC state Vibrios were able to colonise and subsequently multiply within the intestine. Baffone et al. (2003) revealed that the VBNC forms of *V. alginolyticus* and *V. parahaemolyticus* retain virulence characteristics (hemolysin production, adhesive and cytotoxic ability, *in vivo* enteropathogenicity) when isolated by culturing these bacteria from a microcosm consisting of artificial seawater incubated at 5ºC. In this study, hemolytic activity was assayed by plating cells on Wagatsuma agar, adhesiveness was assayed using Hep-2

cells, cytotoxicity was determined using CHO cells and virulence was determined using rat ileal loop assay (Baffone et al., 2003).

In fact, it seems unlikely that pathogens are able to cause disease when present in the VBNC state, although it is conceivable that expressed virulence factors are preserved. Consequently, infection could be triggered following resuscitation to the actively metabolizing state. For instance, VBNC cells of *Vibrio harveyi* ceased to express the hemolysin gene and did not cause death when inoculated into zebra fish, whereas resuscitated cells were lethal. This study demonstrated that VBNC *V. harveyi* cells preserved pathogenic potential (Sun et al., 2008). A similar response has been reported for a range of other pathogenic bacteria including: *V. cholerae*, *Escherichia coli* and *Edwardsiella tarda* (Nair et al., 2007; Pommepuy et al., 1996). Whether these observations reflect maintenance of structures associated with virulence (e.g. fimbriae, adhesins, toxins etc.) by cells in the VBNC state, or *de novo* expression of these virulence factors following resuscitation, remains to be established. However, these observations support the proposition that VBNC state bacterial entero-pathogenic bacteria may pose a potential threat to health.

1.4.4 Gene Expression in the VBNC State

Monitoring changes in gene expression during establishment and maintenance of the VBNC state will be necessary in order to understand the mechanisms responsible for induction, maintenance and escape from the VBNC state. That approach will allow identification of specific genes or regulatory pathways responsible for the development of the VBNC response. For example, Narjol et al. (2006) employed quantitative reverse transcription PCR (qRT-PCR) to analyse and compare levels of expression of specific genes in *V. parahaemolyticus* subjected to starvation conditions and cells in the VBNC state. They selected 16S rRNA and mRNA of the *tuf*A/B, *rpoS* and *relA* genes as molecular targets to explore the utility of the total RNA fraction for culture-independent detection of active *V. parahaemolyticus*. The *tuf*A/B, *rpoS* and *relA* genes are involved in key metabolic processes, such as *tuf*, *relA* presenting protein synthesis and *rpoS* gene products play a role in stress responses. Bacterial cells entering the VBNC state showed a 154, 5100, 24 and 23-fold reduction in the number of copies of 16S rRNA and mRNA for *tuf*, *rpoS* and *relA* in comparison to exponentially growing cells. The differences observed for cells in either a VBNC or a starvation state were

less striking. This result indicated that metabolic processes are likely to decrease in during starvation and the VBNC state. The authors suggested that qRT-PCR methodology, based on selected RNA targets, could be successfully exploited for the identification of bacteria in the VBNC state. Asakura et al. (2008) used qRT-PCR to monitor expression of *ompW* from *Escherichia coli* O157:H7, a gene encoding an outer membrane protein; the work showed that *ompW* mRNA levels markedly increased in cells in the oxidation-induced VBNC state. The authors assumed that *ompW* over-expression was implicated induction of the VBNC state as induction of *ompW* correlated with loss of culturability under oxidative conditions. However, the evidence insufficient to show that *ompW* gene played an important role in regulation of the VBNC state. Nevertheless, this example of application of qRT-PCR methodology supports the view that the approach is a powerful experimental tool in studies designed to understand the mechanism responsible for the VBNC state (Asakura, 2007).

1.4.5 Antibiotic Resistance of VBNC Cells

One of the important consequences of entry into the VBNC state, is the effect on antibiotic resistance. A study by Del Mar Lleò et al. (2007), evaluated the effects of antibiotics that acted on peptidiglycan or protein synthesis of *Enterococcus faecalis* in the VBNC state. They showed that VBNC cells demonstrated such low metabolic activity that the cells became effectively resistant to antibiotics. These antibiotic treated cells were subsequently able to resuscitate and restart infection (Del Mar Lleò et al., 2007). Ehrlich et al. (2002) also demonstrated that antibiotic resistant VBNC cells of *Haemophilus influenzae* present in biofilms were able to initiate chronic infections. In some cases, antibiotic resistance is extraordinary. Vancomycin was reported to be effective against VBNC cells of *Enterococcus faecalis* at doses 500 times higher than the MIC (minimal inhibitory concentration) (Del Mar Lleò et al., 2007) and Anuchin et al. (2009) observed extreme increases in resistance to hydromycin and doxycyclin by VBNC cells of *Mycobacterium smegmatis* (Anuchin et al., 2009). A similar study by River and Steck (2001), provided evidence that indicated uropathogenic *E. coli* cells in the VBNC state were not eliminated by antibiotic therapy. Thus recurrent urinary tract infections are likely a result of cells temporarily in the VBNC state that are able to resist antibiotic therapy and subsequently resuscitate to the active state (Domingue et al., 1995; Mulvey et al., 2001; Rivers & Steck, 2001). A later study suggested that VBNC

cells were present not only in mouse, but also in human urine specimens (Anderson et al., 2004).

Another possible strategy for antibiotic resistance involves the so-called "quinolone-induced VBNC state". Mason et al. (1995) reported that over 90% of culturable *E. coli* cells exposed to various concentrations of quinolone antibiotics such as ciprofloxacin, maintained membrane potential and protein synthesis. Ciprofloxacin apparently promoted the dissociation of metabolic and physical survival from the ability to form colonies on solid media. Thus quinolone-induced VBNC state cells might be capable of continued production of factors relevant for pathogenesis of the host (Mason et al., 1995).

1.5 Resuscitation from the VBNC State

1.5.1 Resuscitation following a Temperature Upshift

The VBNC state can only be important for survival if VBNC cells are able to re-initiate metabolic activity and become culturable. Indeed, an important characteristic of the VBNC state cells that distinguishes them from dead cells, is the ability to be resuscitated in natural and *in vitro* marine environments as a consequence of environmental changes such as an increase in temperature and the presence of nutrients (Nilsson et al., 1991; Weichart et al., 1992; Whitesides & Oliver, 1997). Numerous studies have documented resuscitation from the VBNC state, particularly for *V. vulinificus*. For *Vibrio* species the VBNC state is most commonly induced by a temperature down-shift and the cells resuscitated by a temperature up-shift. For instance, *V. vulinificus* exits the VBNC state by a simple temperature up-shift to 22ºC (Figure 1.8) (Du et al., 2007; Gupte et al., 2003; Wong & Wang, 2004). The molecular mechanism that underpins the change of state is not currently known.

1.5.2 Resuscitation Promoting Factors

Resuscitation of VBNC cells is one of the key issues in the study of non-culturability because it is experimentally difficult to demonstrate major differences between dead cells and potentially viable cells, by other methods. However, there is evidence to suggest that VBNC cells may contain, or express, factors that assist survival and resuscitation of VBNC cells. Several studies have shown that the secreted resuscitation promoter factor (Rpf or YeaZ)

expressed by *Micrococcus luteus* cells assists recovery from a VBNC state. For example, Mukamolova et al. (1998) showed that purified Rpf protein added to suspensions of VBNC cells of *M. luteus*, resulted in a significantly improved recovery compared to untreated cells (Figure 1.9). *M. smegmatis* and *M. tuberculosis* also express similar factors that are implicated in stimulating resuscitation of VBNC state cells (Shleeva et al., 2002; Shleeva et al., 2004). The Rpf protein therefore, may therefore be one mediator of bacterial communication in *M. luteus* involved in resuscitation of VBNC state cells.

Panutdaporn et al. (2006) has shown similar responses can occur in *Salmonella* Typhimurium LT2 and *Salmonella* Oranienburg. The protein encoded by the *yeaZ* gene of *Salmonella* Typhimurium LT2 shares 24.2% homology with *Micrococcus luteus* Rpf (Figure 1.10). YeaZ protein influenced rescuscitation of *Salmonella* Oranienburg cells from a VBNC state in a dose dependent manner (Figure 1.11), when added to 1 mL of suspensions of VBNC state cells containing 10^7-10^8 cells. However, doses of 1 ng mL^{-1} of YeaZ did not affect resuscitation.

YeaZ homologs are ubiquitous among G-ve bacteria. A search of publicly available nucleotide databases has identified homologous *yeaZ* sequences encoded by *V. parahaemolyticus* (Makino et al., 2003) (GenBank accession number: NC_004603). BLAST analysis (Altschul et al., 1990) indicated that the *V. parahaemolyticus* sequence shares 56% amino acid sequence similarity to the YeaZ of *Salmonella* Typhimurium LT2 (Figure 1.12). Surprisingly, a potential linkage between the putative YeaZ protein and the VBNC state in *V. parahaemolyticus* has not been identified, nor is there any experimental evidence to show that the gene is expressed. Given the previous work on YeaZ homologs and their role in recovery from a VBNC or dormant state, future work that aims to understand the function of *yeaZ* gene in *V. parahaemolyticus* would be justifiable and worthwhile.

1.5.3 Biological Mediators of the VBNC State

A number of bacterial pathogens are able to maintain an intracellular lifestyle within host cells. It is possible therefore, that host organisms may play a biological mediator role in the resuscitation of pathogen cells present in the VBNC state. For example, amoebae such as *Acanthamoeba polyphaga* are a natural host for *Legionella pneumophila* and play important roles in bacterial ecology and infectivity to humans. *L. pneumophila* has been shown to enter

the VBNC state following both starvation and exposure to hypochlorite. Interestingly, VBNC cells of *L. pneumophila* are able to resuscitate within the protozoan hosts *A. polyphaga* (García et al., 2007) and *A. castellanii* (Steinert et al., 1997). In other host systems, Sussman et al. (2003) indicated that the marine fireworm *Hermodice caranculata* is a winter reservoir and summer vector for *Vibrio shiloi* (Sussman et al., 2003). These studies lend credence to the idea that the host cell(s) may contain mediators necessary for resuscitation of VBNC cells.

Similar work with mice, chickens and human volunteers lend support to this idea (Colwell et al., 1996). For example, Cappelier et al. (1999) showed that VBNC state cells of *Campylobacter jejuni* could be resuscitated in chicken and mouse animal model systems, although the mouse model permitted better recovery than the chick model. Therefore, it is possible that a wide variety of bacteria-host relationships may play an important role in the survival of bacteria and resuscitation of these bacteria from the VBNC state.

1.5.4 Autoinducers and the VBNC State

Another class of resuscitation factors known as autoinducers has been identified by Reissbrodt et al, (2002). They reported that resuscitation of VBNC state *Salmonella enteric* serovar Typhimurium and enterohemorragic *E. coli* could be effected by a heat-stable Enterobacterial autoinducer. In this study, the three growth factors, trihydroxamate E, the antioxidant Oxyrase and the heat-stable autoinducer, were examined for potential as mediators of resuscitation. The results showed the autoinducer was effective in promoting resuscitation VBNC state cells, whereas trihydroxamate E and Oxyrase had no effect. Furthermore, exposure to the same heat-stable autoinducer also lead to resuscitation of stressed populations of *Citrobacter freundii* and *Enterobacter agglomerans* (Reissbrodt et al., 2002). Freestone et al. (1999) demonstrated a heat-stable autoinducer in a study of seventeen G+ve and six G-ve bacterial species incubated in media including the human norepinephrine. Those strains responded to norepinephrine and synthesised autoinducer. The majority of G-ve strains produced and responded to heat-stable autoinducers of growth. Norepinephrine is a stress-related hormone and produced in large amounts in humans following tissue injury. Bacterial growth occurred in the presence of norepinephrine. These autoinducers indicated a high degree of cross-species activity, suggesting the existence of a novel family of G-ve bacterial signaling molecules, although a number of G+ve bacteria also respond to

norepinephrine (Freestone et al., 1999). Subsequently, Sperandio et al. (2003) identified the factors associated with a novel quorum-sensing system, which they termed Autoinducer (AI-3). Quorum-sensing, known as the interbacterial communication system, utilises hormone-like compounds as autoinducers to regulate bacterial gene expression. Both epinephrine and norepinephrine are able to substitute for AI-3 in regulating entrohemorrhagic *E. coli* virulence gene expression. As epinephrine/norepinephrine or AI-3 were able to block the signaling system, these results suggested that a quorum sensing like mechanism may be involved in bacterium-host communication (Sperandio et al., 2003). Reissbrodt et al. (2002) showed that preparations of VBNC state *Salmonella enterica serovar* Typhimurium and two *E. coli* O157:H7 strains underwent resuscitation to form observable colonies when exposed to autoinducer. The discoveries reported by Reissbrodt et al. (2002) and Sperandio et al. (2003) have major implications for the resuscitation of enteropathogens from the VBNC state, particularly when these are present in the intestinal tract of humans under physiological stress (Sperandio et al., 2003).

1.6 The YjeE/YeaZ/YgjD Signal Transduction Network

Recently, Handford et al. (2009) has reported that the *yjeE*, *yeaZ* and *ygjD* genes from *E. coli* are highly conserved in eubacteria and the *ygjD* gene is also found in *Archea* and *Eukaryotes*. These three genes are essential for the viability of *E. coli* (Handford et al., 2009). To study the role of these proteins in viability, Handford et al. (2009) constructed conditional expression strains for these three genes in *E. coli*. K12 and demonstrated these three genes are necessary for viability. Based on their work, they suggested a model that linked these three genes and their products together in same cellular pathway (Figure 1.13). This complex, essential network involves the regulation of YgjD activity by interaction of YjeE and YeaZ, possibly via proteolysis. Thus, this model creates an important supporting structure for studying the function of these genes in other bacteria to understand their role. YeaZ can interact with YgjD in response to an as yet unidentified signal, and then bind with YjeE. The latter interaction allows free YgjD to accumulate in the cell (Figure 1.13). The reverse partner switch reaction can apparently occur when YjeE binds and hydrolyses ATP. This allows YeaZ to form a partner with YgjD which in turn triggers proteolysis of YgjD (Figure 1.13). But whether YgjD is activated or inactivated through YeaZ-dependent proteolysis still needs

to be investigated; both possibilities are showed in Figure 1.13. YgjD may also be involved in a signaling pathway which results in accumulation of the active, phosphorylated form of RstA or by controlling some specific cellular response (Msadek, 2009). Interestingly, Minagawa et al. (2003) indicated that expression of the *rstAB* operon is controlled by another two component system, PhoP/PhoQ, known to react to magnesium ion concentrations (Minagawa et al., 2003) and it will be important to investigate the relationships of these two signal transduction pathways with the essential YjeE/YeaZ/YgjD protein network.

1.7 YeaZ Protein-Protein Interactions

1.7.1 YeaZ

The *yeaZ* gene product has been inferred, or shown experimentally, to be important for the viability of *E. coli* (Tomoya *et al.*, 2006), *Bacillus subtillis* (Kobayashi et al., 2003), *S. pneumonia* (Zalacain et al., 2003), *Franciscella novicida* (Gallagher *et al.*, 2007), *Pseudomonas aeruginosa* (Liberati et al., 2006), and *Mycoplasma genitalium* (Glass et al., 2006). In *E. coli,* YeaZ forms a complex with YgjD (Butland et al., 2005). A more recent study has showed that the *E. coli* YeaZ associated with either YgjD or YjeE, with YgjD as the preferred partner, suggesting that YeaZ is an important factor in the protein interaction network. This protein interaction network may be associated with the cell division and DNA metabolism (Handford et al., 2009). In fact, YeaZ and YgjD are sequence associated proteins in *E. coli* and interestingly the first 100 amino acids of these proteins share 29% identity.

1.7.2 Structure of YeaZ

Recently, the crystal structure of YeaZ has been solved for a number of bacteria including *S. enteric serovar* Typhimurium ($YeaZ_{ST}$) (Jeudy et al., 2005; Nichols et al., 2006), *Thermotoga maritime* ($YeaZ_{Tm}$) (Xu et al., 2010) and *E. coli* ($YeaZ_{Ec}$) (Jeudy et al., 2005). The structures show that the protein is part of the HSP70 actin-like-fold (HALF) protein family. The HALF protein is one of the largest protein families with functionally difference members such as prokaryotic cell cycle proteins, chaperones, phosphatases and sugar kinases (Kabsch & Sander, 1983).

Nichols et al. (2006) reported the protein structure of YeaZ *of S.* Typhimurium (ST). The conserved HALF structure, $YeaZ_{ST}$ is a two lobed structure with each lobe including one long helix, a β-sheet, and a largely helical subdomain (Figure 1.14). Starting at the N-terminus, the protein chain traces the majority of lobe-A, then crosses into lobe-B before returning to the first lobe once more, such that both the N and C termini reside in lobe-A (Nichols et al., 2006). As demonstrated by actin, Hsc70 and glycerol kinase, the diversity of biological function is provided by the polymorphism of the loops joining the β-strands and helices in the core region and by inserted domains that show high variability (Kabsch & Sander, 1983). Lobe-A has a more conserved structure than lobe-B. These two lobes have unique "glycine-rich regions" suggesting the presence of one or more glycine-rich loops involved in the nucleotide/polyphosphate binding (Nichols et al., 2006). Base on the geometry of such structures, the complete binding site involves one or more residues from another polypeptide chain. Some HALF proteins have been confirmed where the nucleotide binding sites and metal ion are only partly formed by the HALF partner. Therefore, the formation of the complete binding site needs additional residues provided on the surface of a different partner protein. These examples include glycerol kinase and the actin-gelsolin complex (Holtman et al., 2001; Lagarrigue et al., 2003).

Generally, most HALF proteins function as higher-order assemblies, with dimers and tetramers being the most common oligomeric states. YeaZ has been shown that forms dimer and tetramer in *E. coli*, *V. parahaemolyticus*, *S.* Typhimurium LT2 and *Thermotoga maritime* (Aydin et al., 2011; Handford et al., 2009; Jeudy et al., 2005; Nichols et al., 2006; Xu et al., 2010). For example, Nichols et al. (2006) reported that the YeaZ crystal structure suggests a potential "crescent"-shaped dimer, an uncommon arrangement for a HALF protein (Figure 1.15). However, the buried surface area is relatively low and the biologically relevant interaction function is not clear (Nichols et al., 2006).

1.7.3 YgjD

The *ygjD* gene (also called *gcp*) is found in various eubacterial species and eukaryotes. YgjD, like the YeaZ protein, has been inferred to be essential for the viability of many eubacterial species, including: *E. coli* (Arigoni et al., 1998), *S. pneumoniae*, *S. aureus* (Thanassi et al., 2002; Zalacain et al., 2003), *B. subtilis* (Hunt et al., 2006; Kobayashi et al., 2003), *F. novicida*

(Gallagher et al., 2007), *P. aeruginosa* (Liberati et al., 2006), and *M. genitalium* (Glass et al., 2006) and the eukaryote *Saccharomyces cerevisiae* (Giaever et al., 2002). Interestingly, and in contrast to its inferred role in viability, non-lethal *ygjD* mutants of the cyanobacterium *Synechocystis* sp. strain PCC6803 have been shown to be salt-sensitive (Karandashova et al., 2002). Similarly, Zuther et al. (1998) showed *ygjD* (*gcp*) of *Synechocystis* sp. strain PCC 6803 was also associated with salt sensitivity. In this study, a *ygjD* mutant not only displayed reduced salt tolerance, but also lead to nitrogen starvation of the cells accompanied by remarkable changes in pigmentation, ultrastructure, and an increase in the amount of inclusion bodies containing the polymer cyanophycin. The authors suggested glycoprotease activity associated with YgjD (Gcp) might be responsible for degradation of cyanophycin (Zuther et al., 1998).

Based on sequence similarity, YgjD is regarded as a putative glycoprotease (GCP) and at least in *E. coli*, is essential for bacterial survival (Handford et al., 2009). The first identified glycoprotease was shown to be specific for O-glycosylated glycoprotein in *Pasteurella haemolytica* A1 (Abdullah et al., 1991). Recently, many glycoprotease homologues have been identified in G+ve and G-ve bacteria, including *E. coli* (Nesin et al., 1987), *Bacillus anthracis*, and *Streptococus pyogenes* (Zheng et al., 2005), which have 42% amino acid identity. Typically, *yjgD* genes encode proteins of 35 kDa. The glycoprotease is a neutral metalloprotease, and the predicted amino acid sequence contains a putative zinc-binding site (Abdullah et al., 1991). The human ortholog of GCP called OSGEP (O-sialoglycoprotein endopeptidase) has been implicated in proteolysis. OSGEP cleaves misfolded nuclear receptor co-repressor protein (Ng et al., 2006).

In the yeast *S. cerevisiae*, the ortholog of YgjD, called Kae1 (kinase-associated endopeptidase 1), forms a protein complex with a Polarized growth Chromatin-associated Controller 1 (PCC1), a kinase (Bud32p) and two additional proteins encoded by ORFs YJL184w and YMLO36w. Genetic and physical interaction data strongly suggest that this complex forms a functional unit. The Kae1 complex is involved in transcription (Kisseleva-Romanova et al., 2006). Another study indicated that Kae1 formed a complex with Bud32, and uncharacterized proteins (Cgi121 and Gon7). This Kae1complex, named the KEOPS complex, is associated with regulation of the length of telomeres (Downey et al., 2006).

1.7.4 YjeE

Like YeaZ and YgjD, YjeE has been shown to be essential for bacterial viability in a number of bacteria including: *E. coli* (Allali-Hassani et al., 2004; Arigoni et al., 1998) and probably also for *S. enterica* (Knuth et al., 2004), *Streptococcus pneumoniae* (Zalacain et al., 2003) and *Fransicella novicida* (Gallagher et al., 2007). The function of YjeE is not clear. However, *yjeE* genes are absent from the genomes of some *Mycoplasma* species that characteristically lack cell walls. Furthermore, in G-ve bacteria, *yjeE* is located within an operon with a gene that encodes a cell wall amidase. These observations have lead to the prediction that the YjeE protein may be involved in controlling peptidoglycan biosynthesis (Teplyakov et al., 2002). More recently, the *rstA* gene (encoding the response regulator of the RstAB two component signal transduction system) has been shown by Campbell et al. (2007) to act as a multicopy suppressor of a conditional *yjeE* depletion strain in *E. coli*. However, depletion of *yjeE* cannot be complemented by overexpression of RstA. This suggested that the ability of RstA over-expression to suppress the lethal phenotype of YjeE depletion is not the result of turning on YjeE expression. Whether over-expression of RstA results in a very specific set of genes being activated that are related to YjeE function is not clear. It may simply be that over-expression results in a general cellular response that allows cells to better survive under conditions of YjeE depletion, or that depletion of YjeE results in activation of RstAB. Further studies of the RstAB system may help to identify the mechanism of *yjeE* suppression and information on YjeE functions (Campbell et al., 2007).

YjeE is a highly conserved protein in many bacteria, but absent in eukaryotes. The YjeE of *Haemophilus influenzae* has been shown to comprise a typical P-loop ATPase with a molecular weight of 17 kDa. Allali-Hassani et al. (2004) showed that YjeE protein has an ability to bind and hydrolyze ATP. Indeed, structure analysis indicated that YjeE has a nucletoide-binding fold with a four-stranded parallel β-sheet flanked by antiparallel β-sheet on each side. The ATPase activity of YjeE was confirmed in this study by kinetic enzyme assay. YjeE was been suggested as a "molecular switch" initiated by ATP hydrolysis (Allali-Hassani et al., 2004). Furthermore, the phylogenetic pattern of YjeE also suggests involvement in cell wall biosynthesis (Teplyakov et al., 2002).

1.8 Summary

Although the VBNC state of Vibrios has been subject to considerable scrutiny, the study of how these bacteria enter into and exit from the VBNC state is not well understood. While genetic approaches have been utilized as a quick and efficient method to analyse expression of target genes in VBNC state cells proteomic approaches have identified differences in the proteome of normal, dormant and cells. Whether the latter approach will lead to identification of resuscitation factors responsible for recovery from the VBNC state is unknown. Nevertheless, the potential of resuscitation factors for improving recovery from the VBNC state cannot be ignored. Understanding the mechanism of induction of the VBNC state and recovery of these non-culturable cells has potential implications for improved detection of *V. parahaemolyticus* and indeed other pathogenic bacteria. Furthermore, an understanding of key factors involved in recovery from the VBNC state, may lead to identification of specific resuscitation inhibitors. The benefits are an improvement in the assessment of seafood quality and minimization of risk of illness through consumption of contaminated seafoods.

1.9 Hypothesis and Aims

1.9.1 Overall Aims and Hypothesis

Attempts to understand the mechanism for initiation and maintenance of the VBNC state in *V. parahaemolyticus* have to date involved investigation of the environmental conditions required for *V. parahaemolyticus* cells to enter, maintain and resuscitate from the VBNC state. The different factors affecting this process include temperature, salinity, pH and nutrients that influence induction of the VBNC state in *V. parahaemolyticus*. However, most studies have used highly concentrated suspensions of bacteria ($>10^9$ cells mL^{-1}) to demonstrate this effect. This study will use molecular methods to assess the role of rpf homologs in maintenance and escape from the VBNC state as well as use proteomic approaches to identify other proteins that may be required to maintain this physiological state. It is hoped that the results of this study will provide a strong background for development of bacteriological methods that allow future risk assessment of VBNC state *V. parahaemolyticus* in seafood.

1.9.2 Specific Hypothesis

1. The ability of *V. parahaemolyticus* to enter the VBNC state is dependent on cell suspension concentration.
2. Maintenance and resuscitation of *V. parahaemolyticus* VBNC (or dormant) cells is enhanced by resuscitation promoting factor expressed during exposure to nutritional and temperature stresses thought responsible for establishment of the VBNC state.
3. *V. parahaemolyticus* resuscitation promoting factor, YeaZ, is located on the cell surface.
4. The $YeaZ_{Vp}$ protein complex is associated with $YgjD_{Vp}$ and $YjeE_{Vp}$ proteins.

1.9.3 Specific Aims

The specific aims of this study are:

1. Analyse the effect of cell suspension concentrations and different environmental stresses on ability of *V. parahaemolyticus* NCTC 10884 to enter and escape from the VBNC state.
2. Analyse the effect of the resuscitation promoting factor Rpf (YeaZ) in the VBNC state.
3. Use $yeaZ_{Vp}$ mutants to characterise the role of $YeaZ_{Vp}$ in maintenance and escape from the VBNC state.
4. Assess expression of *yeaZ* by *V. parahaemolyticus* NCTC 10884 and identify the location of the protein within the cell.
5. Use a two-hybrid system method to identify $YeaZ_{Vp}$ associated partners in *V. parahaemolyticus* NCTC 10884.

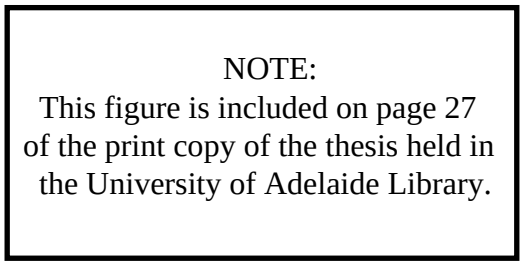

Figure 1.1: Counts of *Vibrio* species from the east coast of North Carolina, USA.
Samples taken from six different sites during July 2000-April 2002.
Figure from Pfeffer et al., (2003).

NOTE:
This figure is included on page 28
of the print copy of the thesis held in
the University of Adelaide Library.

Figure 1.2: Counts of *Vibrio* species(■) and estuarine bacteria (●) in sea sediments.

Counts are expressed as CFU/gram sediment for six sites along the east coast of North Carolina USA. The average water temperatures (○) are shown. Samples were taken during Nov 2001-April 2002.

Figure from Pfeffer et al. (2003).

NOTE:
This figure is included on page 29
of the print copy of the thesis held in
the University of Adelaide Library.

Figure 1.3: Counts of Vibrios and TVC within oysters from South Australia.

Oyster samples from the Eyre Peninsula during the period February, 2005 to March, 2006. Average water temperature is shown. Error bars are standard deviation about the mean, calculated across all sites at a given sampling time.

Figure from Madigan et al. (2007).

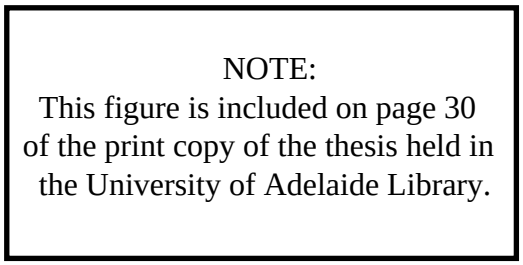

Figure 1.4: Counts of Vibrio and TVC within oyster grow seawater in South Australia.

Water samples taken from five sites along the Eyre Peninsula, South Australia, during the period February, 2005 to March, 2006. Error bars are standard deviation about the mean, calculated across all sites at a given sampling time.

Figure from Madigan et al. (2007).

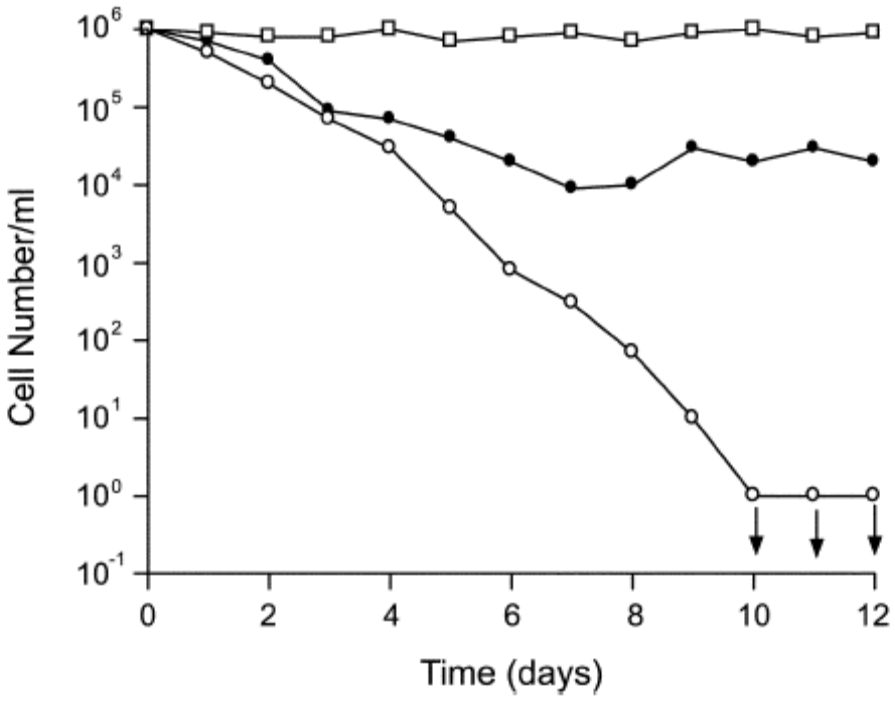

Figure 1.5: Entry of *V. vulnificus* into the VBNC state.

V. vulnificus enter the VBNC state after 10 days incubation at 5°C. Data shown are total cell counts (□), culturable counts (○) and viable counts (●).

Figure from Oliver (2005).

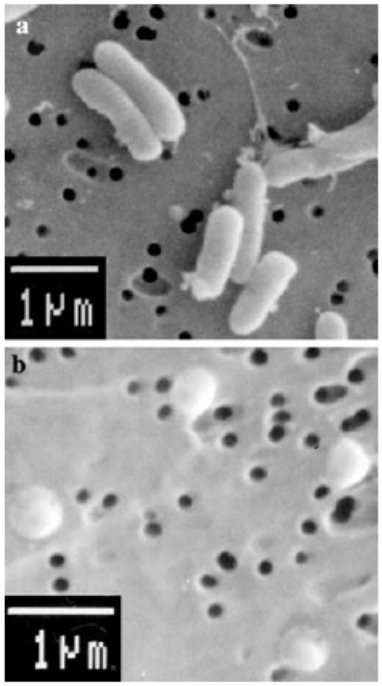

Figure 1.6: Morphological characteristic of *V. alginolyicus* cells analysed by scanning electron microscopy.

Normal cells (a); the VBNC state cells (b).

Figure adapted from Du et al. (2007).

Table 1.1: Bacterial known to enter a VBNC state.

Aeromonas salmonicida	*Lactobacillus plantarum*	*Serratia marcescens*
Agrobacterium tumefaciens	*Lactococcus lactis*	*Shigella dysenteriae*
Alcaligenes eutrophus	*Legionella pneumophila*	*S. flexneri*
Aquaspirillum sp.	*Listeria monocytogenes*	*S. sonnei*
Burkholderia cepacia	*Micrococcus flavus*	*Sinorhizobium meliloti*
B. pseudomallei	*M. luteus*	*Streptococcus faecalis*
Campylobacter coli	*M. varians*	*Tenacibaculum sp.*
C. jejuni	*Mycobacterium tuberculosis*	*Vibrio anguillarum*
C. lari	*M. smegmatis*	*V. campbellii*
Cytophaga allerginae	*Pasteurella piscida*	*V. cholerae*
Enterobacter aerogenes	*Pseudomonas aeruginosa*	*V. fischeri*
E. cloacae	*P. fluorescens*	*V. harveyi*
Enterococcus faecalis	*P. putida*	*V. mimicus*
E. hirae	*P. syringae*	*V. natriegens*
E. faecium	*Ralstonia solanacearum*	*V. parahaemolyticus*
Escherichia coli	*Rhizobium leguminosarum*	*V. proteolytica*
Francisella tularensis	*R. meliloti*	*V. shiloi*
Helicobacter pylori	*Rhodococcus rhodochrous*	*V. vulnificus (types 1&2)*
Klebsiella aerogenes	*Salmonella enteritidis*	*Xanthomonas campestris*
K. pneumoniae	*S. typhi*	
K. planticola	*S. typhimurium*	

Table based on Oliver (2005).

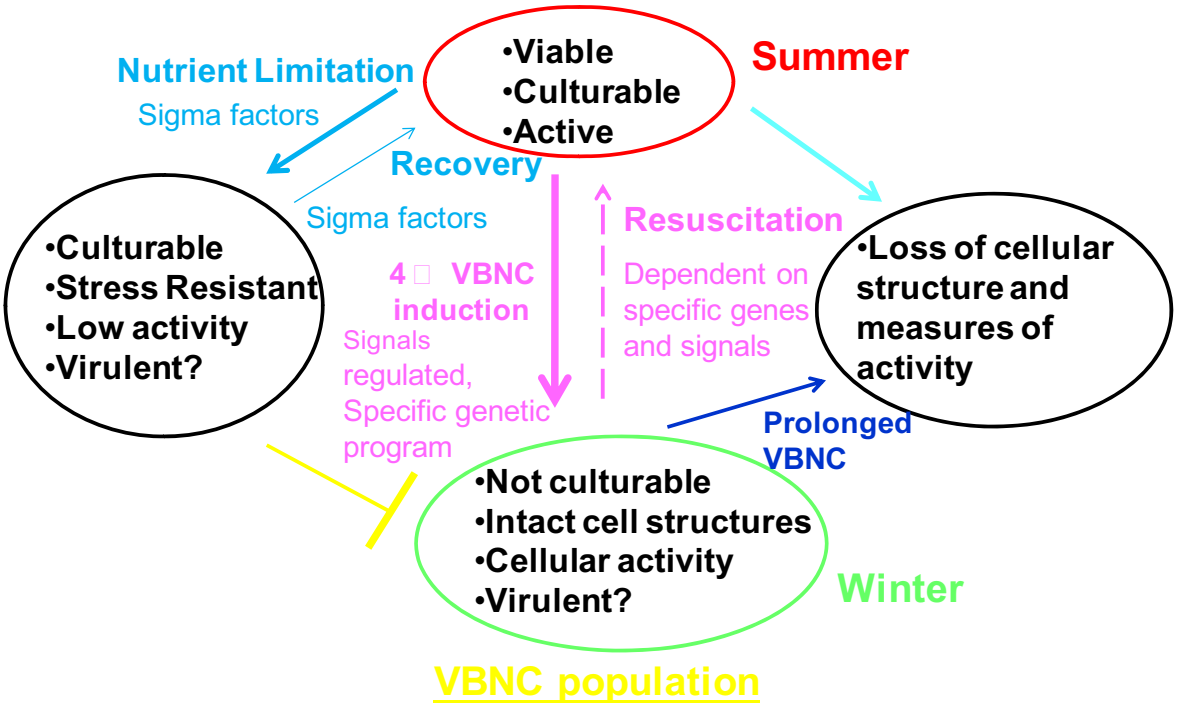

Figure 1.7: Proposed interaction of regulatory factors involved in the VBNC state.

The model depicts the possible physiological states that result from environmental stress or nutrient depletion. Solid arrows depict directions of known response while broken arrows indicate potential lines of induction of physiological states. The sideways "T" indicates the inhibition of blockage of a response. SIMC, Starvation-induced maintenance of culturability.

Adapted from Rice et al. (2000).

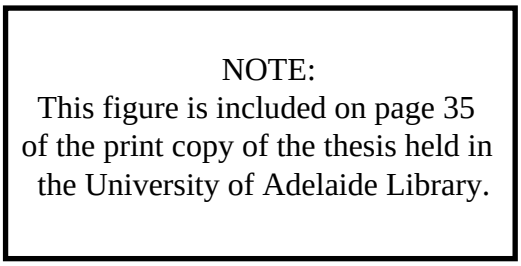

Figure 1.8: Time required for resuscitation of VBNC *V. vulnificus* cells.

Cells from a VBNC microcosm (< 3.3×10^1 CFU/ml) were shifted to 20°C, and aliquots were removed at hourly intervals and plated onto HI agar.

From Whitesides et al. (1997).

NOTE:
This figure is included on page 36
of the print copy of the thesis held in
the University of Adelaide Library.

Figure 1.9: Effect of purified RPF on stimulation of growth of washed *M. luteus* cells.

Washed cells of stationary phase *Micrococcus luteus* were stimulated by addition of resuscitation promoting protein. Stationary phase cells of *M. luteus* grown in lactate minimal medium (LMM) were washed 5 times by suspension and centrifugation in LMM from which lactate had been omitted. Bacteria were finally suspended in the same medium by repeatedly passing them through a syringe, diluted, and inoculated into a 20 mL flask with LMM or LMM in the presence of Rpf (31 pmol/L). The initial cell density was ca. 10^2 viable cells per mL and incubation was at 30°C with intensive shaking. Growth was monitored by plating 0.1 mL samples on Nutrient broth solidified with agar.

From Mukamolova et al. (1998).



Figure 1.10: Alignment of Rpf amino acid sequences.

The sequences for *Salmonella* Typhimurium LT2 (ST-LT2), *Salmonella* Oranienburg (SO) and *Micrococcus luteus* (ML).were aligned using the ClustalW multiple alignment. The homologous portions are boxed with dark background and non-homologies have white background. The homologies between ST-LT2 and SO are indicated by (*). Note the low level of similarity of the *M. luteus* sequence with that of the two *Salmonella* sequences.

From Panutdaporn et al. (2006).

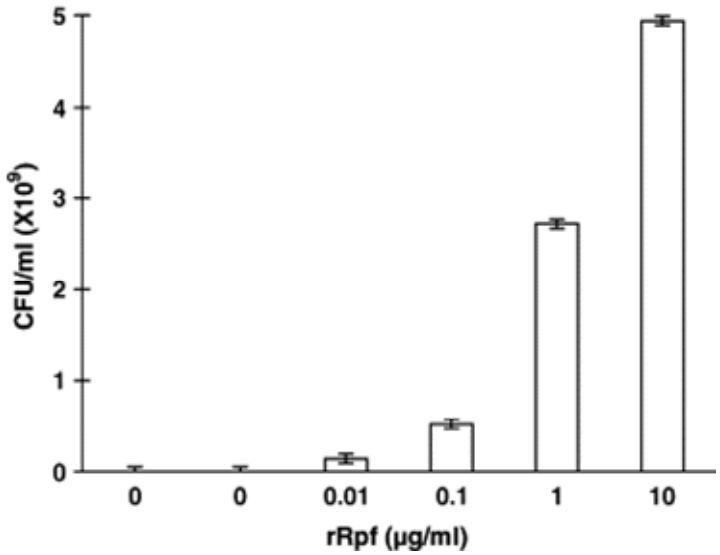

Figure 1.11: Dose-dependency of recombinant Rpf protein in *Salmonella* Oranienburg.

One milliliter of the VBNC cells of *S.* Oranienburg was added to 5% BHI supplemented with 0, 0.001, 0.01, 0.1, 1 and 10 µg/mL of recombinant Rpf protein, followed by incubation at 30°C. After 2 days of incubation, the colony forming units was determined by plating on TSA agar.

From Panutdaporn et al. (2006).

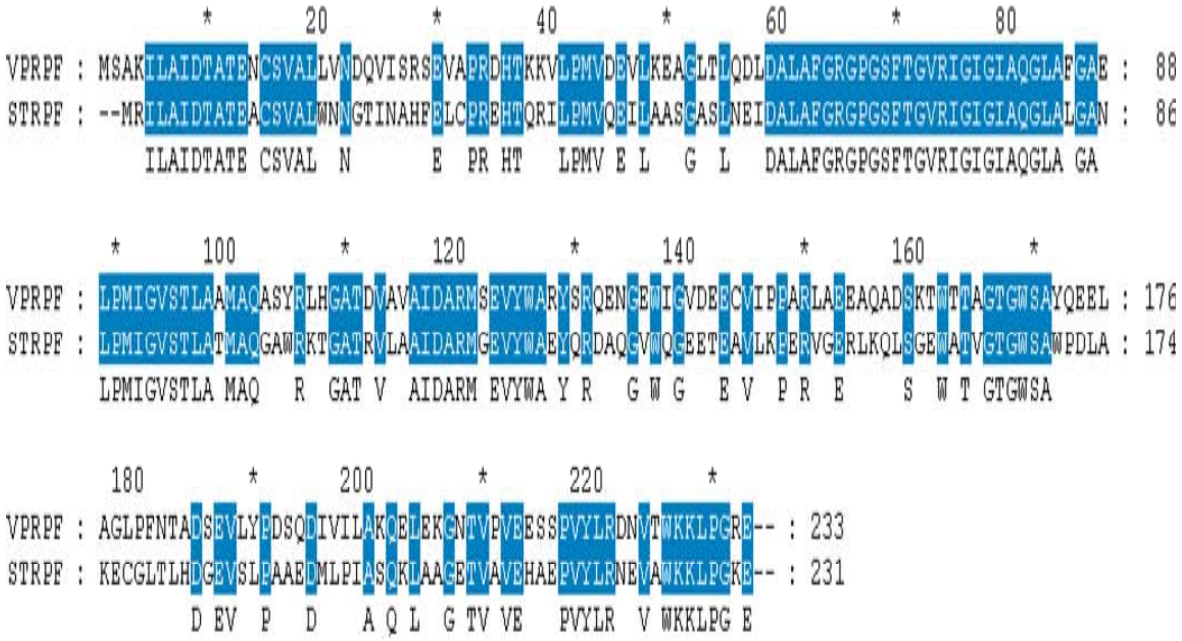

Figure 1.12: Alignment of YeaZ amino acid sequences.

YeaZ sequences were derived from whole from *S. enterica* serovar Typhimurium strain ST4/74 (STRPF) and *Vibrio parahaemolyticus* NCTC 10884 (VPRPF). The sequences were aligned using the ClustalW multiple alignment. The homologous portions are boxed with dark background and non-homologies have white background. The amino acid homologies between STRPF and VPRPF are indicated.

NOTE:
This figure is included on page 40
of the print copy of the thesis held in
the University of Adelaide Library.

Figure 1.13: Model of YjeE, YeaZ and YgjD essential signal transduction network.

Although YeaZ preferentially associates with YgjD, YeaZ also engages in partner switching in response to an undefined signal and binds to YjeE instead. The free YgjD can then accumulate within the cell. ATP binding or hydrolysis by YjeE is thought to reverse the partner switch, allowing YeaZ to form a complex with YgjD, which is then subjected to proteolysis. The RstB histidine kinase phosphorylates its cognate response regulator RstA, thus activating the expression of a specific set of genes whose identity is still unknown. It remains to be determined whether YgjD is in fact activated through proteolysis or simply degraded, where it acts in the cell or within the RstB/RstA pathway to control essential functions, and how RstA overexpression is able to compensate for the absence of YjeE, YeaZ, or YgjD.

From Msadek et al. (2009).

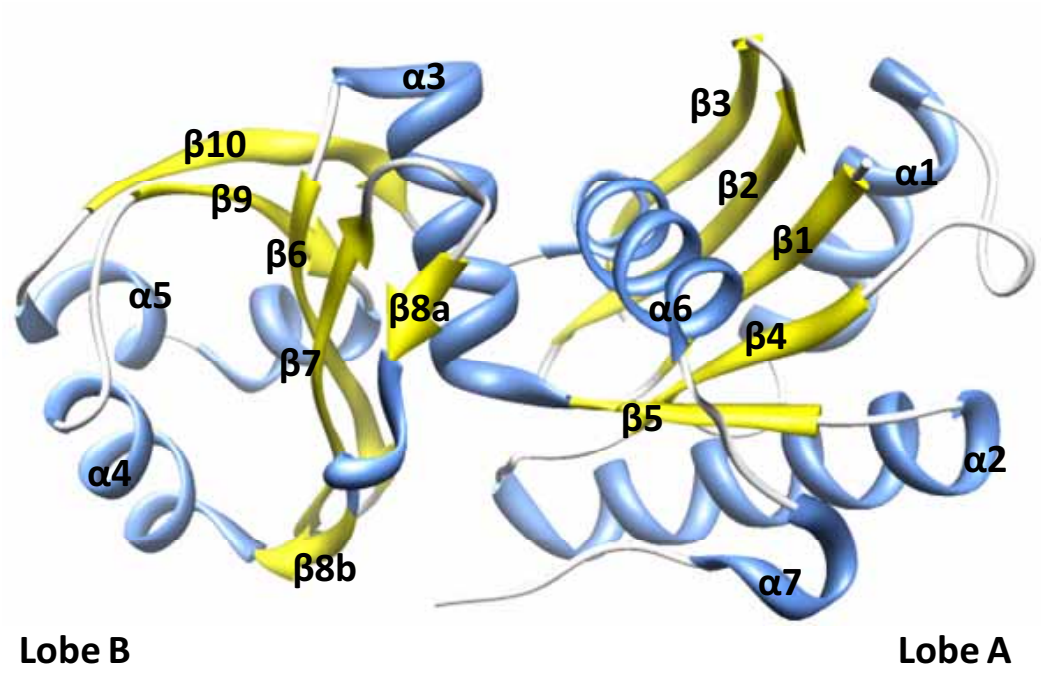

Figure 1.14: Structure of YeaZ from *S.* Typhimurium.

The $YeaZ_{ST}$ crystal structure showing adherence to an overall actin-like fold topology. Blue color represents α-helix; yellow color represents β-sheet.

Figure rendered from PDB Accession 2GEL using Chimera software (Pettersen et al., 2004).

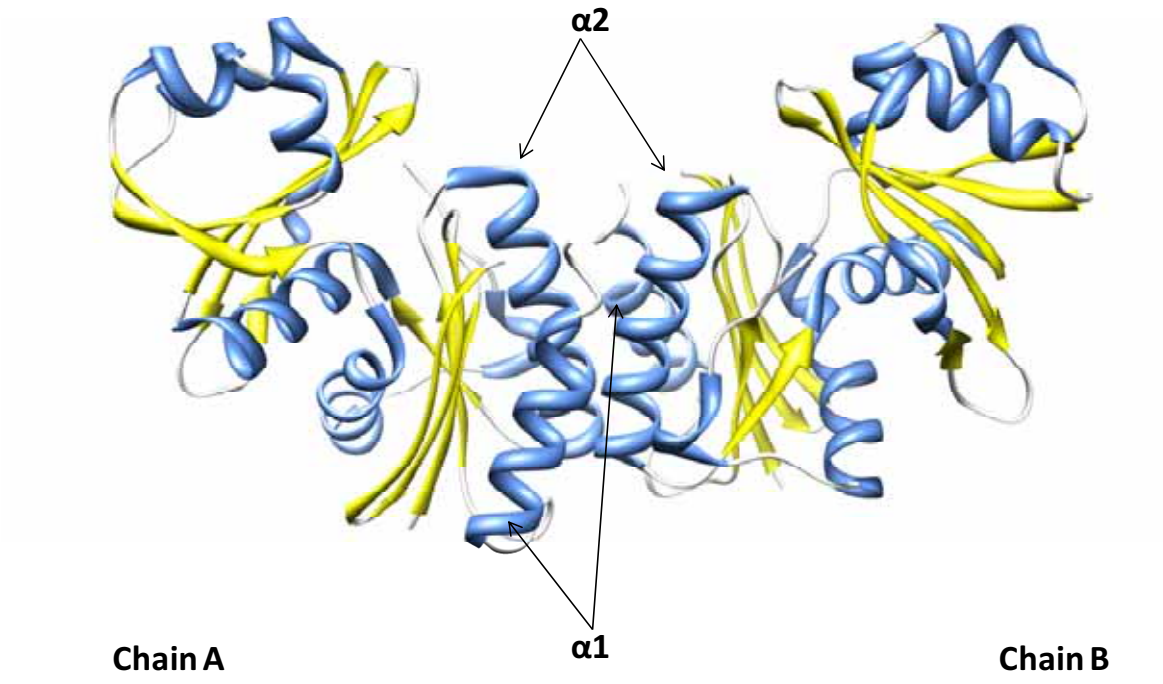

Figure 1.15: The potential YeaZ biological dimer of *S.* Typhimurium.

The potential $YeaZ_{ST}$ biological dimer, conserved in both $YeaZ_{ST}$ crystal forms, using a 2.0 Å probe radius. Blue color represents α-helices; yellow color represents β-sheet. The image was generated by Chimera.

Rendered from PDB Accession 2GEL using Chimera software (Pettersen et al., 2004).

Chapter 2: Materials and Methods

2.1 Chemicals and Reagents

All chemicals, reagents and suppliers are listed in Appendix A. All chemicals and regents were of analytical grade or of the highest purity available.

2.2 Buffers and Solutions

The buffers and solutions used in this study are listed in Appendix B. All buffers and solutions were made up in Milli-Q water and sterilized by autoclaving or filtering with 0.45 μM filter.

The suspension buffer, Artificial Sea Water (ASW), was composed of 24.7g NaCl, 0.67g KCl, 1.36g $CaCl_2H_2O$, 4.66g $MgCl_2$ $6H_2O$, 6.29g $MgSO_4H_2O$ and 0.18g $NaHCO_3$ per liter of deionized water, then adjusted to pH 8.0.

2.3 Bacteria and Yeast Strains

Vibrio parahaemolyticus, *E. coli* and Yeast strains used in this study are included in Table 2.1.

2.4 Growth Media

Vibrio parahaemolyticus strains were growth in Marine Broth (MB) (10 g peptone, 30 g NaCl, 10 g yeast extract per litre of deionized water) at 37°C. Marine agar (MA) was prepared by addition of 3% (w/v) agar to MB. Colony counts on MA plates were incubated at 37 ^{o}C (or as described) for 24 h.

E. coli strains were routinely cultured in LB Broth and on LB Agar. SOC medium was used in transformation studies in *E. coli*. Concentrations of antibiotics used were as follows: Amp 100 μg mL^{-1}; Kan 50 μg mL^{-1}, Tet 10 μg mL^{-1} and Cml 25 μg mL^{-1}.

Yeast strains were cultured using the selective synthetic dropout (SD) medium (Table 2.2).

2.5 DNA and Protein Molecular Weight Markers

DNA ladder and molecular weight marker used in this study are listed in Appendix C and D.

2.6 Plasmids used in this Study

Plasmids used in this study are listed in Table 2.3.

2.7 Oligonucleotide Primers

The oligonucleotide primers used in this study were synthesized by Geneworks (Adelaide, South Australia, Australia) and are listed in Table 2.4.

2.8 Antibodies

Anti-His-Tag Monoclonal Antibody (Novagen, Madison, USA) were used as primary antibody in Western blot to detect expression protein fusion with N-terminal or C-terminal His-tag. The secondary antibody is anti-Rabbit-HRP conjugated and raised by in goat (KPL Inc.**,** Gaithersburg, Maryland, USA). The secondary antibody was used to bind primary antibody for His-tag detection in Western Blot.

2.9 Molecular Biology Techniques

2.9.1 Preparation of Chromosomal DNA

Chromosomal DNA was isolated from 5 ml overnight bacterial cultures using a QIAamp DNA Mini kit (Qiagen, Hilden, Germany) according to the manufacturer's instructions.

2.9.2 Preparation of Plasmid DNA

Plasmid DNA was isolated from 5mL of overnight cultures of *E. coli* using QIAprep Spin Miniprep kit (Qiagen, Hilden, Germany) according to the manufacturer's instructions.

2.9.3 Polymerase Chain Reaction (PCR)

PCR amplification was performed in 25 µL reaction volume including 12.5 µL of GoTaq® Green Master Mix (Promega Corporation, Madison, Wisconsin, USA), 1 µL purified chromosomal DNA or 3 µL of crude DNA extract, 1 µL of each oligonucleotide primer (2-3

μg mL^{-1}) and sterile MQ water. All reactions were amplified using a MyCycler (Bio-Rad, Richmond, California, USA) thermocycler. Standard PCR conditions used comprised 25 cycles of denaturation (95°C, 30 sec), annealing (56°C, 30 sec) and extension (72°C, 1 min). PCR samples were stored at 4°C until further processing.

2.9.4 Restriction Enzyme Digestion

Cleavage of DNA with restriction enzymes was performed using enzymes following the reaction conditions and supplied by the manufacture (New England Biolabs, Beverly, Massachusetts, USA).

2.9.5 Extraction of DNA from Agarose Gel

The extraction of DNA fragments from an agarose gel was performed using a QIAquick Gel Extraction Kit (Qiagen, Hilden, Germany) according to the manufacturer's instructions. DNA fragments were visualized by using long wave UV light and excised from the agarose gel with a clean blade.

2.9.6 DNA Ligation

Ligation reactions were generally performed in 20 μL volumes using T4 DNA ligase (New England Biolabs, Beverly, Massachusetts, USA). Digested DNA and plasmid vector were combined in a 1.5 mL tube at a ratio of 1:3 and where necessary MQ H_2O was added to make the final volume. DNA fragments were ligated by addition of 1 μL of T4 DNA ligase and 2 μL of 10× Ligase buffer. Ligation reactions were incubated overnight at 15ºC.

2.9.7 Transformation of Chemically Competent *E. coli* Cells

Competent cells were prepared by a modification of the method described by Hanahan (Hanahan, 1983). Competent *E. coli* cells were prepared from O/N cultures diluted 1/20 in 10 mL LB broth and incubated at 37°C for 2 h with shaking. Aliquots of 1 mL of cultures were centrifuged 4,000 × g for 10 min at 4°C and the pellet resuspended in 0.3 mL 0.1M $CaCl_2$ prior to centrifugation. Cells were resuspended in 0.3 mL 0.1M $CaCl_2$, kept on ice for 30 min, centrifuged 4,000 × g for 10 min at 4°C and resuspended in 0.3 mL 0.1M $CaCl_2$

solution containing 30% (v/v) glycerol. Aliquots of 200 µL were transferred to sterile 1.5 mL tubes and stored at −80°C until required.

Chemically competent cells were thawed on ice for 15 min and then mixed with 5 µL DNA followed by incubation on ice for 30 min. The mixture was heat shocked at 42°C for 90 sec then incubated on ice for 2 min. Aliquots of 0.8 mL SOC medium was added and the cells incubated at 37°C for 2 h. Transformed cells were then selected by plating LB medium containing the appropriate antibiotics. Plates were incubated O/N at 37°C.

2.9.8 Electro-transformation of *V. parahaemolyticus* Cells

An overnight culture of *V. parahaemolyticus* was used to inoculate 10 mL of fresh MB and incubated with shaking at 37°C until an OD_{600} of 0.8-0.9 was reached. The culture was harvested by centrifugation at 4,000 × g for 15 min and 4°C. The cell pellet was washed three times with ice-cold electroporation buffer (272 mM sucrose, 1 mM $MgCl_2$, 7 mM KH_2PO_4-Na_2HPO_4, pH 7.5) and resuspended in 50 µL of ice-cold electroporation buffer.

The cell suspension was mixed with 1 µL plasmid DNA on ice for 10 min and transferred to a 0.2 cm gap electroporation cuvette. The cells were then electroporated using the following conditions: electric field 10Kv.cm^{-1}, capacitance 25µF and resistance 200 Ω. After electroporation, 500 µL MB was added and the cells incubated at 30°C for 2 h with shaking followed by plating on MA containing the appropriate antibiotic. Plates were incubated O/N at 30°C.

2.9.9 DNA Sequencing

DNA sequencing analysis was performed using ABI Prism Big Dye Terminator version 3.1 reaction technology (Applied Biosystems, California, USA). A standard reaction mix, in a total of 20 µL, contained of 4 µL of Big Dye Terminator mix, 1 µL of forward/reverse primer (2-3 µg mL^{-1}) and 1 µL of plasmid DNA (200 µg mL^{-1}). Sequencing PCR conditions involved 30 cycles of heat denaturation at 95°C for 30 sec, primer annealing at 50°C for 15 sec and extension at 60°C for 4 min.

After amplification, DNA was precipitated using 100% (v/v) isopropanol and incubation at room temperature (~25°C) for 15 min. The DNA pelleted by centrifugation 20,000 × g, 20 min, 4°C. The DNA pellet was washed with 250 µL of 70% (v/v) isopropanol and

centrifuged at 20,000 × g for 20 min at 4°C. The supernatant was discarded and the pellet was dried using centrifuge vacuum for 10 min at room temperature. All sequencing reactions were sent to the Institute for Medical and Veterinary Science (IMVS) sequencing facility (Adelaide, South Australia) for sequencing.

2.9.10 Agarose Gel Electrophoresis

Restricted DNA fragments and PCR product were mixed with 0.1 volumes of loading dye (Appendix B) and separated on 1% (w/v) agarose gels (Appendix B) with 1× TAE buffer (Appendix B) at 120 V for 1 h. DNA was stained by placing gels in distilled H_2O containing 3× Gel Red (Biotium, California, USA). DNA fragments were visualized by trans-illumination using a gel Documentation System (Gel Doc ™XR, Bio-Rad, Richmond, California, USA). Two log DNA markers (New England BioLabs, Massachusetts, USA) were also used to determine the size of DNA fragments.

2.10 RNA Transcript Analysis

2.10.1 RNA Isolation

Total cellular RNA from *V. parahaemolyticus* NCTC 10884 was isolated using the hot phenol method (Aiba et al., 1981). Cells from starvation, VBNC state and resuscitation cultures were harvested by centrifugation at 13,000 rpm for 1 min. The cell pellets transferred to 1.5 mL tube. A 0.5 mL volume of hot acid-phenol:chloroform:isoamyl alcohol at 65°C was added to the pellet and was mixed on a vortex mixer. The sample mixture was incubated at 65°C for 5 min in block heater (Ratek Instrument, Boronia Victoria, Australia). A 0.5mL hot NAES buffer at 65°C was added followed by incubation at 65°C for 5 min. The samples were placed on ice for 1 min then centrifuged for 2 min at 15,500 × g at 4°C. The upper aqueous fraction containing RNA was removed and placed in a new 1.5 mL reaction tube. The RNA was then extracted 2× with hot phenol. RNA was precipitated by addition 0.1 vol of 3 M sodium acetate (pH 5.0) and 2 vol of absolute ethanol and was incubated at -80°C for at least 2 h (or O/N). The RNA was collected by centrifugation for 30 min at 19,300 × g at 4°C. The RNA was washed with 750 µL of 70% ethanol, followed by centrifugation for 5 min at 19,300 × g at 4°C. The RNA pellet was dried under vacuum and resuspended in 50 µL RNase free water.

RNA samples were then heated to 95°C for 2 min, cooled on ice for 1 min before treating with RNasin® Ribonuclease Inhibitor (Promega N251A) to a final concentration of 1U μL^{-1}. Contaminating DNA in the samples was removed by treatment with RNase free DNase (Roche, Penzberg, Germany) at 37°C for 1 h. The purity of the RNA samples (without DNA contamination) was confirmed by one-step RT-PCR with an Access RT-PCR System kit (Promega A1281). The RNA samples then added RQ1 DNase stop buffer (Promega M198A) to inactivate the DNase and storage at -80°C.

2.10.2 RNA Quantification

The concentration of RNA was determined by measurement of absorption at 260 nm assuming an OD_{260} of 1.0 is equal to 40 mg mL^{-1} of RNA (Miller, 1972).

2.10.3 RNA Quality Confirmation

The quality (e.g. DNA contamination) of an RNA preparation was assessed by electrophoresis on a native agarose gel following one-step RT-PCR (Access RT-PCR System kit [Promega A1281]) with and without reverse transcriptase using gene-specific primers according to manufacturer's protocols. Native agarose gel electrophoresis was used to confirm the overall quality of a total RNA preparation by inspection of the one-step RT-PCR bands. A 1.7% (w/v) agarose gel was prepared and 2 µL of RNA was loaded into the well with 1 µL of 6× loading dye.

2.10.4 Quantitative Reverse Transcription PCR

1 µg of RNA was used for cDNA synthesis and PCR in a one-step quantitative RT-PCR using Superscript™ III Platinum® SYBR® Green One-Step qRT-PCR kit (Invitrogen, California, USA) according to the manufacturer's protocols.

2.11 Protein Techniques

2.11.1 Protein Quantification

Protein concentration was determined using a Bradford assay (Bradford, 1976). Briefly, 5 µL of BSA standard (0 to 1 mg mL^{-1}) or protein samples were mixed with 250 µL of Bradford reagent (Appendix B) in wells of a 96-well microtiter plate at room temperature for

10 minutes. Absorbance at 600 nm was measured in an absorbance plate reader (Molecular Dynamics). Samples and BSA standards were carried out in triplicate and averages were used in further calculations. A standard curve was plotted and the sample concentration was determined from the standard curve.

2.11.2 SDS-PAGE

SDS-PAGE was prepared by the method of Lugtenberg et al. (1975) using a Mighty Small II, (Hoefer Scientific Instruments, California, USA) vertical electrophoresis unit. Acrylamide separating gels 12.5% with 4% stacking gels were used. Appendix D describes the compositions of separating and stacking gels. All buffers and solutions used are listed in Appendix B. The GTS buffer was used for the running buffer.

Protein concentrations were determined by Bradford method (Section 2.11.1), using BSA standards (Pierce, Illinois, USA). Protein markers were from New England BioLabs (New England Biolabs, Beverly, Massachusetts, USA). The molecular weight markers were showed in Appendix E. Proteins were detected after samples were denatured by heating at 100ºC for 5 min, then separated on SDS 12.5% polyacrylamide gels in PAGE running buffer at 160 V (Bio-Rad MiniProtean) and stained with Coomassie Blue for visualisation. Coomassie Blue staining was performed by incubating the gel at RT in Coomassie staining solution with agitation for 2 h, followed by incubation in destain solution overnight to remove the background staining.

2.11.3 Western Blot Analysis

Proteins, separated by SDS-PAGE, were transferred to nitrocellulose membranes (NitroBind, Pure nitrocellulose, 0.45 μm, GE Water & Process Technologies) for 1 h at 100 V (Bio- Rad MiniProtean) in Western transfer buffer (Appendix B) by electrophoretic transfer. The membrane was then blocked for 1 h in TTBS (Appendix B) containing 5% (w/v) skim milk at 37°C, and incubated with the primary antibody in TTBS containing 0.5% (w/v) skim milk for 1 h at RT with shaking. The membrane was washed in TBST for 3 × 10 min and subsequently incubated with secondary antibody in TTBS containing 0.5% (w/v) skim milk for 1 h at RT with shaking, washed 3 × in TTBS. The membrane was detected for bound antibody by using chemiluminescent substrate (Sigma, Missouri, USA). All detection was

carried out on X-ray film (AGFA). Film was developed using a CP100 medical X-ray film processing machine (AGFA).

2.11.4 Expression and Purification of His-tagged fusion Protein

A single *E. coli* BL21 colony (carrying His tagged gene constructs) was used to inoculate 10 mL of LB medium containing 100 μg mL^{-1} Amp and incubated overnight at 37°C with shaking. The following morning, 5 mL bacterial culture was added to 0.5 L of LB medium containing 100 μg mL^{-1} Amp and the culture was expanded to an OD_{600nm} of 0.5-0.6. Expression of His tag fusion protein was induced by addition of IPTG to a final concentration of 0.2 mM and the culture incubated with shaking at 30°C for a further 4 h. Bacterial cells were harvested by centrifugation at 4,000 × g at 4°C for 15 min and washed the pellet 2× with PBS by centrifugation at 4,000 × g at 4°C for 15 min. Bacterial pellets were lysed by sonication in PBS buffer supplemented with a protease inhibitor cocktail VI (Astral Scientific, Sydney, Australia). Cell debris was removed by centrifugation at 20,000 × g at 4°C for 15 min and the supernatant filtered through a 0.45 μM filter.

The His-tagged fusion proteins were purified by gravity flow column chromatography using HisLink™ Protein Purification Resin (Promega, Wisconsin, USA), according to the manufacturer's instructions. A HisLink™ resin column was prepared by loading 1 mL of resin slurry into a disposable 5 mL polypropylene column (Pierce, Illinois, USA) Samples were passed through a HisLink™ resin column. After elution with washing buffer (Appendix B) for 5 mL, the His-fusion proteins were eluted with purification elution buffer (Appendix B) for 10 mL at room temperature. The samples from each step of the purification process were analyzed by SDS-PAGE (Section 2.11.2).

2.11.5 Production of a YeaZ specific Polyclonal Antiserum

YeaZ protein purified by gravity flow column chromatography was concentrated using a Vivaspin (Sartorius, Gottingen, Germany) concentrator by centrifugation at 1,700 × g at 4ºC and changed to PBS. The YeaZ preparation was mixed with adjuvant and used to immunise a rabbit at four different sites over a period of 3 months (The immunisation and blood collection procedures were done by Institute of Medical and Veterinary Science (IMVS) staff, Adelaide, Australia.). A pre-immunisation sample of blood was taken. After the initial

immunisation, booster immunizations were performed three and six weeks later. Twelve weeks after the initial immunisation, the rabbit was exsanguinated and the serum was stored at −80°C.

In order to remove the nonspecific antibodies that reacted with *E. coli* antigens, the antiserum was adsorbed with *E. coli* BL21 DE3 cells. A 10 mL overnight broth culture of *E. coli* BL21 DE3, was harvested by centrifugation at 4,000 × g, for 5 min. The pellet was washed in 3× in 10 mL of PBS. The pellet was re-suspended in 5 mL antiserum. The mixture was gently inverted for 3-4 hr at 4°C before the bacteria were removed by centrifugation. The antiserum was then repeatedly adsorbed with *E. coli* cells as described above. The purified antiserum was filter sterilized using 0.2 μm filter, and stored at -20°C until required. The HRP-conjugated goat anti-rabbit IgG was used to test the specificity of the purified antiserum against purified YeaZ protein using Western blot analysis as described in Section 2.11.3.

2.11.6 Co-immunoprecipation

Co-immunoprecipation of proteins was performed using Dynabeads® Protein A (Invitrogen, California, USA) according to the manufacturer's instructions. Briefly, 50 μL of a Dynabeads Protein A suspension were washed twice in 200 μL PBST, and the beads removed from the supernatant by magnetic separation. Resuspended Dynabeads Protein A with 10ug target antibody, and incubated with rotation for 10 min at RT. The Dynabeads-Ab complex was place on magnet, then washed in PBST, resuspended in 1 mL whole cell lysate followed by incubation with rotation for 4 h at RT to allow target antigen to bind to the Dynabeads-Ab complex. The Dynabeads-Ab-Ag complex was washed 3× in 200 μL PBS, removed the supernatant by place the tube on the magnet. The Ab-Ag complex was eluted with 20 μL of 50 mM glycine buffer at pH 2.8 (Appendix B). The Ab-Ag complex was separated by SDS-PAGE (2.11.2) and confirmed by Western blot analysis (2.11.3).

2.11.7 Immunofluoresence Microscopy

Bacterial culture was washed twice in saline (0.85% [w/v] NaCl), centrifuged 20,000 × g for 1 min, resuspended in 1 ml of 3.7% (w/v) formaldehyde (Sigma, Missouri, USA) in saline, and incubated at RT for 20 min. Fixed bacteria were washed in PBS to remove residual formaldehyde, then resuspended in 100 μL PBS.

Sterile glass coverslips were coated with 10% poly-L-lysine in PBS. Formalin fixed bacteria on coverslips were labelled with primary antibody (1:100 in PBS with 10% foetal calf serum (FCS) for 1 h at RT, blocked with PBS containing 10% FCS at RT for 15 min, washed 3× with PBS, and incubated with secondary antibody (1:100 in PBS with 10% FCS) for 30 min at 37°C. Coverslips were washed 2× with PBS and 1× with MQ H2O, mounted on microscope slides with 50 µL Mowiol 4-88 (Calbiochem) containing 20 µg mL^{-1} *p*–phenylenylenediamine (Sigma, Missouri, USA) and sealed with nail polish.

Bacteria were observed by epi-fluorescence microscopy using 100× Phase contrast, oil immersion objective lens with an Olympus 1 × 70 microscope (connected to a Hamamatsu ORCA-ER camera controller, ASI MFC-2000 automatic focus fine-tuning instrument, lamda 10-C shutter instrument, and a Uniblitz2 VMM-D3 three channel shutter drive).

2.11.8 Extraction of Outer Membrane Protein

Outer membrane proteins were separated following the method described by Jung et al. (Jung et al., 2005) centrifugation 6,000 × g for 20 min at 4°C, washed 2× with PBS and suspended in PBS. The suspension was disrupted by sonication (Bronson Sonifier Cell disruptor BLS) on ice for 1 min (60% duty, intensity 7). The cell debris was discarded by centrifugation 6,000 × g for 15 min at 4°C. The supernatant was subjected to ultracentrifugation 105,000 × g for 1 h at 4°C (Beckman Coulter Optima TLX Ultracentrifuge) to separate the cell envelope. The pellet containing the crude envelope protein was suspended in 1% N-lauroylsarcosine (Sigma, Missouri, USA) in PBS for 1 h at RT followed by ultracentrifugation 105,000 × g for 1 h at 4°C by Beckman Coulter Optima TLX Ultracentrifuge. The supernatant was removed and the pellets containing outer membrane protein was suspended in 1% (v/v) TritonX-100 for 1 h at RT, followed by ultracentrifugation at 105,000 × g for 1 h at 4°C. The supernatant containing the purified outer membrane protein were stored at - 20°C until required.

2.11.9 Trichloroacetic Acid (TCA) Precipitation

Culture supernatant was collected following centrifugation and dialysed for 24 h at 4°C in 50 mM Tris-HCl, pH 7.5. Proteins were precipitated by addition of 0.1 vol of 100% (w/v) of ice cold TCA on ice and the mixture incubated for 30 min. The precipitated protein was collected by centrifugation 20,000 × g at 4°C for 10 min. The protein pellet were washed

twice with ice cold acetone, air-dried, and re-suspended in sample loading buffer and stored at −80°C until required.

2.11.10 Formaldehyde Cross-linking

Fresh formaldehyde solution was obtained by dissolving 4% paraformaldehyde in PBS for 2 h at 80°C. Cross-linking was performed essentially as described by (Skare et al., 2004). For cross-linking, bacteria were grown in growth medium until the OD_{600} reached 0.6 and pelleted in 1.5 mL centrifuge tube. The cells were resuspended in PBS. Paraformaldehyde was add to a final concentration of 0.5%, followed by incubation at 65°C for 10 min. The reaction was quenched with 0.5 mL ice-cold 1.25M glycine/PBS for 10 min and subsequently centrifuged immediately to pellet the whole cells. Pellets were washed twice in PBS and then resuspended in protein sample loading buffer (no β-mercaptoethanol). The samples were heated at 65°C for 10 min. Protein samples were analysed by SDS-PAGE (Section 2.11.2) and Western Blot analysis (Section 2.11.3).

2.11.11 MALDI-TOF Mass Spectrometry

The protein band of interest was excised from SDS-PAGE gels and chopped into 1 mm^3 pieces. The gel pieces were stained, reduced and alkylated with iodoacetamide. Consequentially, the sample was digested with 100ng of trypsin. The resulting tryptic peptides were extracted from the gel pieces with 50% aectonitrile containing 1% formic acid (FA) followed by 100% acetonitrile. The final samples were concentrated to 1 mL by vacuum centrifugation. The peptides were diluted to 5 mL FA30 (7 parts of 0.1% FA to 3 parts acetonitrile). The MS and MS/MS spectra were processed by the Adelaide proteomics Centre using flexAnalysis (Version 3.0, Bruker Daltonik GmbH). Peak detection was analysed using the SNAP algorithm with a signal to noise threshold of 3 and a quality factor threshold of 50. The analysed mass lists and spectra were exported to BioTools (Version 3.0, Bruker Daltonik GmbH). The MS and MS/MS spectra were combined and matched to the provided protein sequence using Sequence Editor. The following parameters were used when exporting the theoretical peptide masses from Sequence Editor to BioTools: Global modifications: Carbamidomethyl (C); Variable modifications: Oxidation (M); Mass tol MS: 100 ppm; MS/MS tol: 0.5 Da; Missed cleavages: 1.

2.11.12 Bacterial Two-Hybrid Analysis

2.11.12.1 Construction of Bait and Prey Protein Expressing Strains

Protein-protein interaction using a bacterial two hybrid system was performed as described by Dove and Hochschild (2004). Plasmids pBT and pTRG were used to make fusions to the C-terminal end of λcI and α-NTD. Primers were designed to PCR amplify the bait and prey gene from *V. parahaemolyticus* NCTC 10884 chromosomal DNA (Section 2.7). PCR products, plasmid pBT and pTRG were digested with *Not*I and *Xho*I, and purified and concentrated in a 50 µL volume. Ligation reactions (Section 2.9.6) *E. coli* DH5αZ1 was grown at 30°C and made chemically competent cells (Section 2.9.7), before 100 µL of cells was mixed with 5 µL of ligation reactions and heat shock transformation. The transformants were spread on LB plate containing Amp, Kan and Cml. DNA sequencing confirmed the construction of pBT bait and pTRG prey plasmids. The pBT bait and pTRG prey plasmids were used to cotransform *E. coli* strain KS1. Protein-protein interactions ability was detected by using β-galactosidase assay described below.

2.11.12.2 β-Galactosidase Assay

The β-galactosidase assay used was based on the method originally described by (Miller 1992). Individual colonies were picked up and grown overnight in appropriate antibiotics. IPTG was added to the medium at the final concentration of 20 µM. The strains were sub-cultured in LB broth containing Amp, Kan and Cml at 37°C with aeration until the culture achieved an OD_{600} of 0.3-0.7. To prevent further growth of the cells, the cultures were placed on ice for 20 min. The OD_{600} was measured and recorded for each strain. The culture was mixed with Z buffer (Appendix B) in a total volume of 1 mL in a 1.5 mL reaction tube. Cells were disrupted by adding 30 µL 0.1% (v/v) SDS and 60 µL chloroform and vortexed for 6 sec. The tubes were pre-warmed at 28°C for 10 min prior to the addition of 0.2 mL of 4 mg mL^{-1}ONPG. The tubes were kept at 28°C to allow colour development. The reaction was stopped by addition of 0.5 mL of 1 M Na_2CO_3 and the reaction time recorded. Cells were removed by centrifugation 20,000 × g for 5 min. The supernatant was removed to a fresh 1.5 mL reaction tube. The OD at 420 nm was measured and recorded for each strain. β-galactosidase activity was determined in Miller units by using the following equation:

$$MU = 1000 \times \frac{OD_{420}}{t \times v \times OD_{600}}$$

Where t is the reaction time (min) and v is the volume (mL) of the culture used in the assay.

2.11.13 Yeast Two-Hybrid Analysis

2.11.13.1 Construction of Bait and Prey Protein

The yeast two hybrid system used was originally developed by Fields (Fields & Song, 1989). Plasmids pLexA and pB42AD were used to making fusions to the C-terminal end of DNA-BD and Acid activator Domain (AD). Primers were designed to PCR amplify the bait and prey gene from *V. parahaemolyticus* NCTC 10884 chromosomal DNA. PCR products, plasmid pLexA and pB42AD were digested with *Eco*RI and *Xho*I, and purified and concentrated in a 50 µL volume. Ligation reactions (Section 2.9.6) *E. coli* DH5α was grown at 30°C and made chemically competent cells (Section 2.9.7), before 100 µL of cells was mixed with 5 µL ligation reactions and heat shock transformation. The transformants were spread on LB plate containing Amp. DNA sequencing was used to confirm the construction of pLexA bait and pB42AD prey plasmids. The pLexA bait and pB42AD prey plasmids were used to co-transform *Saccharomyces cerevisiae* EGY48 containing plasmid p8op-lacZ (Table 2.1). Protein-protein interaction ability was detected by using the yeast two hybrid interaction assay (Section 2.11.13.4).

2.11.13.2 Preparation of Competent Yeast Cells

Competent yeast cells were prepared with a *Saccharomyces cerevisiae* EasyComp Transformation kit (Invitrogen, California, USA) using the manufacturer's instructions.

2.11.13.3 Yeast Transformation

Competent yeast cells were prepared by using *Saccharomyces cerevisiae* EasyComp Transformation kit (Invitrogen, California, USA) according to the manufacturer's instructions.

2.11.13.4 β-Galactosidase Assay

Assay of yeast two-hybrid was performed as described by the Matchmarker LexA Tow-Hybrid System's (Clontech, California, USA) instructions. The bait and prey plasmid were co-transformed into *Saccharomyces cerevisiae* EGY48 containing plasmid p8op-lacZ. The co-transformation mixtures were plated on SD/Glu/-His/-Trp/-Ura to select for colonies containing both hybrid plasmids. The co-transformants were transferred to the selection plate SD/Gal/Raf/-His/-Trp/-Ura/-Leu + X-gal at 30°C screening for expression of *LacZ* reporter gene.

2.11.14 Transmission Electron Microscopy (TEM)

Bacterial cells were harvested by centrifugation 20,000 × g for 5 min and the pellets were washed 3× with PBS. The pellets were re-suspended in 0.5mL PBS containing 1.25% (v/v) gluteraldehyde and incubated at 4°C for overnight. The fixed cells were harvested by centrifugation 20,000 × g for 5 min. The cell pellets were then washed once in PBS + 4% (w/v) sucrose, and then postfixed in 2% (w/v) osmium tetroxide (OsO_4) for 1 h. The samples were then dehydrated in a graded ethanol series, and infiltrated with 1:1 propylene oxide/Epoxy resin mixture (10mL of Procure 812, 6 mL of Araldite 502, 22 mL of D.D.S.A. and 0.56 mL of DMP-30). The samples were then infiltrated with 3× changes of 100% Epoxy resin per 8 h. Samples were then embedded in fresh resin and incubated at 70°C for at least 24 h to polymerize the resin. Ultrathin sections were cut using a diamond knife, placed on 300 mesh gold grids and stained with 4% (w/v) uranyl acetate and Reynolds lead citrate (Reynolds, 1963). The stained sections were observed under Philips CM100 Transmission Electron Microscope operated with an accelerating voltage of 80kV.

2.12 Site-directed Mutagenesis by Overlap Extension PCR

Overlap extension PCR was performed as described by Heckman (Heckman & Pease, 2007). Briefly, overlap extension PCR was used to create a point mutation into the *yeaZ* of plasmid pBT (Section 2.6). Three pairs of oligonucleotide (YeaZI75AF/R, YeaZL83AF/R and YeaZF85AF) were used to produce three individual point mutation sites in YeaZ of plasmid pBT (Section 2.7). Oligonucleotide pair YeaZI75AF/YeaZI75AR was designed to introduce nucleotide base change to encode alanine. Oligonucleotide pair YeaZNotI F/YeaZ R was

designed to amplify across the overlapping region containing the point mutation site. The oligonucleotide pair YeaZNotI F/ YeaZ I75AR amplified a region with the point mutation site at 5' end while the oligonucleotide pair YeaZI75AF/YeaZ R amplified a region with the point mutation site at 3' end. These two DNA fragments were combined together as a DNA template for PCR to produce the DNA fragment with point mutation of YeaZ in amino acid 75. The overlap extension PCR was used to produce the point mutation site in amino acid 83 and 85 of the YeaZ sequence.

Table 2.1: Bacteria and Yeast strains used in this study.

Strain	Description	Source/Reference
E .coli		
DH5α	φ80d lacZΔM15, *recA1*, *endA1, gyrA96, thi-1, hsdR17*(Rk – Mk +), supE44, relA1, deoR, Δ(lacZYA*argF*) U169	Laboratory stock
DH5αZ1	φ80d lacZΔM15, *recA1, endA1, gyrA96, thi-1 hsdR17 supE44*	(Lutz and Bujard, 1997)
BL21	*E. coli* B F– *dcm ompT hsdS*(Rb– Mb–) *gal*	Laboratory stock
KS1	λ(DE3) F' $lacI^q$(Kan^R)	Laboratory stock
V. parahaemolyticus	NCTC 10884	Laboratory stock
S. cerevisiae		
$EGY48^C$	MATα, his 3,trp 1,ura 3,LexAop(x6)-LEU2	Clontech
$EGY48^C$ (p8op-lacZ)	MATα, his 3,trp 1,ura 3,LexAop(x6)-LEU2,(p8op-lacZ)	Clontech

Table 2.2: Composition of SD medium.

Nutrient	25X Concentration
Adenine hemisulfate salt	500 mg/L
Arginine HCl	500 mg/L
Histidine HCl monohydrate	500 mg/L
Isoleucine	750 mg/L
Leucine	2500 mg/L
Lysine HCl	750 mg/L
Methionine	500 mg/L
Phenylalanine	500 mg/L
Threonine	5000 mg/L
Tryptophan	500 mg/L
Tyrosine	750 mg/L
Uracil	500 mg/L
Valine	3750 mg/L

Table 2.3: Plasmids used in this study.

Plasmid	Description	Source
pGEM-T Easy	Cloning vector; Amp^R	Promega
pET21a	Expression vector; Amp^R	Novagen
pET21b	Expression vector; Amp^R	Novagen
pCACTUS	Suicide vector; Cml^R; 30^{oC}	(Clark)
pWSK29	Low copy cloning vector ; Amp^R	(Wang & Kushner, 1991)
pET-Duet	Amp^R	Novagen
pBT	Cml^R	Stratagene
pTRG	Tet^R	Stratagene
pBT-LGF2	Cml^R, positive control	Stratagene
pTRG-Gal11^p	Tet^R, positive control	Stratagene
pLexA	Amp^R	Clontech
pB42AD	Amp^R	Clontech
pLexA-53	Amp^R , positive control	Clontech
pB42AD-T	Amp^R , positive control	Clontech
pUC18K	Kam^R	(Menard et al., 1993)
pCTX100	pGEMT-Easy carrying a 859 bp flanking fragment of the *yeaZ* gene from *V. parahaemolyticus*	This study; Chapter 4
pCTX101	pCTX100 with a 850 kanamycin resistance cartridge from pUC18K into the *Eco*RI and *Xho*I site to create a *yeaZ::kan* mutation	This study; Chapter 4
pCTX102	pCACTUS carrying a 1866 bp *yeaZ::kan* DNA fragment from pCTX101	This study; Chapter 4
pCTX103	pWSK29 carrying a 3.0kb *yeaZ* fragment	This study; Chapter 4
pCTX104	pGEMT-Easy carrying a 702 bp DNA fragment of the *yeaZ* gene from *V. parahaemolyticus*	This study; Chapter 4

Table 2.3 continued.

pCTX105	pET21b carrying a 702 bp DNA fragment of the *yeaZ* gene from *V. parahaemolyticus*	This study; Chapter 4
pCTX106	pBT carrying a 702 bp DNA fragment of the *yeaZ* gene from *V. parahaemolyticus*	This study; Chapter 5
pCTX107	pTRG carrying a 702 bp DNA fragment of the *yeaZ* gene from *V. parahaemolyticus*	This study; Chapter 5
pCTX108	pTRG carrying a 485 bp DNA fragment of the *yjeE* gene from *V. parahaemolyticus*	This study; Chapter 5
pCTX109	pTRG carrying a 1,017 bp DNA fragment of the *ygjD* gene from *V. parahaemolyticus*	This study; Chapter 5
pCTX110	pLexA carrying a 702 bp DNA fragment of the *yeaZ* gene from *V. parahaemolyticus*	This study; Chapter 5
pCTX111	pB42AD carrying a 485 bp DNA fragment of the *yjeE* gene from *V. parahaemolyticus*	This study; Chapter 5
pCTX112	pB42AD carrying a 1,017 bp DNA fragment of the *yjeE* gene from *V. parahaemolyticus*	This study; Chapter 5
pCTX113	pET-Duet carrying a 702 bp DNA fragment of the *yeaZ* gene from *V. parahaemolyticus*	This study; Chapter 5
pCTX114	pET-Duet carrying a 702 bp DNA fragment of the *yeaZ* gene and a 458 bp DNA fragment of the *yjeE* from *V. parahaemolyticus*	This study; Chapter 5
pCTX115	pET-Duet carrying a 702 bp DNA fragment of the *yeaZ* gene and a 1,017 bp DNA fragment of the *ygjD* from *V. parahaemolyticus*	This study; Chapter 5

Table 2.3 continued.

pCTX116	pBT carrying a 702 bp DNA fragment of the *yeaZ* gene with I75A point mutation from *V. parahaemolyticus*	This study; Chapter 5
pCTX117	pBT carrying a 702 bp DNA fragment of the *yeaZ* gene with L83A point mutation from *V. parahaemolyticus*	This study; Chapter 5
pCTX118	pBT carrying a 702 bp DNA fragment of the *yeaZ* gene with F85A point mutation from *V. parahaemolyticus*	This study; Chapter 5

Table 2.4: Primer pairs used in this study.

Primer name	Oligonucleotide sequence	Target	Source
pGEM-T EASY			
M13F	5'-GTCATAGCTGTTTCCTGTGTG-3'	pGEM-T easy	Promega
M13R	5'-GTCGTGACTGGGAAAACCCTGGCG -3'	pGEM-T easy	Promega
pET 21			
T7F	5'-TAATACGACTCACTATAGG-3'	pET21	This study; Chapter 4
T7R	5'- GCTAGTTATTGCTCAGCG-3'	pET21	This study; Chapter 4
***rpf*-specific primers**			
rpf F	5'-GAGTCATATGAGCGCAAAAATTCTTGCTAT-3'	*yeaZ* gene	This study; Chapter 4
rpf R	5'-TAATTACTCGAGGCCTGGAAGCTTCTTCCA-3'	*yeaZ* gene	This study; Chapter 4
rpfmut F	5'-GCATGCCTGAGCCAAACAGCCCAGGCTTAGCGGACA-3'	400bp upstream *yeaZ*	This study; Chapter 4
rpfmut R	5'-GCATGCTTGGGACTCATCAACTTGTTTTATGG-3'	2185bp upstream *yeaZ*	This study; Chapter 4
rpfcom F	5'-GGATCCTAAATCAGATACTTCCATGC-3'	300bp downstream *yeaZ*	This study; Chapter 4
rpfcom R	5'-CTCGAGTTTTGAGCTTTCTTTACCTGCCCT-3'	146bp downstream *yeaZ*	This study; Chapter 4

Table 2.4 continued.

***yjeE*- specific primers**			
yjeE F	5’-GCACATATGAGCACGAAACAATTTAC-3’	*yjeE* gene	This study; Chapter 5
yjeE R	5’-GACTCACTCGAGCTCCAATCGACTGAG-3’	*yjeE* gene	This study; Chapter 5
B2H primers			
pBT 5’	5’-TCCGTTGTGGGGAAAGTTATC-3’		This study; Chapter 5
pBT 3’	5’GGGTAGCCAGCAGCATCC-3’		This study; Chapter 5
pTRG 5’	5’-TGGCTGAACAACTGGAAGCT-3’		This study; Chapter 5
pTRG 3’	5’-ATTCGTCGCCCGCCATAA-3’		This study; Chapter 5
YeaZ NotI F	5’-GAGGCGGCCGCAATGAGCGCAAAAATTCTTGCTATCG-3’	*yeaZ* gene	This study; Chapter 5
YeaZ R	5’-TAATTACTCGAGGCCTGGAAGCTTCTTCCA-3’	*yeaZ* gene	This study; Chapter 5
YjeE Not I F	5’-GAGGCGGCCGCAATGAGCACGAAACAATTTAC-3’	*yjeE* gene	This study; Chapter 5
YjeE R	5’-GACTCACTCGAGCTCCAATCGACTGAG-3’	*yjeE* gene	This study; Chapter 5
YgjD Not I F	5’-GAGGCGGCCGCAATGCGCATTATTGGTATCG-3’	*ygjD gene*	This study; Chapter 5
YgjD R	5’-TGATTACTCGAGTGGCGTTAGCTGGTC-3’	*ygjD gene*	This study; Chapter 5
YeaZ I75AF	5'-GTAGCTTTACTGGTGTTCGTGCGGGTATTGGCATCGCTCAAGG-3'		This study; Chapter 5
YeaZ I75AR	5'-CCTTGAGCGATGCCAATACCCGCACGAACACCAGTAAAGCTAC-3’		This study; Chapter 5
YeaZ L83AF	5'-GTATTGGCATCGCTCAAGGCGCGGCATTTGGTGCAGAACTGCC-3’		This study; Chapter 5
YeaZ L83AR	5'-GGCAGTTCTGCACCAAATGCCGCGCCTTGAGCGATGCCAATAC-3’		This study; Chapter 5
YeaZ F85AF	5'-GCTCAAGGCCTAGCAGCTGGTGCAGAACTGCC-3'		This study; Chapter 5
YeaZ F85AR	5'-GGCAGTTCTGCACCAGCTGCTAGGCCTTGAGC-3'		This study; Chapter 5

Table 2.4 continued.

Y2H primers			
pLexA	5’-CGTCAGCAGAGCTTCACCATTG-3’		This study; Chapter 5
pB42AD	5’-CCAGCCTCTTGCTGAGTGGAGATG-3’		This study; Chapter 5
pLexA-YeaZ F	5’-CGGGAATTCATGAGCGCAAAAATTCTTGCTATCG-3’	*yeaZ* gene	This study; Chapter 5
pLexA-YeaZ R	5’-TAATTACTCGAGGCCTGGAAGCTTCTTCCA-3’	*yeaZ* gene	This study; Chapter 5
pB42AD-YjeE F	5’-GGCCTCGAGATGAGCACGAAACAATTTAC-3’	*yjeE* gene	This study; Chapter 5
pB42AD-YjeE R	5’-GACTCACTCGAGCTCCAATCGACTGAG-3’	*yjeE* gene	This study; Chapter 5
pB42AD-YgjD F	5’-GAGGAATTCATGCGCATTATTGGTATCG-3’	*ygjD* gene	This study; Chapter 5
pB42AD-YgjD R	5’-TGATTACTCGAGTGGCGTTAGCTGGTC-3’	*ygjD* gene	This study; Chapter 5
Co-expression primers			
pET-duet RPF F	CGGGAATTCGATGAGCGCAAAAATTCTTGCTATCG	*yeaZ* gene	This study; Chapter 5
pET-duet RPF R	AATGCGGCCGCGCCTGGAAGCTTCTTCCAA	*yeaZ* gene	This study; Chapter 5
pET-duet GCP F	GAGAGATCTCATGCGCATTATTGGTATCG	*ygjD* gene	This study; Chapter 5

Table 2.4 continued.

Q-RT PCR primers			
Vp 16S rRNA F	5'-CAGCCACACTGGAACTGAGA-3'	16s rRNA	This study; Chapter 4
Vp 16S rRNA R	5'-TTAGCCGGTGCTTCTTCTGT-3'	16s rRNA	This study; Chapter 4
Vp yeaZ RT F	5'-GATGTCGCTGTAGCGATTGA-3'	*yeaZ* gene	This study; Chapter 4
Vp yeaZRT R	5'-CCCGCCAGTTCTTCTTGATA-3'	*yeaZ* gene	This study; Chapter 4
Vp rpoS RT F	5'-CGGGTAAGACCAATCTCTCG-3'	*rpoS* gene	This study; Chapter 4
Vp rpoS RT R	5'-CCTGACGCAAACAACTCTGA-3'	*rpoS* gene	This study; Chapter 4

Chapter 3: Factors affecting Resuscitation and Entry to the VBNC State

3.1 Introduction

Vibrio parahaemolyticus inhabits warm seawater, however this Vibrio is seldom isolated by cultural methods when the water temperature is below 13–15°C (Kaneko & Colwell, 1974). Most of the Vibrios that inhabit similar marine environments (Oliver & Bockian, 1995) including *V. parahaemolyticus*, may be present in a Viable But Non-Culturable (VBNC) state during the winter months when water temperatures are low, and therefore cannot be cultured on nutrient growth media.

The VBNC state may represent a dormant state that improves the survival of non-sporulating bacteria in a stressful environments (Colwell, 2000). For example, VBNC state bacteria show enhanced resistance to mechanical and ethanol stresses (Weichart & Kjelleberg, 1996) and some pathogenic bacteria maintain virulence following recovery from this physiological state (Rahman, 1996). Thus VBNC state pathogenic bacteria may be a potential risk for public health. This risk factor has not yet been systematically evaluated for seafoods contaminated by Vibrios, but should be considered as these cells may impact the food inspection process and microbiological evaluation of seafoods.

The mechanism involved in the establishment of the VBNC state in bacteria is not well characterized. *V. parahaemolyticus* present in natural and food processing environments are often maintained at low temperature, low salinity and nutrient deprivation. These stress conditions induce the VBNC state in other bacteria (Oliver et al., 1991) and in *V. parahaemolyticus*. Indeed the stress of nutrient deprivation and exposure to low temperature, have been shown to be major causes of the induction of VBNC state in some pathogenic bacteria. VBNC state *V. parahaemolyticus* cells have been detected in populations of starved cells at low temperature (Jiang, 1996). However, the effect of extrinisic factors, such as pH and NaCl concentration, on the kinetics of entry and escape to or from the VBNC state have not been examined. To address this issue for *V. parahaemolyticus*,

this chapter presents data that demonstrates the impact of water pH, NaCl concentration and the initial numbers of *V. parahaemolyticus* NCTC 10884 cells on entry to the VBNC state.

3.2 Experimental Approach

To determine whether cell concentration is an important factor in the VBNC state induction and resuscitation, *V. parahaemolyticus* NCTC 10884 cell were incubated in an artificial seawater medium (ASW) at 4°C and 20°C to monitor entry and exit respectively, of the cell suspension to/from the VBNC state. Suspensions of cells incubated at 20°C were used as controls. The impact of NaCl concentration and pH on induction and resuscitation was also evaluated.

3.3 Results

3.3.1 Effect of Initial Cell Concentration and NaCl Concentration on Culturability

ASW containing different NaCl concentrations (2.5%, 5% and 10% at pH 8.0) were used to investigate the effect of initial cell concentration and NaCl concentration on induction of the VBNC state.

V. parahaemolyticus NCTC 10884 was tested for loss of culturability when suspended at 10^9, 10^7, 10^5 and 10^3 cells mL^{-1} in 1 L volumes of sterile ASW solution containing 2.5% NaCl at pH 8.0, followed by incubation, without agitation, in the dark at 4°C or 20°C for up to 43 d (Figure 3.1 Panel A, B, C and D). Culturability was assessed by plate count methods using ASW as a diluent and plating on the non-selective MA medium, with incubation at 30°C. Estimates of viability were obtained using a *Bac*Light Cell Viability kit[2]. The culturability of suspensions initially containing 10^9 cells mL^{-1} bacteria when incubated at 20°C, remained *ca.* 10^9 cells mL^{-1} for the entire 43 d period of the experiment. In contrast,

[2] *Bac*Light™ Bacterial Viability Kits use green-fluorescent SYTO® 9 stain and red-fluorescent propidium iodide stain that differ in ability to penetrate viable bacterial cells. SYTO® 9 stain labels both live and dead bacteria, whereas, propidium iodide penetrates only bacteria with damaged membranes, reducing SYTO® 9 fluorescence when both dyes are present. Thus, viable bacteria fluoresce green, while dead bacteria with damaged membranes fluoresce red. Direct microscopic counts of differentially stained cells allows estimation of viable cells *vs*. dead cells.

the culturability of cell suspensions incubated at 4°C decreased to undetectable levels within in 36 d. Similar trends were also observed for suspensions prepared with 10^7, 10^5 and 10^3 cells mL^{-1} incubated at 4°C. For example, the culturability of the 10^7 cells mL^{-1} suspensions decreased to an undetectable level within 20 d at 4°C, whereas the culturability of the same suspensions incubated at 20°C decreased to 10^5 cells mL^{-1}. Moreover, cell suspensions with initial cell numbers of 10^5 and 10^3 cells mL^{-1} lost culturability within 8 d when incubated at 4°C. The results presented in Figure 3.1 suggest that the time to loss of culturability occurs more rapidly with suspensions of low cell concentration. Counts of viable cells in cell suspensions were confirmed using a *Bac*light cell viability kit (Figure 3.1 Panel A and B). The culturable counts result showed that the 10^9 cells mL^{-1} suspension entered into the VBNC state in 36 d at 4°C in 2.5% NaCl ASW solution. For suspensions prepare with 10^9 and 10^7 cells mL^{-1} at the commencement of the storage experiment, *ca.* 10^8 and 10^6 cells mL^{-1} respectively of viable cells remained when these suspensions were stored for 43 d at 4°C in 2.5% NaCl ASW solution. The viability of cell suspensions containing 10^5 and 10^3 cells mL^{-1} were not recorded as the cell numbers of the starting suspensions were below the detection limit of the viability assay.

Results obtained for suspensions prepared in ASW containing 5% NaCl at pH 8 are shown in Figure 3.2. Panels C and D show the changes in culturability for suspensions prepared with 10^3 and 10^5 cells mL^{-1} and incubated at 4°C. As described above, the times to loss of culturability recorded were shorter (<8 d) than those recorded for high concentration cell suspensions incubated under identical conditions (24 and 36 d respectively) (Figure 3.2 Panel A and B). Similarly, estimates of viable counts obtained using the *Bac*light cell viability kit (Figure 3.2 Panel A and B) showed that although loss of culturability was observed after 36 d for suspensions containing 10^9 cells mL^{-1} incubated at 4°C, viable counts of *ca.* 10^8 cells mL^{-1} remained after 43 d of incubation (Figure 3.2 Panel A). The viability of suspensions containing 10^7 cells mL^{-1} also remained high (Figure 3.2 Panel B).

The described trends of changes in culturability and viability of cell suspensions stored at 4°C were essentially the same for cell suspensions prepared in ASW containing 10% NaCl at pH 8.0 (Figure 3.3). All suspensions lost culturability within 16 d. Furthermore, counts of viable cells in suspensions containing 10^9 and 10^7 cells mL^{-1} were maintained at ca. 10^8 and 10^6 cells mL^{-1}. However, with the exception of cell suspensions prepared with 10^9 cells mL^{-1},

all other suspensions incubated at 20°C were noted to rapidly lose culturability. By contrast, the 10^9 cells mL^{-1} suspensions maintained culturability at a cell concentration of *ca*. 10^4 cells mL^{-1} (Figure 3.3 Panel A).

Figure 3.4 shows the time to loss of culturability as a function of initial cell suspension concentration when suspensions were incubated at 4°C. The data sets were obtained for cultures suspended in ASW containing 2.5, 5.0 and 10% NaCl. Cells suspended in ASW containing a high NaCl concentration (10% NaCl), required a shorter time to loss of culturability compared with cell suspensions incubated in either 2.5% and 5% NaCl. Moreover, the data shown indicates that the time to loss of culturability is dependent on initial cell suspension concentration. High concentration suspensions lose culturability more slowly than low concentration suspensions.

To further investigate the apparent effect of suspension concentration on time to loss of culturability at 4°C, the data for each initial suspension concentration presented in Figure 3.1, 3.2 and 3.3 were normalized and plotted against time of incubation. Figure 3.5 shows plots of $\ln(N/N_0)$[3] *vs* incubation time for suspensions prepared in ASW containing different concentrations of NaCl. Regression lines are fitted to the plotted data. Linear regression analysis indicated the data sets conformed to a first order equation[4]. Regression coefficients (r^2) obtained were highly significant. Irrespective of the NaCl concentration used to formulate the ASW media used, the analysis indicated the rate of loss of cell culturability is inversely dependent on initial cell concentration (Figure 3.5 Panel A, Panel B and Panel C). Visual inspection of Figure 3.5 indicates that the rate of loss of culturability for each initial cell suspension concentration are not the same, although the rate order is the same irrespective of NaCl concentration used to formulate the ASW. This observation is in marked contrast with widely accepted observations that the rate of cell death is independent of the concentration of viable cells present at any time. Consequently, these results indicate that the kinetics of loss of culturability of *V. parahaemolyticus* NCTC 10884 at 4°C is different from either cell death and growth.

---

[3] N_0 is the culturable count at the beginning of the incubat ion. N is the culturable count at any time t (d).

[4] First order equation : ln (N/N0) = -kt N: cell counts N0: initial cell counts k: constant t: time (d)

3.3.2 Effect of Initial Cell Concentration and pH on Culturability

To examine the impact of pH on establishment of the VBNC state, *V. parahaemolyticus* NCTC 10884 was suspended in ASW containing 2.5% NaCl adjusted to pH 5, pH 8 and pH 9.5 and incubated at either 4 or 20°C. The culturability of the cells in suspension was monitored by plating samples on MA. Data obtained are presented as Figure 3.6, 3.7 and 3.8.

Figure 3.6 presents changes in culturability over a period of 28 d for cell suspensions prepared in ASW adjusted to pH 5. The culturability of suspensions with an initial cell concentration of 10^9 cells mL^{-1} incubated at 20°C did not fall below 10^8 cells mL^{-1} (Figure 3.6 Panel A). In fact, the culturable counts increased to *ca.* 10^{10} cells mL^{-1} in 28 d (Figure 3.6 Panel A). By contrast, suspensions with initial counts of 10^7, 10^5 and 10^3 cells mL^{-1}, became unculturable within 5 d at 20°C (Figure 3.6, Panels B, C and D). Suspensions containing initial cell numbers 10^9, 10^7, 10^5 and 10^3 cells mL^{-1} with incubation at 4°C became unculturable within 24, 12, 8 and 4 d respectively. Furthermore, the viability of suspensions containing 10^9 and 10^7 cells mL^{-1} incubated at 4°C (Figure 3.6 Panel A and B) did not fall below 10^8 and 10^6 cells mL^{-1}. As described in Section 3.3.1, the time to loss of culturability was dependent on initial suspension cell concentration. Importantly, ASW adjusted to pH 5 had a detrimental effect on the culturability of cell suspensions, for all cell concentrations used (except 10^9 cells mL^{-1}) and all incubation temperatures. This effect is evident from a comparison of data presented in Figure 3.1 and 3.6.

The changes in culturability of cell suspensions in ASW at pH 8 and stored in the dark at 4°C or 20°C without agitation for up to 38 d, followed trends similar to that reported for Figure 3.1. The culturability of suspensions of 10^9, 10^7, 10^5 and 10^3 cells mL^{-1} incubated at 20°C, retained culturability, although suspensions containing 10^9 cells mL^{-1} increased to *ca.* 10^{10} cells mL^{-1} over a period 38 d (Figure 3.7 Panel A), whereas all other suspensions were maintained at no less than 1 log unit lower than the initial counts at the beginning of the experiment. By contrast, the culturability of suspensions containing 10^9, 10^7, 10^5 and 10^3 cells mL^{-1} incubated at 4°C, decreased to undetectable levels in 38, 34, 8 and 12 d respectively (Figure 3.7 Panel B, C and D). The viability of suspensions incubated at 4°C or 20°C, did not change appreciably across the course of the experiment.

When cells were suspended in ASW adjusted to pH 9.5 followed by incubation in the dark at 4°C without agitation for up to 28 d, the counts of culturable cells decreased to rapidly

(Figure 3.8). The time to loss of culturability for suspensions containing 10^9, 10^7, 10^5 and 10^3 cells mL^{-1} was 12, 8, 8 and 4 d respectively. Counts of viable cells in suspensions incubated at 4°C remained stable throughout the course of the experiment. Of the suspensions incubated at 20°C, all except that containing 10^9 cells mL^{-1} (Figure 3.8, Panel A) were observed to undergo significant loss of culturability.

Figure 3.9 presents the time to loss of culturability as a function of the suspension cell concentration for each of the different pH conditions tested. As reported in Section 3.3.1 the time to loss of culturability was inversely related to suspension concentration, irrespective of the pH of the suspending medium. However, the time to loss of culturability for cells in a suspending medium with a near neutral condition (pH 8), was significantly longer than for cells incubated in suspending media with a pH of 5 or 9.5.

To further analyse the apparent effect of suspension concentration and pH on the rate of entry into the unculturable state at 4°C, the individual data for each initial suspension concentration presented in Figure 3.6, 3.7 and 3.8 were normalized and plotted against time of incubation. Figure 3.10 shows plots of $\ln(N/N_0)$ *vs* incubation time for suspensions prepared in ASW adjusted to pH 5, 8 or 9.5. Regression lines are fitted to the plotted data. Linear regression analysis indicated the data sets conformed to a first order equation[5]. Regression coefficients (r^2) obtained were highly significant. Irrespective of the suspending medium pH, the analysis indicated the rate of loss of cell culturability (slope of the regression line) is inversely dependent on initial cell concentration (Figure 3.10 Panel A, Panel B and Panel C). As described in Section 3.3.1, inspection of Figure 3.10 shows that the rate of loss of culturability for each initial cell suspension concentration are not the same, although the rate order is the same irrespective of the pH of the ASW. This observation supports the contention that the kinetics of loss of culturability of *V. parahaemolyticus* NCTC 10884 at 4°C is different from that observed for cell death and growth.

3.3.3 Effect of Cell Concentration and NaCl Concentration on Resuscitation

To further determine the possible impact of the cell concentration and NaCl concentration on the VBNC state resuscitation. Cells suspended in ASW containing 2.5, 5.0 or 10% NaCl at

[5] First order equation : $\ln (N/N0) = -kt$ N: cell counts N0: initial cell counts k: constant t: time (d)

pH 8, were incubated at 4°C until the culturability was reduced to an undetectable level. These non-culturable cells were then subjected to a temperature upshift to 20°C and the culturability monitored by plating samples of cells on MA. The changes in culturability observed are presented in Figure 3.11.

When suspensions of VBNC cells suspended in ASW containing 2.5% NaCl were shifted from 4°C to 20°C, the VBNC state cultures underwent resuscitation to a culturable state (Figure 3.11 Panel A). Interestingly, only suspensions that contained initial cell numbers of 10^9 and 10^7 cells mL^{-1} could be resuscitated. The culturability of preparations of VBNC cells derived from suspensions with initial cell concentrations of 10^9 cells mL^{-1} increased to 4.7×10^5 cells mL^{-1} 1 d after the temperature upshift and to 2.2×10^{11} cells mL^{-1} within 9 d. Similar changes in culturability were observed for VBNC cells derived from suspensions containing 10^7 cells mL^{-1} (63 cells mL^{-1} in 3 d and 7.5×10^5 cells mL^{-1} after 9 d). Preparations of VBNC cells prepared from lower concentrations of cells could not be resuscitated.

VBNC state cells suspended in ASW containing 5% NaCl (Figure 3.11 Panel B), but not 10% NaCl (data not shown), could also be resuscitated by temperature upshift from 4 to 20°C, albeit that only preparations containing an initial cell concentration of 10^9 cells mL^{-1} could be resuscitated (1.2×10^4 cells mL^{-1} after 1 d and 1.1×10^{10} cells mL^{-1} after 9 d).

3.3.4 Effect of Cell Concentration and pH on Resuscitation

To further determine the possible impact of the cell concentration and pH on the VBNC state resuscitation, cells suspended in ASW containing 2.5% NaCl adjusted to pH 5, 8 and 9.5 were incubated at 4°C until the culturability was reduced to an undetectable level. These non-culturable cells were then subjected to a temperature upshift to 20°C and the culturability monitored by plating samples of cells on MA. The changes in culturability observed are presented in Figure 3.12.

VBNC state cells prepared from suspensions in ASW at pH8 containing initial concentrations of 10^9 and 10^7 cells mL^{-1} were able to be resuscitated. For example, the culturability of VBNC suspensions prepared with 10^9 cells mL^{-1} increased to 4.7×10^5 cells mL^{-1} after 1 d and 6×10^9 cells mL^{-1} after 9 d at 20°C. Similarly the culturability of suspensions prepared from 10^7 cells mL^{-1} suspension increased to 3.6×10^3 cells mL^{-1} and 3.2×10^7 cells mL^{-1} after 1 and 9 d respectively. However, no resuscitation occurred for

suspensions of VBNC cells of lower concentration. Furthermore, the non-culturable suspensions prepared in ASW adjusted to pH 5 and pH 9.5 at 4°C could not be resuscitated (data not shown).

3.4 Discussion

The primary purpose of this work described in this chapter was to examine the impact of intrinsic (cell concentration) and extrinsic (NaCl concentration and pH) factors on induction of the VBNC state in suspensions of *V. parahaemolyticus* NCTC 10884. The effect of these factors on resuscitation was also evaluated.

The VBNC state induction of *V. parahaemolyticus* is not easily achieved (Wolf & Oliver, 1992). However, Jiang et al. (1996) indicated that *V. parahaemolyticus* cells can reach the VBNC state within 35 to 80 d at 3.5°C when suspended in starvation medium (2.6% NaCl and pH 7.8) (Jiang, 1996). For this reason, induction of VBNC state in *V. parahaemolyticus* is a very time consuming process if supplies of VBNC cells are to be prepared for both physiological and pathological studies.

Wong et al. (2004) indicated that the time of the VBNC state induction can be reduced to about 35 d by suspending mid-exponential phase cells in 0.5% NaCl of a starvation medium followed by incubation at 4°C. However, when the cells were incubated at higher NaCl concentrations (1 - 3%), the induction time required increased to 40 to 55 d (Wong & Wang, 2004). In results reported in this chapter, early exponential phase cells entered a VBNC state within 36 d when suspended in ASW containing 2.5% NaCl at pH 8.0 (Figure 3.1). Overall, the times to loss of culturability presented are consistent with data reported by other studies. For example, (Bates & Oliver, 2004) reported that cell suspensions of 10^5 cells mL^{-1} *V. parahaemolyticus* Kanagawa Postive (Kp) and Kanagawa Negative (Xu et al., 1994a) strains achieved nonculturability within 7 d. Furthermore, Wong et al. (2004) showed that suspensions containing 10^8 cells mL^{-1} of *V. parahaemolyticus* NCTC 10884 need more than 20 d to reach the VBNC state. Although, the 0.5 to 3% NaCl concentrations were used in Wong's study, the time to reach the VBNC state required more than 20 d (Wong & Wang, 2004). Indeed the results reported here showed that the times to loss of culturability in ASW containing a range of NaCl concentrations vary. However suspensions incubated in ASW containing 2.5 - 5% NaCl allow *V. parahaemolyticus* NCTC 10884 to enter the VBNC state,

whereas NaCl concentrations outside this range (eg. 10%) may represent a potentially lethal environmental stress to the bacteria that results in rapid loss of culturability (see the following discussion)

Similarly, the pH of the ASW medium was determined to affect the time to induction of the VBNC state. The pH required for induction of the VBNC state was pH 8.0 in ASW containing 2.5% NaCl concentrations of salt. Exposure to lower (pH 5.0) or higher (pH 9.5) resulted in more rapid loss of culturability (Figure 3.9), although no loss in viability was observed. This suggested that *V. parahaemolyticus* NCTC 10884 was able to enter a viable but non-culturable state irrespective of the NaCl concentration or the suspending medium pH used in this study. These results are consistent with other studies (Wong et al., 1998).

Although the NaCl concentration and pH of the suspending medium affected the rate of loss of culturability, these factors apparently did not affect cell viability. The combination of these observations indicated that these cells had entered a VBNC state from a definitional point of view. However it is clear from attempts to resuscitate these VBNC state cells, that there are important differences in the physiological status (of the VBNC state cells) that are dependent on the prevailing NaCl concentration and pH of the suspending medium. Typically VBNC state cells can be resuscitated to a culturable state by exposure to a temperature upshift (Whitesides & Oliver, 1997). The resuscitation results presented, suggest that VBNC cells suspended in media adjusted to NaCl concentrations and pH close to the *V. parahaemolyticus* growth optima (2.5% NaCl, pH8.5) (see ICMSF, 1996) were able to be resuscitated. Conversely, VBNC cells suspended in media adjusted to NaCl concentrations (10% NaCl) and pH (5.0 or 9.5) typical of the biological extremes for this organism, were not able to be resuscitated by a temperature upshift to 20°C. Whether these results reflect intrinsic differences in VBNC state cells that are the result of exposure to the inducing medium, or simply the adverse effects of high suspending medium NaCl concentration and pH extremes on the normal function of cellular transport systems, electron transport and the activity of various essential cellular enzymes, is unclear. Nevertheless, it is clear from the work presented, that suspending medium NaCl concentration and pH can have profound effects on the rate of entry into the VBNC state and probably more importantly, resuscitation from that state.

Interestingly, analysis of the rate of loss of culturability by *V. parahaemolyticus* NCTC 10884 cell suspensions at 4°C, showed a dependence on the initial cell suspension population size. This rate dependence on initial cell suspension concentration was consistent across the range of salinities and pH tested. This observation has not been previously reported and may have gone unnoticed because all studies of induction of a VBNC state have employed a single initial cell suspension concentration. Typically the cell concentrations used have been in excess of 10^7 cells mL^{-1}.

The dependence of the rate of loss of culturability on the initial cell suspension population density is remarkable. Bacterial cell population growth and death are universally described as conforming to a log-linear, first order reaction model in which the growth rate, or death rate constant in the log phase of population is independent of the initial cell concentration. This suggests that the rate entry into the non-culturable state represents a situation where there is a dependence on other neighbouring cells. There are several possible explanations for the observed response. It is interesting to speculate that this dependence could involve any of the following:

- supply of maintenance nutrients/energy from dead cell neighbours.
- population density critical molecular signals that govern entry into the VBNC state, or
- a distribution of cells with differing sensitivities to stress. At low densities, these may not be detected using plating methods, although at high densities these cells would be easily enumerated and these cells may influence the rate of loss of culturability.

Any of these possibilities would be dependent on the initial population density size of suspensions incubated under conditions required to initiate the VBNC state. The more cells present, the more nutrients available as a source of maintenance energy, or the higher the concentration of some required molecular signal needed to initiate effective entry to the VBNC state.

This observation is made more interesting by the fact that cell suspensions containing 10^5 cells mL^{-1} or less could not be resuscitated by a temperature upshift. Failure to resuscitate may reflect the maintenance energy status of VBNC cells, sub-critical concentrations of an essential molecular signal required for resuscitation, or the presence of subpopulations of

stress resistant cells. The lower the initial population density, the lower the concentration of maintenance nutrients released from dead cells.

Thus VBNC state cells that lack an adequate source of maintenance energy, may well be unfit to resuscitate to the culturable state under permissive extrinsic conditions. Although VBNC state cells undergo major decreases in rates of respiration and macromolecular synthesis, plasmid DNA is retained and cellular levels of ATP and membrane potential are maintained. In addition Rahman et al. (1994) has reported that VBNC cells are able to take up amino acids and incorporate these into protein. Indeed, studies by Oliver and co-workers have shown that *V. vulnificus* cells are able to metabolize exogenously supplied nutrient at low temperatures (Oliver & Wanucha, 1989). Other studies that utilized RT-PCR have demonstrated that VBNC cells remain metabolically active. For example, rRNA genes are expressed by non-culturable *E. coli* cells (Yaron & Matthews, 2002). Clearly VBNC state cells are not inactive and consequently must require a source of maintenance energy to enable the sorts of basic cellular activities required to ensure survival. Thus if only a small proportion of cells from high density populations were to die and release nutrients, then these may provide the necessary maintenance requirements that could not be provided by low density populations of cells. This scenario could be tested by simple experimental systems that allow removal (eg. dialysis) of small molecular weight molecules that could act as a source of nutrients from the cell suspension medium.

A similar scenario would apply to suspensions that lacked the critical concentrations of a molecular signal(s) needed to initiate resuscitation. Studies by Oliver (1995) however, have shown that VBNC state cells placed in a diffusion chamber were able to be resuscitated using standard methods. This observation suggested that molecular signals may not be required for initiating resuscitation.

Counts of *V. parahaemolyticus* in refrigerated foods are known to rapidly decrease. Whether this reduction in culturable counts is the result of establishment of VBNC state cells has yet to be proven. If this were the case, then it could be argued that these bacteria convert to VBNC state cells in a biologically compatible environment that may provide the maintenance nutrients necessary for rapid resuscitation at elevated temperatures. During starvation conditions (eg. open sea environments) however, VBNC state cells may not have access to sufficient reserves of nutrients to allow efficient resuscitation.

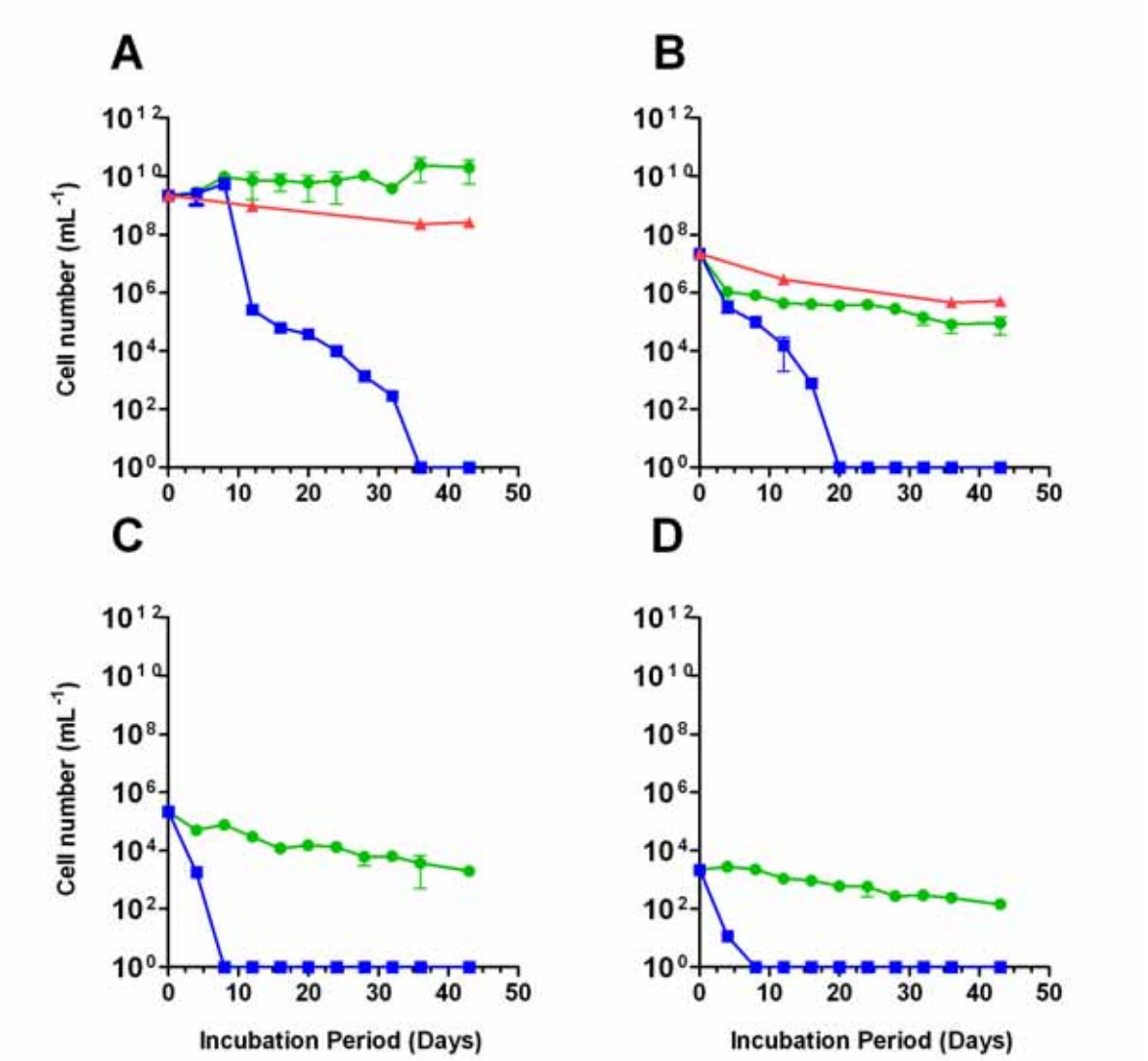

Figure 3.1: Counts of *V. parahaemolyticus* cells incubated in ASW containing 2.5% NaCl at 4°C and 20°C.

Data shows cell counts of washed cell suspensions of *V. parahaemolyticus* NCTC 10884 adjusted to approximately 10^9 (Panel A), 10^7 (Panel B), 10^5 (Panel C) and 10^3 (Panel D) cells mL^{-1} in ASW containing 2.5% NaCl (pH 8). These suspensions were incubated at 4°C (blue square) and 20°C (green circle). Counts of culturable cells were estimated by plating on Marine Agar and total viable cell counts were determined using a *Bac*light Live/Dead kit (red triangle). Counts are showed on a Log_{10} scale. Each data point is the mean of three independent measurements. Error bars represent the standard deviation about the mean.

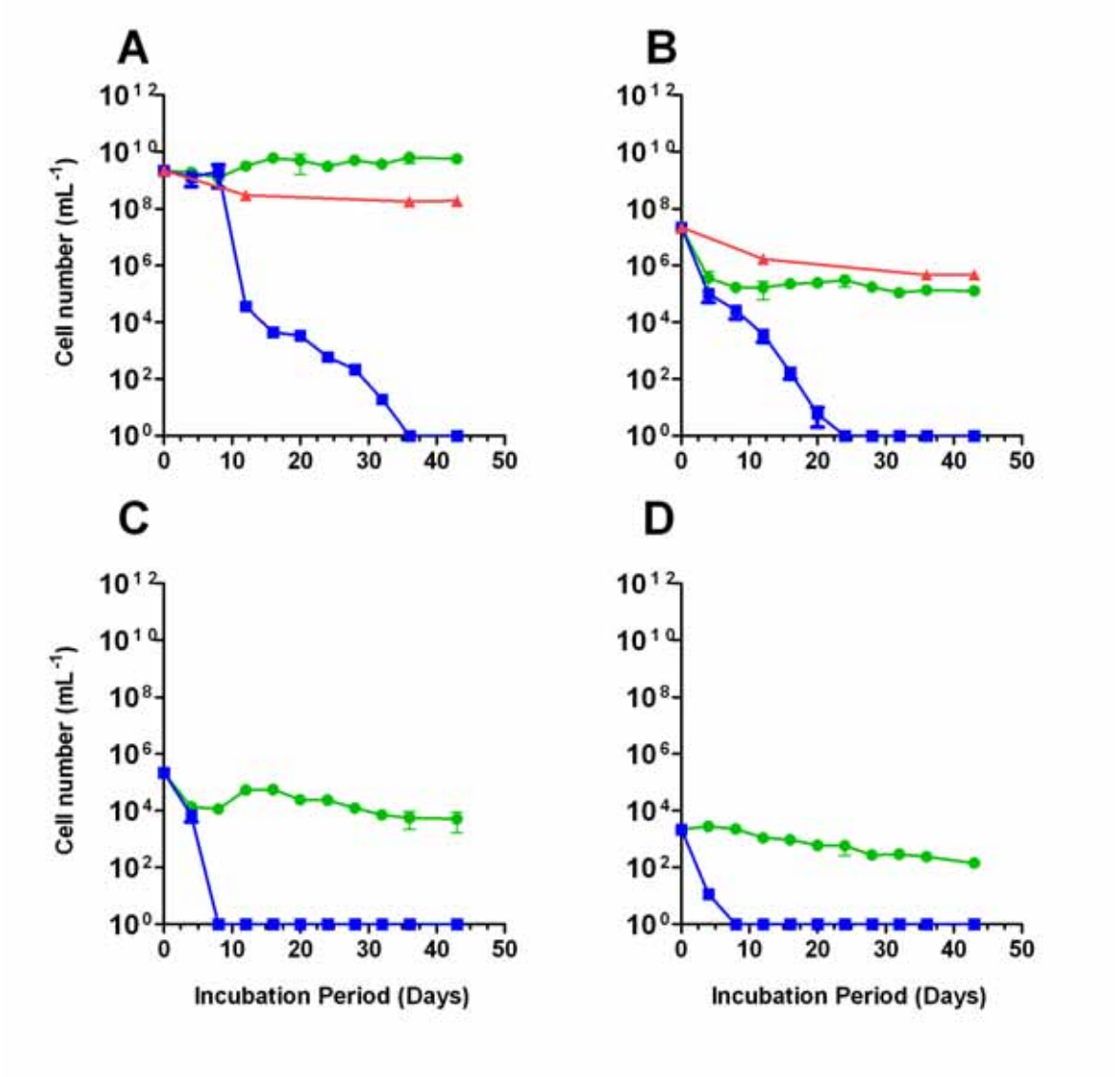

Figure 3.2: Counts of *V. parahaemolyticus* cells incubated in ASW containing 5.0% NaCl at 4°C and 20°C.

Data shows cell counts of washed cell suspensions of *V. parahaemolyticus* NCTC 10884 adjusted to approximately 10^9 (Panel A), 10^7 (Panel B), 10^5 (Panel C) and 10^3 (Panel D) cells mL^{-1} in ASW containing 5.0% NaCl (pH 8). These suspensions were incubated at 4°C (blue square) and 20°C (green circle). Counts of culturable cells were estimated by plating on Marine Agar and total viable cell counts were determined using a *Bac*light Live/Dead kit (red triangle). Counts are showed on a Log_{10} scale. Each data point is the mean of three independent measurements. Error bars represent the standard deviation about the mean.

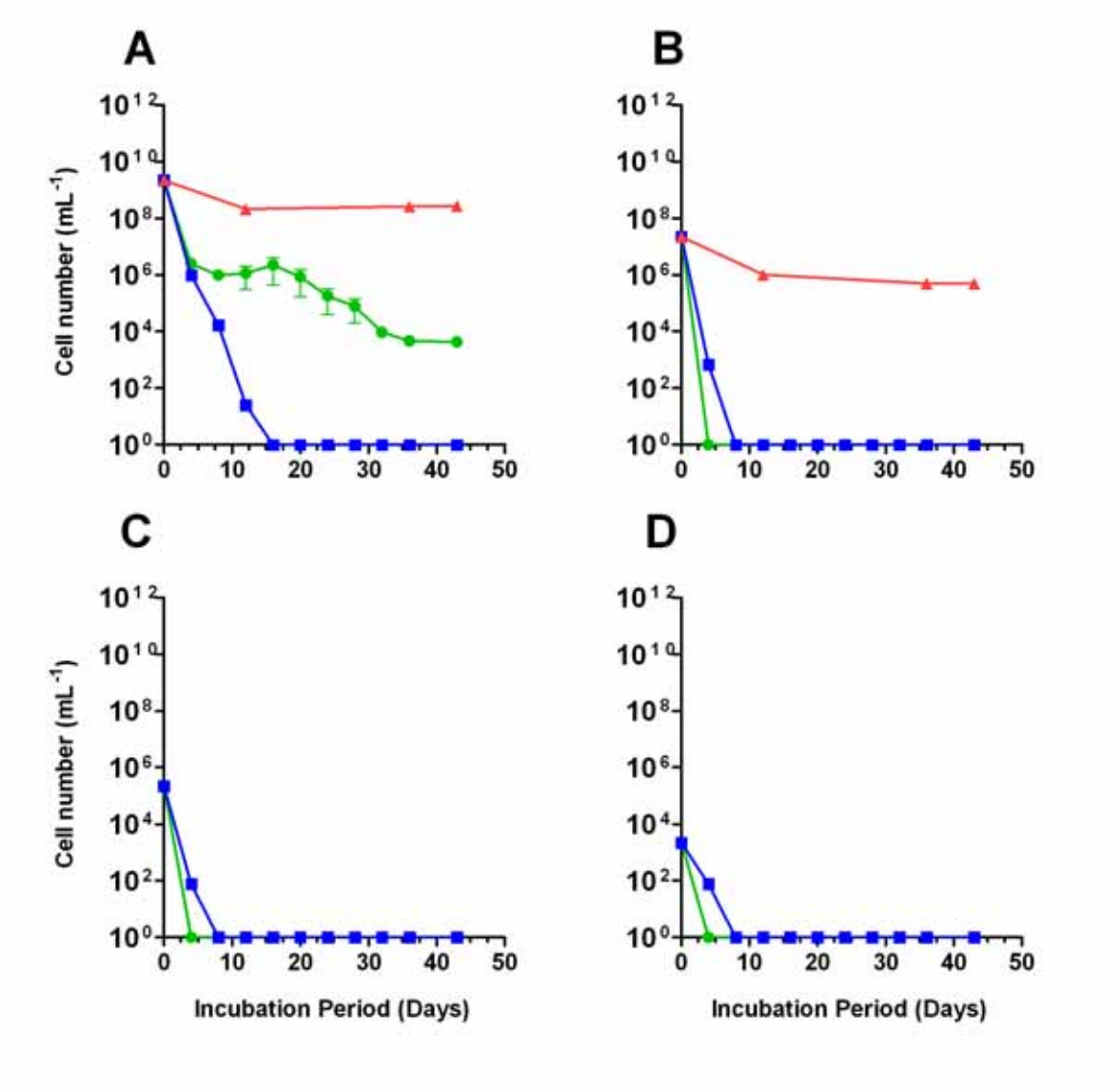

Figure 3.3: Counts of *V. parahaemolyticus* cells incubated in ASW containing 10% NaCl at 4°C and 20°C.

Data shows cell counts of washed cell suspensions of *V. parahaemolyticus* NCTC 10884 adjusted to approximately 10^9 (Panel A), 10^7 (Panel B), 10^5 (Panel C) and 10^3 (Panel D) cells mL^{-1} in ASW containing 10% NaCl (pH 8). These suspensions were incubated at 4°C (blue square) and 20°C (green circle). Counts of culturable cells were estimated by plating on Marine Agar and total viable cell counts were determined using a *Bac*light Live/Dead kit (red triangle). Counts are showed on a Log_{10} scale. Each data point is the mean of three independent measurements. Error bars represent the standard deviation about the mean.

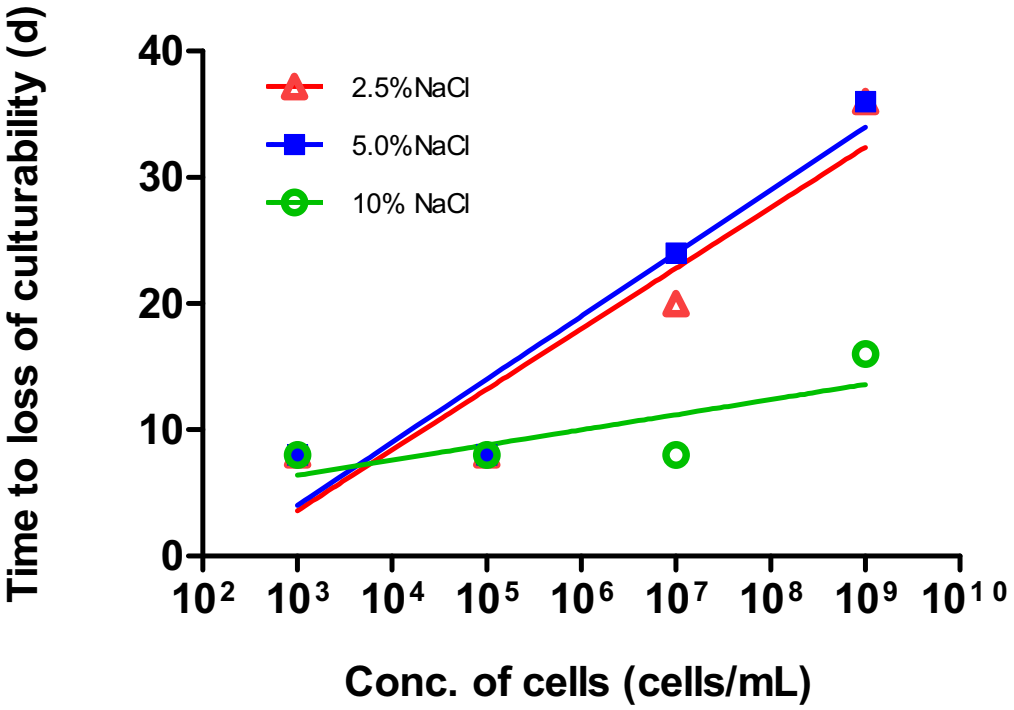

Figure 3.4: Time to loss of culturability of *V. parahaemolyticus* cells suspended in ASW containing different levels of NaCl.

Estimates of the time to loss of culturability for *V. parahaemolyticus* NCTC 10884 suspended in ASW containing different concentrations of NaCl were determined from data shown in Figures 3.1, 3.2 and 3.3. Data were plotted as a function of suspension concentration. The cells were incubated at 4°C pH 8 in ASW containing 2.5%, 5% and 10% NaCl.

Figure 3.5: Plots of $\ln(N/N_0)$ *vs.* time at 4°C in ASW with different levels of NaCl.

Estimates of the $\ln(N/N_0)$ for *V. parahaemolyticus* NCTC 10884 suspended in ASW containing 2.5, 5.0 or 10% NaCl adjusted to pH 8 were determined from data shown in Figures 3.1, 3.2 and 3.3. Data were plotted as a function of time (d) incubation for each initial suspension concentration used. Data sets reflecting different initial concentrations (N_0) of *V. parahaemolyticus* NCTC 10884 are shown as: 1×10^9 (purple), 1×10^7 (blue) and 1×10^5 (green) cells mL^{-1}, Panel A: ASW containing 2.5% NaCl; Panel B: ASW containing 5.0% NaCl; Panel C: ASW containing 10.0% NaCl.

The solid lines are the linear regression lines fitted to indicate the rate of decrease in culturable cell counts of *V. parahaemolyticus* NCTC 10884. The values of r^2 are shown in Appendix F, G and H.

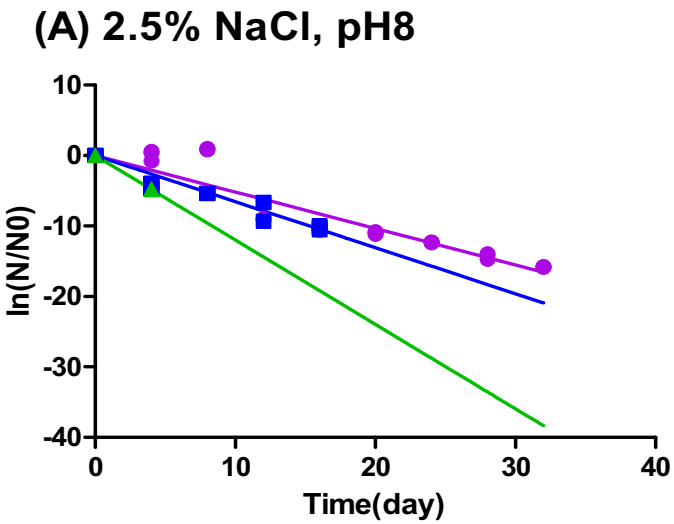
(A) 2.5% NaCl, pH8
ln(N/N0)
10
0
-10
-20
-30
-40
0
10
20
30
40
Time(day)

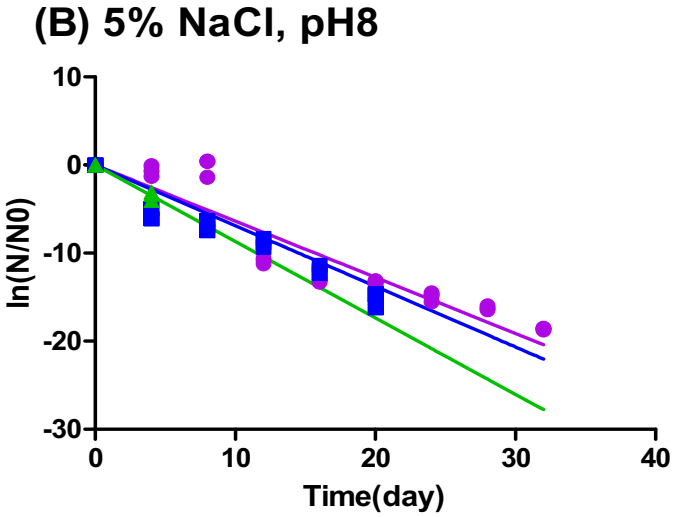
(B) 5% NaCl, pH8
ln(N/N0)
10
0
-10
-20
-30
0
10
20
30
40
Time(day)

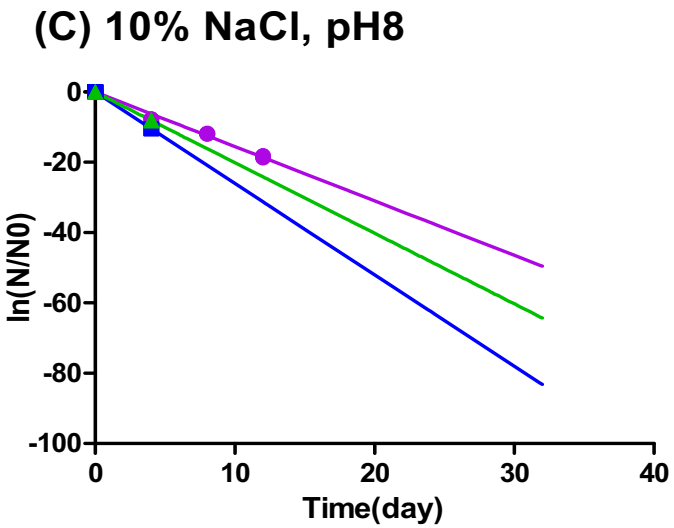
(C) 10% NaCl, pH8
ln(N/N0)
0
-20
-40
-60
-80
-100
0
10
20
30
40
Time(day)

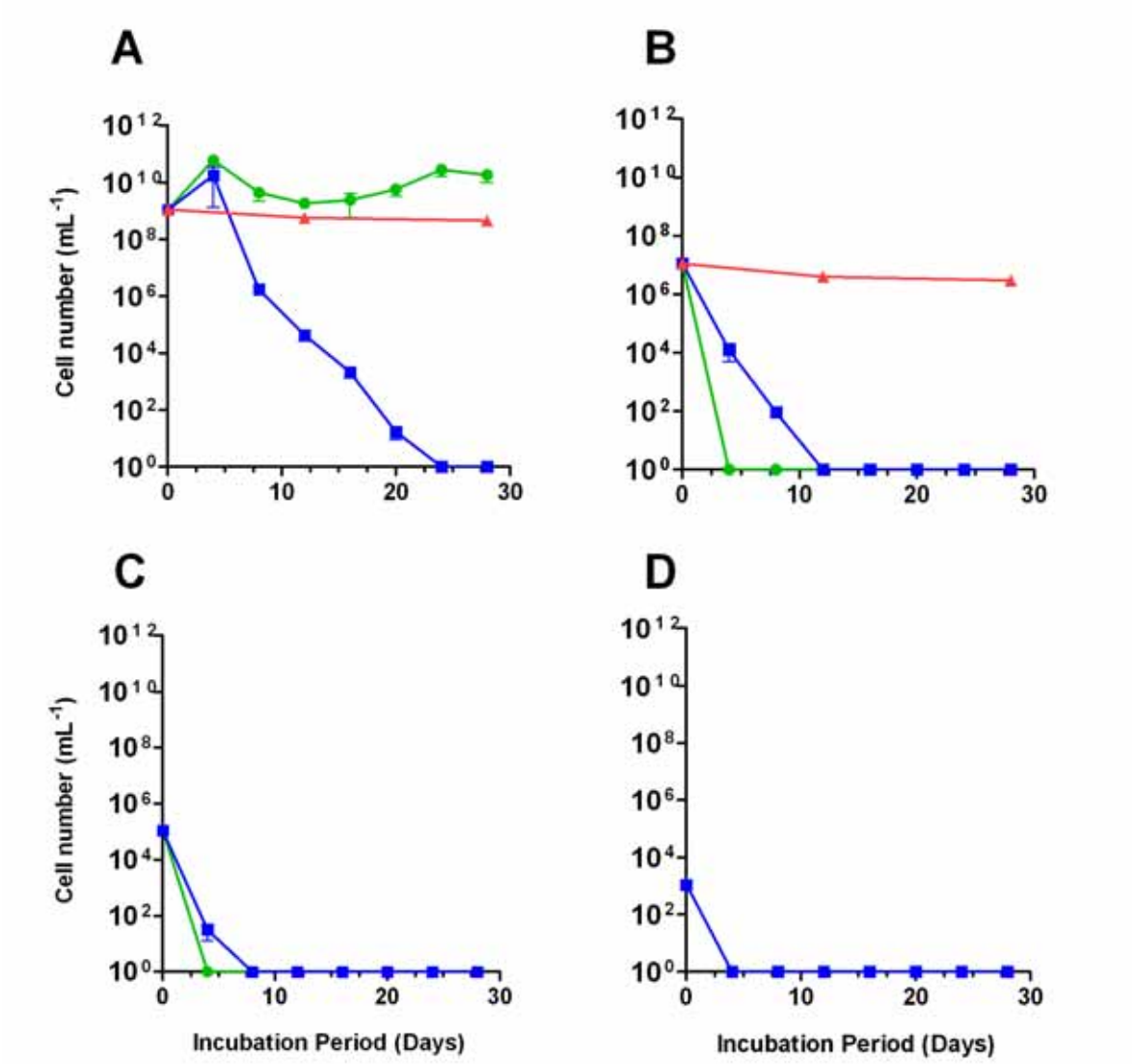

Figure 3.6: Counts of *V. parahaemolyticus* incubated at 4°C and 20°C in ASW at pH 5.

Data shows cell counts of washed cell suspensions of *V. parahaemolyticus* NCTC 10884 adjusted to approximately 10^9 (Panel A), 10^7 (Panel B), 10^5 (Panel C) and 10^3 (Panel D) cells mL^{-1} in ASW adjusted to pH 5. These suspensions were incubated at 4°C (blue square) and 20°C (green circle). Counts of culturable cells were estimated by plating on Marine Agar and total viable cell counts were determined using a *Bac*light Live/Dead kit (red triangle). Counts are showed on a Log_{10} scale. Each data point is the mean of three independent measurements. Error bars represent the standard deviation about the mean.

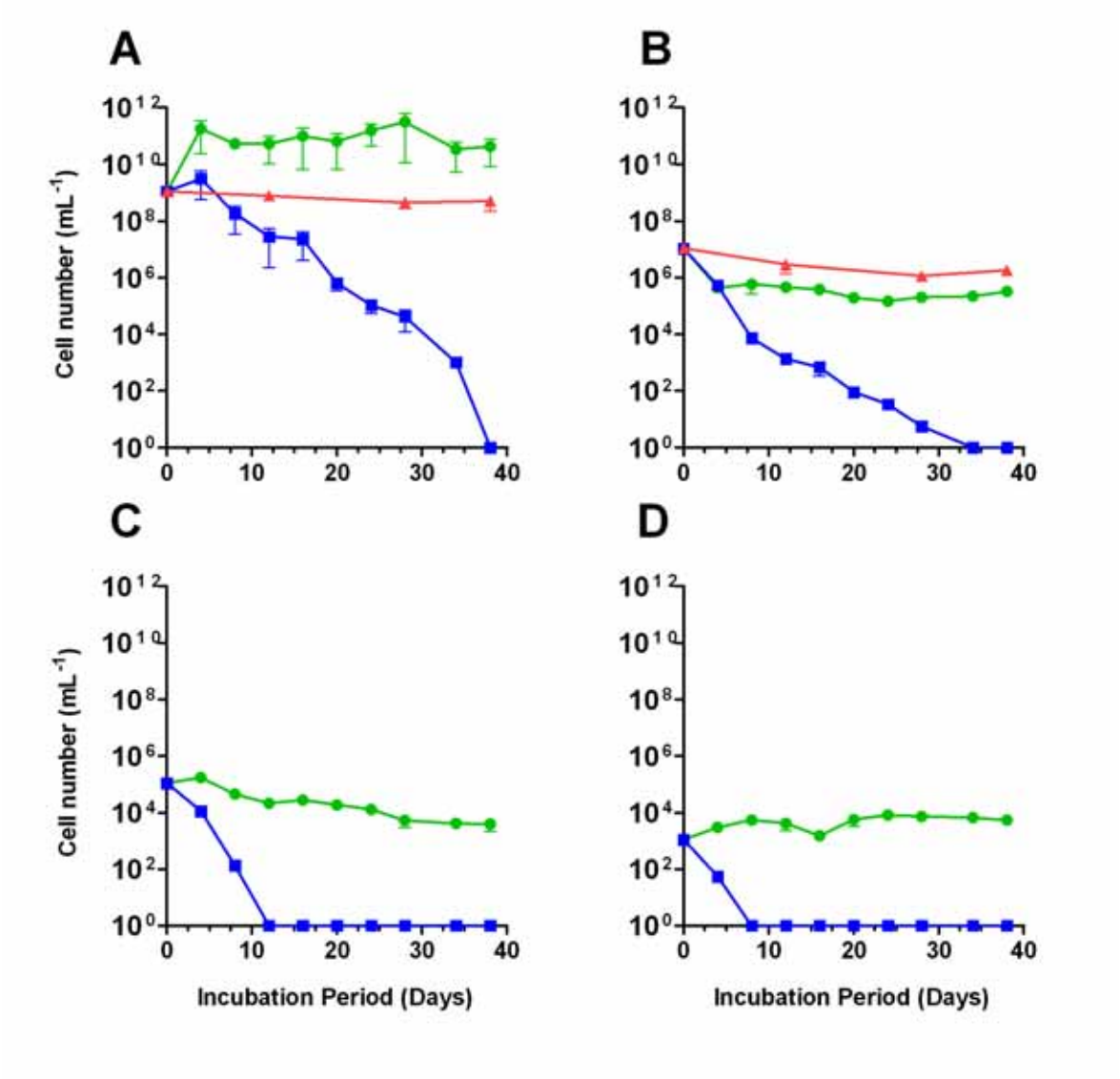

Figure 3.7: Counts of *V. parahaemolyticus* incubated at 4°C and 20°C in ASW at pH 8.

Data shows cell counts of washed cell suspensions of *V. parahaemolyticus* NCTC 10884 adjusted to approximately 10^9 (Panel A), 10^7 (Panel B), 10^5 (Panel C) and 10^3 (Panel D) cells mL^{-1} in ASW adjusted to pH 8. These suspensions were incubated at 4°C (blue square) and 20°C (green circle). Counts of culturable cells were estimated by plating on Marine Agar and total viable cell counts were determined using a *Bac*light Live/Dead kit (red triangle). Counts are showed on a Log_{10} scale. Each data point is the mean of three independent measurements. Error bars represent the standard deviation about the mean.

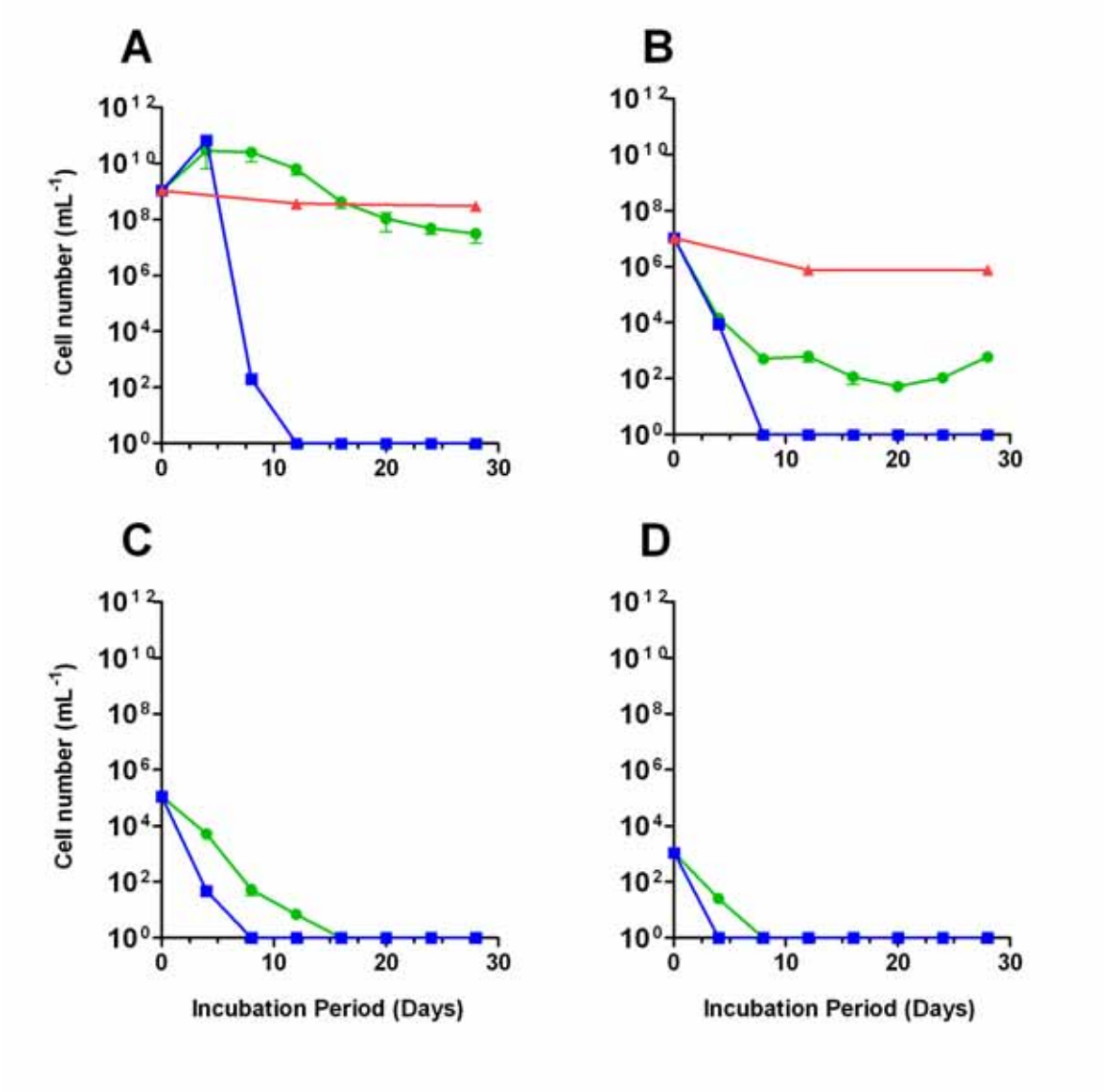

Figure 3.8: Counts of *V. parahaemolyticus* incubated at 4°C and 20°C in ASW at pH 9.5.

Data shows cell counts of washed cell suspensions of *V. parahaemolyticus* NCTC 10884 adjusted to approximately 10^9 (Panel A), 10^7 (Panel B), 10^5 (Panel C) and 10^3 (Panel D) cells mL^{-1} in ASW adjusted to pH 9.5. These suspensions were incubated at 4°C (blue square) and 20°C (green circle). Counts of culturable cells were estimated by plating on Marine Agar and total viable cell counts were determined using a *Bac*light Live/Dead kit (red triangle). Counts are showed on a Log_{10} scale. Each data point is the mean of three independent measurements. Error bars represent the standard deviation about the mean.

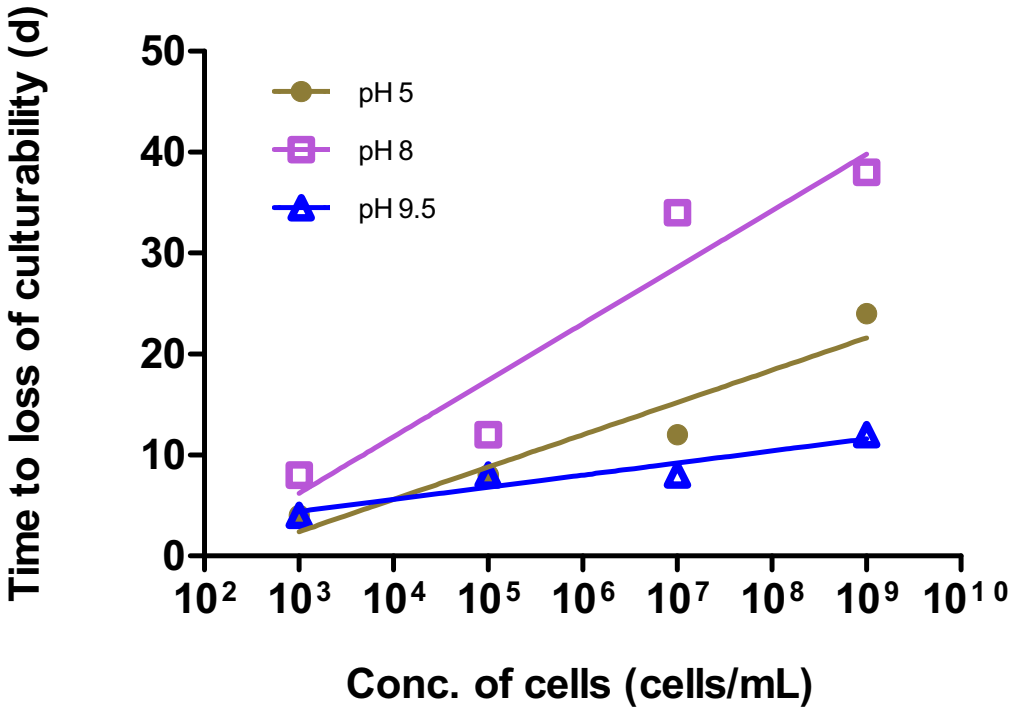

Figure 3.9: Effect of pH on time to loss of culturability of *V. parahaemolyticus* cells in ASW adjusted to different pH.

Estimates of the time to loss of culturability at 4°C for *V. parahaemolyticus* NCTC 10884 cells suspended in ASW containing 2.5% NaCl adjusted to pH 5, pH 8 and pH 9.5, were determined from data shown in Figures 3.6, 3.7 and 3.8. Data were plotted as a function of suspension concentration.

Figure 3.10: Plot of $\ln(N/N_0)$ versus time at 4°C in ASW adjusted to different pH.

Estimates of the $\ln(N/N_0)$ for *V. parahaemolyticus* NCTC 10884 suspended in ASW containing 2.5% NaCl adjusted to pH 5, pH 8 and pH 9.5, were determined from data shown in Figures 3.6, 3.7 and 3.8. Data were plotted as a function of time (d) incubation for each initial suspension concentration used. Data sets reflecting different initial concentrations (N_0) of *V. parahaemolyticus* NCTC 10884 are shown as: 1×10^9 (purple), 1×10^7 (blue) and 1×10^5 (green) cells mL^{-1}, Panel A: ASW adjusted to pH 5; Panel B: ASW adjusted to pH 8; Panel C: ASW adjusted to pH 9.5.

The solid lines are the linear regression lines fitted to indicate the rate of decrease in culturable cell counts of *V. parahaemolyticus* NCTC 10884. The values of r^2 are shown in Appendix I, J and K.

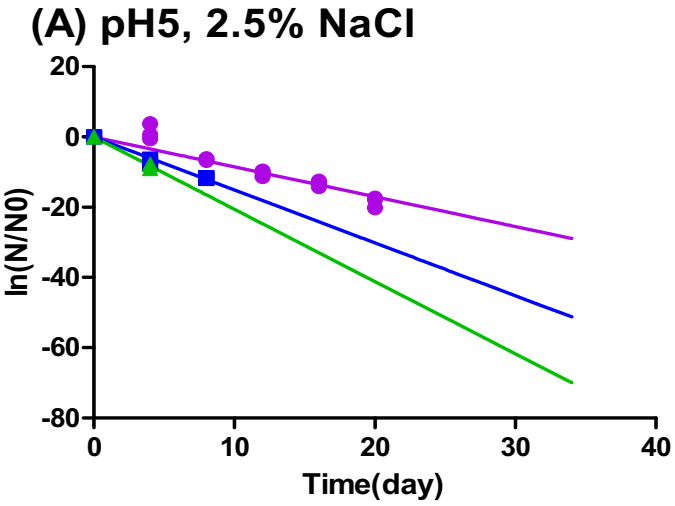
(A) pH5, 2.5% NaCl
ln(N/N0)
20
0
-20
-40
-60
-80
0
10
20
30
40
Time(day)

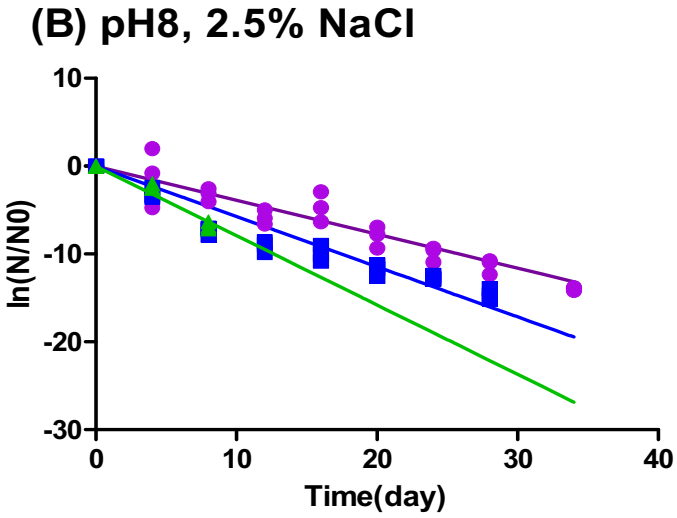
(B) pH8, 2.5% NaCl
ln(N/N0)
10
0
-10
-20
-30
0
10
20
30
40
Time(day)

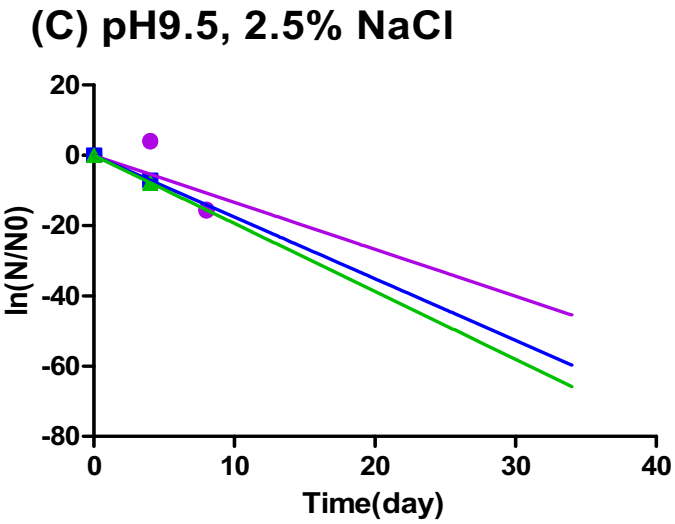
(C) pH9.5, 2.5% NaCl
ln(N/N0)
20
0
-20
-40
-60
-80
0
10
20
30
40
Time(day)

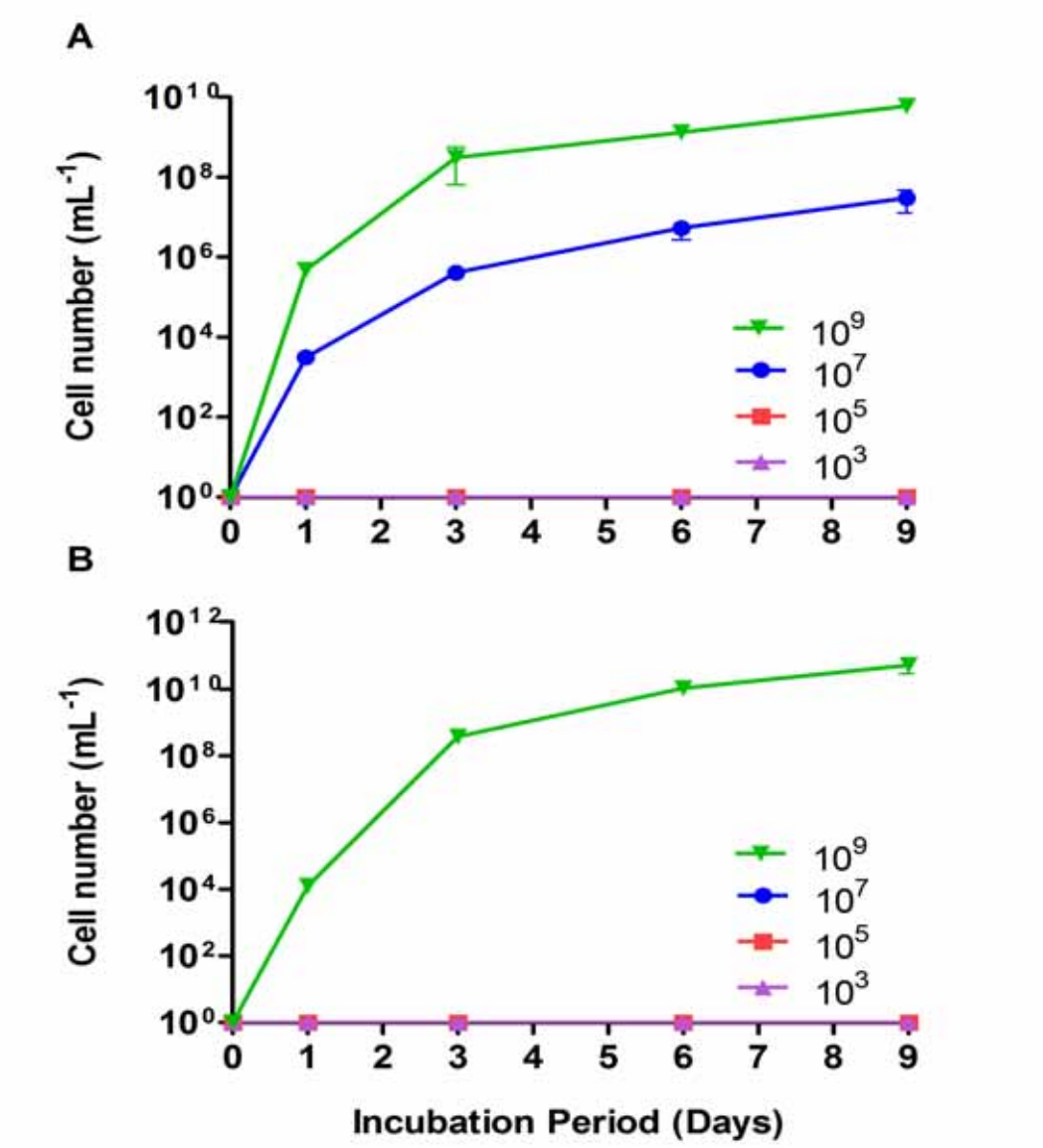

Figure 3.11: Counts of *V. parahaemolyticus* during resuscitation from the VBNC state from 4°C upshift to 20°C in 2.5% NaCl (Panel A) and 5% NaCl (Panel B) of ASW.

VBNC state cells, prepared by incubation at 4°C were resuscitated by incubation at 20. Cell counts were estimated by plating cell suspensions on Marine Agar. Counts are showed on a Log_{10} scale. Each data point shown is the mean of three independent measurements. Error bars represent the standard deviation about the mean.

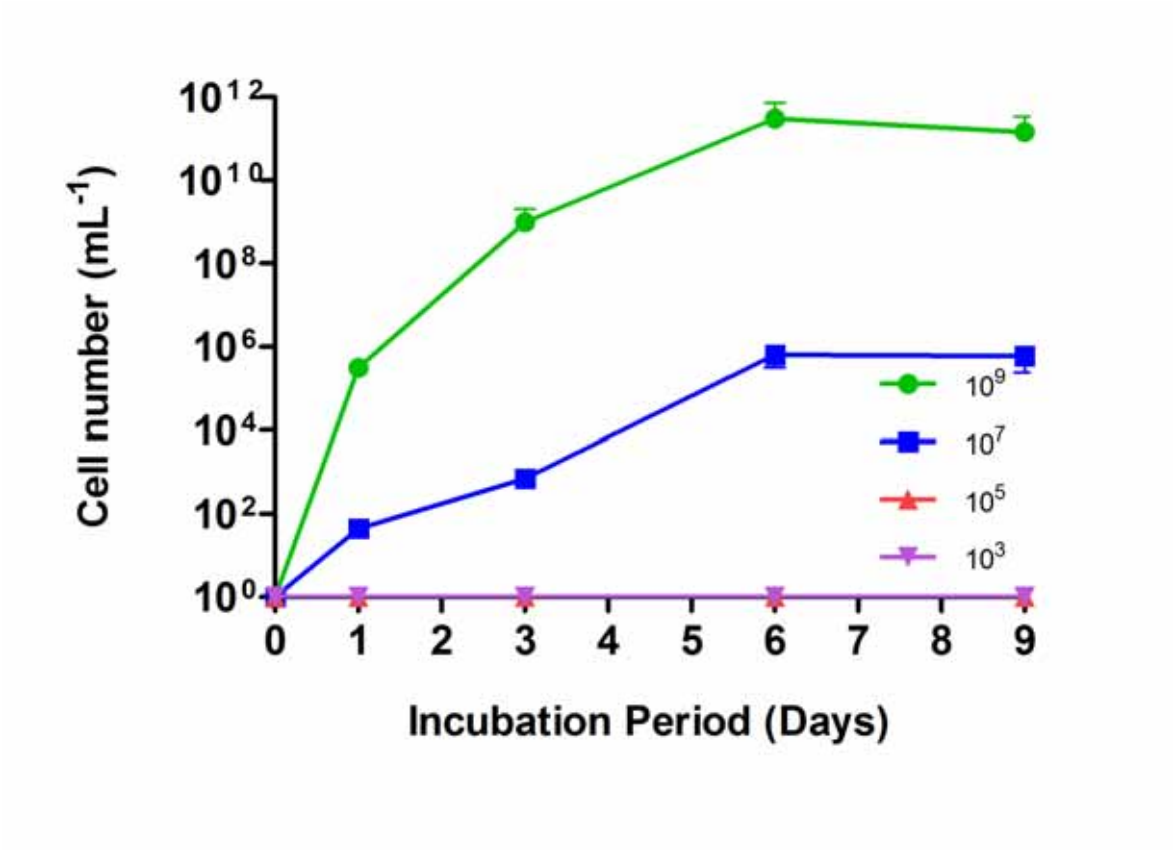

Figure 3.12: Counts of *V. parahaemolyticus* NCTC 10884 during resuscitation from the VBNC state from 4°C upshift to 20°C in pH 8 of ASW.

VBNC state cells, prepared by incubation at 4°C, were resuscitated by incubation at 20°C. Cell counts were estimated by plating cell suspensions on Marine Agar. Counts are showed on a Log_{10} scale. Each data point shown is the mean of three independent measurements. Error bars represent the standard deviation about the mean.

Chapter 4: The role of YeaZ in the VBNC state

4.1 Introduction

The induction of the VBNC state can be achieved by exposure of bacteria to starvation (Cook & Bolster, 2007) and low temperature conditions (Maalej et al., 2004; Valérie et al., 2002; Wong & Wang, 2004). Results presented in Chapter 3, provided evidence that the starvation and low temperature stresses are able to induce the VBNC state in *V. parahaemolyticus* NCTC 10884. Furthermore, a temperature upshift is able to stimulate recovery from the VBNC state. However, what has not been previously appreciated is the fact that induction of VBNC *V. parahaemolyticus* NCTC 10884 by exposure to low temperatures occurs in a cell concentration dependent manner and that resuscitation only occurred for high cell concentration (10^9 and 10^7cells mL^{-1}). It is interesting to speculate that dead cells in high density suspensions may release nutrients and other small molecular weight molecules that provide maintenance energy requirements for VBNC cells and assist recovery of VBNC state cells. Indeed various factors have been shown to mediate resuscitation from stress conditions e.g. temperature upshift (Du et al., 2007; Gupte et al., 2003; Nilsson et al., 1991; Weichart et al., 1992; Whitesides & Oliver, 1997; Wong & Wang, 2004), biological mediators (Cappelier et al., 1999; Colwell et al., 1996b; García et al., 2007; Sussman et al., 2003), autoinducers (Freestone et al., 1999; Reissbrodt et al., 2002; Sperandio et al., 2003) and resuscitation promoting factors (Mukamolova et al., 1998; Shleeva et al., 2002; Shleeva et al., 2004). Significantly, a resuscitation promoting factor in Gram negative bacteria called YeaZ in *S.* Typhimurium LT2 ($YeaZ_{ST}$) has been recently described (Panutdaporn et al., 2006). $YeaZ_{ST}$ is a 233 amino acid protein with a molecular weight of 25 kDa that apparently plays an important role in resuscitation of both *S.* Typhimurium LT2 and *S. enterica* serotype Oranienburg cells from the VBNC state (Panutdaporn et al., 2006).

YeaZ homologs are ubiquitous among G-ve bacteria. Sequence alignment analysis indicated that the YeaZ protein sequence in *V. parahaemolyticus* NCTC 10884 shared 56% similarity in amino acid sequence to the YeaZ of *S.* Typhimurium LT2 (Figure 1.12). In addition, $YeaZ_{ST}$ has been reported as a putative homolog of *Pasteurella haemolytica* M22 Gcp O-sialoglycoprotein endopeptidase (Nichols et al., 2006). Amino acid sequence BLAST

analysis (Altschul et al., 1990) showed that *V. parahaemolyticus* NCTC 10884 YeaZ ($YeaZ_{Vp}$) protein also has been proposed to have M22 O-sialoglycoprotein endopeptidase homolog. However, the role of the $YeaZ_{Vp}$ in resuscitation correlation with the VBNC state is not known.

Given that $YeaZ_{ST}$ has a demonstrated role in maintenance and escape from the VBNC state, it is of interest to examine whether $YeaZ_{Vp}$ has a function in resuscitation for *V. parahaemolyticus* NCTC 10884. Therefore, the principal aim of the work described in this chapter was to confirm a role for $YeaZ_{Vp}$ in the *V. parahaemolyticus* NCTC 10884 VBNC state.

4.2 Experimental Approach

The following approaches were used to characterize aspects of the role of the *yeaZ* in the VBNC state induction and resuscitation.

1. To investigate the role of *yeaZ* in the VBNC state, a *V. parahaemolyticus* NCTC 10884 non-polar *yeaZ* insertion mutant and *yeaZ* complement were constructed. The two constructs were used to determine the role of *yeaZ* by comparing the VBNC state induction and resuscitation in the wild-type *V. parahaemolyticus* NCTC 10884.
2. C-terminal His tag technologies were used to express the YeaZ recombinant protein.
3. Purified YeaZ recombinant protein was used to prepare rabbit polyclonal antiserum for immunoblotting. The YeaZ protein localization in *V. parahaemolyticus* NCTC 10884 was investigated by western blot and immuno-fluorescence (IF) microscope.
4. The YeaZ expression in *V. parahaemolyticus* NCTC 10884 during the VBNC state induction and resuscitation was investigated by quantitative real-time polymerase chain reaction (qRT-PCR).
5. The cell morphology changes in the VBNC state and resuscitation state *V. parahaemolyticus* NCTC 10884 were examined by transmission electron microscopy (TEM).

4.3 Results

4.3.1 Characterization of *yeaZ$_{Vp}$* Nucleotide and Amino Acid Sequence

The YeaZ ORF comprises 699 nucleotides (Genbank accession BA000031) and encodes 233 amino acids with a predicted molecular weight of 25 kDa (Figure 4.1). A BLAST comparison (Altschul et al., 1990) of the YeaZ$_{Vp}$ amino acid sequence with other sequences from the GenBank non-redundant amino acid sequence data base indicated that the sequence is similar to hypothetical proteins, M22 O-sialoglycoprotein endopeptidase and inactive metal-dependent protease (Nichols et al., 2006). Notably, the YeaZ$_{Vp}$ sequence shares 56% amino acid sequence similarity to the YeaZ$_{ST}$ (Chapter 1, Figure 1.12).

4.3.2 Cloning the *yeaZ* gene from *V. parahaemolyticus* strain NCTC 10884

Chromosomal DNA was isolated from *V. parahaemolyticus* NCTC 10884 using methods described in Chapter 2 (Section 2.9.1). This DNA was used as a template to PCR amplify a 1561 bp fragment encoding *yeaZ*. The primer pair RPFmu*Sph*IF/R introduced two *Sph*I sites at each end of the amplicon to facilitate cloning. The amplicon was purified by agarose gel electrophoresis and then isolated by gel extraction (Figure 4.2). The 1561 bp amplicon was then ligated to pGEM-T Easy vector (Promega) (Table 2.3) to produce plasmid pCTX100 (Figure 4.3). Plasmid pCTX100 was used to transform chemically competent *E. coli* DH5α cells (Table 2.1 and Chapter 2, Section 2.9.7). Transformants were selected based on blue/white colour selection on LB plates containing Amp, X-gal and IPTG with O/N incubation at 37°C. White colonies were selected, used to extract plasmid DNA and these clones confirmed to contain the 1561 bp insert by PCR and DNA sequencing (Appendix L).

4.3.3 Mutagenesis of *yeaZ$_{Vp}$*

In order to produce a deletion mutation of the ORF *yeaZ*, an 850 bp kanamycin resistance (*aphA3*) cartridge DNA fragment was isolated from pUC18K and cloned into *Eco*RI/*Pst*I digested pCTX100 to produce plasmid pCTX101 (Figure 4.4). This construct resulted in deletion of a 521 bp fragment from *yeaZ* followed by insertion of the kanamycin resistance cartridge. Plasmid pCTX101 was used to transform chemically competent *E. coli* DH5α cells. Transformants containing pCTX101 were selected by plating on LB containing Kan with

incubation at 37°C O/N. Colonies containing pCTX101 were confirmed by PCR amplification using the primer pair RPFcom*Sph*IF/R. A single PCR positive colony that resulted in a PCR fragment of 1866 bp was used for further analysis (Figure 4.5).

4.3.4 Construction of a *V. parahaemolyticus yeaZ*::*kan* Mutant

4.3.4.1 Cloning the *yeaZ::kan* insertion Mutation into Plasmid pCACTUS

The 1.9 kbp *yeaZ::kan Sph*I fragment isolated from pCTX101 was subcloned into *Sph*I digested pCACTUS vector[6] to yield the 6.2 kbp plasmid pCTX102 (Figure 4.6). Plasmid DNA was then used to transform chemically competent *E. coli* DH5α cells. Transformants were plated on LB plates containing Kan and Cml with incubation at the permissive temperature of 30°C O/N. A single Kan^R, Cml^R colony was selected and confirmed by PCR amplification (Appendix M) and restriction digestion analysis to contain the 1.9 kbp *yeaZ::kan* DNA fragment (Figure 4.7).

4.3.4.2 Allelic Exchange Mutagenesis

The suicide vector pCTX102 was used to introduce the *yeaZ::kan* mutation into *V. parahaemolyticus* NCTC 10884 using the principle of allelic exchange. Plasmid pCTX102 was introduced into *V. parahaemolyticus* NCTC 10884 strain by electro-transformation (Chapter 2, Section 2.9.8). Transformants were cultured at the permissive temperature of 30°C on marine agar containing Kan and Cml. In order to select co-integrates, transformants were then plated on MA containing Kan and Cml at the non-permissive temperature of 42°C O/N. Putative allelic exchange mutants were then selected by loss of chloramphenicol resistance following plating of co-integrates on marine agar containing Kan and 6% sucrose cultured at 30°C. Colonies were isolated and incubated on marine agar containing Kan at 37°C O/N. Allelic exchange mutants were confirmed by PCR amplification of a 1.9 kbp fragment using a primer pair RPFmu*Sph*IF/R1 (Figure 4.8).

---

[6] pCACTUS (see Chapter 2, Table 2.3 for detailed plasmid information) is a counter-selectable suicide vector that contains a temperature sensitive origin of replication (ori_{ts}), chloramphenicol resistance marker (Cm^R) and a negative selection marker, *sacB*.

4.3.5 Complementation Analysis

To complement the loss of YeaZ in the *V. parahaemolyticus yeaZ::kan* mutant, PCR amplified DNA encoding the wild type *yeaZ* was amplified by PCR and cloned into the low copy number shuttle vector pWSK29 as plasmid pCTX103 (Chapter 2, Table 2.3). Figure 4.9 illustrates the strategy used to construct this plasmid pCTX103. A 3.0 kbp DNA fragment including $yeaZ_{Vp}$ and its cognate promoter region was amplified from *V. parahaemolyticus* NCTC 10884 using PCR. A primer pair RPFcom F/R (Chapter 2, Table 2.4) was used to amplify the *yeaZ* region with *Bam*HI and *Xho*I restriction sites at the 5' and 3' ends respectively. *Bam*HI and *Xho*I digested amplicon was then ligated to similarly digested pWSK29 plasmid DNA to form plasmid pCTX103. This construct was then used to electro-transform the *V. parahaemolyticus yeaZ* mutant (Chapter 2, Section 2.9.8). Transformants were cultured at 37°C on marine agar plates containing Kan and Amp to select mutants carrying plasmid pCTX103. Nucleotide sequence analysis was used to confirm the pCTX103 construct following PCR amplification using primer pair M13F/R (Figure 4.10).

4.3.6 Overexpression and Purification of $YeaZ_{Vp}$

4.3.6.1 Cloning of $yeaZ_{Vp}$ into the Expression Vector pET21b

The primer pair RPF F/R (Table 2.4) was used to amplify the $yeaZ_{Vp}$ gene and introduce an *Nde*I site at the 5' end of the gene and a *Xho*I site at the 3'end. A 0.7 Kbp DNA fragment of the full length *yeaZ* carrying *Nde*I/*Xho*I restriction sites was cloned into pGEM-T Easy vector (Figure 4.11) to create a construct pCTX104. Plasmid pCTX104 was introduced into *E. coli* DH5α cells (Chapter 2, Section 2.9.7) and selected on LB plates containing Amp, X-gal and IPTG as described previously. Plasmid pCTX104 was extracted from the *E. coli* DH5α cells using plasmid extraction kit (Chapter 2, Section 2.9.2) and then subcloned into pET21b expression vector (Chapter 2, Table 2.3) using *Xho*I/*Nde*I restriction enzymes to yield a construct pCTX105 (Figure 4.12). The constructed plasmid pCTX105 was confirmed by restriction enzymes digestion analysis using the same enzymes (*Xho*I/*Nde*I). Plasmid pCTX105 encoding $YeaZ_{Vp}$ with a C-terminal histidine tag, was sequenced by the T7F/R primer pair (Chapter 2, Table 2.4) to confirm the DNA sequence (Appendix N). After the sequence was confirmed, pCTX105 was then transformed into the expression host, *E. coli* BL21 DE3 cells (Table 2.1).

4.3.6.2 Overexpression of $YeaZ_{Vp}$ from *E. coli* BL21 [pCTX105]

A single colony of *E. coli* BL21 [pCTX105] was cultured in 10 mL LB broth containing 100 mg mL^{-1} Amp with incubation at 37°C O/N with vigorous shaking. The O/N culture was sub-cultured into 50 mL fresh LB/Amp broth and then *yeaZ* expression was induced at cell concentration of OD_{600} ~ 0.6 by addition of 0.2 mM IPTG followed by incubation at 30°C for 4 h with shaking. The *E. coli* BL21 DE3 cells were harvested by centrifugation at 4,000 × g for 15 min and the cells were lysed using three 30 sec burst of sonication. The cell lysate was affinity purified using gravity flow column chromatography on a HisLink™ Protein Purification Resin column (Promega, Wisconsin, USA). Purified protein samples were collected and analyzed by SDS-PAGE (Figure 4.13). Figure 4.13 shows that the induced protein band was at the expected size for the YeaZ fusion protein (~25kDa). The purified $YeaZ_{Vp}$ fusion protein was collected and stored at -80°C for further applications.

4.3.7 Generation of a Polyclonal Antiserum for $YeaZ_{Vp}$

4.3.7.1 Immunization Protocol

The purified $YeaZ_{Vp}$ protein from Section 4.3.6.2, was used to produce a polyclonal antiserum. Briefly, the anti-$YeaZ_{Vp}$ polyclonal antibody was generated from a female rabbit immunised with $YeaZ_{Vp}$ protein by injecting four boosters consisting of 2 mg $YeaZ_{Vp}$ protein each, subcutaneously into the rabbit at different sites. Sera from the rabbit before and after immunisation with purified $YeaZ_{Vp}$ protein were collected and examined for the antigen ($YeaZ_{Vp}$) and antibody (Anti-$YeaZ_{Vp}$) specificity using ELISA (Data not shown). The ELISA was performed by the IMVS Antibody facility. The rabbit was ex-sanguinated and the blood serum that contained polyclonal anti-$YeaZ_{Vp}$ antibodies was stored at -80°C for further use (Chapter 2, Section 2.11.5).

4.3.7.2 Specificity of the $YeaZ_{Vp}$ Polyclonal Antiserum

In order to remove non-specific antibodies, the polyclonal antiserum was repeatedly adsorbed at 4°C using *E. coli* BL21 [pET21b] cells (Chapter 2, Section 2.11.5). The adsorbed antiserum was sterilized by filtration through 0.2 μM disk membrane filters.

The adsorbed antiserum was tested for specificity of the expressed native $YeaZ_{Vp}$ protein (Western Blotting) in whole cell lysates of *V. parahaemolyticus* NCTC 10884 wild-type, a *yeaZ* mutant and a *yeaZ* complemented strain (Figure 4.14). Western blotting using the adsorbed antiserum diluted 1:20000, was able to detect the *ca.* 25 kDa $YeaZ_{Vp}$ protein present in whole cell lystes of wild type *V. parahaemolyticus* NCTC 10884 and the *yeaZ*$_{Vp}$ complemented strain (Figure 4.14). This data indicated that the $YeaZ_{Vp}$ protein was expressed in *V. parahaemolyticus* NCTC 10884 and *yeaZ*$_{Vp}$ complemented strains. Furthermore, these immunoblot data confirmed that the antiserum was specific for the $YeaZ_{Vp}$ protein in *V. parahaemolyticus* NCTC 10884 and *yeaZ*$_{Vp}$ complemented strains. Moreover, the adsorbed antiserum did not bind to any proteins present in lysates of the *V. parahaemolyticus yeaZ::kan* mutant. Together, this data confirmed the specificity of the antiserum for $YeaZ_{Vp}$ and showed that the *yeaZ::kan* insertion mutant was unable to express $YeaZ_{Vp}$ protein.

4.3.8 Characterisation of the *yeaZ*$_{Vp}$ Mutant

4.3.8.1 Effect of the *yeaZ*$_{Vp}$ Mutation on Entry into the VBNC State

V. parahaemolyticus NCTC 10884, *yeaZ*$_{Vp}$ mutant and *yeaZ*$_{Vp}$ complemented strains were prepared for the VBNC state induction. Cells from overnight culture in MB were harvested, washed and resuspended in sterile ASW containing 2.5% NaCl (pH 8) at a density of 10^9 cells mL^{-1}. The suspension was incubated without agitation in the dark at 4°C or 20°C for up to 140 d (Figure 4.15) and monitored regularly to assess culturability. The culturability of suspensions of the wild type, *yeaZ*$_{Vp}$ mutant and *yeaZ*$_{Vp}$ complemented strains incubated at 20°C remained approximately 10^9 cells mL^{-1} over 140 d. By contrast, all of three strains lost the culturability when incubated at 4°C. Wild type suspensions completely lost culturability within 60 d (Figure 4.15). Similarly, the *yeaZ*$_{Vp}$ complemented strain lost culturability after 75 d, whereas the *yeaZ*$_{Vp}$ mutant achieved a non-culturable state after incubation at 4°C for 140 d. This data indicated that the *yeaZ::kan* mutation resulted in a more than doubling of the time to loss of culturability compared to the wild type.

4.3.8.2 Resuscitation of the *yeaZ$_{Vp}$* Mutant

To determine whether the *yeaZ::kan* mutation affected recovery from the non-culturable state, non-culturable suspensions prepared as described in Section 4.3.8.1 were incubated at 20°C and samples of cells suspensions tested for culturability on MA. Table 4.1 lists the changes in culturability observed over a 6 d period. None of the strains tested regained culturability for the first day of incubation at 20°C. However, the wild type and *yeaZ$_{Vp}$* complemented strains rapidly regained culturability 2 d following the temperature up-shift. Counts of culturable cells in suspensions of these two strains increased to 6.5×10^6 cells mL^{-1} and 8×10^6 cells mL^{-1} respectively and reached 10^8 cells mL^{-1} after 6 d following resuscitation. However, the *yeaZ$_{Vp}$* mutant did not regain culturability failed to do so under the same conditions. This data indicated that non-culturable *V. parahaemolyticus* NCTC 10884 cells unable to express a functional $YeaZ_{Vp}$ protein, were not able toregain culturability after a temperature upshift from 4 to 20°C.

4.3.9 The Effect of YeaZ$_{Vp}$ Fusion Protein on Resuscitation

The purified $YeaZ_{Vp}$ fusion protein was used to investigate the extracellular effect in the VBNC state resuscitation. The purified $YeaZ_{Vp}$ fusion protein was added in 10 mL VBNC state induced cells from VBNC state cells after 60 d at 4°C (Figure 4.15) with the final concentration of 10ug mL^{-1} purified $YeaZ_{Vp}$ fusion protein and incubated at 37°C for 2 d (Figure 4.16). This data indicated that both of these two samples are able to recover from the VBNC state in 1 d and 2 d. However, there is no significant difference between added $YeaZ_{Vp}$ fusion protein or not. Therefore, the exogenous $YeaZ_{Vp}$ protein resulted in a no additional effect on the VBNC state resuscitation.

4.3.10 Cellular Location of YeaZ in *V. parahaemolyticus* NCTC 10884

To determine the cellular location of $YeaZ_{Vp}$ protein, cell preparations of the wild type strain were separated into cytoplasmic, cell envelope and outer membrane fractions and each fraction tested for $YeaZ_{Vp}$ by Western immunoblot analysis. Log phase *V. parahaemolyticus* NCTC 10884 cells were harvested from MA cultures, washed, and lysed using three 30 sec burst of sonication. The cell lysates were ultra-centrifuged at 105,000 × g for 1 h and cell fractions separated into the cytoplasmic protein, cell envelope protein and cell membrane

protein fractions according to methods described in Section 2.11.8. Protein from the culture supernatant was TCA precipitated as described in Section 2.11.9. All protein samples were analysed using SDS-PAGE and Western Blot.

SDS-PAGE and Western blot analyses are shown in Figure 4.17. These data show that the 25 kDa $YeaZ_{Vp}$ protein was mainly concentrated in the cell envelope (Lane 5) and cell outer membrane fractions (Lane 6). However, $YeaZ_{Vp}$ protein was also detected in the cytoplamic protein fraction (Lane 4), although the signal intensity was lower compared with the $YeaZ_{Vp}$ signal in the envelope and the membrane protein fractions. $YeaZ_{Vp}$ protein was not observed in the culture supernatant protein fraction (data not shown).

To determine whether $YeaZ_{Vp}$ protein was displayed on the surface of *V. parahaemolyticus* NCTC 10884 cells, immuno-fluorescence microscopy (Chapter 2, Section 2.11.7) using a fluorescein isothiocyanate (FITC)-labelled goat anti-rabbit antibody. The *V. parahaemolyticus* NCTC 10884 *yeaZ*$_{Vp}$ mutant was used as a negative control. The IF results shown in Figure 4.18 indicated that the fluorescence signal was detected on the cell surface of the *V. parahaemolyticus* NCTC 10884 wild type (Figure 4.18, Panel A), but not on the surface of *yeaZ*$_{Vp}$ mutant cells (Figure 4.18, Panel C). This data suggested that the *V. parahaemolyticus* NCTC 10884 $YeaZ_{Vp}$ protein is exported to the cell surface.

4.3.11 $YeaZ_{Vp}$ Levels during VBNC Induction and Resuscitation

The presence and relative levels of $YeaZ_{Vp}$ protein in cells during induction of the VBNC state at 4°C was determined by Western blot analysis. Whole cell lysates of 1 mL samples of cell suspensions of *V. parahaemolyticus* NCTC 10884 incubated at 4°C in ASW (pH 8.0) were subjected to SDS-PAGE and Western transfer. The Western blot data shown in Figure 4.19, Panel A indicated that $YeaZ_{Vp}$ protein was present at similar levels in all samples collected suspensions incubated at 4°C. This analysis was not done for control suspensions in ASW incubated at 20°C.

$YeaZ_{Vp}$ protein levels in VBNC state *V. parahaemolyticus* NCTC 10884 cells during resuscitation at 20°C was also examined by Western blot analysis of whole cell lysates of samples of cell suspensions. Samples were harvested daily for up to 3 d. The Western blot data is shown in Figure 4.19, Panel B. This indicated that the $YeaZ_{Vp}$ protein was present at similar levels in resuscitating cell populations for the 3 d period of resuscitation.

4.3.12 Transcriptional Analysis of VBNC State and Resuscitating Cells

Results presented above suggest that the $YeaZ_{Vp}$ may affect the ability of cells to maintain viability during induction of the VBNC state and/or resuscitation. $YeaZ_{Vp}$ protein was clearly present in cells during induction of the VBNC state at 4°C (Figure 4.19, Panel A) and during resuscitation of VBNC state cells at 20°C (Figure 4.19, Panel B). However, these results do not indicate whether *de novo* synthesis of $YeaZ_{Vp}$ protein occurred during induction and resuscitation. To monitor *de novo* synthesis, mRNA levels of *yeaZ*$_{Vp}$ at different stages of induction and resuscitation were examined using quantitative reverse transcription PCR (qRT-PCR). The effect of temperature changes on transcription of the *rpoS* (sigma factor, response to stresses such as near-UV radiation, acid, temperature or osmotic shock, oxidative stress, and nutrient deprivation) and *yeaZ*$_{Vp}$ at different stages of establishment of the VBNC state, was investigated by qRT-PCR using gene specific primer pairs (Chapter 2, Table 2.4). The housekeeping gene 16S rRNA was used as an internal control, as it is constitutively expressed in the cells[7].

V. parahaemolyticus NCTC 10884 was cultured in marine broth until cells reached log phase. Cells in log phase were harvested by centrifugation (20,000 × g) at 4°C and then suspended in ASW (pH 8.0) and incubated at 4°C to induce the VBNC state VBNC state cells were then resuscitated by incubation at 20°C (temperature upshift). Total RNA (Chapter 2, Section 2.10.1) from cells at the commencement of incubation at 4°C, from VBNC state cells after 60 d at 4°C, from cells at the end of 1 d of resuscitation and after 6 d of resuscitation, was extracted, DNase treated and subjected to qRT-PCR using gene specific primers to amplify fragments of *yeaZ*, *rpoS* and *16S* rRNA genes. No template controls (NTC) and no reverse transcriptase control (NRTC) were examined for each samples to eliminate contamination of reagents and RNA purity. No PCR product was detected in the absence of either template or reverse transcriptase for any RNA samples prepared.

[7] Although 16S rRNA is used as an internal control, it is accepted that levels can vary widely depending on the physiological state of the cells. This possibility could lead to problems when this marker is used to eliminate variation in mRNA quantity in samples. This could be partially resolved by normalizing RNA levels to the starting input levels.

Threshold cycle (Ct) is the metric used for analyzing qRT-PCR results. The Ct value represents the number of cycles needed for fluorescence to reach threshold background fluorescence. The fewer cycles needed to attain a detectable fluorescence level indicates the greater the amount of starting template. Therefore, the lower the Ct, the higher the gene expression (Nolan et al., 2006).

All RNA samples were analysed in quadruplicate and the best three out of four in each quadruplicate were selected for qRT-PCR data analysis (SD of less than 0.5). The ΔΔCt method (Livak & Schmittgen, 2001) was used for relative quantitation of target genes in different samples. Gene expression level of *rpoS* and *yeaZ* in all samples were first normalized with 16S rRNA reference gene to eliminate for variation in RNA quantity to obtain the ΔCt values which were then used to compute relative ΔΔCt values in different groups. The computing formula is as follows: $\Delta\Delta Ct_{yeaZ} = \Delta Ct_{yeaZ} - \Delta Ct_{16S}$

The qRT-PCR results shown in Figure 4.20 indicate that the fold change in expression of the $yeaZ_{Vp}$ measured in freshly prepared suspensions of cells (starvation), VBNC state cells, and cells from the early stage of resuscitation (day 1) and the late stage of resuscitation (day 6) were 0.83, 0.02, 0.0039 and 4, respectively. A similar trend was observed for *rpoS* gene expression. Fold changes of *rpoS* gene in freshly prepared suspensions of cells (starvation), VBNC state, early stage of resuscitation (day 1) and late stage of resuscitation (day 6) were 5.3, 0.052, 0.019 and 12, respectively. Together this data suggests that expression of the *rpoS* and *yeaZ* genes declines during the transition to the VBNC state, but is elevated during resuscitation (Figure 4.20).

4.3.13 TEM of *V. parahaemolyticus* NCTC 10884 Cells in the VBNC State

TEM was used to visualise the cell morphology of *V. parahaemolytcus* NCTC 10884 wild type and the $yeaZ_{Vp}$ mutant during the log phase and VBNC state induction. Figure 4.21 presents micrographs of cell sections in log phase (Panel A and B) and VBNC state (Panel C and D). Log phase cells were uniformly rod-shaped with well-defined, intact walls. These cells were characterized by a densely stained cytoplasm with a clear definition of the chromosomal DNA (Figure 4.21, Panel A and B). However, VBNC state wild type cells induced in ASW pH 8.0 at 4°C were coccoid in shape with a large variation in size. In addition, cell sections of VBNC cells displayed a reduced cytoplasmic staining intensity

compared to normal cells. The chromosomal DNA of VBNC cells was also difficult to visualize. Furthermore, many of the VBNC cells examined appeared to have lost cell integrity (Figure 4.21, Panel C and D).

Changes similar to those observed for VBNC state cells were also identified in sections of the *yeaZ*$_{Vp}$ mutant. Figure 4.22 presents micrographs of cell sections from log phase (Panel A and B) and VBNC state (Panel C and D) of *V. parahaemolyticus* NCTC 10884 *yeaZ*$_{Vp}$ mutant strain. TEM images suggested that *yeaZ::kan* mutant cells displayed an unsual-shaped cell envelope in log phase (Figure 4.22, Panel A and B). Culture of the *yeaZ::kan* mutant at 4°C resulted in smaller cell sizes compared with the cell preparations from log phase cultures (Figure 4.22, Panel C and D). Similarly, ribosome density in VBNC state *yeaZ*$_{Vp}$ mutant cells was lower than that in the log phase preparations of the mutant. Many *yeaZ*$_{Vp}$ mutant cells incubated under conditions used to prepare VBNC state cells have disrupted cell membranes and cell wall complexes (Figure 4.22, Panel C and D).

4.4 Discussion

The exact role of the VBNC state and mechanisms that control the VBNC state in bacteria is yet to be elucidated. It is likely that its role and significance differ from one bacterial type to another. Intriguingly, recent studies have described a role for resuscitation protein factors (Rpf) in the recovery of culturability by VBNC state cells for several different types of bacteria. Treatment of VBNC state cells with exogenous sources of Rpf result in improved recovery of culturability (Mukamolova et al., 1998; Mukamolova et al., 2002; Shleeva et al., 2004). Furthermore, in G-ve bacteria at least, Rpf (or YeaZ) homologs have been demonstrated to be essential for viability in *E. coli* and *S.* Typhimurium (Handford et al., 2009; Panutdaporn et al., 2006). Together, these studies have lead to suggestions that YeaZ protein is implicated in establishment of the VBNC state and/or resuscitation from this state (Oliver, 2010; Panutdaporn et al., 2006). It is against this background that the objective of work described in this chapter, was designed to determine the involvement and role of the *yeaZ*$_{Vp}$ in establishment of the VBNC state and subsequent resuscitation for *V. parahaemolyticus* NCTC 10884. Experimental strategies used to address this objective included construction of a deletion mutation within the *yeaZ*$_{Vp}$ using cloning techniques,

localization of the $YeaZ_{Vp}$ protein using immunoblot methodologies and monitoring changes in cell morphology and structure using TEM.

V. parahaemolyticus NCTC 10884 carrying an insertion mutation in $yeaZ_{Vp}$ was constructed by allelic exchange using insertion mutations carried on the suicide vector pCACTUS. This mutant was confirmed by antibiotic selection, PCR and Western blot analysis. Plasmid pCACTUS was developed specifically to engineer allelic replacement of wild type alleles in G-ve bacteria such as *V. cholera* (Ogierman et al., 1997). Specifically, vector pCACTUS is a derivative of plasmids containing the *sacB* gene of *Bacillus subtilis* (pIB279) and pIB307, the product of which is toxic to bacteria when they are grown in the presence of sucrose. The vector pCACTUS also contains a temperature-sensitive pSC101 replicon, a *mob* region and a chloramphenicol resistance gene (Blomfield et al., 1991). The temperature sensitive replicon is inoperative at 42°C but supports plasmid replication at 30°C.

The preparation of a viable *yeaZ* mutation is particularly interesting given recent reports that YeaZ protein has been shown or inferred to be essential for viability for *E. coli*, *Streptococcus pneumoniae*, *Staphylococcus aureus*, *Bacillus subtilis, Francisella novicida*, *Pseudomonas aeruginosa* and *Mycoplasma genitalium* (Baba et al., 2006; Gallagher et al., 2007; Glass et al., 2006; Hunt et al., 2006; Kobayashi et al., 2003; Liberati et al., 2006; Zalacain et al., 2003). In cases where there is experimental evidence for this requirement, the function of YeaZ has been demonstrated through the use of *yeaZ* conditional depletion mutants. In *E. coli*, depletion of YeaZ leads to significant changes in cell morphology and ultrastructure that include changes in cell size and nucleoid condensation (Handford et al., 2009) that are apparently consistent with a block in protein synthesis. In the current study, a non-polar *yeaZ* insertion mutation was demonstrated to be viable under normal laboratory culture conditions. However, these mutants did display some differences in ultrastructure when cultured in MB at 37°C compared with the wild type. Typically, the $yeaZ_{Vp}$ mutant cells were slightly longer than the wild type, had a more condensed nucleoid and many cells showed polar separation of the cell membrane from the cell wall complex (Figure 4.22 Panel B). These changes are consistent with those described by Handford et al. (2009) for *E. coli* YeaZ depletion mutants. The most startling changes were observed when these mutants were incubated under starvation conditions in ASW at 4°C. These cells were more rounded,

smaller, and contained a condensed nucleoid. Many cells displayed disrupted cell membrane/cell wall complexes typical of lysed cells. Furthermore, extended incubation under these conditions leads to loss of culturability that cannot be recovered by incubation under conditions permissive for resuscitation. All of these changes indicate cells under significant stress. This suggests that in *V. parahaemolyticus* at least, YeaZ may be important in maintaining cell viability and integrity under stressful conditions.

This observation is novel and suggests that $yeaZ_{Vp}$ mutations may be lethal only under certain conditions eg. incubation under starvation conditions at low temperatures. Why the mutant lost culturability when incubated at 4°C, but not at 20°C is unclear. Nevertheless the experimental data implicate $YeaZ_{Vp}$ not only in establishment of the VBNC state, but more particularly, in recovery from that state. Given the proposed role of YeaZ proteins in viability of bacterial cells, this data adds support for $YeaZ_{Vp}$ as an important factor required for viability of VBNC state cells.

Previous reports have shown that depletion of YeaZ (and other partner proteins) results in loss of cell viability (Handford et al., 2009; other references). It is possible that for wild type *V. parahaemolyticus* NCTC 10884 cells exposed to low temperatures, under starvation conditions (specifically in low cell density environments in ASW) that YeaZ levels cannot be maintained and fall below critical levels required to maintain viability. The fact that Western immunoblot analysis and qRT-PCR data showed that $YeaZ_{Vp}$ protein was expressed in cells throughout incubation of wild type cells at 4°C and during resuscitation may only be representative for the high concentration suspensions tested. Levels of YeaZ were not determined for low density suspensions (because of the technical difficulty of obtaining sufficient numbers of cells). If levels of YeaZ decreased to subcritical levels during incubation of low density suspensions at 4°C, then this scenario could explain why VBNC state cells are unable to be resuscitated by a temperature upshift. Considering this scenario, it would not be surprising that a *yeaZ* mutant was unable to survive conditions known to induce the VBNC state, irrespective of suspension concentration or nutrient status. A more careful analysis of YeaZ levels in low concentration suspensions may provide some support for this hypothesis.

However, it is also plausable that the apparent role of $YeaZ_{Vp}$ is the result of pleiotrophic effects caused by the mutation itself and consequent loss of an important cellular protein. In this study, *yeaZ*$_{Vp}$ was inactivated by insertion of a non-polar kanamycin resistance cassette. This should have resulted in inactivation of the *yeaZ*$_{Vp}$ gene without affecting transcription of downstream co-transcribed genes, but does not eliminate the possibility that loss of $YeaZ_{Vp}$ protein could lead to other as yet unidentified changes in cell chemistry that could ultimately be responsible for the loss of viability effects described above. Ideally, a deletion mutation rather than an insertion mutation should be constructed to ensure that pleiotrophic effects were eliminated. Ultimately however, these observations could be confirmed by use of the conditional depletion model described by Handford et al. (2009) and Hunt et al. (2006).

A role for *yeaZ* in resuscitation of VBNC cells has been previously examined. *M. luteus* cells are reported to secrete Rpf protein that assists resuscitation of VBNC cells prepared by extended starvation culture (Mukamalova et al., 1998). When purified recombinant Rpf was added to VBNC cells resuspended in fresh growth medium, these cells recovered culurability at a greater rate than cultures without added Rpf. Asakura et al. (2002) have also shown that *S.* Orianenberg secretes a factor that promotes recovery of VBNC cells. Similarly, purified $YeaZ_{ST}$ can assist VBNC state *S.* Typhimurium cultures to recover culturability in a dose dependent manner (Panutdaporn, Kawamoto et al. 2006). These studies suggested that Rpf/YeaZ proteins are secreted out of cells. However, attempts to demonstrate that purified, recombinant $YeaZ_{Vp}$ could assist recovery of culturability in low temperature induced VBNC state *V. parahaemolyticus* NCTC 10884 cells, were unsuccessful (Figure 4.16).

In view of the fact that several studies of interactions between YeaZ and partner proteins (YgjD and YjeE) have confirmed these important interactions take place in the cell cytoplasm, it is difficult to understand how YeaZ can also be secreted by these cells. There is little definitive information in the literature to indicate the principal cellular compartments for YeaZ. The landmark study by Handford et al. (2009) used Western analysis of whole cell lysates to show that this protein is expressed by *E. coli*. Hunt et al. (2006) used GFP fusions to indicate that the YeaZ homolog (YdiC) was cytoplasmic. This approach however is only useful for tracking intracellular proteins. In the present study, Western immunoblot analysis of fractionated cells was carried out together with immunofluorescence microscopy of intact log phase cells of *V. parahaemolyticus* NCTC 10884 as a way to identify cellular

compartments containing $YeaZ_{Vp}$. These definitive experiments confirmed for the first time that YeaZ was secreted to the outer membrane, although traces of protein were also located in the cytoplasm. No $YeaZ_{Vp}$ was located in the culture supernatant. Immunofluorescence microscopy confirmed that $YeaZ_{Vp}$ protein decorated the outer surface of intact cells. These data imply that $YeaZ_{Vp}$ can be both a cytoplasmic protein that interacts with partner proteins involved in viability, as well as a secreted protein that somehow associates with the external surface of the *V. parahaemolyticus* NCTC 10884 cells.

How $YeaZ_{Vp}$ is secreted is unknown. Amino acid sequence analysis indicated that the protein does not have an N-terminal signal peptide that might facilitate Sec-dependent secretion (data not shown). This analysis is consistent with findings for YeaZ protein sequences for *S.* Typhimurium LT2 (Nichols et al., 2006; Panutdaporn et al., 2006). Therefore, it is still unclear how $YeaZ_{Vp}$ protein is secreted out of the cell or translocate to the outer membrane. It is interesting to speculate that secretion of YeaZ to the culture supernatant may be an essential step that is needed for this protein to assist recovery of culturability of VBNC cells. It may be that sequestration of $YeaZ_{Vp}$ on the outer surface of *V. parahaemolyticus* NCTC 10884 cells prevented proper interaction with extracellular components involved in recovery[8].

The observation that $YeaZ_{Vp}$ is somehow involved in recovery of culturability of low temperature induced VBNC state cells of *V. parahaemolyticus* NCTC 10884, suggested that it may be possible to use small molecular weight molecules to inhibit interactions between this protein and other protein partners. If specific inhibitors that affect the interaction between YgjD and YeaZ can be identified, these may be developed as broad spectrum, antibacterial agents that affect cell viability and cell multiplication. Furthermore, if it can be shown that the rapid reduction in culturability of *Vibrio* cells that occurs when contaminated seafood is refrigerated (see Mutanda-Garriga et al., 1995; Oliver, 1981) is an indication that these cells enter a VBNC state, then YeaZ specific inhibitors might be used to treat seafood so that these VBNC cells are unable to recover culturability. The combined effects of these inhibitors on recovery of culturability, together with the potential impact on cell multiplication, could be

[8] Sequestration of $YeaZ_{Vp}$ at the surface of *V. parahaemolyticus* will be discussed in more detail in Chapter 5 of this thesis.

used to engineer significant reductions in risk of illness associated with consumption of seafood.

```
  1 - ATGAGCGCAAAAATTCTTGCTATCGATACCGCAACTGAAAACTGTTCAGTTGCACTACTG - 60
  1 - M  S  A  K  I  L  A  I  D  T  A  T  E  N  C  S  V  A  L  L   - 20
      Start codon
 61 - GTTAATGACCAAGTGATTTCACGCAGCGAAGTGGCACCTCGTGACCACACGAAAAAAGTA - 120
 21 - V  N  D  Q  V  I  S  R  S  E  V  A  P  R  D  H  T  K  K  V   - 40
121 - CTGCCAATGGTTGACGAAGTGCTGAAAGAAGCGGGTCTAACTCTACAAGACTTGGATGCA - 180
 41 - L  P  M  V  D  E  V  L  K  E  A  G  L  T  L  Q  D  L  D  A   - 60
181 - CTAGCGTTTGGCCGTGGCCCTGGTAGCTTTACTGGTGTTCGTATCGGTATTGGCATCGCT - 240
 61 - L  A  F  G  R  G  P  G  S  F  T  G  V  R  I  G  I  G  I  A   - 80
241 - CAAGGCCTAGCATTTGGTGCAGAACTGCCGATGATTGGTGTTTCAACATTGGCTGCGATG - 300
 81 - Q  G  L  A  F  G  A  E  L  P  M  I  G  V  S  T  L  A  A  M   - 100
301 - GCACAAGCAAGCTACCGCCTGCATGGTGCAACTGATGTCGCTGTAGCGATTGATGCGCGC - 360
101 - A  Q  A  S  Y  R  L  H  G  A  T  D  V  A  V  A  I  D  A  R   - 120
361 - ATGAGCGAGGTTTACTGGGCACGTTATTCTCGCCAAGAAAACGGCGAATGGATCGGTGTT - 420
121 - M  S  E  V  Y  W  A  R  Y  S  R  Q  E  N  G  E  W  I  G  V   - 140
421 - GATGAAGAATGTGTGATTCCACCAGCTCGTTTGGCGGAAGAAGCACAAGCTGACTCTAAA - 480
141 - D  E  E  C  V  I  P  P  A  R  L  A  E  E  A  Q  A  D  S  K   - 160
481 - ACGTGGACAACAGCTGGTACAGGTTGGTCTGCATATCAAGAAGAACTGGCGGGCCTGCCG - 540
161 - T  W  T  T  A  G  T  G  W  S  A  Y  Q  E  E  L  A  G  L  P   - 180
541 - TTTAACACTGCAGACAGTGAGGTATTGTACCCTGACTCACAAGACATTGTGATTTTAGCT - 600
181 - F  N  T  A  D  S  E  V  L  Y  P  D  S  Q  D  I  V  I  L  A   - 200
601 - AAGCAAGAACTAGAAAAAGGCAATACGGTTCCTGTTGAAGAATCTAGCCCGGTTTACCTG - 660
201 - K  Q  E  L  E  K  G  N  T  V  P  V  E  E  S  S  P  V  Y  L   - 220
661 - CGTGATAACGTGACTTGGAAGAAGCTTCCAGGCCGCGAATAA                    - 702
221 - R  D  N  V  T  W  K  K  L  P  G  R  E  *                     - 240
                                            Stop codon
```

Figure 4.1: DNA and amino acid sequence for $YeaZ_{Vp}$.

Sequence data is from GenBank Accession BA000031. Start and stop codons are underlined. The deduced polypeptide contains 233 amino acids.

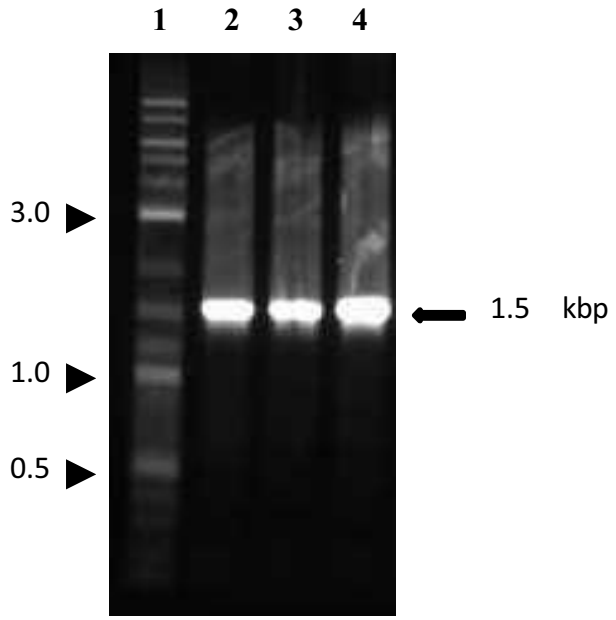

Figure 4.2: PCR amplification of the 1561bp fragment *yeaZ*$_{Vp}$.

The 1561 bp DNA fragment encoding YeaZ was amplified by using a primer pair RPFmuSphIF/R1. This primer pair introduced *Sph*I sites at each end of the amplicon. The amplicons were separated on 1 % (w/v) agarose gel. Lane 1, 2 log size markers; Lanes 2, 3 and 4, 1.5 kbp amplicons encoding *yeaZ*.

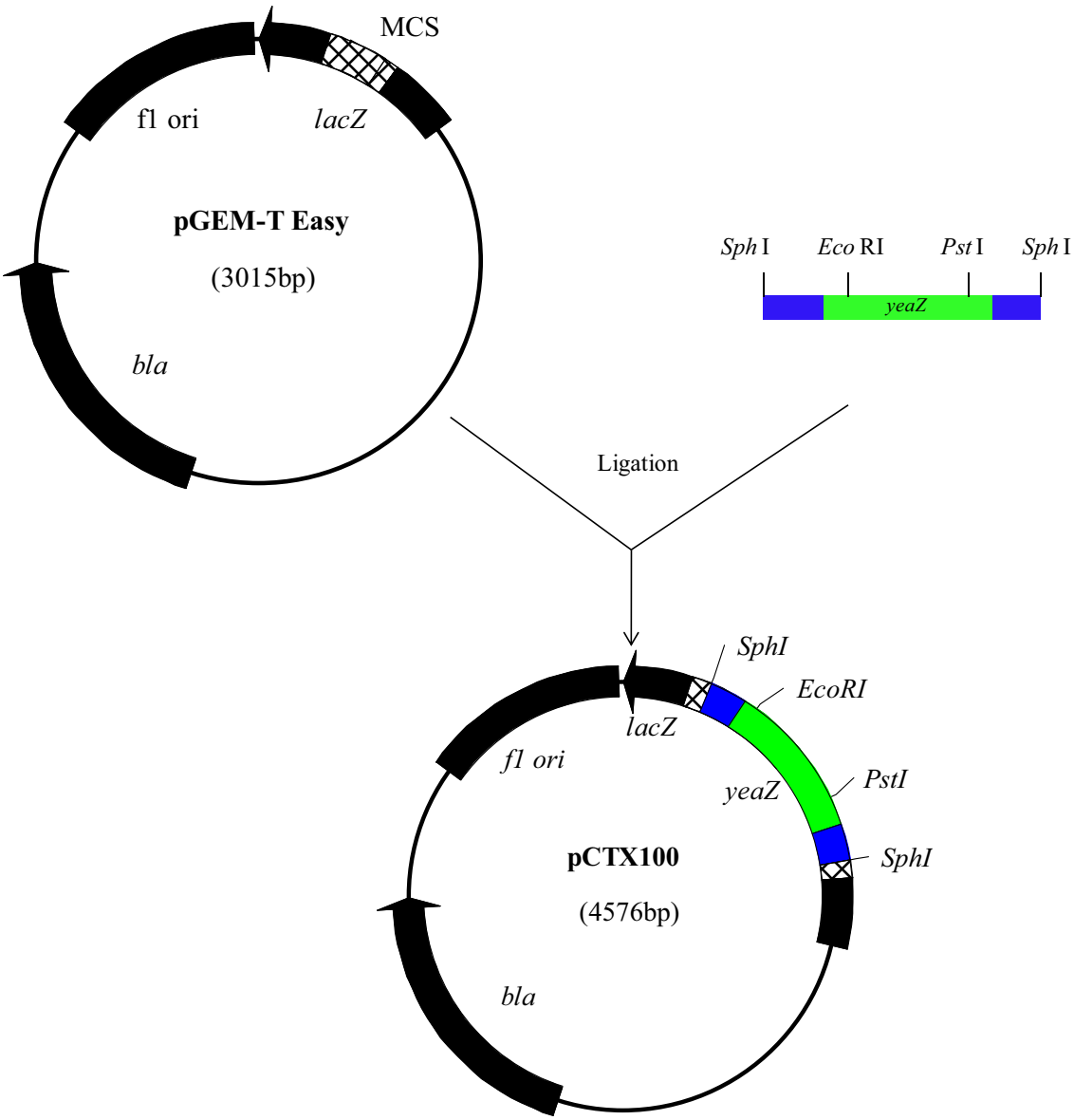

Figure 4.3: Construction of plasmid pCTX100.

The PCR amplified 1561bp fragment encoding $YeaZ_{Vp}$ was ligated into pGEM-T Easy to create plasmid pCTX100.

Abbreviation: *bla*, ampicillin resistance; *f1 ori*, f1 origin; *lacZ*, *lacZ* gene; MCS, multiple cloning sites.

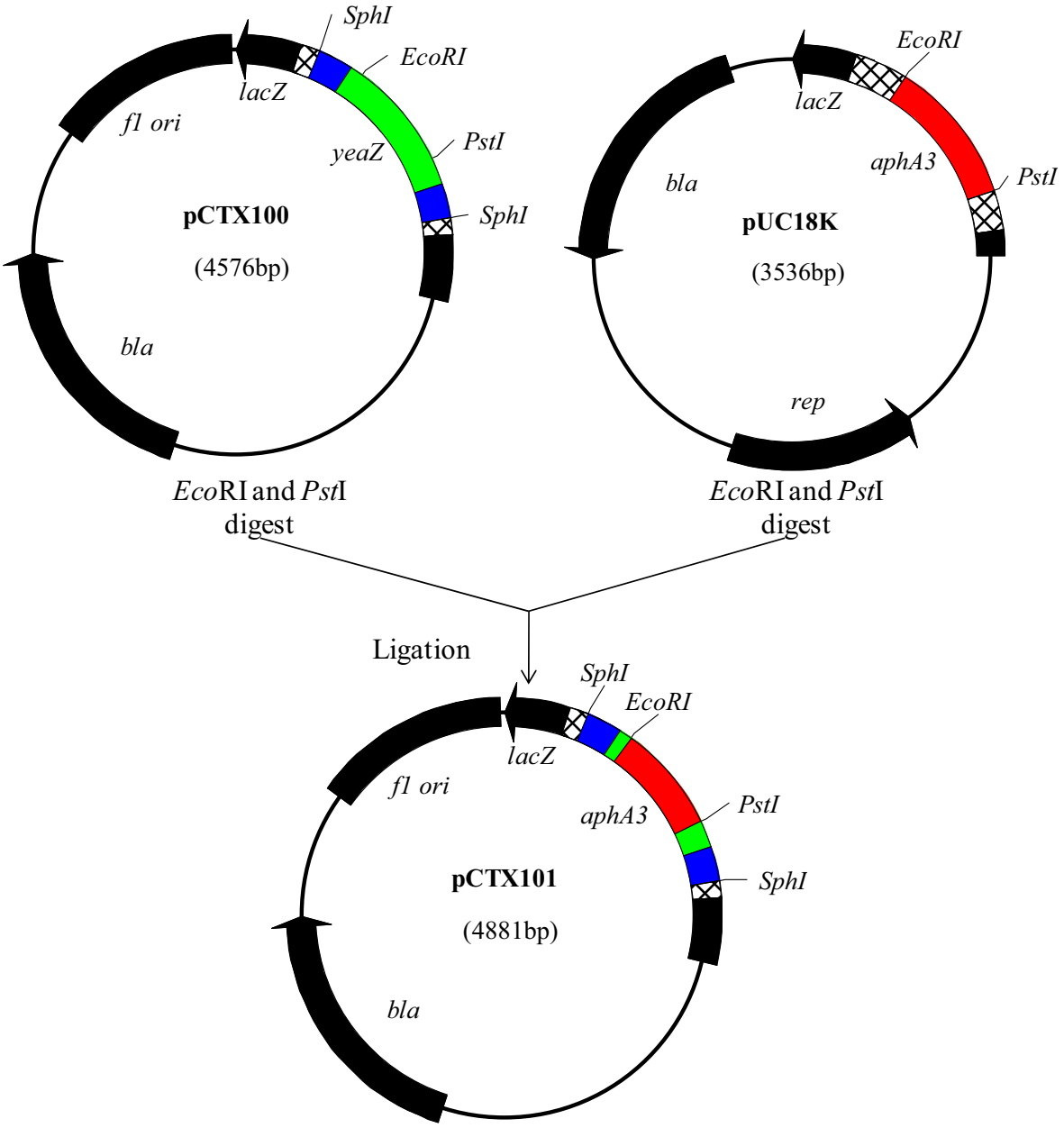

Figure 4.4: Construction of plasmid pCTX101.

The 850 bp *Eco*RI/*Pst*I kanamycin resistance (*aphA3*) cartridge isolated from pUC18K was ligated into *Eco*RI and *Pst*I digested pCTX100 to create a *yeaZ::kan* insertion mutation encoded on plasmid pCTX101.

Abbreviation: *bla*, ampicillin resistance; *aph*A3, Kanamycin resistance; *f1 ori*, f1 origin; *lacZ*, *lacZ* gene; MCS, multiple cloning sites.

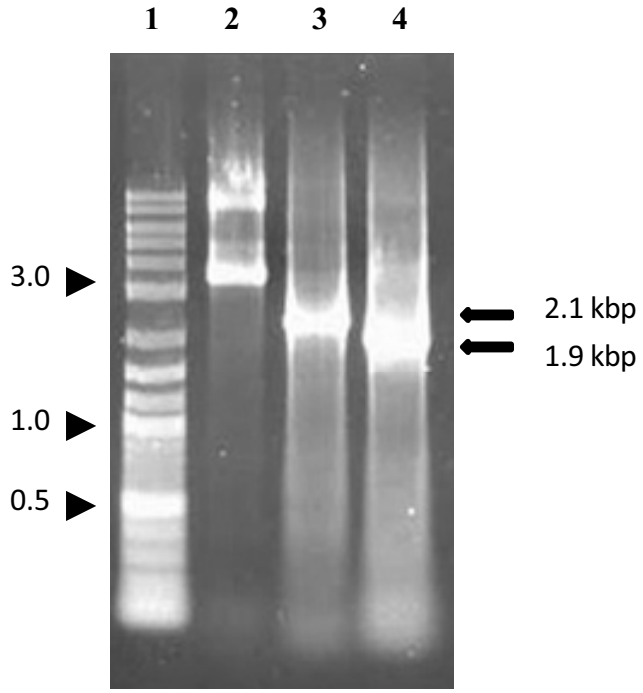

Figure 4.5: PCR confirmation of the 1.9 kbp *yeaZ::kan* fragment of pCTX101.

The DNA amplified with primer pairs of M13F/R and RPFmuSphIF/R1. Amplicons analyzed on a 1% agarose gel. Plasmid pCTX101 includes 1.9 kbp DNA fragment containing the *yeaZ::kan* and *yeaZ* flanking DNA.

Lanes are marked as below:

1. 2 log DNA marker.
2. Plasmid pCTX101.
3. 2.1 kbp *yeaZ* PCR amplicons using a primer pair M13F/R.
4. 1.9 kbp *yeaZ* PCR amplicons using a primer pair RPFmuSphIF/R1.

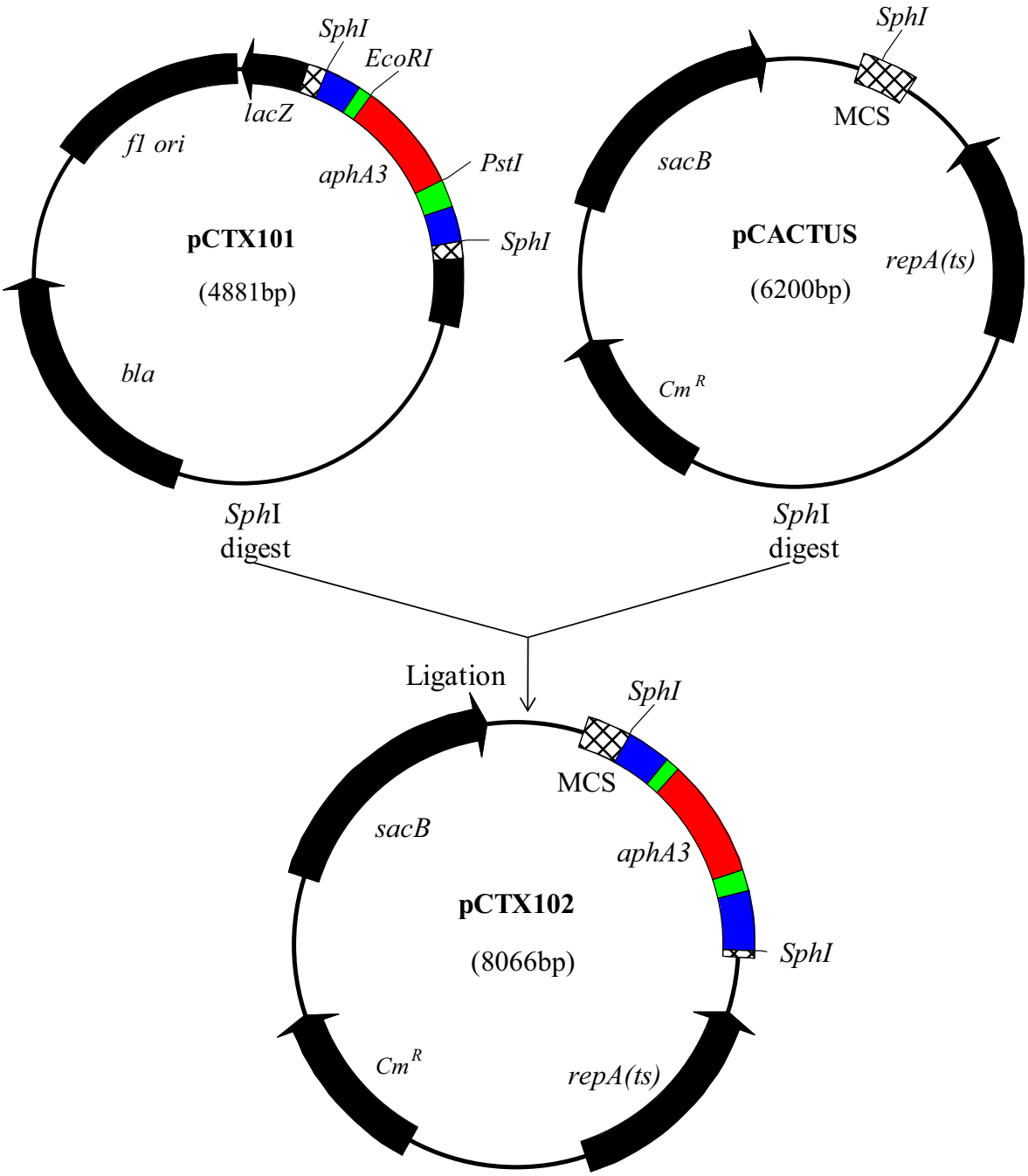

Figure 4.6: Construction of plasmid pCTX102.

The 1.9 kbp DNA fragment was isolated from pCTX101 as an *Sph*I fragment and ligated into *Sph*I digested pCACTUS to form pCTX102.

Abbreviation: *bla*, ampicillin resistance; *f1 ori*, f1 origin; *lacZ*, lacZ gene; MCS, multiple cloning site; *aphA 3*, kanamycin resistance; *repA* (ts), temperature sensitive replicon; Cm^R chloramphenicol resistance; *sacB*, levansucrase gene.

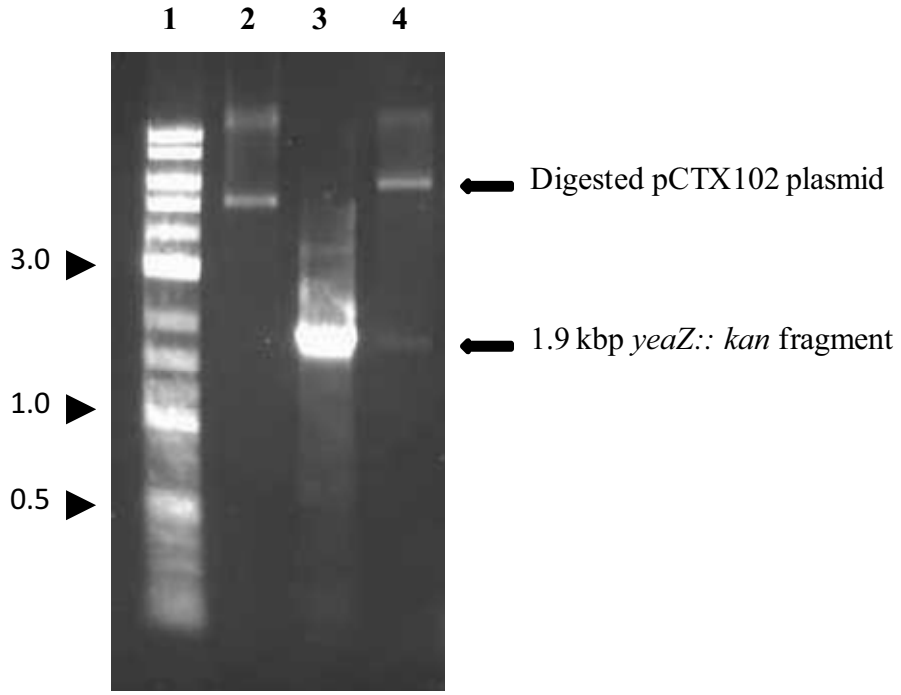

Figure 4.7: PCR confirmation of the 1.9 kbp fragment of the pCTX102.

Primer pair RPFmu*Sph*IF-R1 was used to PCR amplify a 1.9 kbp fragment encoding the *yeaZ::kan* construct from plasmid pCTX102 DNA. Amplicons were analyzed on a 1% agarose gel. Lanes are marked as below:

Lane 1: 2 log size marker.

Lane 2: pCTX102 plasmid.

Lane 3: 1.9 kbp *yeaZ* amplicon PCR amplified from pCTX102 DNA using the primer pair RPFmu*Sph*IF/R1.

Lane 4: pCTX102 plasmid digested with *Sph*I to release the 1.9 kbp *yeaZ::kan* construct.

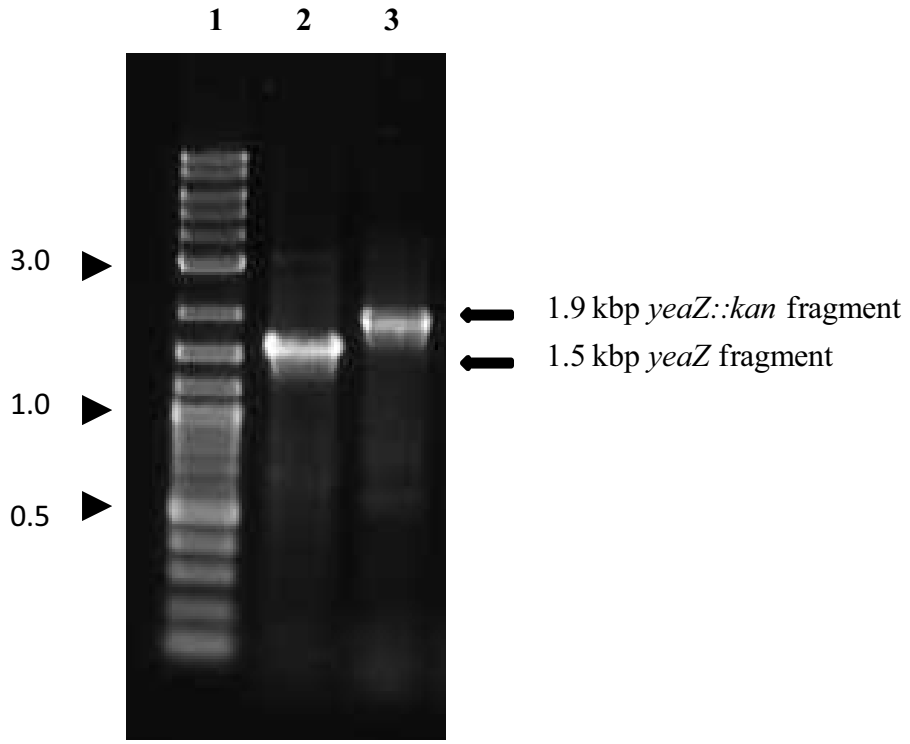

Figure 4.8: PCR confirmation of the *V. parahaemolyticus yeaZ*$_{Vp}$ mutant.

DNA isolated from the *V. parahaemolyticus* NCTC 10884 wild type and the *yeaZ* mutant were used as a template to amplify DNA encoding *yeaZ* and the 1.9 kbp *yeaZ::kan* fragment using primer pair RPFmuSphIF-R1. Amplicons were analyzed on a 1% (w/v) agarose gel.

Lanes are marked as described below:

1. 2 log size DNA marker
2. 1.5 kbp *yeaZ* PCR amplicon prepared using primer pair RPFmuSphIF/R1 and DNA extracted from the wild type *V. parahaemolyticus* NCTC 10884.
3. 1.9 kbp *yeaZ::kan* PCR amplicons prepared using primer pair RPFmuSphIF/R1 and DNA extracted from the *yeaZ* mutant.

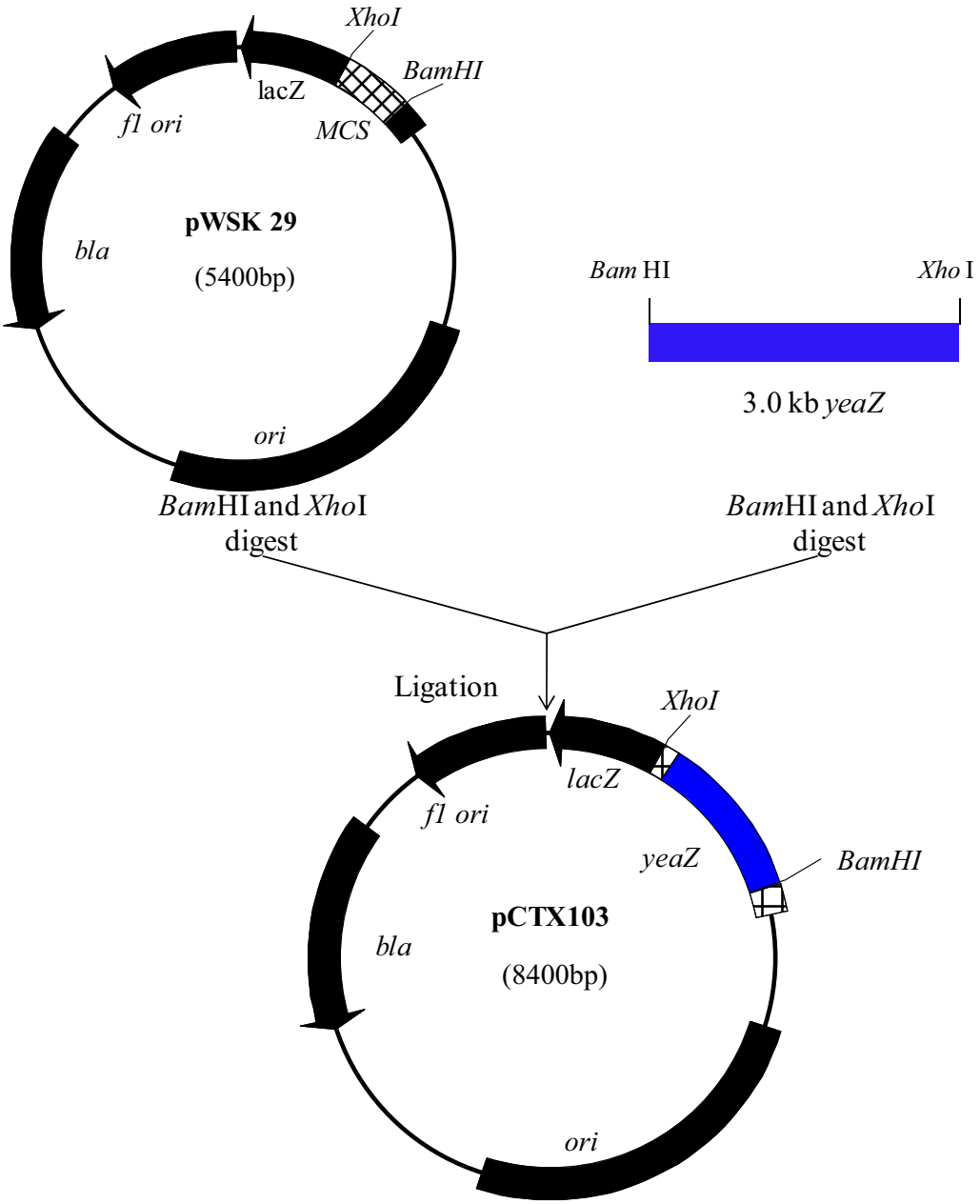

Figure 4.9: Construction of plasmid pCTX103.

The 3.0 kbp DNA fragment encoding *yeaZ* and sufficient flanking DNA to encode the cognate promoter, was amplified from *V. parahaemolyticus* NCTC 10884 and ligated into *Bam*HI and *Xho*I digested pWSK29 to create pCTX103.

Abbreviation: *bla*, ampicillin resistance; *f1 ori*, f1 origin; *lacZ*, *lacZ* gene; MCS, multiple cloning sites.

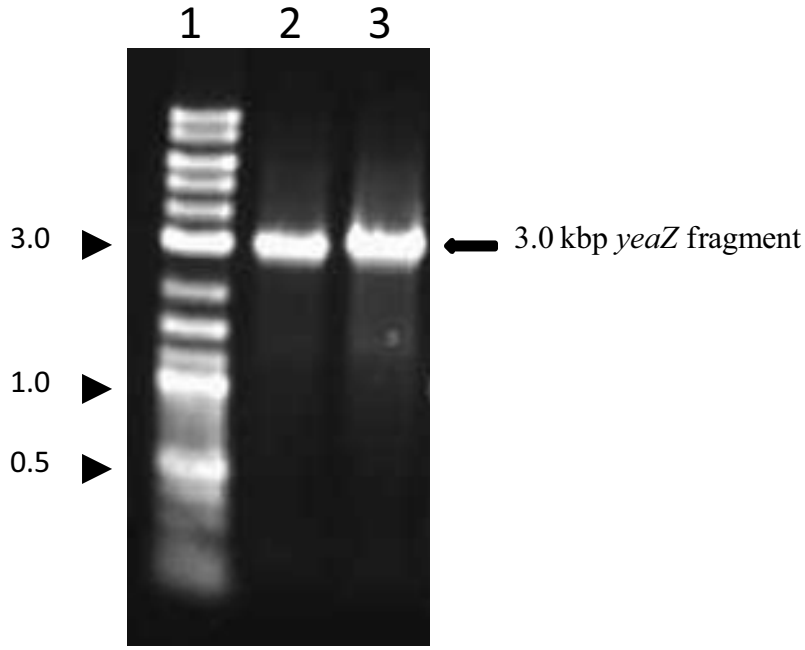

Figure 4.10: PCR amplification of the 3 kbp *yeaZ*$_{Vp}$ fragment.

The 3 kbp fragment cloned into pCTX103 was confirmed by PCR amplification using a primer pair M13F/R and plasmid pCTX103 as a template. Amplicons were separated on a 1% (w/v) agarose gel.

Lanes are marked as below:

1. 2 log size DNA marker.
2. 3 kbp *yeaZ* amplicons.
3. replicate of Lane 2.

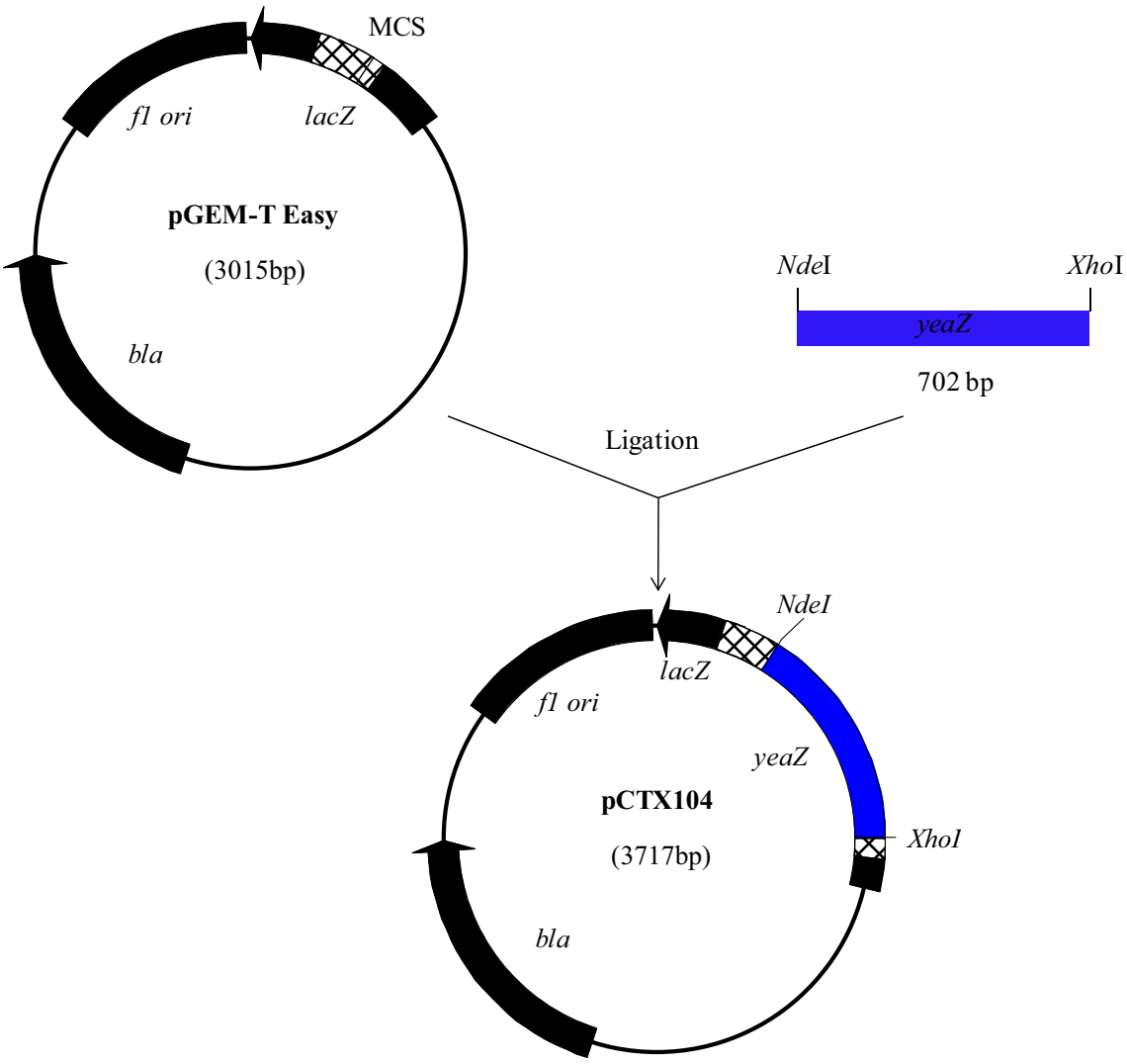

Figure 4.11: Construction of pCTX104.

The PCR amplified 702bp $yeaZ_{Vp}$ DNA fragment carrying *Nde*I/*Xho*I restriction sites was ligated into pGEM-T Easy to create plasmid pCTX104.

Abbreviation: *bla*, ampicillin resistance; *f1 ori*, f1 origin; *lacZ*, *lacZ* gene; MCS, multiple cloning sites.

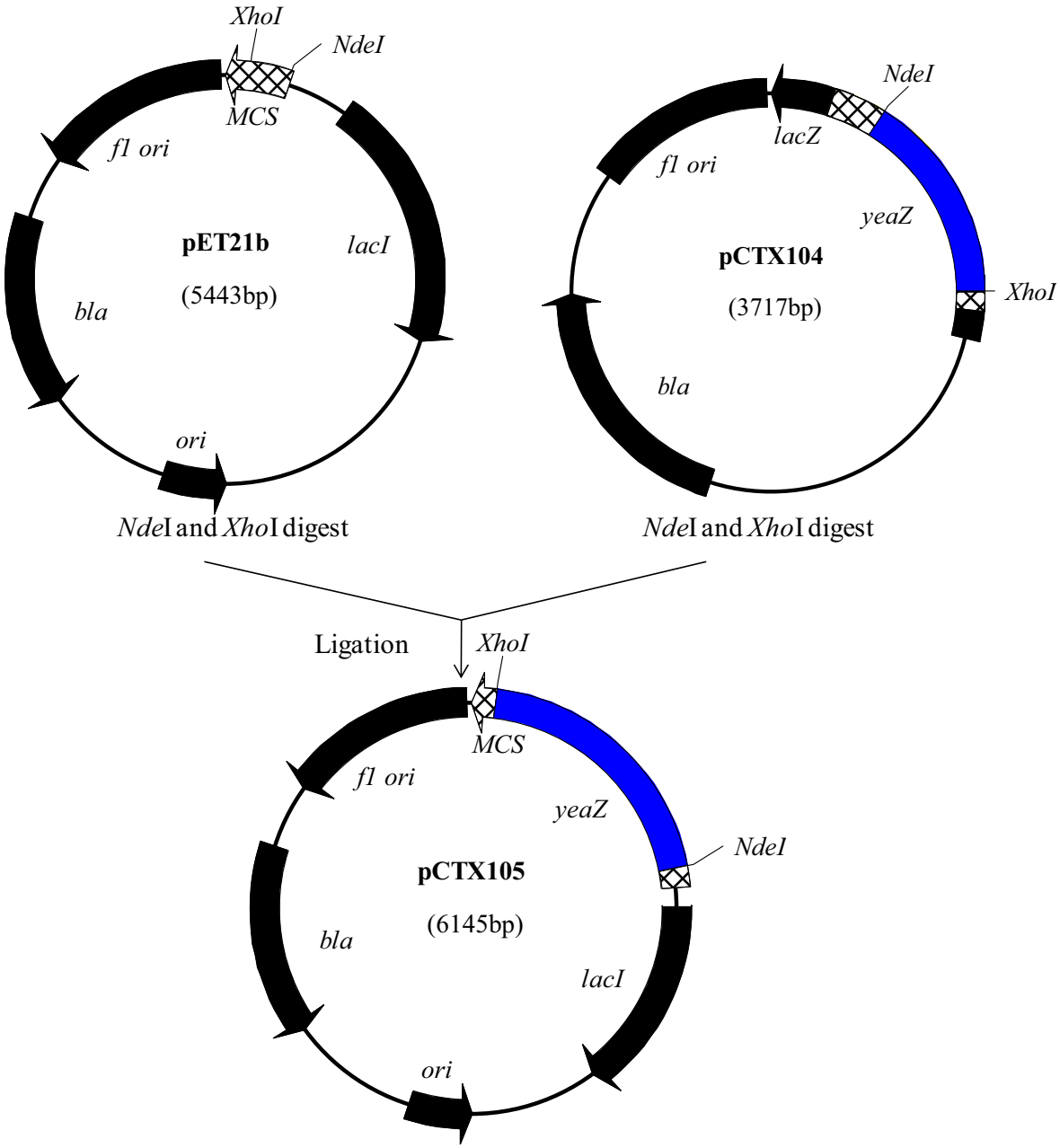

Figure 4.12: Construction of pCTX105.

A 702bp NdeI/XhoI *yeaZ*$_{Vp}$ DNA fragment was digested from pCTX104 plasmid and then ligated into similarly digested plasmid pET21b to create plasmid pCTX105. This plasmid construct was used to overexpress a C-terminal His tagged YeaZ hybrid protein.

Abbreviation: *bla*, ampicillin resistance; *f1 ori*, f1 origin; *lacI*, *lacI* gene; MCS, multiple cloning sites.

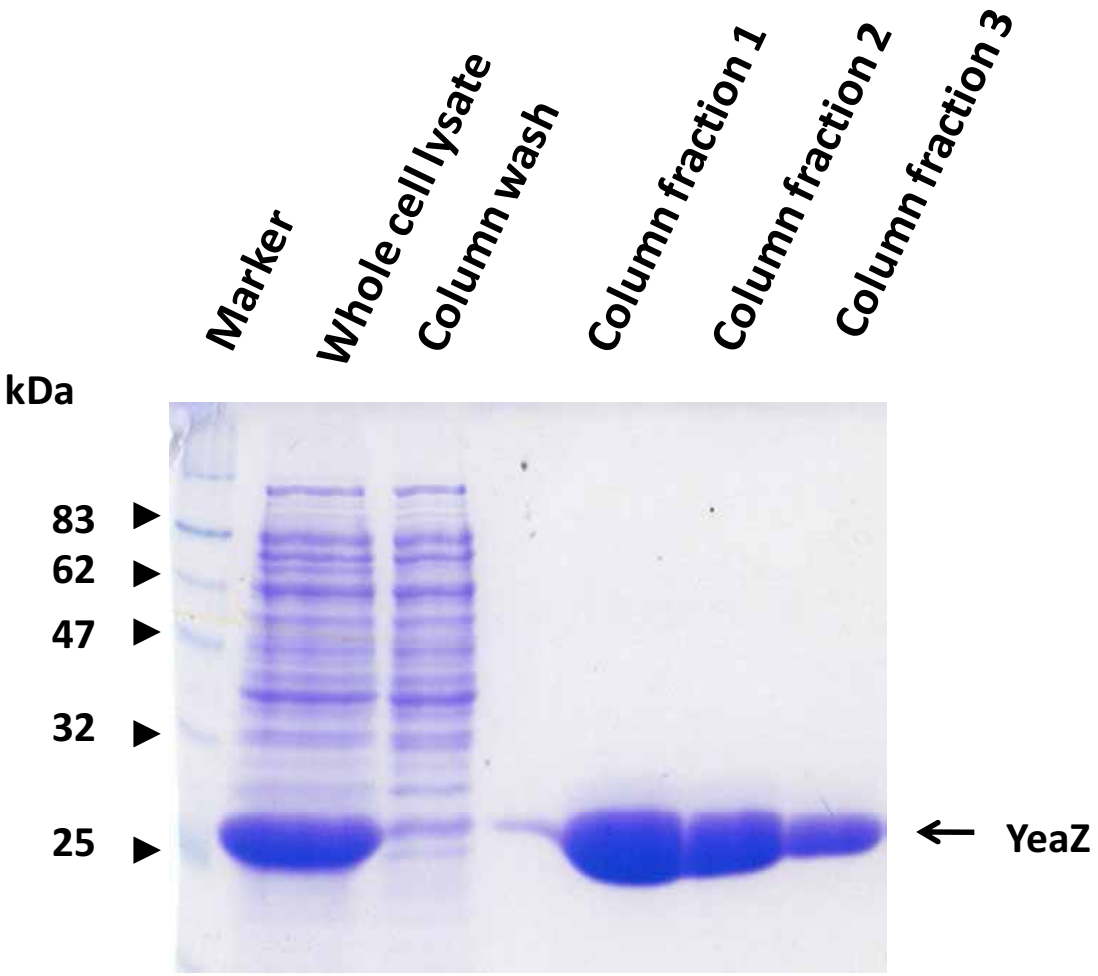

Figure 4.13: Purification of $YeaZ_{Vp}$ protein.

The C-terminal His-tagged $YeaZ_{Vp}$ fusion protein was overexpressed in *E. coli* BL21 cells and the protein purified by Ni-NTA column chromatography. Protein was induced in the presence of 0.2mM IPTG. Cells were then harvested by centrifugation. Cell pellets were resuspended in PBS buffer and treated with 0.5mg/mL lysozyme followed by three 30 sec burst of sonication. Cell debris was removed by centrifugation and supernatant passed through a Ni-NTA column. After washing with 10 column volumes of washing buffer, the His-tagged $YeaZ_{Vp}$ fusion protein was eluted and samples separated by SDS-PAGE. The protein bands were stained with Coomassie blue.

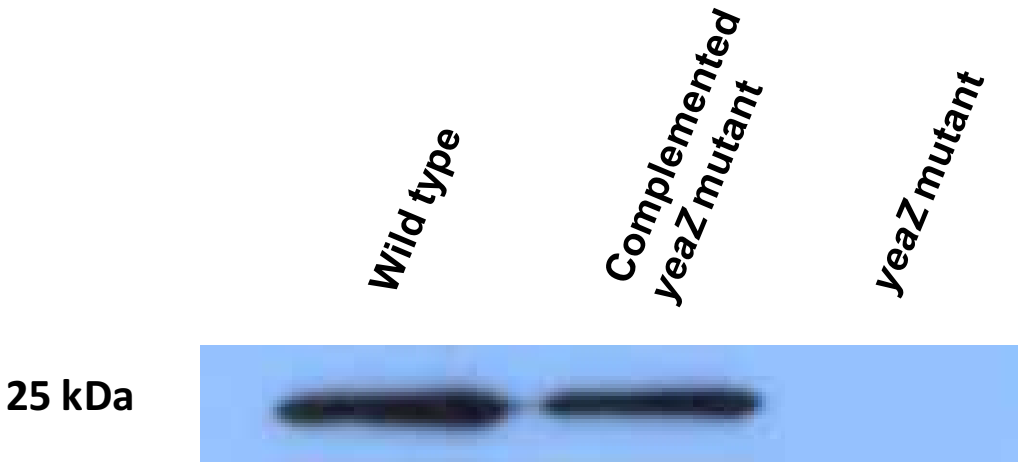

Figure 4.14: Western blot analysis of $YeaZ_{Vp}$ proteins.

Whole cell lysate were prepared from *V. parahaemolyticus* NCTC 10884 wild type, complemented *yeaZ*$_{Vp}$ and *yeaZ*$_{Vp}$ mutant strains and separated on 12.5% SDS-PAGE. The SDS-PAGE separated proteins were transferred to a Nitrocellulose membrane, probed with a rabbit anti-$YeaZ_{Vp}$ polyclonal antiserum and detected using a goat anti-rabbit-HRP conjugate secondary antibody.

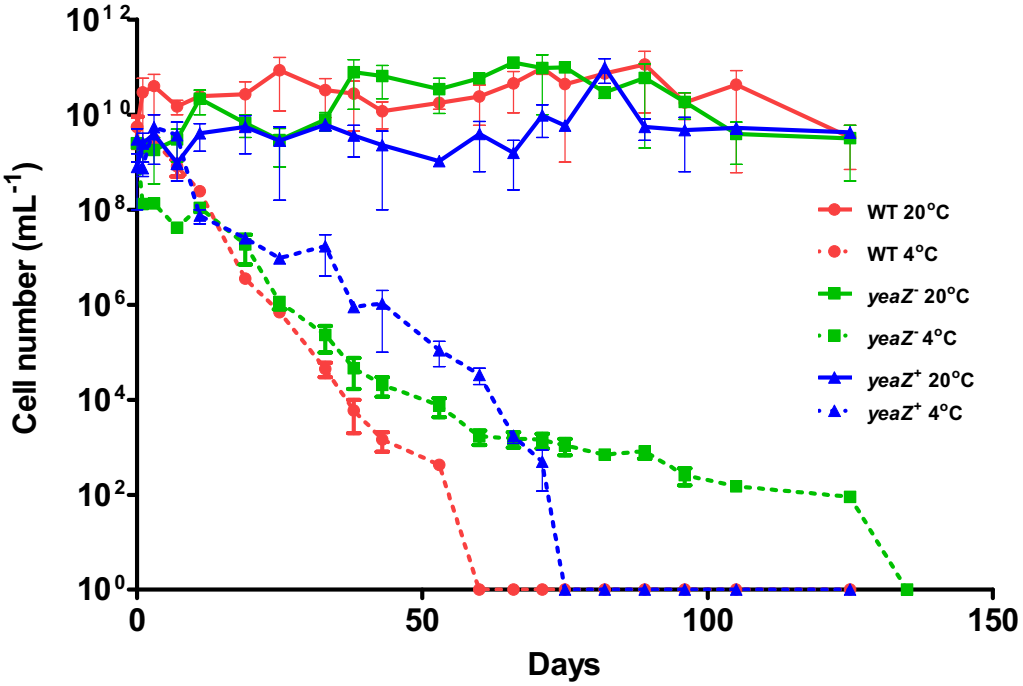

Figure 4.15: Effect of a *yeaZ* mutation on entry into the VBNC state.

Data shows the counts of culturable cells of *V. parahaemolyticus* NCTC 10884 wild type (WT), *yeaZ* mutant (yeaZ$^-$) and *yeaZ* complemented (yeaz$^+$) cultures during incubation in ASW at 4°C and 20°C for 140 d. Counts of culturable cells were performed on Marine agar. Each data point shown is the mean of two independent measurements. Error bars indicate the standard deviation of the mean value.

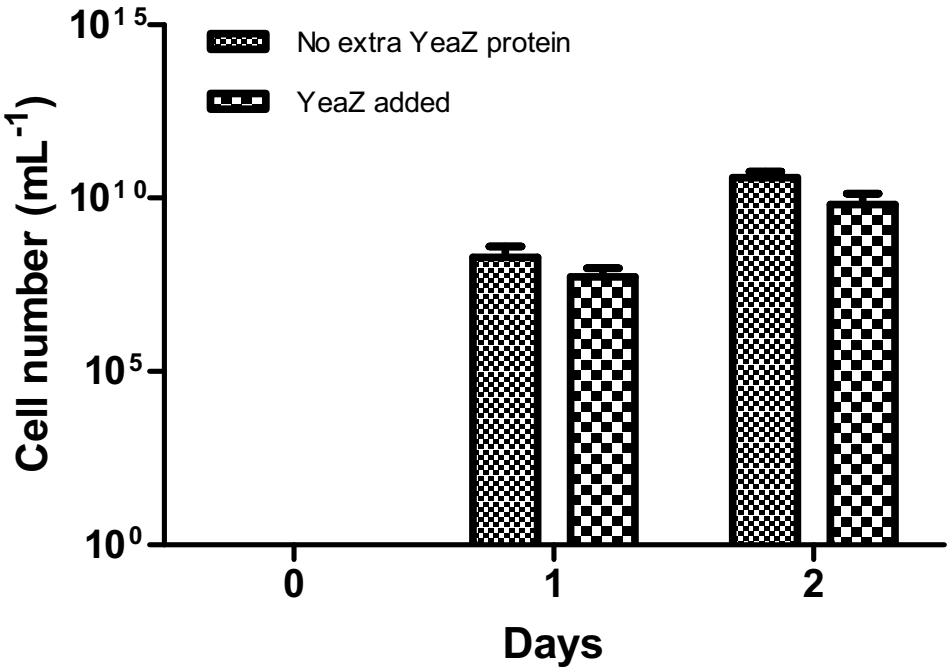

Figure 4.16: Effect of exogenous $YeaZ_{Vp}$ protein on resuscitation from the VBNC state.

Data shows change in culturability of VBNC state *V. parahaemolyticus* NCTC 10884 wild type and wild type added $YeaZ_{Vp}$ fusion protein, following resuscitation at 20°C for up to 2 d. The count of culturable cells was performed on Marine agar. Each data point shown is the mean of two independent measurements. The results are expressed as the mean ± SD.

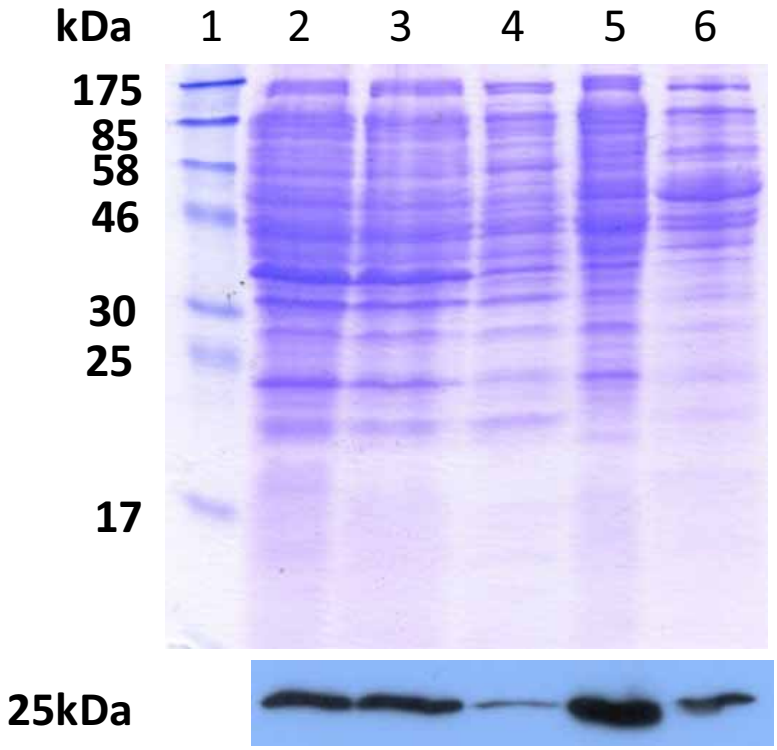

Figure 4.17: SDS-PAGE separation of proteins from *V. parahaemolyticus*.

Protein extracts were prepared from *V. parahaemolyticus* NCTC 10884 cells. Preparations were separated by 15% SDS-PAGE. Each lane was loaded with 10 ng of protein. Western blot analysis of a 25 kDa $YeaZ_{Vp}$ protein separated by SDS-PAGE is shown below.

Lanes are marked as below:

1. Protein prestained markers.
2. Whole cell lysate protein fraction.
3. Whole cell lysate crude protein fraction.
4. Cytoplasmic protein fraction.
5. Cell envelope protein fraction (cytoplasmic membrane plus outer membrane).
6. Outer membrane protein fraction.

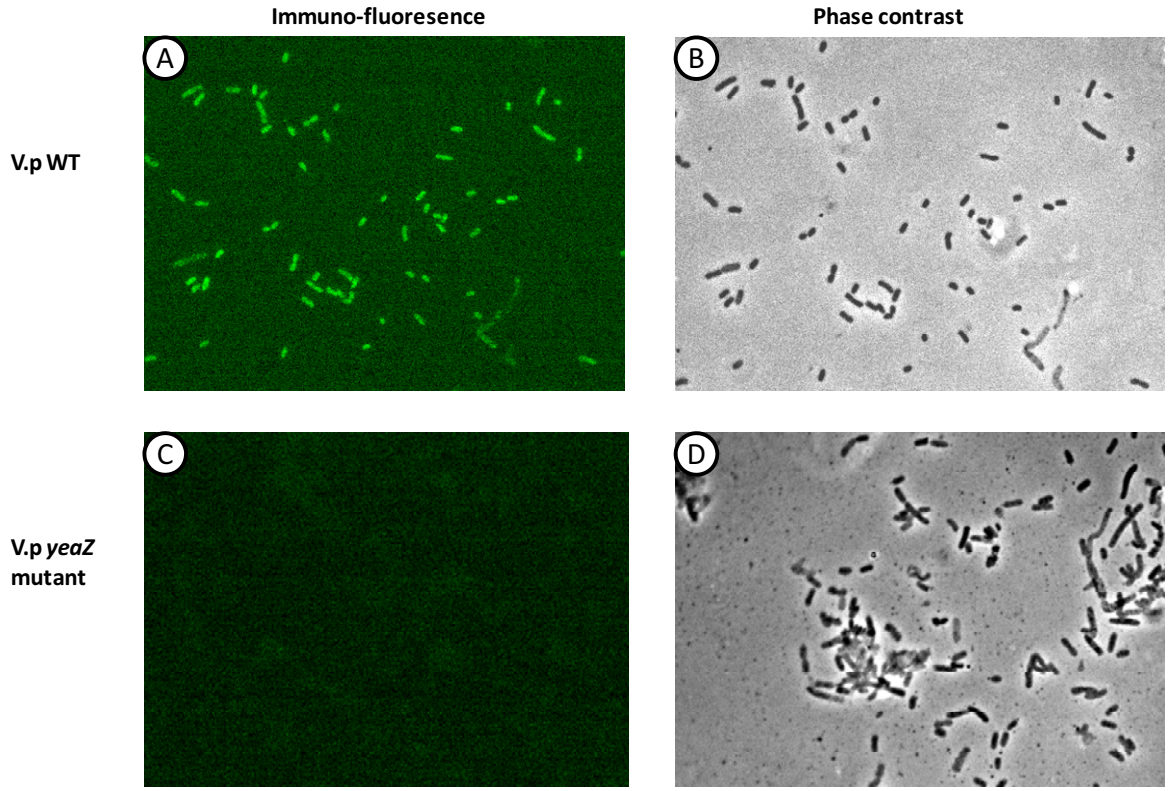

Figure 4.18: Detection of cell surface associated $YeaZ_{Vp}$ by IF.

Strains were grown in MB at 37°C to an OD 600 of 0.2-0.4, formalin fixed, and labelled with rabbit anti-$YeaZ_{Vp}$ serum followed by goat anti-rabbit IgG-FITC conjugated secondary antibody. Bacteria were observed by phase contrast and epi-fluorescence microscopy.

Panels A and B: Micrographs of *V. parahaemolyticus* NCTC 10884 wild type cells viewed by epi-fluorescence and phase contrast, respectively.

Panels C and D: Micrographs of *V. parahaemolyticus* NCTC 10884 $yeaZ_{Vp}$ mutants viewed by epi-fluorescence and phase contrast, respectively.

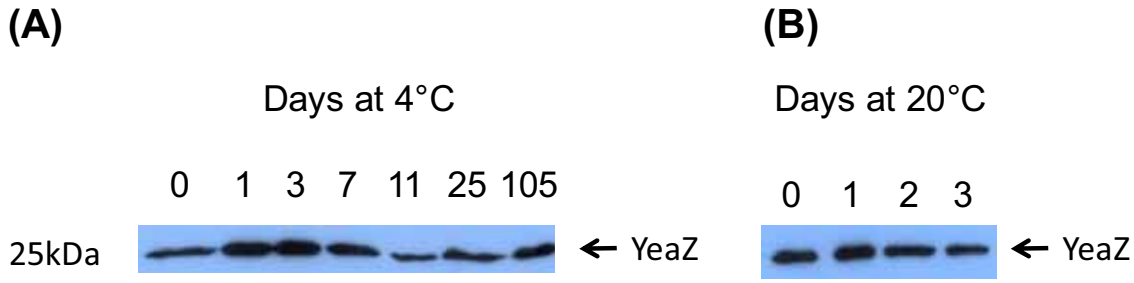

Figure 4.19: $YeaZ_{Vp}$ prepared from VBNC state cells and Resuscitated Cells.

V. parahaemolyticus NCTC 10884 wild type cells were cultured in MB. The cells were harvested and suspended in ASW (pH 8.0) and incubated at 4°C to induce the VBNC state. Preparations of non-culturable cells were resuscitated by temperature upshift to 20°C. The image shows Western blot analysis of SDS PAGE separated whole cell lysates of cell samples. $YeaZ_{Vp}$ was detected using specific rabbit polyclonal antiserum followed by goat anti-rabbit-HRP conjugate.

Panel A: $YeaZ_{Vp}$ extracted from samples of cell suspensions incubated at 4°C for up to 105 d.

Panel B: $YeaZ_{Vp}$ extracted from samples of cell suspensions of VBNC state cells resuscitated by temperature upshift to 20°C.

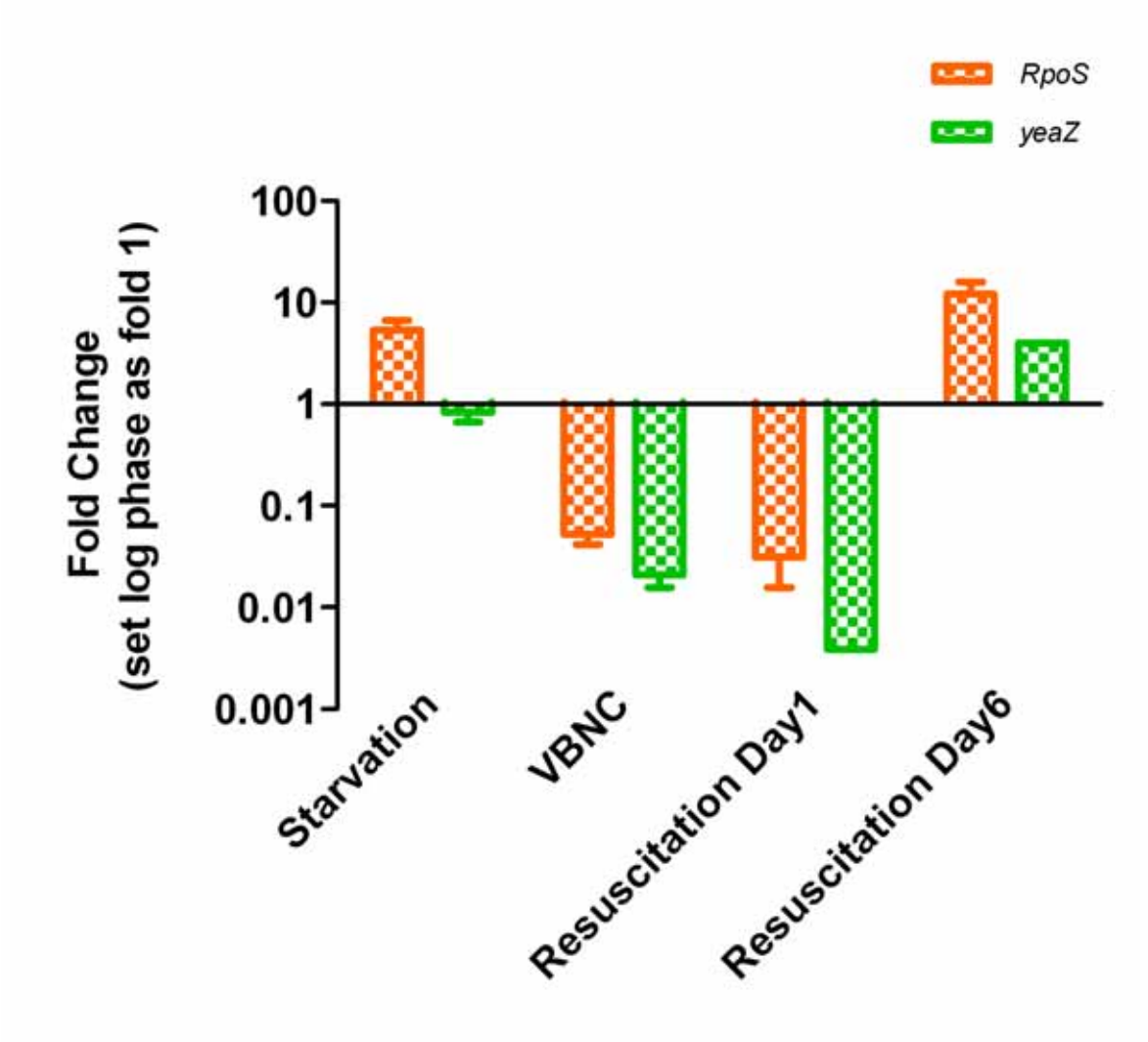

Figure 4.20: Expression of the *rpoS* and *yeaZ* genes in different states.

The fold changes of *rpoS* and *yeaZ* gene expression as determined by qRT-PCR. Data shows the fold changes for freshly prepared cell suspension in ASW (pH 8.0) prior to storage at 4°C, VBNC state cells, and VBNC state cells after resuscitation at 20°C for 1 and 6 d.

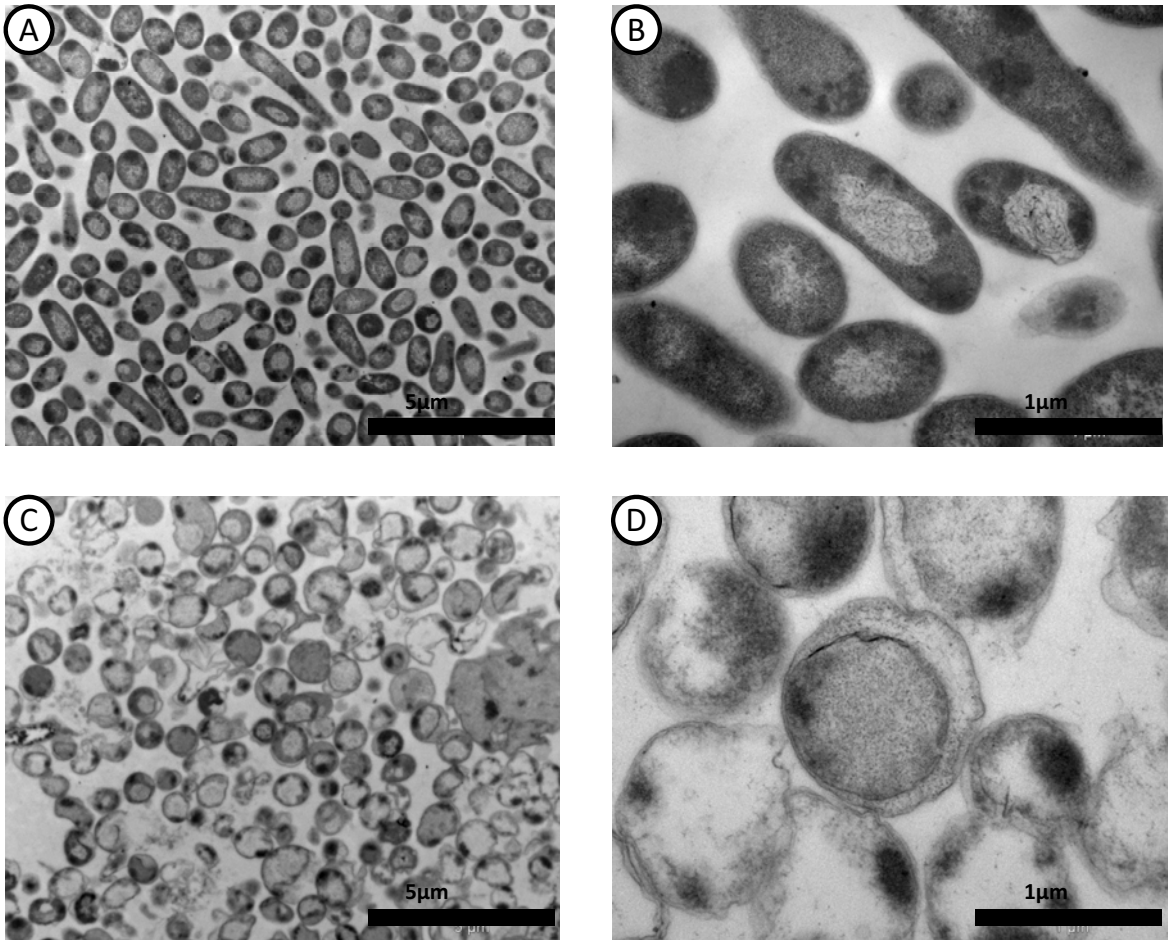

Figure 4.21: TEM images of sections of wild type *V. parahaemolyticus* cells.

Cells harvested from Log phase cultures were suspended in ASW incubated at 4°C until the culture reached the VBNC state. The bacterial cells from each culture were harvested by centrifugation and prepared for TEM.

Panels A and B: Sections of log phase *V. parahaemolyticus* NCTC 10884 wild type cells following culture in Marine Broth at 37°C.

Panels C and D: Sections of log phase of *V. parahaemolyticus* NCTC 10884 wild type cell suspensions in the VBNC state at 4°C.

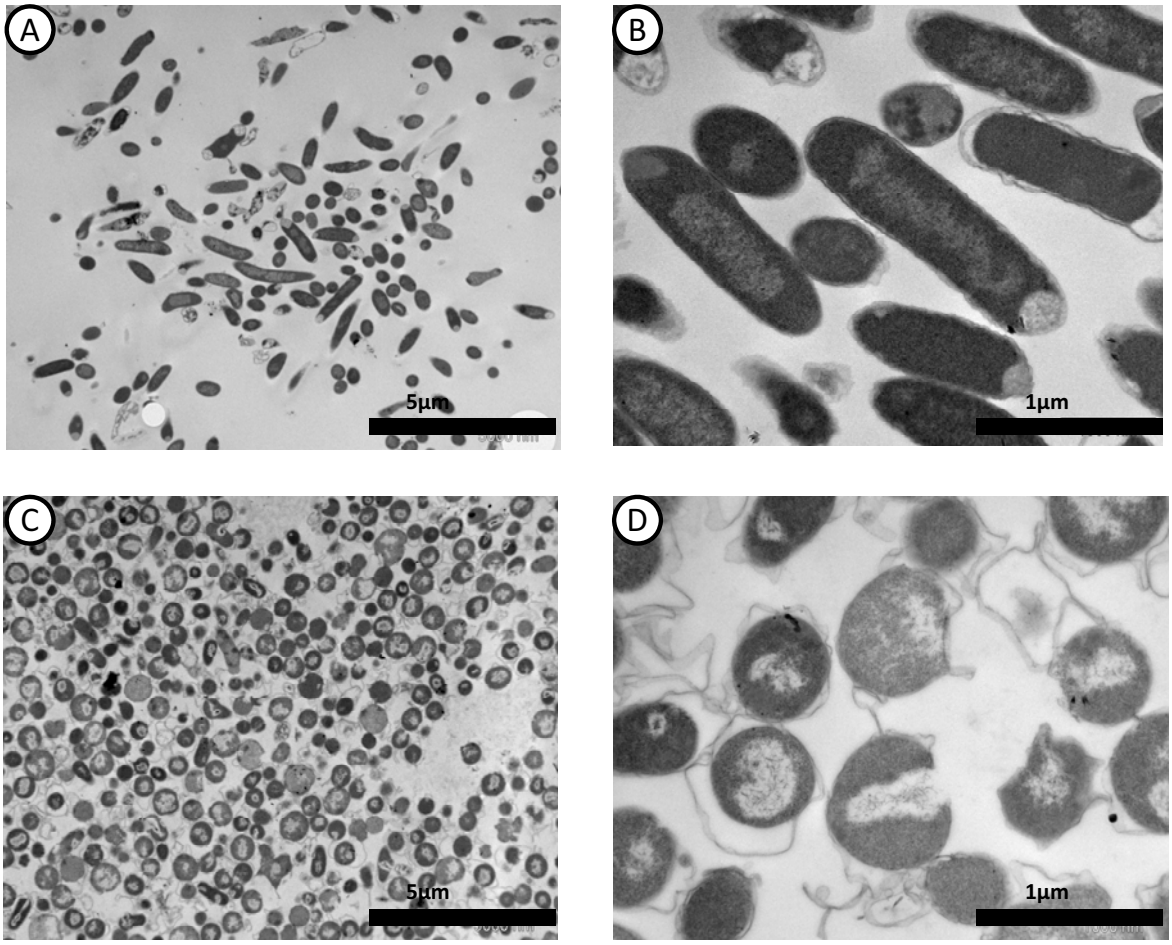

Figure 4.22: TEM images of sections of *V. parahaemolyticus yeaZ* mutant cells.

Log phase cultures or log phase cultures were used to suspend in ASW incubation at 4°C for reach the VBNC state. The bacteria cells from each culture were harvested by centrifugation and prepared for TEM.

Panels A and B: Sections of log phase *V. parahaemolyticus* NCTC 10884 $yeaZ_{Vp}$ mutant cells after culture in Marine Broth at 37°C.

Panels C and D: Sections of *V. parahaemolyticus* NCTC 10884 $yeaZ_{Vp}$ mutant cell suspensions in the VBNC state at 4°C.

Table 4.1: Effect of a *V. parahaemolyticus yeaZ* mutation on resuscitation from the VBNC state.

Days	Counts of viable cells		
	Wild type	*YeaZ* mutant	Complemented
0	ND	ND	ND
1	ND	ND	ND
2	$6.5 \times 10^6 \pm 2.1 \times 10^6$	ND	$8.0 \times 10^6 \pm 1.4 \times 10^6$
3	$7.6 \times 10^7 \pm 4.9 \times 10^7$	ND	$4.6 \times 10^7 \pm 6.3 \times 10^7$
4	$6.1 \times 10^8 \pm 4.1 \times 10^8$	ND	$1.8 \times 10^8 \pm 2.3 \times 10^8$
5	$6.5 \times 10^8 \pm 2.1 \times 10^8$	ND	$1.1 \times 10^9 \pm 2.1 \times 10^8$
6	$5.3 \times 10^8 \pm 3.2 \times 10^8$	ND	$5.5 \times 10^8 \pm 2.1 \times 10^8$

Data shows change in culturability of VBNC state *V. parahaemolyticus* NCTC 10884 wild type, $yeaZ_{Vp}$ mutant and $yeaZ_{Vp}$ complemented mutant following resuscitation in ASW at 20°C for up to 6 d. The count of culturable cells was performed on Marine agar. Each data point shown is the mean of two independent measurements. The results expressed as averages ± SD. ND: not detected.

Chapter 5: YeaZ Protein-Protein Interactions

5.1 Introduction

Results presented in Chapter 4 suggest that the YeaZ protein may be involved in the resuscitation of VBNC state in *V. parahaemolyticus* NCTC 10884, although, the actual molecular mechanism regulating resuscitation and other potential involved factors, are still unclear. If $YeaZ_{Vp}$ is directly involved then this protein is likely to interact with other protein partners to direct this process. Recently, it has been shown that $YeaZ_{Ec}$ and another protein, $YgjD_{Ec}$, are two interacting and sequence-related proteins in *E. coli* that are intimately involved in maintenance of viability of these organisms (Handford et al., 2009). Given the role of $YeaZ_{Ec}$ in viability, it is not surprising that the *yeaZ* gene and the *yjeE* gene homologs have been found in all bacterial genomes sequenced to date, except for the highly reduced genomes of the obligate endosymbionts *Carsonella ruddii* and *Sulcia muelleri* (McCutcheon & Moran, 2007; Nakabachi et al., 2006). Furthermore, the three genes *yjeE*, *yeaZ* and *ygjD*, have been shown to be highly conserved in each bacteria genome examined, although only, in a limited number of studies, have these genes been demonstrated to be essential for viability under standard laboratory culture conditions (Handford et al., 2009). To overcome the requirement of these genes for viability, Handford et al. (2009) constructed conditional expression strains for the three genes in *E. coli* that allowed depletion of these proteins without compromising viability. These constructs were then used to study interactions between these proteins. Interestingly, their work suggested that depletion of the proteins encoded by these genes can be complemented by multi-copy clones harboring the *rstA* gene[9]. This suggested that Rst proteins were also involved in the same essential cellular pathway (Chapter 1, Figure 1.13). This interaction network of three proteins essential for bacterial viability provided evidence that not just YeaZ, but also other proteins may interact with each other and regulate the VBNC state resuscitation in *V. parahaemolyticus* NCTC 10884.

[9] The *rstA* gene encodes the response regulator of the RstAB two component signal transduction system shown to act as a multicopy suppressor of a strain depleted for *yjeE* expression (Campbell et al., 2007).

Rajagopala et al. (2010) recently systematically examined protein-protein interactions between gene products YgjD, YjeE and YeaZ from *E. coli* in the *E. coli* ORF collection and other Gram-positive pathogens such as *S. aureus* and *S. pneumoniae* collections, using yeast two-hybrid system. They reported that *E. coli* YeaZ and YgjD protein interacted with each other. Moreover, the YeaZ protein from *E. coli* was observed to be able to interact with YgjD protein from both *S. aureus* and *S. pneumonia*. Although the biological function of YeaZ, YjeE and YgjD remains poorly understood, it has been suggested that in *E. coli*, YeaZ was able to proteolyse YgjD. This indicated that YeaZ has protease activity (Rajagopala et al., 2010).

V. parahaemolyticus genomes sequenced thus far encode proteins YjeE, YgjD and YeaZ homologs respectively. In Chapter 4 of this thesis, the $YeaZ_{Vp}$ mutants were shown to be involved in VBNC state resuscitation in *V. parahaemolyticus* NCTC 10884. However, in the context of this chapter, it is of particular interest that the non-polar insertion mutation within the *yeaZ*$_{Vp}$ gene was apparently not lethal for strain NCTC 10884. Whether this observation means that the function of $YeaZ_{Vp}$ is different in subtle ways from $YeaZ_{Ec}$ is unclear. One approach that could be used to unravel this difference may be to first determine whether the known protein interaction network exists between the YeaZ, YjeE and YgjD proteins expressed by *V. parahaemolyticus* NCTC 10884. Indeed this approach is the basis for the principal objective of this chapter. An additional objective of work described in this chapter was to determine the $YeaZ_{Vp}$ domains involved in protein-protein interactions. Study of protein-protein interaction of $YeaZ_{Vp}$ and its related partners would help to understand the function of this protein complex, the YeaZ/YjeE/YgjD essential signal transduction network and perhaps the mechanism that regulates VBNC state resuscitation in this marine pathogen.

5.2 Aims and Approaches

The following outline describes approaches used in this chapter to analyze the interaction of YeaZ/YjeE and YeaZ/YgjD protein complex in *V. parahaemolyticus* NCTC 10884.

1. To determine whether $YeaZ_{Vp}$ interacts with $YjeE_{Vp}$ and $YgjD_{Vp}$, bacterial two-hybrid and yeast two-hybrid systems were used to investigate the protein-protein interaction between protein pairs, $YeaZ_{Vp}$/$YjeE_{Vp}$, $YeaZ_{Vp}$/$YgjD_{Vp}$ or $YeaZ_{Vp}$/$YeaZ_{Vp}$ (bacterial two-hybrid).

2. Native protein-protein interactions between $YeaZ_{Vp}$/$YjeE_{Vp}$ and $YeaZ_{Vp}$/$YgjD_{Vp}$ pairs were examined following over-expression by an *E. coli* host carrying plasmids capable of co-expression of each protein pair. Protein-protein interactions were examined using His-tag affinity technologies and cross-linking approaches designed to stabilize protein complexes.
3. Immuno-precipitation together with Matrix-assisted laser desorption/ionization (MALDI-TOF) were used to investigate other $YeaZ_{Vp}$ protein complexes formed in *V. parahaemolyticus* NCTC 10884.
4. Site-direct mutagenesis together with bacterial two-hybrid technology was used to identify the potential interaction/binding sites of $YeaZ_{Vp}$.

5.3 Results

5.3.1 Characterization of the $YgjD_{Vp}$ and $YjeE_{Vp}$ Nucleotide and Amino Acid Sequences

Nucleotide and amino acid sequences of $YeaZ_{Vp}$ associated protein $YgjD_{Vp}$ was determined. The YgjD ORF (GenBank Accession no. BA000031), comprises 1,017 bp nucleotides and encodes a 339 amino acid protein with a predicted molecular weight of 37 kDa (Figure 5.1). BLASTP (Altschul et al., 1990) sequence analysis of *V. parahaemolyticus* YgjD was indicated that the YgjD polypeptide is similar to a large number of O-sialoglycoprotein endopeptidases including *Mannheimia haemolytica* (GenBank Accession no, AAA80282.1 GI:150502), *Photobacterium profundum* (GenBank Accession no, YP_128667.1 GI:54307647), *S. enterica* (GenBank Accession no, ZP_02697497.1 GI:168463580), *E. coli* (GenBank Accession no, YP_001745336.1 GI:170682206) and *Aeromonas hydrophila* (GenBank Accession no, YP_855374.1 GI:117621272). As the *Mannheimia haemolytica* YgjD protein has been shown to have O-sialoglycoprotein endopeptidase activity for O-sialoglycoprotein, this suggests that the *V. parahaemolyticus* YgjD may have a similar function. In addition, a search for conserved domains indicated that the N-terminal region of YgjD amino acid sequence was similar to COG1214 superfamily of M22 O-sialoglycoprotein endopeptidase homologs. Other conserved domain presents include a universal genome maintenance protein (UGMP) homolog and a HMEGH motif (Figure 5.1). The latter is a

histidine rich motif conserved in bacteria and is a potential metal ion binding site (Abdullah et al., 1991). In *V. parahaemolyticus*, the presence of this motif in YgjD, may indicate that the putative protein is associated with metal binding.

The YjeE ORF comprised of 465 bp nucleotides that encoded a 155 amino acid protein (GenBank Accession no., NP_799200 GI:28899595) with a predicted molecular weight of 17 kDa (Figure 5.2). BLASTP analysis (Altschul et al., 1990) indicated that the YjeE polypeptide has high similarity to the ATPase or nucleotide binding proteins of *Photobacterium profundum* (YP_131454.1 GI:54310434), *S. enterica* (NP_458793.1 GI:16763176), *E. coli* (ZP_03001004.1 GI:188493734) and *Aeromonas salmonicida* (YP_001143099.1 GI:145300258). Like the *E. coli* YjeE protein, YjeE has a typical P-loop ATPase that binds and hydrolyses ATP (Teplyakov et al., 2002). Furthermore, the $YjeE_{Vp}$ amino acid sequence was conserved to ATPase YjeE family. Members of this family have a conserved nucleotide-binding motif GXXGXGKT and a nucleotide-binding fold (Figure 5.2) and the YjeE protein of *Haemophilus influenza* has been shown to have ATPase activity (Lerner et al., 2007). Taken together, this data indicated that the presence of this motif may act as a nucleotide-binding site in the *V. parahaemolyticus* YjeE.

5.3.2 Protein-protein Interactions in Bacterial Two-hybrid Analysis

Bacterial two-hybrid systems are a genetic approach for detecting protein–protein interactions *in vivo* using a prokaryotic host. In this study, a bacterial two-hybrid system described by (Dove & Hochschild, 2004) was used to examine potential protein-protein interactions using $YeaZ_{Vp}$ as a bait. Plasmid pBT (Chapter 2, Table 2.3) is a bait expression plasmid that carries a low copy p15A replication origin and a chloramphenicol resistance gene. The bait plasmid encodes the full length bacterial phage λcI protein under the control of the IPTG-inducible la*c-UV*5 promoter. Plasmid pTRG (Chapter 2, Table 2.3) is a prey plasmid which carries a low-copy ColEl replication origin and confers tetracycline resistance. The plasmid directs transcription of the amino-terminal domain of RNA polymerase α subunit, through a multiple cloning site at the 3' end of α subunit gene. Expression is and under the control of the IPTG-inducible, tandem promoter lpp/lac-UV5.

For this analysis, the *yeaZ*$_{Vp}$ gene was cloned into the bait plasmid pBT. The YeaZ$_{Vp}$ bait was then used to examine interactions with YeaZ$_{Vp}$, YgjD$_{Vp}$ and YjeE$_{Vp}$ expressed from the pTRG prey plasmid.

5.3.2.1 Cloning of the *yeaZ*$_{Vp}$ Gene into Plasmid pBT

The oligonucleotide pair of YeaZNotI F and YeaZ R (Chapter 2, Table 2.4) was used to PCR amplify the *yeaZ*$_{Vp}$ gene from strain NCTC 10884. The 0.7 kbp DNA fragment encoding the full length *yeaZ*$_{Vp}$ was digested with *Not*I and *Xho*I and cloned into similarly digested pBT plasmid to create pCTX106 (Chapter 2, Table 2.3) as described in Figure 5.3. Plasmid pCTX106 was then used to transform into chemically competent *E. coli* DH5αZ1 cells (Chapter 2, Section 2.9.7). Transformants were selected by plating on LB plates containing Cml. After O/N culture at 37°C, colonies were collected and screened for insert DNA by digestion with *Not*I and *Xho*I. Clones that contained the 702 bp insert, were confirmed by both PCR analysis and DNA sequencing. Plasmid pCTX106 was extracted from confirmed *E. coli* DH5αZ1 transformants using a plasmid extraction kit (Chapter 2, Section 2.9.2). Plasmid pCTX106 nucleotide sequence was confirmed by sequencing using primers pBT 5'/3' (Appendix O).

5.3.2.2 Cloning the *yeaZ*$_{Vp}$, *ygjD*$_{Vp}$ and *yjeE*$_{Vp}$ Genes into Plasmid pTRG

Similar cloning methodology was used to clone *yeaZ*$_{Vp}$ into the pTRG prey expression plasmid. Primers YeaZNotI F and YeaZ R (Chapter 2, Table 2.4) were used to amplify a 702 bp DNA fragment that encoded a full length *yeaZ*$_{Vp}$ flanked by *Not*I/*Xho*I restriction sites. A *Not*I/*Xho*I *yeaZ*$_{Vp}$ full length sequence was cloned into similarly digested pTRG plasmid to create pCTX107 (Chapter 2, Table 2.3). Figure 5.4 illustrates the major steps in construction of plasmid pCTX107. Plasmid pCTX107 was used to transform *E. coli* DH5αZ1 cells as described previously (Chapter 2, Section 2.9.7). Clones were screened and selected from LB plates containing Tet with incubation O/N at 37°C O/N. PCR and DNA sequencing were performed to confirm clones containing the 702 bp insert. Plasmid pCTX107 extracted from *E. coli* DH5αZ1 cells (Chapter 2, Section 2.9.2) was sequenced to confirm its nucleotide accuracy using primers pTRG 5'/3' (Chapter 2, Table 2.4) (Appendix P).

Similarly, oligonucleotide primers YjeENotIF/YjeE R (Chapter 2, Table 2.4) were used to amplify the *yjeE* gene to generate a 485 bp DNA fragment from *V. parahaemolyticus* NCTC 10884 that encoded the full length $yjeE_{Vp}$ gene on a *Not*I/*Xho*I restriction fragment. This fragment was then cloned into plasmid pTRG to generate pCTX108 (Chapter 2, Table 2.3) as described in Figure 5.4. Plasmid pCTX108 was introduced into *E. coli* DH5αZ1 chemically competent cells (Chapter 2, Section 2.9.7) and transformants screened on LB plates containing Tet with incubation O/N at 37°C. Transformants were selected and screened for insert DNA. Clones that carried the 485 bp insert, were confirmed by PCR and DNA sequencing. DNA was extracted (Chapter 2, Section 2.9.2) from plasmid *E. coli* DH5αZ1 [pCTX108] and oligonucleotide primers pTRG 5'/3' were used to confirm the nucleotide sequence of the insert (Appendix Q).

Similarly, oligonucleotide primers YgjD NotI F and YgjD R (Chapter 2, Table 2.4) were used to amplify the *ygjD* gene to generate a 1.017 kbp DNA fragment from *V. parahaemolyticus* NCTC 10884. The full length *ygjD* carried on a *Not*I/*Xho*I restriction fragment was cloned to similarly digested plasmid pTRG to create pCTX109 (Chapter 2, Table 2.3) as described in Figure 5.4. Plasmid pCTX109 was introduced into chemically competent *E. coli* DH5αZ1 cells as described previously and transformants screened on LB plates containing Tet, with O/N incubation at 37°C. PCR and DNA sequencing were used to confirm whether clones contained the 1,017 bp insert. Plasmid pCTX109 was extracted from *E. coli* DH5αZ1 cells and the plasmid nucleotide sequence was confirmed by DNA sequencing using oligonucleotide primers pTRG 5'/3' (Appendix R).

5.3.2.3 β-Galactosidase Assays

The β-galactosidase assay (Chapter 2, Section 2.11.12.2) was used to examine the protein-protein interactions between bait and prey hybrid proteins. Plasmid pCTX106/pCTX107, pCTX106/pCTX108 and pCTX106/pCTX109 were co-transformed into *E. coli* KS1 cells (Chapter 2, Table 2.1). Plasmids pBT and pTRG were used as negative controls. Plasmid pBT-LGF2 and pTRG-Gal11p was used as positive controls. All plasmid pairs were used to transform into chemically competent *E. coli* KS1 cells (Chapter 2, Table 2.1 and Section 2.9.7). Transformants were selected on LB plates containing Cm, Kan and Tet, with incubation O/N at 37°C. Transformants collected from selection plates and activities were

examined for protein-protein interaction between $YeaZ_{Vp}$, $YjeE_{Vp}$ and $YgjD_{Vp}$ proteins based on β-galactosidase activity (Chapter 2, Section 2.11.12.2).

Constructs including pCTX106/pCTX107, pCTX106/pCTX108, pCTX106/pCTX109, a negative control (pBT and pTRG) and a positive control (pBT-LGF2 and pTRG-Gal11p), were measured the β-galactosidase activity. Data presented in Figure 5.5 showed that the pCTX106/pCTX109 construct (*yeaZ*$_{Vp}$/*ygjD*$_{Vp}$) had the highest β-galactosidase activity ($P<0.05$) compared to the pCTX106/pCTX107 (*yeaZ*$_{Vp}$/*yeaZ*$_{Vp}$) and pCTX106/pCTX108 (*yeaZ*$_{Vp}$/*yjeE*$_{Vp}$) constructs. This data indicated a strong interaction between protein $YeaZ_{Vp}$ and $YgjD_{Vp}$. In the same figure, the β-galactosidase activity of the pCTX106/pCTX107 (*yeaZ*$_{Vp}$/*yeaZ*$_{Vp}$) construct shown, was slightly higher ($P<0.05$) than the negative control construct (pBT and pTRG), indicating that $YeaZ_{Vp}$ may have ability to form dimers or higher multimeric units. Transformants containing pCTX106/pCTX108 did not express β-galactosidase activity, indicating that no significant interaction was observed between $YeaZ_{Vp}$ and $YjeE_{Vp}$.

5.3.3 Protein-protein Interactions in Yeast Two-hybrid Analysis

For this analysis, the *yeaZ*$_{Vp}$ gene was cloned into the bait plasmid pLexA. The expressed $YeaZ_{Vp}$ bait was then used to examine interactions with $YgjD_{Vp}$ and $YjeE_{Vp}$ expressed from the pB42AD prey plasmid.

5.3.3.1 Cloning of *yeaZ*$_{Vp}$ into Plasmid pLexA

The interactions between protein pairs $YeaZ_{Vp}$/$YjeE_{Vp}$ and $YeaZ_{Vp}$/$YgjD_{Vp}$ described in Section 5.3.2, were confirmed by a eukaryotic model, the yeast two-hybrid system. The construction of pCTX110 is shown in Figure 5.6. Primers pLexAyeaZF/R (Chapter 2, Table 2.4) were used to PCR amplify the *yeaZ*$_{Vp}$ gene from *V. parahaemolyticus* NCTC 10884 to generate a 702 bp *yeaZ*$_{Vp}$ fragment that was then isolated as an *Eco*RI/*Xho*I restriction fragment. This fragment was ligated to similarly digested pLexA (Chapter 2, Table 2.3) bait plasmid to create construct pCTX110 (Chapter 2, Table 2.3). Plasmid pCTX110 was then introduced into chemically competent *E. coli* DH5α cells (Chapter 2, Section 2.9.7) and transformants selected by culture on LB plates containing Amp with O/N incubation at 37°C. Transformants were selected and screened for insert DNA by extracting plasmid pCTX110

from *E. coli* DH5α cells using plasmid extraction kit (Chapter 2, Section 2.9.2). A forward primer pLexA 5' (Chapter 2, Table 2.4) was used to confirm the nucleotide sequence of the construct (Appendix S).

5.3.3.2 Cloning of *ygjD*$_{Vp}$ and *yjeE*$_{Vp}$ into Plasmid pB42AD

The *ygjD*$_{Vp}$ and *yjeE*$_{Vp}$ genes were cloned into the pB42AD plasmid using similar methods to those (Chapter 2, Table 2.3). Primers pB42AD-YjeE F/R (Chapter 2, Table 2.4) were used to PCR amplify the *yjeE* gene from *V. parahaemolyticus* NCTC 10884 as a 465 bp *Xho*I fragment of the full length *yjeE* gene. The *yjeE*$_{Vp}$ was then cloned into pB42AD plasmid to create pCTX111 (Chapter 2, Table 2.3) as described in Figure 5.7. Plasmid pCTX111 was then introduced into chemically competent *E. coli* DH5α cells, followed by culture O/N at 37°C on LB plates containing Amp. Clones that contained the 465 bp *yjeE*$_{Vp}$ insert, were screened by PCR and DNA sequencing. The pB42AD sequencing primers (Chapter 2, Table 2.4) were used to confirm the sequence of plasmid pCTX111 (Appendix T).

Primers pB42AD-YgjD F/R (Chapter 2, Table 2.4) were also used to PCR amplify the *ygjD*$_{Vp}$ gene. The 1017 bp *EcoR*I/*Xho*I fragment of the full length *ygjD*$_{Vp}$ was cloned into pB42AD plasmid to generate pCTX112 (Chapter 2, Table 2.3) as described in Figure 5.7. Plasmid pCTX112 was introduced into chemically competent *E. coli* DH5α cells, cultured O/N at 37°C on LB plates containing Amp. DNA sequencing using the pB42AD sequencing primers confirmed that clones contained the 1.017 kbp *ygjD*$_{Vp}$ construct (Chapter 2, Table 2.4) (Appendix U).

5.3.3.3 Interactions between YeaZ$_{Vp}$ and Proteins YjeE$_{Vp}$ or YgjD$_{Vp}$

Pairs of constructs were co-transformed to confirm the protein-protein interactions. Plasmid pCTX110 (pLexA-YeaZ$_{Vp}$) was together with pCTX111 (pB42AD-YjeE$_{Vp}$) used to co-transform *Saccharomyces cerevisiae* (*S. cerevisiae*) EGY48[p8op-lacZ] cells (Chapter 2, Table 2.3) using a yeast *S. cerevisiae* EasyComp Transformation kit (Chapter 2, Section 2.11.13.2). Cells were grown on SD/Glu/-His/-Trp/-Ura selective medium to select colonies of cells containing both hybrid plasmids. Plasmid pCTX112 (pB42AD-YgjD$_{Vp}$) was also co-transformed with pCTX110 (pLexA-YeaZ$_{Vp}$) into *S. cerevisiae* EGY48[p8op-lacZ] cells.

Colonies with co-transformed plasmids pLexA-53 and pB42AD-T were used as a positive control. A total of three negative controls were used in this experiment:

1. Plasmid pLexA and pB42AD co-transformed yeast cells.
2. Plasmid pCTX110 (pLexA-YeaZ$_{Vp}$) transformed cells.
3. Plasmid pCTX110 (pLexA-YeaZ$_{Vp}$) and pB42AD co-transformed cells.

Protein-protein interactions were examined by using the recommended induction plate activity assay for this two-hybrid system[10]. Cells were streaked on SD/Gal/Raf/-His/-Trp/-Ura/-Leu + X-gal and cultured at 30°C for 24 to 72 hr to induce expression of bait and prey proteins and allow screening of expression of *LacZ* reporter gene. This medium contains Galactose and Leucine required for expression of bait and prey proteins from the P_{Gal} and P_{ADH1} promoters located on pB42AD and pLexA respectively. The appearance of blue colonies (expressing β-galactosidase) indicated an interaction between bait and prey proteins. All transformed cell lines that carried plasmids encoding different bait and prey pairs were tested on both induced and un-induced selective plates. Results for the interaction assays are shown as Figure 5.8. On the induction plate (Figure 5.8, Panel A), growth of blue (β-galactosidase positive) colonies was observed for the positive control (colony no. 6) and the YeaZ$_{Vp}$/YgjD$_{Vp}$ co-transformants (colony no. 5). This result indicated that the YeaZ$_{Vp}$ protein interacted with YgjD$_{Vp}$ protein. However transformants expressing the YeaZ$_{Vp}$ and YjeE$_{Vp}$ proteins (colony no. 4) were β-galactosidase negative as were the negative controls (colonies 1, 2 and 3). The lack of a response indicated that YeaZ$_{Vp}$ was unable to interact with YjeE$_{Vp}$ in this two-hybrid system. The response produced by the vector only transformants (colony 3). The transformants containing either YeaZ$_{Vp}$ bait plasmid plus empty prey vector (pB42AD) (colony 2) or the YeaZ$_{Vp}$ bait plasmid alone (colony 1) was expected, as none of these transformants can express both bait and prey proteins.

As expected, under non-inducing conditions (transformed yeast cells plated on SD/Glu/-His/-Trp/-Ura medium that lacks Galactose and Leucine required for induction of bait and

[10] The assay was based on the fact that many eukaryotic transacting transcriptional regulators are composed of physically separable, functionally independent domains, such as a DNA-binding domain, that bind to a specific promoter sequence and an active domain that directs the RNA polymerase II complex to transcribe the gene downstream of the DNA-binding site (Keegan et al., 1986). Therefore, the conditional expression of a nutritional reporter gene is used to select the potential interacting proteins.

prey genes), all of the transformed yeast strains were β-galactosidase negative (Figure 5.8, Panel B). In addition, all cell lines grew at similar rates on the un-induced plate, except for the negative control cells (colony 1, Figure 5.8, Panel B) that contained a single plasmid pCTX110 (pLexA-YeaZ$_{Vp}$). This result was expected, as this cell line was unable to grow on the SD/Glu/-His/-Trp/-Ura medium without also carrying a pB42AD based prey plasmid. However, the transformed cells carrying the empty vectors pLexA and pB42AD, were able to survive on the un-induced SD/Glu/-His/-Trp/-Ura medium plate. Moreover, the fact that all cell lines grew on the selection plate indicated that all constructs had been successfully used to transform the yeast cells (Figure 5.8, Panel B).

5.3.4 Protein-protein Interactions in Pull-down Analysis

This section describes experiments designed to determine whether His tagged YeaZ$_{Vp}$ could be used to selectively isolate interacting proteins. To achieve this, gene pairs were co-expressed from pET-Duet in *E. coli* and protein complexes isolated from cytoplasmic extracts by affinity chromatography methods.

5.3.4.1 Cloning of *yeaZ$_{Vp}$* and *ygjD$_{Vp}$* into Plasmid pET-Duet

Plasmid pET-Duet allows co-expression of two target genes, one with a N-terminal His-tag and the other with an S-tag. This co-expression system was used to natively analyse protein-protein interactions between YeaZ$_{Vp}$/YjeE$_{Vp}$ or YeaZ$_{Vp}$/YgjD$_{Vp}$ pairs within an *E. coli* background.

Figure 5.9 describes the construction of plasmid pCTX113. Primers pET-Duet RPF F/R (Chapter 2, Table 2.4) were used to PCR amplify the *yeaZ$_{Vp}$* gene and generate a 702 bp *yeaZ$_{Vp}$* fragment on a *Eco*RI/*Not*I restriction fragment from *V. parahaemolyticus* NCTC 10884. This full length *yeaZ$_{Vp}$* was then ligated into the *Eco*RI/*Not*I sites of pET-Duet plasmid (Chapter 2, Table 2.3) to create pCTX113. This construction allowed expression of YeaZ$_{Vp}$ with a N-terminal His tag. The *ygjD$_{Vp}$* gene was then introduced into pCTX113 in a manner that allowed expression of this gene with a C-terminal S tag as follows. Primers pET-DuetGCPF/R (Chapter 2, Table 2.4), were used to PCR amplify the *ygjD$_{Vp}$* gene to generate a 1017bp *Bgl*II/*Xho*I fragment carrying the full length *ygjD$_{Vp}$* gene. This fragment was cloned into similarly digested pCTX113 to generate plasmid pCTX115 (Chapter 2, Table 2.3) as

outlined in Figure 5.10. Plasmid pCTX115 was then introduced into *E. coli* DH5α cells as described previously (Chapter 2, Section 2.9.7) and transformants selected by plating on LB plates containing Amp with O/N incubation at 37°C. Clones containing the 1017bp *ygjD*$_{Vp}$ construct were extracted from cells and confirmed by PCR (Figure 5.11, Panel B). DNA sequencing was also performed to confirm the cloned *ygjD*$_{Vp}$ nucleotide sequence.

5.3.4.2 Cloning of *yeaZ*$_{Vp}$ and *yjeE*$_{Vp}$ into Plasmid pET-Duet

Primers yjeE F/R (Chapter 2, Table 2.4) were used to amplify the *yjeE* gene to generate a 465 bp *Nde*I/*Xho*I fragment carrying the full length *yjeE* gene. This was cloned into similarly digested pCTX113 plasmid (Section 5.3.4.1) to create pCTX114 (Chapter 2, Table 2.3) as described in Figure 5.10. Plasmid pCTX114 was then introduced into *E. coli* DH5α cells as described previously (Chapter 2, Section 2.9.7) and transformants were cultured on LB plates containing Amp with O/N incubation at 37°C. PCR and DNA sequencing were performed to confirm the insert size and nucleotide sequence respectively (Figure 5.11, Panel A).

5.3.4.3 Co-expression of YeaZ$_{Vp}$/YgjD$_{Vp}$ or YeaZ$_{Vp}$/YjeE$_{Vp}$ Protein Complexes

To co-express the YeaZ$_{Vp}$/YjeE$_{Vp}$ protein pair from plasmid pCTX114 and YeaZ$_{Vp}$/YgjD$_{Vp}$ protein pair from plasmid pCTX115, these plasmids were separately introduced into *E. coli* BL21DE3 chemically competent cells (Chapter 2, Section 2.9.7). Colonies were cultured and selected on LB plates containing Amp with O/N incubation at 37°C O/N. Protein expression was induced by incubation of these cultures at 30°C for 6 h in the presence of 0.2 mM IPTG. The cells were harvested, washed and used to prepare cytoplasmic extracts from both induced and non-induced cultures. Soluble, non-denatured protein extracts were prepared by first perforating the cell membranes of washed cells with BugBuster® reagent. SDS-PAGE (Chapter 2, Section 2.11.2) analysis of BL21DE3 [pCTX114] of the protein extracts allowed identification of the *ca.* 17 kDa YjeE$_{Vp}$ and 25 kDa YeaZ$_{Vp}$ proteins expressed from *E. coli* BL21DE3 [pCTX114] (Figure 5.12, Lane 3). Two protein bands ca. 37 kDa and 25 kDa in size, ° were also observed in extracts of induced *E. coli* BL21DE3 [pCTX115] (Figure 5.12, Lane 5), indicating the presence of proteins YgjD$_{Vp}$ and YeaZ$_{Vp}$ respectively. As expected, none of the cloned genes were expressed by un-induced cultures (Figure 5.12, Lanes 2 and 4).

Prestained markers proteins were used as an approximate guide to molecular weight (Appendix E).

5.3.4.4 Pull-down Assay of $YeaZ_{Vp}$/$YgjD_{Vp}$ or $YeaZ_{Vp}$/$YjeE_{Vp}$ Protein Complexes

To assess whether $YeaZ_{Vp}$ and partner proteins formed native complexes when expressed together in *E. coli*, HisLink™ Protein Purification Resin (Promega) (Chapter 2, Section 2.11.4) was used to co-purify any native $YeaZ_{Vp}$/$YjeE_{Vp}$ and $YeaZ_{Vp}$/$YgjD_{Vp}$ protein complexes co-expressed in *E. coli* BL21DE3 [pCTX114] and *E. coli* BL21DE3 [pCTX115], respectively. Soluble, non-denatured protein extracts prepared as described in Section 5.3.4.3 from induced *E. coli* BL21DE3 [pCTX114] and *E. coli* BL21DE3 [pCTX115] cultures were subjected to affinity chromatography on a gravity flow column of HisLink resin to isolate His-tagged $YeaZ_{Vp}$ protein and any complexed $YjeE_{Vp}$ or $YgjD_{Vp}$ protein. SDS-PAGE was performed to analyse protein profiles of the soluble protein extracts and the column eluted fractions (Figure 5.13). Results shown in Figure 5.13 indicated that both the His-tagged $YeaZ_{Vp}$ protein and the $YjeE_{Vp}$ protein (Figure 5.13, Lane 5) were co-purified with the HisLink™ resin column. Moreover, His-tagged $YeaZ_{Vp}$ protein and the co-expressed $YgjD_{Vp}$ protein (Figure 5.13, Lane 6) were also both purified from extracts prepared from induced *E. coli* BL21DE3 [pCTX115] (Figure 5.13, Lane 7). This data indicated that $YeaZ_{Vp}$ was able to form complexes with $YjeE_{Vp}$ and $YgjD_{Vp}$ when co-expressed at high copy number in *E. coli*.

5.3.4.5 Cross-linking of $YeaZ_{Vp}$/$YjeE_{Vp}$ or $YeaZ_{Vp}$/$YjeE_{Vp}$ Protein Complexes

Formaldehyde mediated cross-linking methods (Chapter 2, Section 2.11.10) were performed to confirm whether protein pairs $YeaZ_{Vp}$/$YjeE_{Vp}$ and $YeaZ_{Vp}$/$YgjD_{Vp}$ formed protein complexes. Soluble protein extracts were prepared from *E. coli* BL21DE3 [pCTX113], *E. coli* BL21DE3 [pCTX114] and *E. coli* BL21DE3 [pCTX115] cultures as described in Section 5.3.4.3. These preparations were cross-linked with formaldehyde (Chapter 2, Section 2.11.10), followed by SDS-PAGE (Chapter 2, Section 2.11.2) and Western Blot analysis using adsorbed polyclonal anti-$YeaZ_{Vp}$ serum to identify $YeaZ_{Vp}$ protein complexes (Figure 5.14). When used at a final dilution of 1/20,000, this antiserum was able to detect protein bands with a size of *ca.* 25 kDa in both cross-linked and non-cross-linked extracts that represented $YeaZ_{Vp}$ monomer (Figure 5.14, Lane 2-7). In addition, a *ca.* 50 kDa protein was also detected in all of the cross-linked samples (Figure 5.14, Lane 5-7), indicating a formation

of a $YeaZ_{Vp}$ dimer. However, $YeaZ_{Vp}$/$YjeE_{Vp}$ or $YeaZ_{Vp}$/$YgjD_{Vp}$ protein complexes were not detected by Western Blot analysis from any sample tested (Figure 5.14, Lane 5-7).

5.3.5 Co-immunoprecipitation of $YeaZ_{Vp}$ Associated Proteins

Protein co-immunoprecipitation was performed to further investigate the $YeaZ_{Vp}$ associated protein complex by isolating the potential protein complexes from *V. parahaemolyticus* NCTC 10884 (Chapter 2, Section 2.11.6). Potential protein bands were precipitated from whole cell lysates using the adsorbed polyclonal anti-$YeaZ_{Vp}$ serum. Pre-bleed normal rabbit serum (nonimmune rabbit serum) was used as a negative control. Figure 5.15 shows that Dynabeads® coupled Protein A (Invitrogen, California, USA) was able to affinity purify $YeaZ_{Vp}$ as well as a potential $YeaZ_{Vp}$ associated protein with a molecular size of *ca.* 35 kDa (Figure 5.15, Lane 4 and 5). Interestingly, protein bands consistent with the size of $YgjD_{Vp}$ and $YjeE_{Vp}$ were not present. As expected, the heavy and light chain fragments of IgG were also isolated. No other potential $YeaZ_{Vp}$ interacting proteins were observed from the two negative control groups (Figure 5.15, Lane 2 and 3).

MALDI-TOF mass spectrometry (Chapter 2, Section 2.11.11) was performed to determine the amino acid sequence of the *ca.* 35 kDa protein co-purified with $YeaZ_{Vp}$. The sequence data obtained was similar to outer membrane protein U (OmpU) of *V. parahaemolyticus*. The predicted protein molecular weight of the OmpU was 36.3 kDa, consistent with the observed molecular weight (35kDa) of the protein band isolated by SDS-PAGE (Figure 5.15, Lane 4-5).

5.3.6 $YeaZ_{Vp}$ Domains involved in Protein-Protein Interactions

5.3.6.1 Structural analysis of $YeaZ_{Vp}$

Amino acid sequences of YeaZ protein in *Salmonella* Typhimurium LT2, *E. coli*, *V. parahaemolyticus* and *Pasteurella haemolytica* were aligned using ClustalW multiple alignment software (Figure 5.16). YeaZ has total 8 α-helices based on the *Salmonella* YeaZ structure (Nichols et al., 2006). The alignment presented in Figure 5.16 indicated that the α-helices 1 and 2 in particular are highly conserved in YeaZ protein among various strains. This analysis is consistent with reports by reference. Using Chimera software (Pettersen et al., 2004), together with Protein Data Bank PDB structure data for $YeaZ_{ST}$, to the predicted

structure of the $YeaZ_{Vp}$ protein was threaded on the $YeaZ_{ST}$ structure as described in Figure 5.17. The $YeaZ_{ST}$ (Figure 5.17, Panel A) and the $YeaZ_{Vp}$ (Figure 5.17, Panel B) has a similar two lobed structure (labeled Lobe A and B).

The structure of the *S.* Typhimurium LT2 $YeaZ_{ST}$ dimer was visualised by Chimera software (Pettersen et al., 2004) using data published by Nicholls et al. (2006). This dimeric structure indicated that the two monomeric $YeaZ_{ST}$ units interacted at potential binding motifs located within the α-helix 1 and 2, as well as three potential binding sites, I73, L81 and F83 within $YeaZ_{ST}$ dimer structure (Figure 5.18). Having identified amino acids that were potentially involved in interactions resulting in formation of $YeaZ_{ST}$ dimers, site directed mutagenesis was used to confirm the role of these residues in $YeaZ_{Vp}$ protein-protein interactions. The bacterial two-hybrid system previously described was used to quantitate the effects of site directed mutagenesis of *yeaZ*$_{Vp}$.

5.3.6.2 Site-directed Mutagenesis of $YeaZ_{Vp}$

To determine the role of specific residues located within α-helix 2 in interactions that enable $YeaZ_{Vp}$ to form dimers, specific point mutations in the *yeaZ*$_{Vp}$ sequence were constructed and these mutated versions of *yeaZ*$_{Vp}$ cloned in the pBT bait plasmid used in the bacterial two-hybrid system described above, together with the $YgjD_{Vp}$ and $YeaZ_{Vp}$ prey constructs (Section 5.3.2.2). The interaction between baits and a wild type $YeaZ_{Vp}$ prey was quantitatively assessed using the ß-Galactosidase assay. Wild type bait and prey proteins were used as positive controls.

The strategy used to create point mutations within the *yeaZ*$_{Vp}$ of plasmid pCTX106 is shown in Appendix V. Briefly, a point mutation site was first introduced into the pCTX106 which carrying a *yeaZ*$_{Vp}$ fragment using overlap extension PCR (Chapter 2, Section 2.12). Oligonucleotide primer pairs of YeaZNot*I*F/YeaZR and YeaZI75AF/YeaZI75AR (Chapter 2, Table 2.4) were designed to amplify *yeaZ*$_{Vp}$ gene. Three nucleotide changes at codon position 225 (ATC → GCG), resulted in an Ile75Ala substitution. Primers YeaZNotIF/YeaZI75AR amplified a 225 bp region with the point mutation site at 5' end while the oligonucleotide pair YeaZI75AF/YeaZR amplified a 477 bp region with the point mutation site at 3' end. PCR amplification of each fragment was confirmed by gel electrophoresis (data not shown).

The two 225 bp and 477 bp DNA fragments that overlapped the alanine site in amino acid sequence of the mutated *yeaZ*$_{Vp}$ gene were combined at equal final concentrations, denatured at 95°C and then rapidly cooled to allow formation of an overlapping DNA hybrid that representing the *yeaZ*$_{Vp}$ fragment. The hybrid was used as a template DNA for PCR amplification using primers yeaZNotIF/yeaZR to generate a 702 bp fragment (225 bp + 477 bp). The 702 bp yeaZ DNA fragment carrying a amino acid point mutation site was double digested with *Not*I/*Xho*I restriction enzymes, followed by a ligation of the 702 bp *yeaZ*$_{Vp}$ DNA and plasmid pBT to form a pCTX116 construct (Chapter 2, Table 2.3 and Figure 5.19) for further bacterial two-hybrid assay. DNA sequencing was performed to confirm the amino acid point mutation site was successful introduced into the pCTX116 construct (Appendix W, Panel A).

The same overlapping extension PCR strategy was also performed to generate a point mutation site in residues L83 and F85 of the YeaZ$_{Vp}$. Primer pairs of YeaZL83AF/R and YeaZF85AF/R (Chapter 2, Table 2.4) were used to introduce nucleotide base changes which resulted in a L83A substitution and a F85A substitution. Figure 5.19 illustrates the construction of the pCTX117 construct carrying a L83A mutation and the pCTX118 construct carrying a F85A mutation. These constructs were confirmed by nucleotide sequencing (Appendix W, Panels B and C). The 702 bp *yeaZ*$_{Vp}$ DNA fragment carrying L83A and F85A were separately ligated into plasmid pBT to form plasmid pCTX117 and pCTX118 respectively.

The three constructed plasmids pCTX116, pCTX117 and pCTX118 were then expressed in *E. coli* KS1 cells together with wild type YeaZ$_{Vp}$ and YgjD$_{Vp}$ prey protein to investigate the effect of the mutations on the ability of YeaZ$_{Vp}$ to initiate protein-protein interactions as described below.

5.3.6.3 Effect of YeaZ$_{Vp}$ Mutations on Protein-Protein Interactions

The β-galactosidase assay (Chapter 2, Section 2.11.12.2) was used to provide quantitative data that reflected the strength of the interaction between bait and prey proteins used in the bacterial two-hybrid system. In order to examine the effect of mutated YeaZ$_{Vp}$ on interaction with YgjD$_{Vp}$, constructed plasmids including pCTX106/pCTX109 (YeaZ$_{Vp}$/YgjD$_{Vp}$), pCTX116/pCTX109 (YeaZI75A/YgjD$_{Vp}$), pCTX117/pCTX109 (YeaZL83A/YgjD$_{Vp}$) and

pCTX118/pCTX109 (YeaZF85A/YgjD$_{Vp}$) were used to co-transform *E. coli* KS1 cells. The plasmid pair of pBT/pTRG (Chapter 2, Table 2.4) was used as a negative control and the plasmid pair pBT-LGF2/pTRG-Gal11p as a positive control. All required transformants were selected by growth on LB plates containing the antibiotics Cml, Kan and Tet with O/N incubation at 37°C. A total of six constructs, each expressing YeaZ$_{Vp}$/YgjD$_{Vp}$, YeaZI75A/YgjD$_{Vp}$, YeaZL83A/YgjD$_{Vp}$ or YeaZF85A/YgjD$_{Vp}$ bait and prey protein hybrids respectively together with the negative control and positive control cultures. The β-galactosidase activity (measured in Millers units) was determined for each culture. The results are presented as Figure 5.20. Cultures transformed with empty vectors expressed little or no β-galactosidase activity, while the positive control cultures expressed *ca.* 1000 Miller units of activity. These data indicated that the assay was working correctly. Cultures that expressed the wild type YeaZ$_{Vp}$ bait and YgjD$_{Vp}$ prey expressed 839 Miller's units of β-galactosidase activity, whereas the cultures expressing the YeaZI75A/YgjD$_{Vp}$ bait and prey pair expressed significantly less activity (637 Millers units). Cultures that expressed the YeaZL83A/YgjD$_{Vp}$ and YeaZF85A/YgjD$_{Vp}$ bait and prey pairs expressed only low levels of activity compared to the wild type protein pair. These data indicated that the I75A mutation, but most particularly the L83A and F85A mutations in YeaZ$_{Vp}$ are important in establishing protein-protein interactions between YeaZ$_{Vp}$ and YgjD$_{Vp}$.

The same strategy was used to determine whether the same amino acid substitutions influence the interaction of YeaZ$_{Vp}$ monomer to form dimeric forms of this protein. *E. coli* KS1 cells that expressed YeaZ$_{Vp}$/YeaZ$_{Vp}$, YeaZI75A/YeaZ$_{Vp}$, YeaZL83A/YeaZ$_{Vp}$, YeaZF85A/YeaZ$_{Vp}$, a pBT/pTRG (negative control) and a pBT-LGF2/pTRG-Gal11p (positive control) (Chapter 2, Table 2.4) were used for this analysis. Data presented in Figure 5.21 shows that cultures expressing YeaZ$_{Vp}$ bait proteins with I75A, L83A and F85A substitutions together with wild type YeaZ$_{Vp}$ prey, produced produced significantly less β-galactosidase activity than that of the wild type bait and prey expressing cultures. This data provided strong experimental evidence to indicate that I75, or L83 and F85 are individually important for protein-protein interactions between two molecules of YeaZ$_{Vp}$.

5.3.6.4 Confirmation of the λcI-YeaZ$_{Vp}$ Expression

In order to show that the protein-protein interactions described in Section 5.3.6.3 were the result of interactions between YeaZ$_{Vp}$ expressed from the bait plasmid and not from natively expressed *E. coli* YeaZ$_{Vp}$, Western blot analysis was performed to confirm that the λcI-YeaZ$_{Vp}$ bait protein was expressed. The samples from Section 5.3.6.3 were collected and separated by SDS-PAGE.

Protein samples were analyzed by Western blot with anti-YeaZ$_{Vp}$ serum to examine the λcI-YeaZ$_{Vp}$ fusion protein. Results presented in Figure 5.22 indicated that there was a *c.a.* 50 kDa protein, a 25 kDa λcI protein fused with a *c.a.* 25 kDa YeaZ$_{Vp}$, presented in cell lysates of the *E. coli* KS1 cell carrying plasmid pair pCTX106/pCTX109 (YeaZ$_{Vp}$/YgjD$_{Vp}$), pCTX116/pCTX109 (YeaZI75A/YgjD$_{Vp}$), pCTX117/pCTX109 (YeaZL83A/YgjD$_{Vp}$) and pCTX118/pCTX109 (YeaZF85A/YgjD$_{Vp}$), lane 3, 4, 5 and 6, respectively. As expected, no λcI-YeaZ$_{Vp}$ fusion protein was observed in the cell lysates of the negative control cultures, or cultures carrying bait and prey plasmid positive control plasmids (Figure 5.22). Therefore, these data has confirmed that the λcI-YeaZ$_{Vp}$ fusion proteins were expressed, in the β-galactosidase assay.

To further confirm the expression of λcI-YeaZ$_{Vp}$ fusion protein in the cultures designed to examine interactions involved in dimerisation of YeaZ$_{Vp}$, a Western Blot, using adsorbed anti-YeaZ$_{Vp}$ serum, was performed to detect YeaZ$_{Vp}$ protein expression. Data presented in Figure 5.23indicated that the λcI-YeaZ$_{Vp}$ was also detected in *E. coli* KS1 cell lysates of cells carrying plasmid pair pCTX106/pCTX107 (YeaZ$_{Vp}$/YeaZ$_{Vp}$), pCTX116/pCTX107 (YeaZI75A/YeaZ$_{Vp}$), pCTX117/pCTX107 (YeaZL83A/YeaZ$_{Vp}$) or pCTX118/pCTX107 (YeaZF85A/YeaZ$_{Vp}$). Again, as expected, no λcI-YeaZ$_{Vp}$ fusion protein band was detected in either negative or positive controls (Figure 5.23). Data here suggested that the λcI-YeaZ$_{Vp}$ fusion protein was able to be expressed and detected in the interaction between YeaZ$_{Vp}$ mutants with YgjD$_{Vp}$ or wild-type YeaZ$_{Vp}$ in the β-galactosidase assay.

5.4 Discussion

The purpose of work described in this chapter was to gather evidence to support the hypothesis that YeaZ$_{Vp}$/YjeE$_{Vp}$ and YeaZ$_{Vp}$/YgjD$_{Vp}$ protein pairs work as partners or complexes in *V. parahaemolyticus* NCTC 10884 in the same manner as previously reported

for other bacterial systems (Handford et al., 2009). This was achieved by detection of specific protein-protein interactions between these proteins using two-hybrid systems. To confirm that these interactions occurred natively within the cytoplasm of bacteria, the presence of these complexes was tested following cross-linking and immunoprecipitation analysis of cytoplasmic extracts prepared from *V. parahaemolyticus* and from *E. coli* strains overexpressing individual pairs of $YeaZ_{Vp}$/$YeaZ_{Vp}$, $YeaZ_{Vp}$/$YjeE_{Vp}$ and $YeaZ_{Vp}$/$YgjD_{Vp}$. Finally, to identify amino acid residues involved in interaction between partner proteins, site-directed mutagenesis of selected $YeaZ_{Vp}$ residues was combined with a bacterial two-hybrid system to test the effect of sequence changes.

The bacterial two-hybrid system used in this study (developed by Dove et al., 1997), relies on transcriptional activation of a reporter gene following recruitment of RNA polymerase. In *E. coli*, specific interactions between a DNA-bound activator and the C-terminal domain of the α-subunit of RNA Polymerase allow activation of transcription. Dove and colleagues showed that these contacts can be replaced by artificial protein-protein interactions. Thus interacting chimeric proteins based on the λcI repressor and the α-subunit of RNA Polymerase allow oligomerisation of the DD domains of both proteins. Thus in the presence of λcI, Rα-cI can stimulate transcription of a *lacZ* gene under control of an artificial *lac* promoter carrying an upstream λ operator (Dove et al., 1997). Furthermore, Dove and colleagues showed that the magnitude of transcriptional activation of the *lacZ* correlated with the strength of the interaction between λcI and the chimeric Rα-cI. This two-hybrid system comprises the pBT vector (to prepare fusions with a sequence specific DNA-binding protein, in this case the λcI repressor protein) and the pTRG vector (to express an RNAP α-subunit fusion protein).

The yeast two-hybrid system used is a LexA based interaction trap for detecting specific protein-protein interactions in yeast (Golemis et al., 2001). The pLexA plasmid is designed to express the DNA-binding domain-fused bait protein. The DNA-binding domain-fused bait protein is used to transform yeast possessing a dual reporter system responsive to transcriptional activation through the LexA operators. In addition, the pB42AD plasmid is used to induce GAL1 promoter to express a transcription activation domain (AD) that functions as a portable transcriptional activation motif. These two plasmids were introduced into *S. cerevisiae* $EGY48^{C}$ (p8op-lacZ) which contains the lacZ reporter gene under control of

8 LexA operators. The protein-protein interaction between two protein pairs was determined by β-galactosidase activity assay on X-gal agar plates.

The bacterial two-hybrid system allowed demonstration that $YeaZ_{Vp}$ formed strong interactions with other $YeaZ_{Vp}$ protein and with $YgjD_{Vp}$, but not $YjeE_{Vp}$ (Figure 5.5). This data suggested that $YeaZ_{Vp}/YgjD_{Vp}$ and $YeaZ_{Vp}/YeaZ_{Vp}$ could form protein complexes in the cytoplasm of *V. parahaemolyticus* NCTC 10884. These results were confirmed by the yeast two-hybrid data. This outcome is consistent with interactions between $YeaZ_{Ec}/YgjD_{Ec}$ and $YeaZ_{Ec}/YeaZ_{Ec}$ of *E. coli* reported by (Handford et al., 2009). In that study, $YeaZ_{Ec}$ was shown to strongly interact with $YgjD_{Ec}$ and $YeaZ_{Ec}$ through the use of a two-hybrid system based on reconstitution of a signaling cascade. That system exploits functional complementation between two fragments of the adenylate cyclase of *Bordetella pertussis* (Karimova et al., 1998). Handford and colleagues also demonstrated that $YeaZ_{Ec}$ formed a complex with $YgjD_{Ec}$ when expressed natively. Indeed the native form of the $YeaZ_{Ec}$ protein was shown to have a strong propensity to homo-dimerise. Rajagopal and colleagues obtained similar results for the YeaZ, YgjD and YjeE homologs from *E. coli* K-12, *Staphylococcus aureus* and *Streptococcus pneumoniae* when expressed in a yeast two-hybrid system (Rajagopala et al., 2010). The fact these three independent studies report consistent protein-protein interactions in different genera of bacteria, lends strong support for the hypothesis that these proteins are likely interact in the same manner across most bacterial genera/species. Interestingly, while these proteins are highly conserved across most bacterial species, the latter authors found that YeaZ, YgjD and YjeE from different organisms do not necessarily interact. Indeed, Handford et al. (2009) have concluded that there are differences in the way YeaZ/YgjD complexes are regulated in across species.

Although the bacterial two-hybrid and yeast two-hybrid data in this thesis provide strong support for $YeaZ_{Vp}/YgjD_{Vp}$ protein pair interaction, it was of interest to confirm whether these interactions also occur natively in *V. parahaemolyticus* or in *E. coli strains* co-expressing *yeaZ/ygjD, yeaZ/yjeE and yeaZ/yeaZ* pairs. When $YeaZ_{Vp}$ carrying a N-terminal His tag was co-expressed with appropriate partner proteins in *E. coli*, YeaZ/YgjD and YeaZ/YjeE complexes could be isolated from cytoplasmic extracts by affinity chromatography. However, after the extracts were cross-linked with formaldehyde, only YeaZ/YeaZ dimeric complexes were observed. Taken together, this data indicated that all of

the protein-protein interactions identified by two-hybrid systems could also be demonstrated to occur when expressed natively in *E. coli*. The data also confirmed that $YeaZ_{Vp}$, like other homologs, has a strong propensity to dimerise. However, none of these complexes could be separated from cytoplasmic extracts of *V. parahaemolyticus* NCTC 10884 by immuno-precipitation using a specific polyvalent anti-$YeaZ_{Vp}$ serum. This apparently confounding result may be a reflection of the following:

1. $YeaZ_{Vp}$ and partner proteins may be expressed at low levels in *V. parahaemolyticus* and may consequently affect the abililty of immuno-precipitation methods to isolate detectable quantities of complexes.

2. As YeaZ is proposed to be a protease that specifically cleaves YgjD it is possible that any YeaZ/YgjD complexes may have been degraded during preparation of cytoplasmic extracts used for immuno-precipitation.

3. Protein complexes involving $YeaZ_{Vp}$ may be only short-lived in the cytoplasm of bacteria and may not survive processing time for immuno-precipitation. This limitation might only be overcome by over expression of $YeaZ_{Vp}$ and partner proteins as is clearly the case when tagged proteins were over expressed in *E. coli.*

Interestingly, while $YeaZ_{Vp}$ protein complexes with $YgjD_{Vp}$ and $YjeE_{Vp}$ could not be immuno-precipitated from cytoplasmic extracts prepared from NCTC 10884, immune complexes comprising $YeaZ_{Vp}$ and outer membrane protein U (OmpU) were identified. OmpU is a porin that is critical in *Vibrio* species for resistance to bile salts. The significance of this interaction is not obvious, nor is it clear why this protein should be found in association with an outer membrane protein. Data presented in Chapter 4, indicated $YeaZ_{Vp}$ is co-located on the surface of NCTC 10884. It is possible that cytoplasmic $YeaZ_{Vp}$ secreted by these cells is displayed on the surface of the cell following interaction with OmpU. However it is possible that this interaction may simply be the result of a spurious interaction that occurs following extraction of cytoplasmic proteins in their native state. Nevertheless, the observation that $YeaZ_{Vp}$ interacts with a molecule exposed on the cell surface of NCTC 10884 warrants further study.

The OmpU interaction may also be interesting for another reason. This protein has been identified as a starvation inducible protein during long term starvation in *V. parahaemolyticus*

and *V. alginolyticus* (Ben Abdallah et al., 2010). Furthermore, ToxRS regulates the production of OmpU and OmpT (Crawford et al., 1998; Li et al., 2000; Miller & Mekalanos, 1988). Thus OmpU requires ToxR for expression and confers resistance to antimicrobial peptides and may also relate to the function of adhesion (Sperandio et al., 1995). The ToxR gene encodes a transcriptional activator controlling the cholera toxin, Tcp pilus, and OmpU (Miller et al., 1987). In addition, extracellular signals such as pH, osomolarity, temperature and oxygen tension are involved in ToxR-regulated genes (Gardel & JJ, 1994; Miller & Mekalanos, 1988). Recently, Whitaker et al. (2010) demonstrated that the *V. parahaemplyticus toxRS* operon is responsible for controlling expression of OmpU. They suggested that OmpU is responsible for resistance to acid and temperature stress (Whitaker et al., 2010). Although there is no published evidence to show that $YeaZ_{Vp}$ protein is regulated by the ToxRS regulon, it is interesting to speculate that YeaZ/YjeE/YgjD expression might be regulated through the ToxRS two-component regulatory system and hence may be involved in establishment/recovery of/from the VBNC state of *V. parahaemolyticus*.

Although there is good evidence to indicate that $YeaZ_{Vp}$ forms a dimer, little is known about the potential interaction domains required to establish $YeaZ_{Vp}$ dimers and complexes with $YgjD_{Vp}$. The crystal structure of *Salmonella* Typhimurium YeaZ has recently been solved (Nichols et al., 2006). Analysis of the $YeaZ_{ST}$ structure identified two α helical domains (helices 1 and 2) as potential interaction domains required for formation dimeric structures. Since that publication, two additional dimers that represent the physiologically relevant forms of YeaZ homologs in *Thermotoga maritime* have been identified (Xu et al., 2010). Given the high level of similarity between $YeaZ_{ST}$ and $YeaZ_{Vp}$ the potential interaction domains in $YeaZ_{Vp}$ were located by using the $YeaZ_{ST}$ structure as a scaffold for predicting the structure for $YeaZ_{Vp}$. Using this deduced structure, it was possible to identify amino acid residues that may allow interactions via α helices 1 and 2 interaction domain identified by Nicholls et al. (2006). In particular, the close proximity of residues I75, L83 and F85 in dimeric forms were identified as candidates for site directed mutagenesis. The bacterial two-hybrid system was then used to identify which of these mutations lead to abolishment of interactions between YeaZ and YeaZ mutants, or reduction in the strength of interaction with $YeaZ_{Vp}$ chimeric proteins. As shown in Figure 5.21, he I75A, L83A and F85A mutations in $YeaZ_{Vp}$ protein abolished interaction to levels equivalent to the –ve

control. This observation is the first report that attempts to quantify the contribution of selected residues in the interaction that occurs between YeaZ molecules during formation of dimers. Whether I75, L83 and F85 are involved in interaction between YeaZ and YgjD is less clear, although L83A and F85A YeaZ mutants (Figure 5.20) interacted less strongly ($p>0.05$) with YgjD than the I75A mutant. Certainly the structure associated with the N-terminal domain of YgjD is similar to Lobe A of YeaZ, and it is generally accepted that it is this part of the molecule that interacts with YeaZ (Nicholls et al., 2006). This interaction could easily be examined using the two-hybrid system already described in this thesis, although YgjD constructs carrying mutations in selected amino acid residues would need to be prepared in order to examine the effects of individual changes in YeaZ and YgjD. There are other potential residues that may contribute to the interaction of YeaZ with either itself or with YgjD. For example, Nicholls et al. (2006) has identified glycine rich loops normally associated with nucleotide/polyphosphate binding (G-X-G-XX-G). Indeed this unusual sequence is semi-conserved across YeaZ orthologs with six glycines located in α helical domain 2. This helix region is directly connected to the β-strand connecting lobe A and lobe B in the YeaZ structure. This helix region has been speculated to be involved in large domain movement applied to one end of the protein that is a prerequisite for dimerisation of YeaZ protein and the catalytic cycle involving interaction with YgjD. Thus the conserved glycines rich region may allow the YeaZ structure to flex and accommodate a reorientation of lobe B (Nichols et al., 2006). Interestingly, Nicholls and co-workers showed that three of these glycines are proposed to be aligned on one side of this helix, with the remaining glycines located on the other. Examination of the predicted model for YeaZ indicated the orientation of these glycines is likely to be preserved in this homolog. For these reasons, it would be interesting for future studies to determine whether the glycines present within helix 2 are involved in protein-protein interactions.

The experimental data presented in this chapter indicates $YeaZ_{Vp}$ protein is able to dimerise, but also able to form a complex with $YgjD_{Vp}$. However, a cellular role for YeaZ, $YgjD_{Vp}$ and $YjeE_{Vp}$ in *V. parahaemolyticus* is not known. The similarities between these proteins and their counterparts in other organisms, is striking. Indeed as described in Chapter 4, loss of $YeaZ_{Vp}$ leads to formation of cell morphologies similar to those of depletion mutants described by other authors (Campbell et al., 2007; Handford et al., 2009). These

changes lead Handford et al. (2009) to suggest that loss of these proteins is consistent with a link to cell envelope processes. It is interesting, that unlike other *yeaZ* genes examined, mutations within the *yeaZ* carried by *V. parahaemolyticus* NCTC 10884 are apparently not lethal. These mutants grow normally under standard laboratory conditions, but lose viability when exposed to long term, low temperature stress. Whether this observation implies this bacterium encodes a gene product that may complement the loss of YeaZ, has not been considered. For example, Campbell et al. (2007) has already suggested that the RstAB system may suppress otherwise lethal phenotypes leading to depletion of YjeE, YeaZ or YgjD, although these workers acknowledge that other gene products subject to control by RstA are likely to be involved in rescue of cells depleted of YeaZ and YgjD. Nevertheless, if YeaZ forms an integral part of a system that results in processing of YgjD, it is reasonable to expect that a *yeaZ* mutation might lead to a disruption to a system that has an integral role to play in cell viability.

```
   1 - ATGCGCATTATTGGTATCGAAACCTCTTGTGACGAGACAGGAATCGCGATTTACGACGAT - 60
   1 - M  R  I  I  G  I  E  T  S  C  D  E  T  G  I  A  I  Y  D  D   - 20
       Start codon
  61 - GAAAAAGGCCTGTTGGCGCACAAGCTTTACAGCCAAGTAAAACTTCACGCGGATTACGGC - 120
  21 - E  K  G  L  L  A  H  K  L  Y  S  Q  V  K  L  H  A  D  Y  G   - 40
 121 - GGCGTGGTGCCAGAGTTGGCTTCACGTGACCATGTAAAGAAAACCATTCCTCTTATTAAA - 180
  41 - G  V  V  P  E  L  A  S  R  D  H  V  K  K  T  I  P  L  I  K   - 60
 181 - GAGGCACTAAAAGAAGCAAACTTAACATCCCAAGACATCGACGGCGTGGCTTACACGGCC - 240
  61 - E  A  L  K  E  A  N  L  T  S  Q  D  I  D  G  V  A  Y  T  A   - 80
 241 - GGTCCTGGTTTGGTTGGTGCTTTGCTAGTGGGTGCAACCATCGGTCGCAGTATTGCTTAC - 300
  81 - G  P  G  L  V  G  A  L  L  V  G  A  T  I  G  R  S  I  A  Y   - 100
 301 - GCATGGGGTGTTCCTGCTGTTCCTGTTCATCATATGGAAGGTCATTTACTTGCGCCAATG - 360
 101 - A  W  G  V  P  A  V  P  V  H  H  M  E  G  H  L  L  A  P  M   - 120
 361 - CTAGAAGACAACCCACCACCATTCCCATTTGTGGCGGTGTTGGTTTCTGGCGGTCACTCG - 420
 121 - L  E  D  N  P  P  P  F  P  F  V  A  V  L  V  S  G  G  H  S   - 140
 421 - ATGATGGTGGAAGTAAAAGGCATTGGTGAATACAAGATTCTAGGCGAATCCATTGATGAT - 480
 141 - M  M  V  E  V  K  G  I  G  E  Y  K  I  L  G  E  S  I  D  D   - 160
 481 - GCAGCCGGTGAAGCATTTGATAAGACGGCTAAGCTGATGGGGTTAGATTACCCAGGCGGT - 540
 161 - A  A  G  E  A  F  D  K  T  A  K  L  M  G  L  D  Y  P  G  G   - 180
 541 - CCTCTGTTATCCAAGCTAGCAGAGAAAGGTACTCCGGGTCGCTTTAAGTTCCCACGACCA - 600
 181 - P  L  L  S  K  L  A  E  K  G  T  P  G  R  F  K  F  P  R  P   - 200
 601 - ATGACCAATGTGCCGGGTTTGGATATGAGTTTCTCTGGTTTGAAAACCTTCACGGCAAAC - 660
 201 - M  T  N  V  P  G  L  D  M  S  F  S  G  L  K  T  F  T  A  N   - 220
 661 - ACGATTGCAGCGAATGGCGATGACGAGCAGACTCGTGCTGATATTGCGTACGCTTTTGAA - 720
 221 - T  I  A  A  N  G  D  D  E  Q  T  R  A  D  I  A  Y  A  F  E   - 240
 721 - GAAGCCGTGTGTGCAACGTTGGCAATTAAATGTAAGCGTGCATTAGAGCAAACCGGTATG - 780
 241 - E  A  V  C  A  T  L  A  I  K  C  K  R  A  L  E  Q  T  G  M   - 260
 781 - AAGCGCATCGTTATTGCTGGTGGTGTAAGTGCGAACCGCCGCTTGCGTGCAGAGCTTGAG - 840
 261 - K  R  I  V  I  A  G  G  V  S  A  N  R  R  L  R  A  E  L  E   - 280
 841 - AAGCTTGCGAAGAAAATCGGTGGTGAAGTGTATTACCCACGTACCGAGTTCTGTACTGAC - 900
 281 - K  L  A  K  K  I  G  G  E  V  Y  Y  P  R  T  E  F  C  T  D   - 300
 901 - AACGGTGCAATGATTGCGTATGCGGGTATGCAACGTTTGAAGAACGGTGAAGTCGCAGAT - 960
 301 - N  G  A  M  I  A  Y  A  G  M  Q  R  L  K  N  G  E  V  A  D   - 320
 961 - ATGTCGGTGGAAGCGCGTCCGCGCTGGCCAATTGACCAGCTAACGCCAATCGCGTAA     - 1017
 321 - M  S  V  E  A  R  P  R  W  P  I  D  Q  L  T  P  I  A  *      - 340
                                                        Stop codon
```

Figure 5.1: Nucleotide and deduced amino acid sequence for $YgjD_{Vp}$.

The sequence presented was taken from NCBI GenBank Accession NP_796787. Start and stop codons are underlined. A HMEGH metal ion binding motif is located at amino acid 111 – 115 (red underlined text). The deduced polypeptide contains 339 amino acids with a predicted MW of 37 kDa. A search for conserved domains in using the NCBI Conserved Domain database indicated the N-terminal part of $YgjD_{Vp}$ amino acid sequence is similar to COG1214 superfamily of M22 O-sialoglycoprotein endopeptidase and universal genome maintenance protein homolog.

```
  1 - ATGAGCACGAAACAATTTACTTTAAAAGATGAGCAAGAAACGGTAGCACTGGGCACCGAG - 60
  1 - M  S  T  K  Q  F  T  L  K  D  E  Q  E  T  V  A  L  G  T  E   - 20
      Start codon
 61 - CTGGCTCAACTTTGTTCTCAACAAACCACTATTTATCTGCATGGTGATTTAGGTGCAGGT - 120
 21 - L  A  Q  L  C  S  Q  Q  T  T  I  Y  L  H  G  D  L  G  A  G   - 40
121 - AAAACAACCTTCAGTCGTGGTTTTGTCCGTGCTCTTGGGCATCAAGGAAACGTGAAAAGT - 180
 41 - K  T  T  F  S  R  G  F  V  R  A  L  G  H  Q  G  N  V  K  S   - 60
181 - CCGACTTATACGCTTGTCGAACCTTACCAATTAGATAAGTGGCAGGTTTACCACTTTGAT - 240
 61 - P  T  Y  T  L  V  E  P  Y  Q  L  D  K  W  Q  V  Y  H  F  D   - 80
241 - CTTTACCGATTGGCAGATCCTGAAGAATTGGAATTCATGGGGATCCGAGACTACTTCACA - 300
 81 - L  Y  R  L  A  D  P  E  E  L  E  F  M  G  I  R  D  Y  F  T   - 100
301 - GATGATGCGATCTGCTTGGTTGAATGGCCTGAAAAAGGGCAAGGATTGCTGCCACAACCA - 360
101 - D  D  A  I  C  L  V  E  W  P  E  K  G  Q  G  L  L  P  Q  P   - 120
361 - GATTTAGATGTAGAAATTCGTTATCAAGGTGAGCAACGCGTCGCTGAGATAACGGCGAAC - 420
121 - D  L  D  V  E  I  R  Y  Q  G  E  Q  R  V  A  E  I  T  A  N   - 140
421 - AATGATTACGGTGTGCAGTTACTCAGTCGATTGGAGCTATGTTGA                 - 465
141 - N  D  Y  G  V  Q  L  L  S  R  L  E  L  C  *                  - 160
                                                 Stop codon
```

Figure 5.2: Nucleotide and deduced amino acid sequence for $YjeE_{Vp}$.

Sequence presented is taken from NCBI GenBank Accession NP_799200. Start and stop codons are underlined. A GXXGXGKT nucleotide binding motif is located at amino acid 35 – 42 (underlined red text). The deduced polypeptide comprises 155 amino acids with a predicted MW of 17 kDa. A search for conserved domains in using the NCBI Conserved Domain database indicated the entire polypeptide sequencing is similar to the ATPase YjeE family.

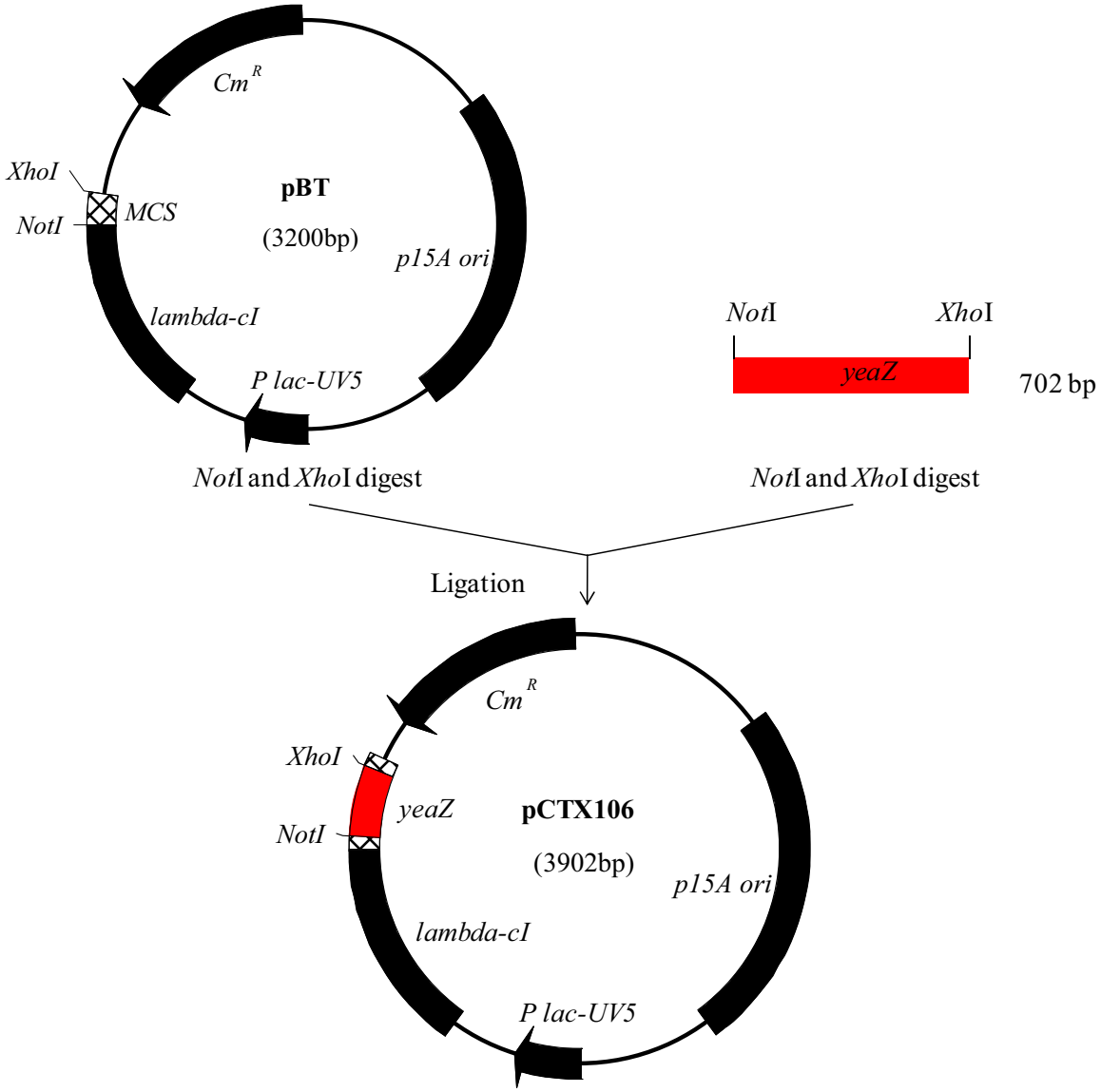

Figure 5.3: Construction of plasmid pCTX106.

The 702 bp *yeaZ* fragment containing *Not*I and *Xho*I restriction enzymes recognition sites was PCR amplified from *V. parahaemolyticus* NCTC 10884. The *Not*I/*Xho*I digested *yeaZ* fragment was ligated into *Not*I/*Xho*I digested pBT to create plasmid pCTX106. This plasmid was used to express a λcI YeaZ fusion protein for use in bacterial two-hybrid analysis.

Abbreviations: Cm^R, chloramphenciol resistance; p15A ori, p15A origin; *lambda-cI*, *λ-cI* gene; MCS, multiple cloning sites.

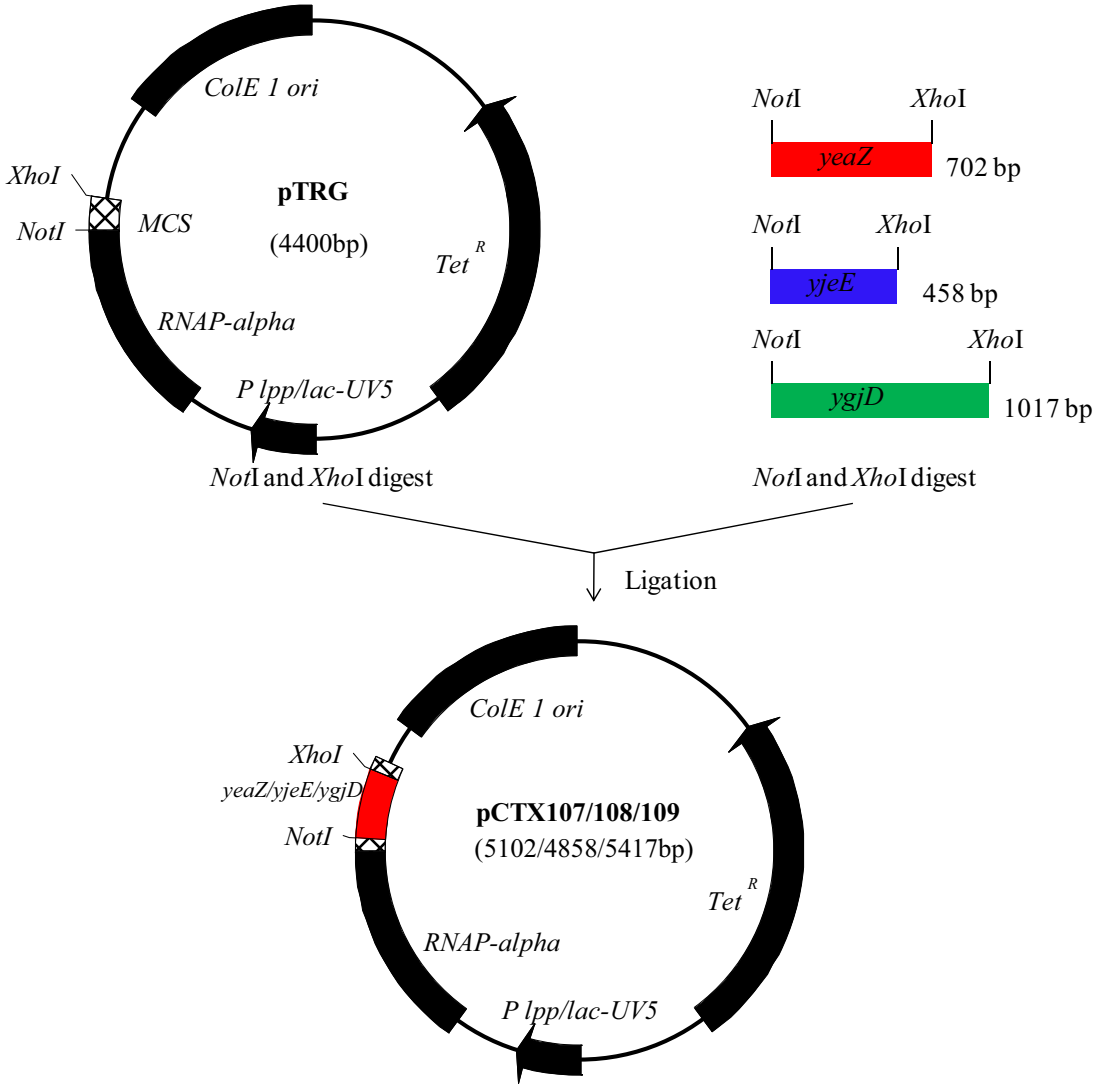

Figure 5.4: Construction of plasmids pCTX107, pCTX108 and pCTX109.

The 702 bp *yeaZ,* 465 bp *yjeE* and 1017 bp *ygjD* fragments containing flanking *Not*I and *Xho*I restriction enzymes recognition sites were separately PCR amplified from *V. parahaemolyticus* NCTC 10884. The *Not*I and *Xho*I sites were introduced on the primers used to amplify each gene. The *Not*I/*Xho*I digested *yeaZ*, *yjeE* and *ygjD* fragment were ligated into *Not*I/*Xho*I digested pTRG to create plasmid pCTX107, pCTX108 and pCTX109. Theses plasmid constructs were used to express a RNAP-α fusion protein for use in bacteria two-hybrid analysis.

Abbreviations: Tet^R, tetracycline resistance; ColE 1 *ori*, p15A origin; RNAP-α, RNA polymerase-α gene; *P lpp/lac*, promoter lpp/lac; MCS, multiple cloning sites.

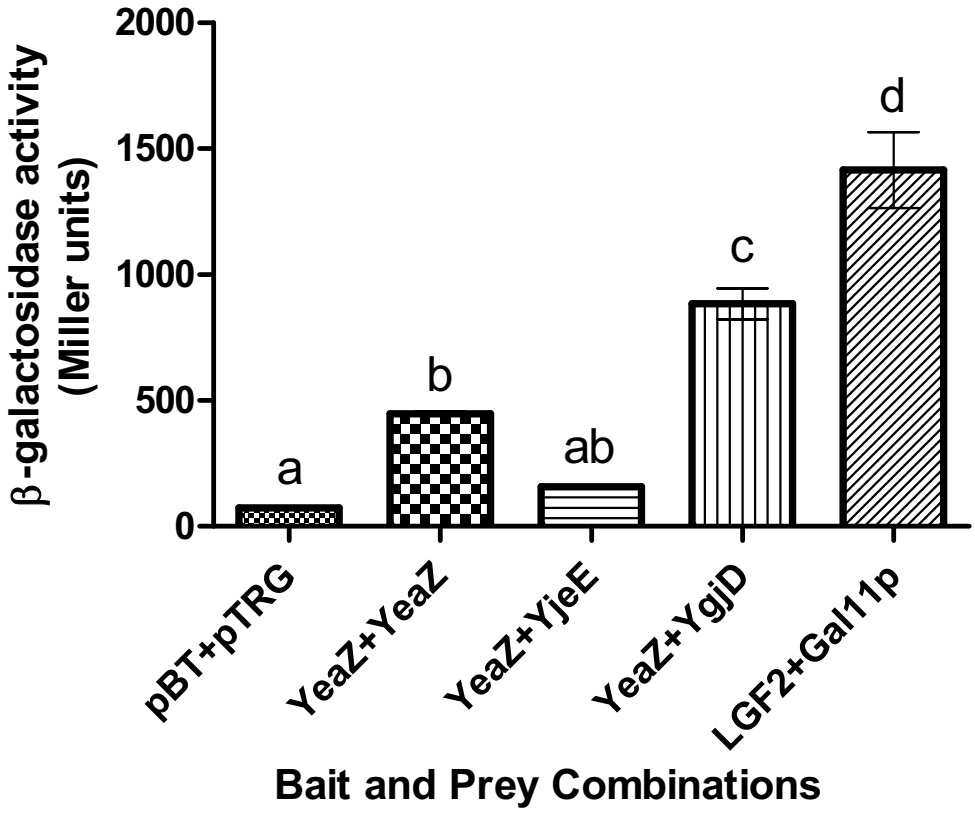

Figure 5.5: $YeaZ_{Vp}$ interaction with $YeaZ_{Vp}$, $YgjD_{Vp}$ and $YjeE_{Vp}$.

Bacterial two-hybrid interaction analysis was carried out using $YeaZ_{Vp}$ and each of $YeaZ_{Vp}$, $YjeE_{Vp}$ and $YgjD_{Vp}$. The strength of protein-protein interactions is indicated by β-galactosidase activity. The yeaZVp gene was cloned into pBT as a bait plasmid pCTX106. The yeaZVp, yjeEVp and ygjDVp were cloned into pTRG as prey plasmids pCTX107, pCTX108 and pCTX109 respectively. The negative control was empty vector pBT and pTRG. The positive control bait and prey constructs used were plasmids pBTLGF2 and pTRGGal11p. *E. coli* KS1 strain was co-transformed with pBT and pTRG plasmid derivatives. A single transformant was picked and inoculated in LB medium applied with appropriate antibiotics and β-galactosidase assays were used to analyse the interaction activity by following the method of Miller (1992). GraphPad prism was used to analyse data by performing a one way ANOVA with a Tukey-Kramer multiple comparison test to make pairwise comparisons of each data set. Data set with the same single letter label are not significantly different ($p>0.05$). Error bars represent standard error of the means; n= 5. Columns lacking error bars have standard errors to small to be plotted.

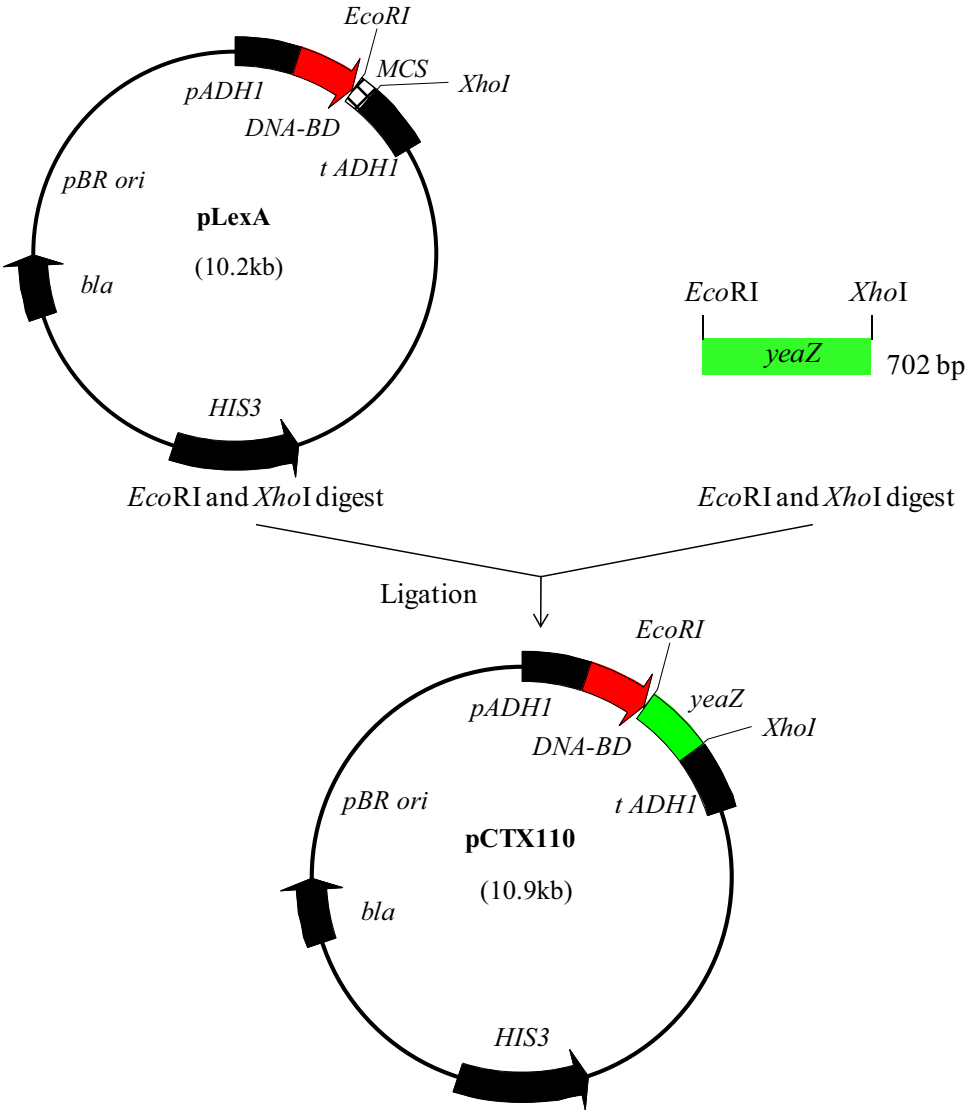

Figure 5.6: Construction of plasmid pCTX110.

The 702 bp *yeaZ*$_{Vp}$ fragment encoding flanking *Eco*RI and *Xho*I restriction enzymes recognition sites were PCR amplified from *V. parahaemolyticus* NCTC 10884. The *Eco*RI /*Xho*I digested *yeaZ*$_{Vp}$ fragment was ligated into *Eco*RI/*Xho*I digested pLexA to create plasmid pCTX110. This plasmid construct was used to express a DNA-BD YeaZ$_{Vp}$ fusion protein for use in yeast two-hybrid analysis.

Abbreviations: *bla*, ampicillin resistance; pBRA *ori*, pBR origin; pADH1, *ADH1* promoter; DNA-BD, DNA-binding domain; tADH1, *ADH1* terminator MCS, multiple cloning sites.

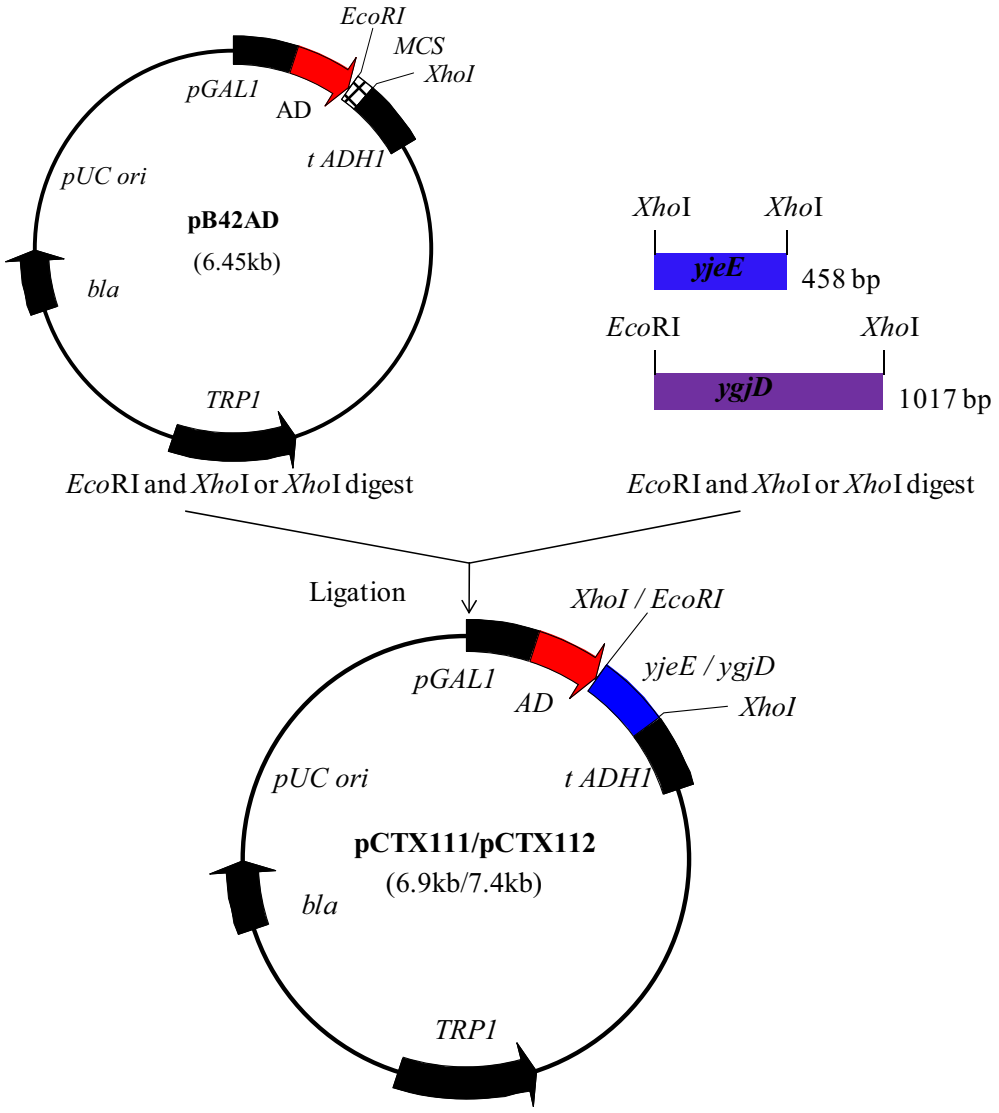

Figure 5.7: Construction of plasmids pCTX111 and pCTX112.

The 465 bp *yjeE* and 1,017 bp *ygjD* fragments carrying flanking *Xho*I or *Eco*RI/*Xho*I restriction enzyme recognition sites were PCR amplified from *V. parahaemolyticus* NCTC 10884. The *Eco*RI/*Xho*I or *Xho*I sites were introduced on the primers used to amplify individual gene respectively. The *Xho*I digested *yjeE* fragment was ligated into *Xho*I digested pB42AD to create plasmid pCTX111. The *Eco*RI/*Xho*I digested *ygjD* fragment was ligated into *Eco*RI/*Xho*I digested pB42AD to create plasmid pCTX112. These plasmid constructs were used to express acidic activator fusion YjeE or YgjD protein for use in yeast two-hybrid analysis.

Abbreviations: *bla*, ampicillin resistance; pUC *ori*, pUC origin; pGAL1, GAL promoter; AD, acidic activator; tADH1, ADH1 terminator; MCS, multiple cloning sites.

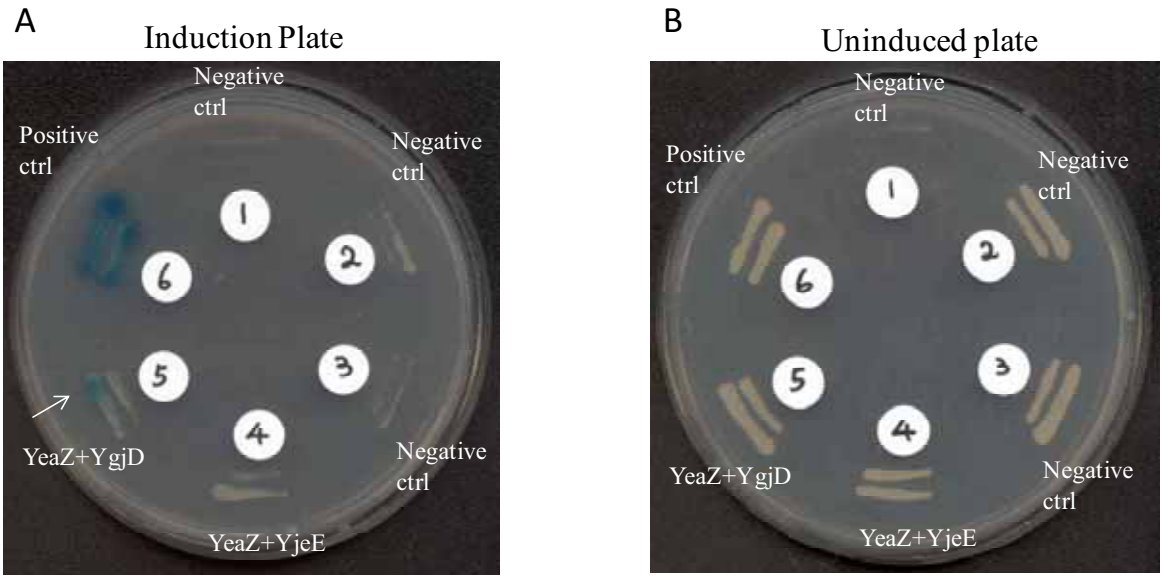

Figure 5.8: Protein interaction in yeast two-hybrid.

Yeast two-hybrid interaction analysis was carried out using YeaZ as a bait protein and either YgjD and YjeE as prey proteins. Interactions were tested using the induction plate β-galactosidase activity assay. The *yeaZ* gene was cloned into pLexA as bait plasmid pCTX110. The *yjeE* or *ygjD* was cloned into pB42AD as prey plasmids pCTX111 and pCTX112 respectively. The negative control plasmids used were empty vector pLexA, or pLexA+pB42AD, or pLexA-yeaZ+pB42AD. The positive control plasmid pair used was pLexA-53 and pB42AD-T. *S. cerevisiae* EGY 48 strain, p8Op-LacZ, was co-transformed with paired pLexA and pB42AD plasmid derivatives. Transformants were picked and patched on SD/Gal/Raf/-Ura-His-Trp-Leu induction plates (Panel A) and SD/Glu/-Ura-His-Trp uninduced plate (Panel B) to assess protein-protein interactions.

Number descriptions are marked as below:

1. pLexA-YeaZ only in p8Op-LacZ Yeast EGY 48 (negative control)
2. pLexA-YeaZ + pB42AD in p8Op-LacZ Yeast EGY 48 (negative control)
3. pLexA + pB42AD in p8Op-LacZ Yeast EGY 48 (negative control)
4. pLexA-YeaZ + pB42AD-YjeE in p8Op-LacZ Yeast EGY 48
5. pLexA-YeaZ + pB42AD-YgjD in p8Op-LacZ Yeast EGY 48
6. pLexA-53 + pB42AD-T in p8Op-LacZ Yeast EGY 48 (positive control)

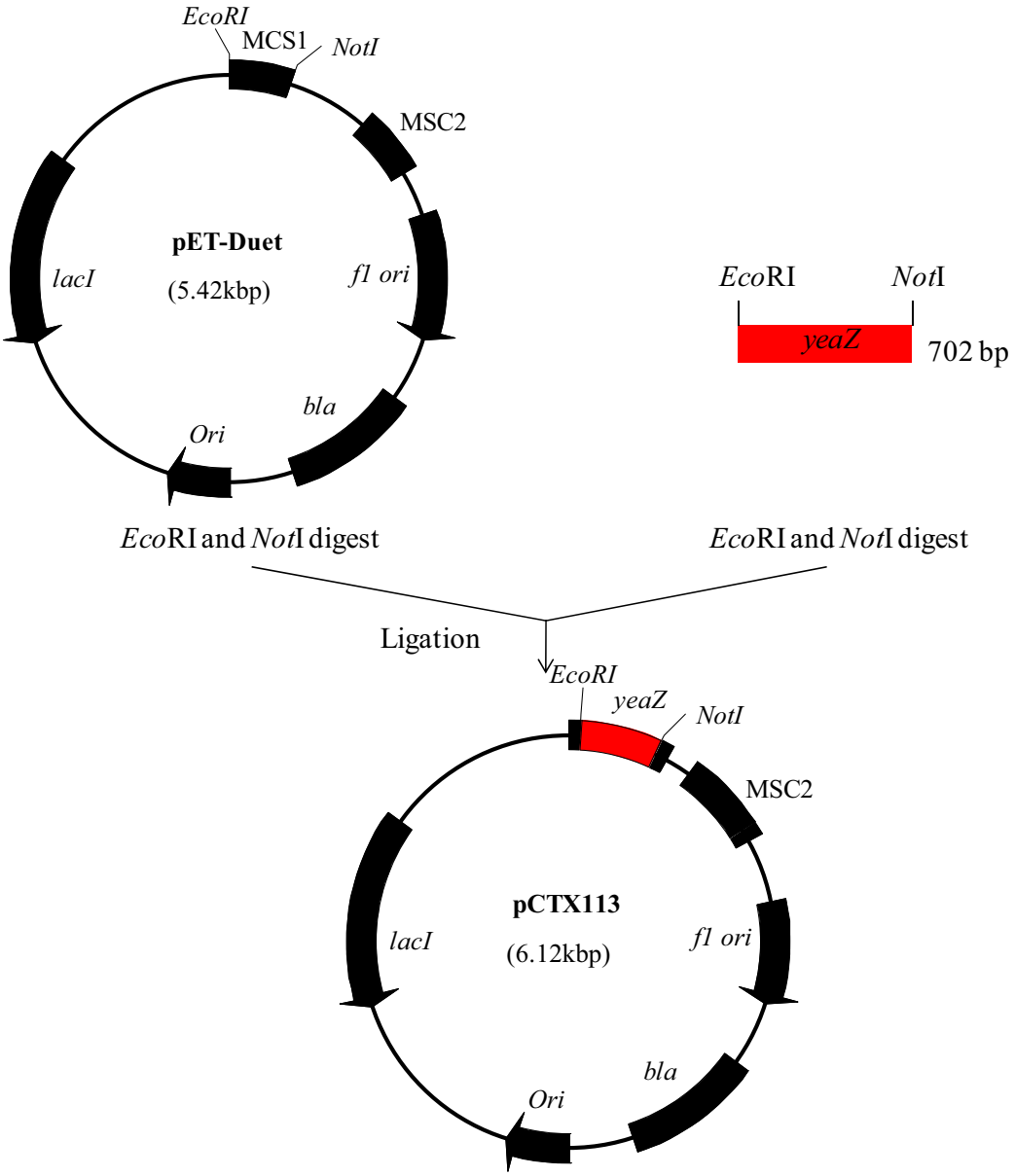

Figure 5.9: Construction of plasmid pCTX113.

A 702 bp *yeaZ* fragment was PCR amplified from *V. parahaemolyticus* NCTC 10884 using oligonucleotide primers encoding the *Eco*RI and *Not*I sites. The *Eco*RI/*Not*I digested *yeaZ* fragment was ligated into *Eco*RI/*Not*I digested pET-Duet to create plasmid pCTX113. This plasmid was used to express a N-terminal His-tag YeaZ fusion protein for use in co-expression analysis.

Abbreviations: *bla*, ampicillin resistance; *f1 ori*, f1 origin; lac I, *lac I* gene; MCS1, multiple cloning site 1; MCS2, multiple cloning site 2.

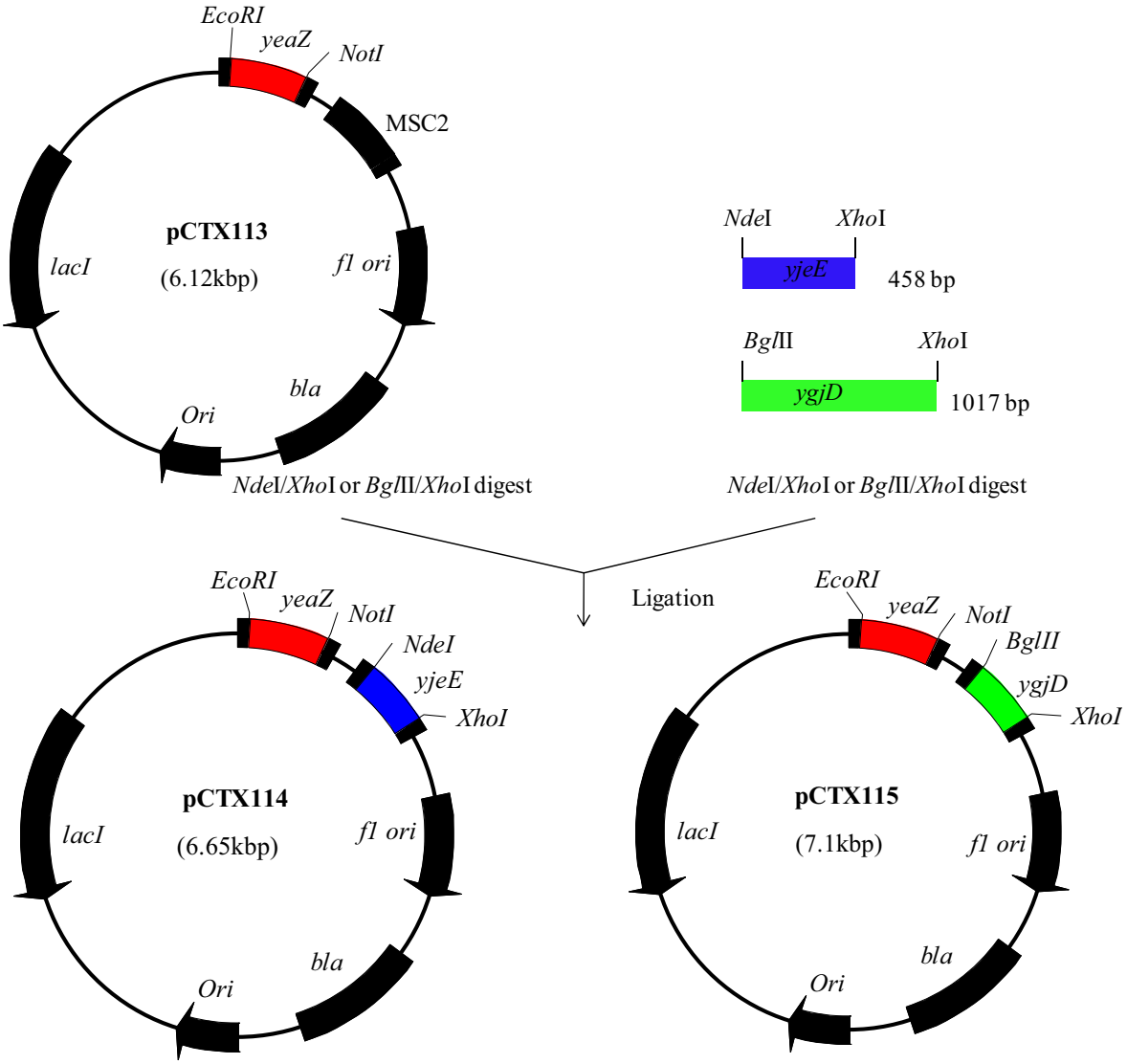

Figure 5.10: Construction of plasmids pCTX114 and pCTX115.

The 465 bp *yjeE* and 1,017 bp *ygjD* fragments encoding flanking *Nde*I/*Xho*I or *Bgl*II/*Xho*I restriction enzyme cutting sites were PCR amplified from *V. parahaemolyticus* NCTC 10884. The *Nde*I/*Xho*I digested *yjeE or Bgl*II/*Xho*I digested *ygjD* fragment was ligated into *Nde*I/*Xho*I or *Bgl*II/*Xho*I digested pET-Duet to create plasmid pCTX114 or pCTX115. YeaZ was expressed with N-terminal His tag. YjeE and YgjD were expressed with a C-terminal S tag.

Abbreviations: bla, ampicillin resistance; *f1 ori*, f1 origin; lac I, *lac I* gene; MCS1, multiple cloning site 1; MCS2, multiple cloning site 2.

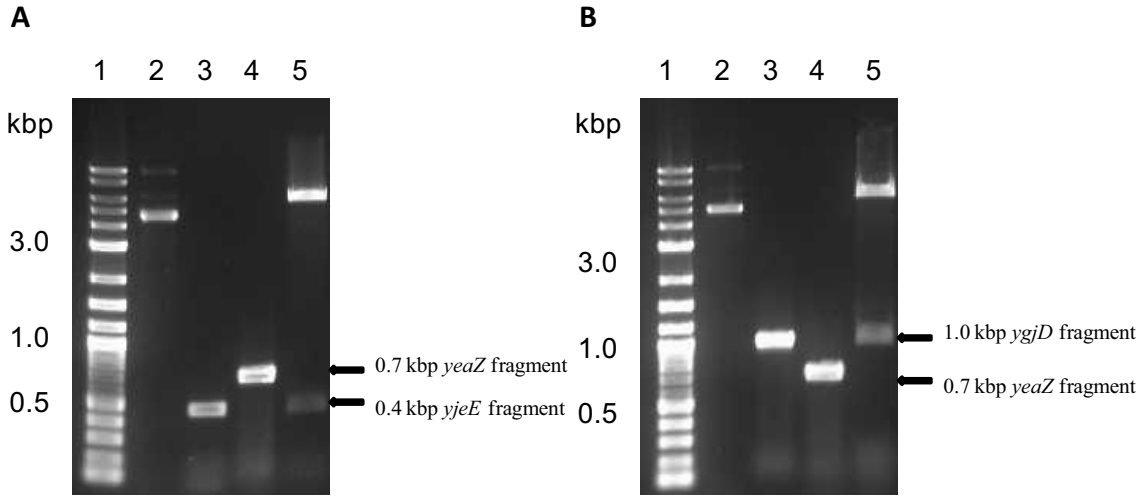

Figure 5.11: Confirmation of pCTX114 and pCTX115.

Panel A. Plasmid pCTX114 comprises a total of 6.65 kbp. Oligonucleotide pairs yjeEF/R and pET-DuetRPFF/R were used to confirm presence of a 0.4 kbp fragment of *yjeE* and a 0.702 kbp fragment of *yeaZ*. Restriction enzyme digestion was used to confirm the expected 0.4 kbp *Nde*I/*Xho*I fragments comprising plasmid pCTX114. All DNA fragments were separated on a 1 % (w/v) agarose gel. Lanes are marked as below:

1. 2 log DNA marker
2. pCTX114 plasmid
3. *yjeE* fragment amplicon
4. *yeaZ* fragment amplicon
5. *Nde*I/*Xho*I digested plasmid pCTX114.

Panel B. A total of 7.1 kbp of DNA plasmid from plasmid pCTX115 has been constructed. Nucleotide pairs pET-DuetGCPF/R and pET-DuetRPFF/R were used to confirm the 1.0 kbp *ygjD* and 0.7 kbp *yeaZ* fragments. Plasmid pCTX115 was digested with *Nde*I and *Xho*I. The DNA fragments were analysis by 1 % agarose gel. Lanes are marked as below:

1. 2 log marker
2. pCTX115 plasmid
3. *ygjD* fragment amplicon
4. *yeaZ* fragment amplicon
5. *Nde*I/*Xho*I digested plasmid pCTX115.

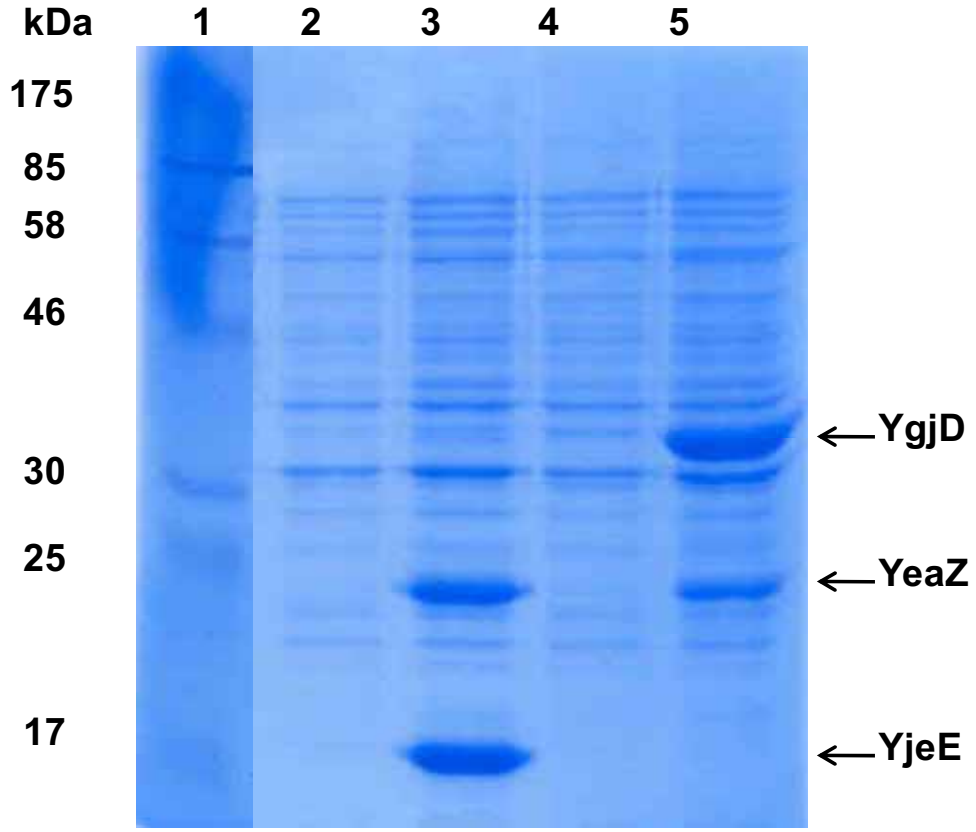

Figure 5.12: Co-expression of $YeaZ_{Vp}$ with $YgjD_{Vp}$ or $YjeE_{Vp}$ in *E. coli* BL21DE3.

Whole cell lysates prepared from *E. coli* BL21DE3 strains carrying pCTX114 or pCTX115 were cultured in LB with Amp and protein expression induced with IPTG. Proteins from lysates of induced and non-induced cultures were separated on 12.5 % SDS-PAGE gel and stained with Coomassie blue. Each lane was loaded with 10 µg of protein.

Lanes are marked as below:

1. Prestained protein marker.
2. Cell lysate from non-induced *E. coli* BL21DE3 [pCTX114].
3. Cell lysate from induced *E. coli* BL21DE3 [pCTX114] expressing $YeaZ_{Vp}$ and $YjeE_{Vp}$ protein.
4. Cell lysate from non-induced *E. coli* BL21DE3 [pCTX115].
5. Cell lysate from induced *E. coli* BL21DE3 [pCTX115] expressing $YeaZ_{Vp}$ and $YgjD_{Vp}$ protein.

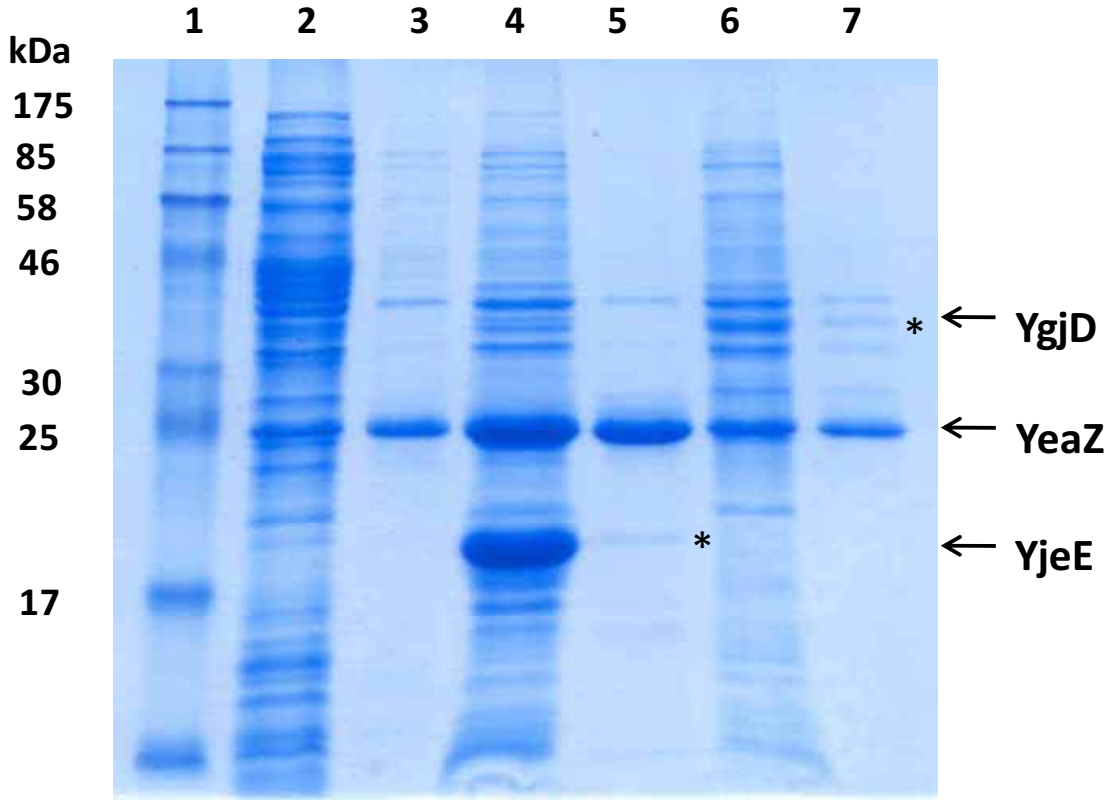

Figure 5.13: The His-tag pull down assay of $YeaZ_{Vp}$ complexes.

Cytoplasmic protein was prepared from *E. coli* strains carrying pCTX113, pCTX114 and pCTX115. The strains were cultured in LB with Amp and protein expression induced with IPTG. Cytoplasmic protein extracts were affinity purified on a Ni-NTA column. Isolated proteins obtained were separated on a 12.5 % SDS-PAGE gel and stained with Coomassie blue. Each lane was loaded with 10 µg of protein.

Lanes are marked as below:

1. Prestained protein marker.
2. Cell lysate from *E. coli* BL21DE3 [pCTX113] expressing $YeaZ_{Vp}$ protein.
3. $YeaZ_{Vp}$ eluate.
4. Cell lysate from *E. coli* BL21DE3 [pCTX114] expressing $YeaZ_{Vp}$ and $YjeE_{Vp}$ protein.
5. $YeaZ_{Vp}$ and $YjeE_{Vp}$ eluate.
6. Cell lysate from *E. coli* BL21DE3 [pCTX115] expressing $YeaZ_{Vp}$ and $YgjD_{Vp}$ protein.
7. $YeaZ_{Vp}$ and $YgjD_{Vp}$ eluate.

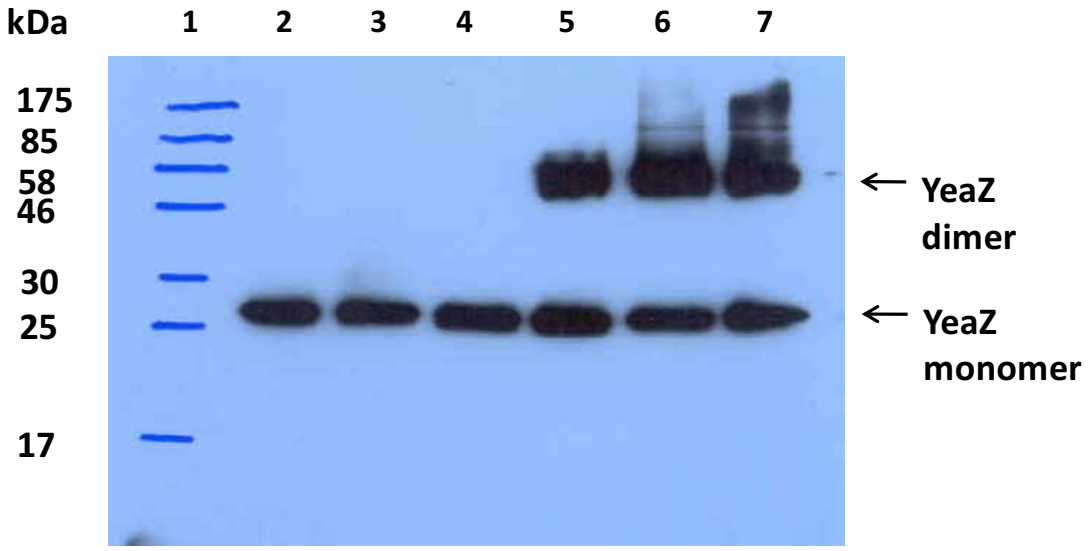

Figure 5.14: Western blot detection of cross-linked $YeaZ_{Vp}$ complexes.

Whole cell lysate protein was prepared from *E. coli* BL21DE3 strains carrying pCTX113, pCTX114 and pCTX115 plasmids. The strains were cultured in LB with Amp and protein expressioninduced with IPTG. Cytoplasmic extracts containing the expressed proteins were cross-linked by treatment with formaldehyde to stabilize protein complexes. Proteins were then separated on 12.5 % SDS-PAGE gel. After migration the bands were stained with Coomassie blue. Each lane was loaded with 10 µg of protein.

Lanes are marked as below:

1. Prestained protein marker.
2. Cell lysate from *E. coli* BL21DE3 [pCTX113] expressing $YeaZ_{Vp}$ protein.
3. Cell lysate from *E. coli* BL21DE3 [pCTX114] expressing $YeaZ_{Vp}$ and $YjeE_{Vp}$ protein.
4. Cell lysate from *E. coli* BL21DE3 [pCTX115] expressing $YeaZ_{Vp}$ and $YgjD_{Vp}$ protein.
5. Cell lysate from *E. coli* BL21DE3 [pCTX113] expressing $YeaZ_{Vp}$ protein (crosslinked).
6. Cell lysate from *E. coli* BL21DE3 [pCTX114] expressing $YeaZ_{Vp}$ and $YjeE_{Vp}$ protein (crosslinked).
7. Cell lysate from *E. coli* BL21DE3 [pCTX115] expressing $YeaZ_{Vp}$ and $YgjD_{Vp}$ protein (crosslinked).

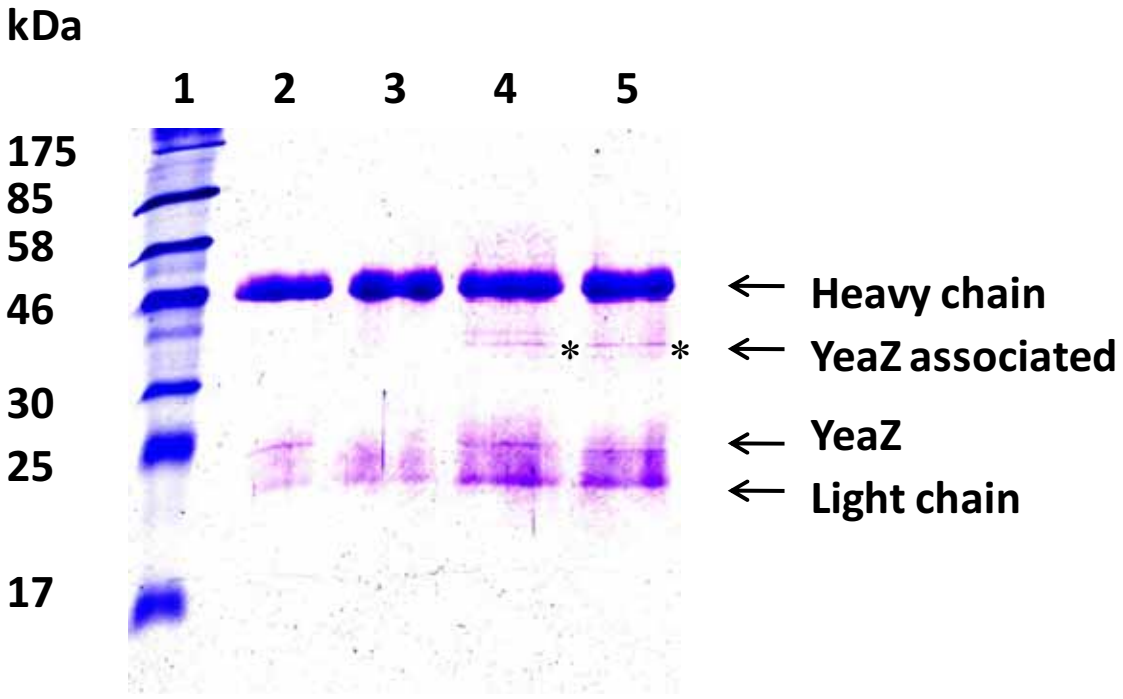

Figure 5.15: Immuno-precipitation of $YeaZ_{Vp}$ associated protein.

Whole cell lysates were prepared from *V. parahaemolyticus* NCTC 10884. Protein was reacted with an adsorbed polyvalent anti-$YeaZ_{Vp}$ serum coupled to Protein A-Dynabeads. Dynabeads were then collected, washed and bound protein eluted. These protein samples were then separated on 12.5 % SDS-PAGE gel and after migration the bands were stained with Coomassie blue. Each has loaded with 10 µg of protein.

Lanes are marked as below:

1. Prestained protein marker.
2. Immunoprecipitated recombinant $YeaZ_{Vp}$ protein fraction (Negative control).
3. Immunoprecipitated whole cell protein extracts treated with prebleed rabbit serum (Negative control).
4. and 5. Immunoprecipitated whole cell protein extracts.

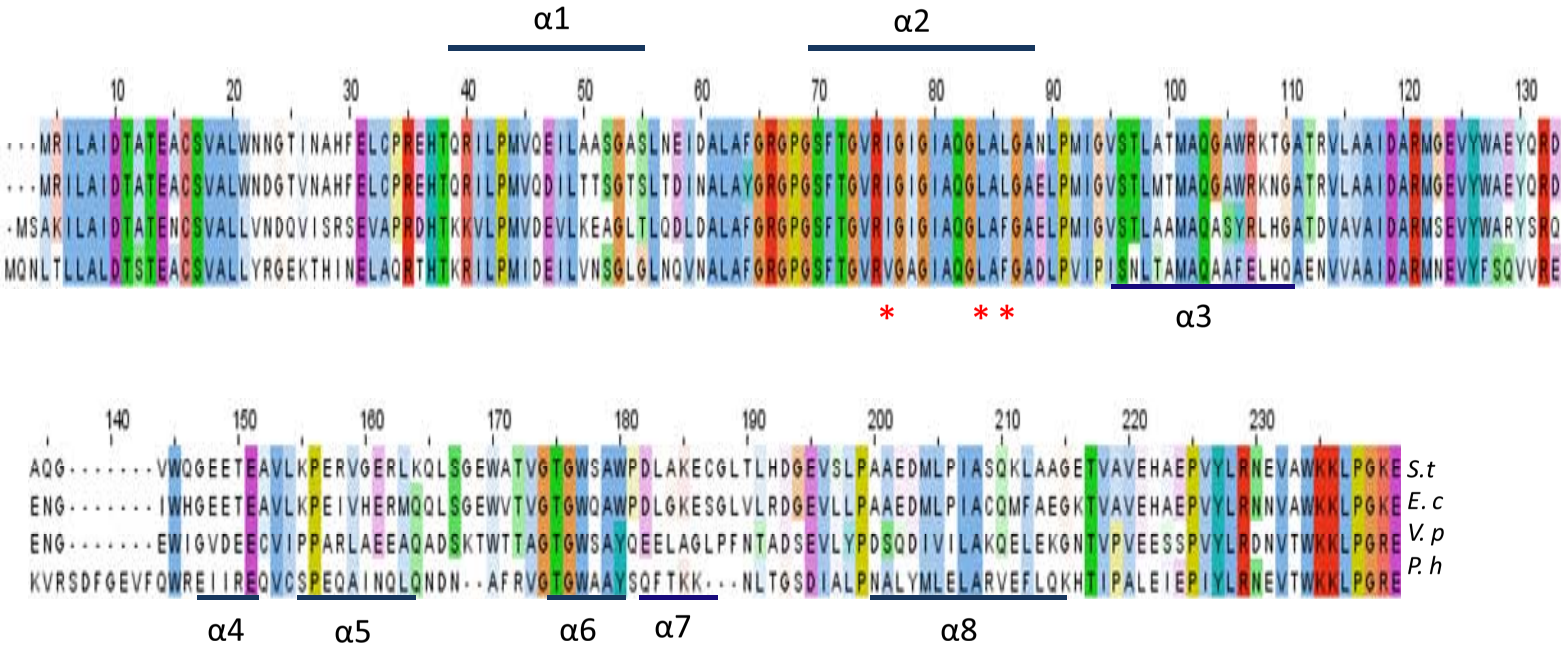

Figure 5.16: YeaZ amino acid sequence alignments.

Amino acid sequence of the YeaZ protein from *Salmonella* Typhimurium LT2 (*S. t*), *E. coli* (*E. c*), *V. parahaemolyticus* (*V. p*) and *Pasteurella haemolytica* (*P. h*) were aligned using ClutalW2 (http://www.ebi.ac.uk/Tools/msa/clustalw2/). Alignments were sorted by slow pairwise comparison. The alignment was displayed using Jalview (http://www.jalview.org/download.html) configured to display predicted α-helical regions. Residues were colored according to ClustalX schema. $YeaZ_{Vp}$ has 8 α helices based on the structure of *Salmonella* YeaZ (underlined). $YeaZ_{Vp}$ residues proposed to be potential interaction sites within α-helix 2 are indicated by red asterisks (I75, L83 and F85).

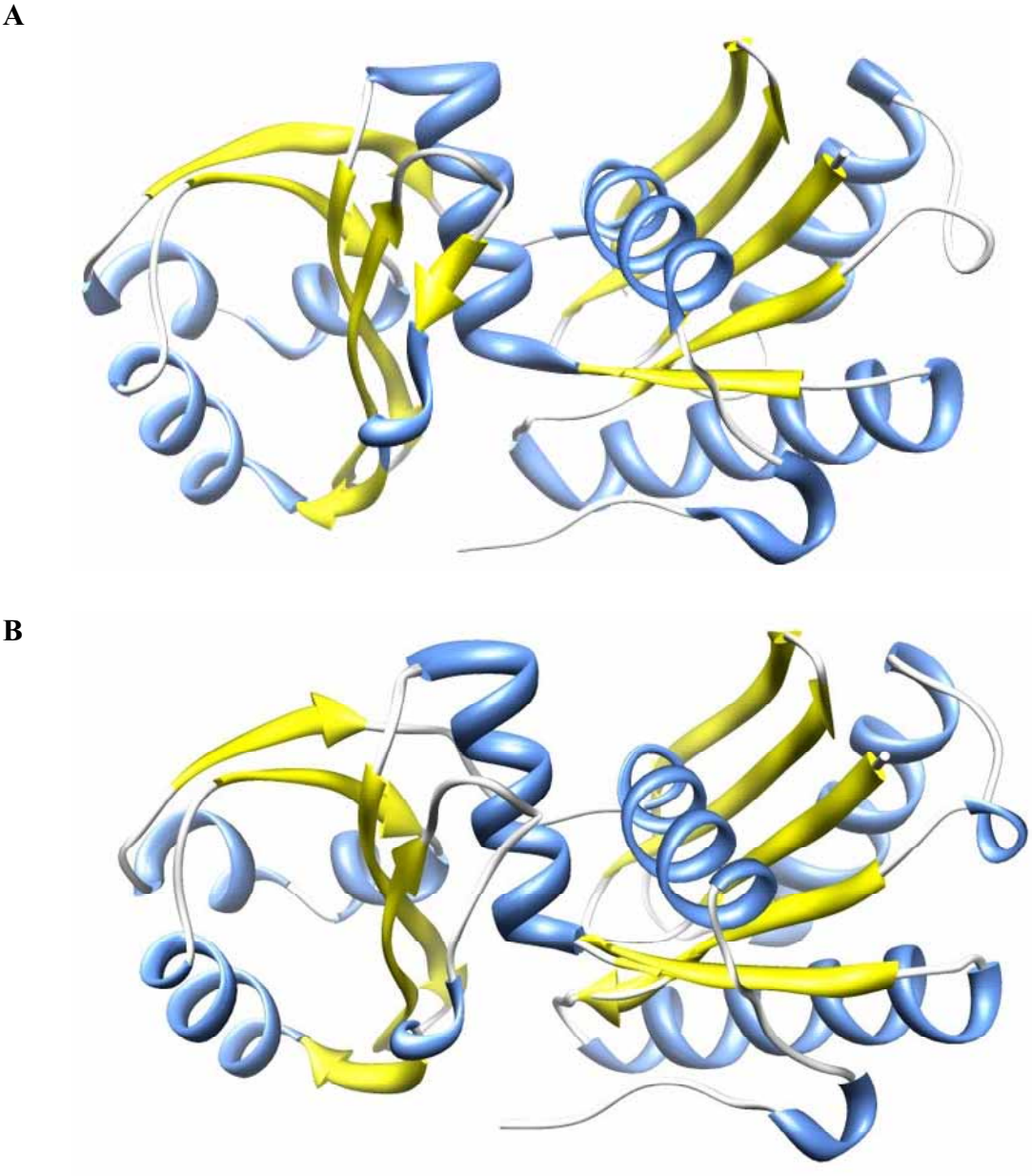

Figure 5.17: The structure of $YeaZ_{ST}$ and predicted structure of $YeaZ_{Vp}$.

$YeaZ_{ST}$ (Panel A) and $YeaZ_{Vp}$ (Panel B) comprise two lobes A and B. The $YeaZ_{Vp}$ structure was deduced by threading the amino acid sequence onto that of the $YeaZ_{ST}$ structure. Blue color represents α-helix; yellow color represents β-sheet. The images were generated from PBD data using Chimera software (Pettersen et al., 2004).

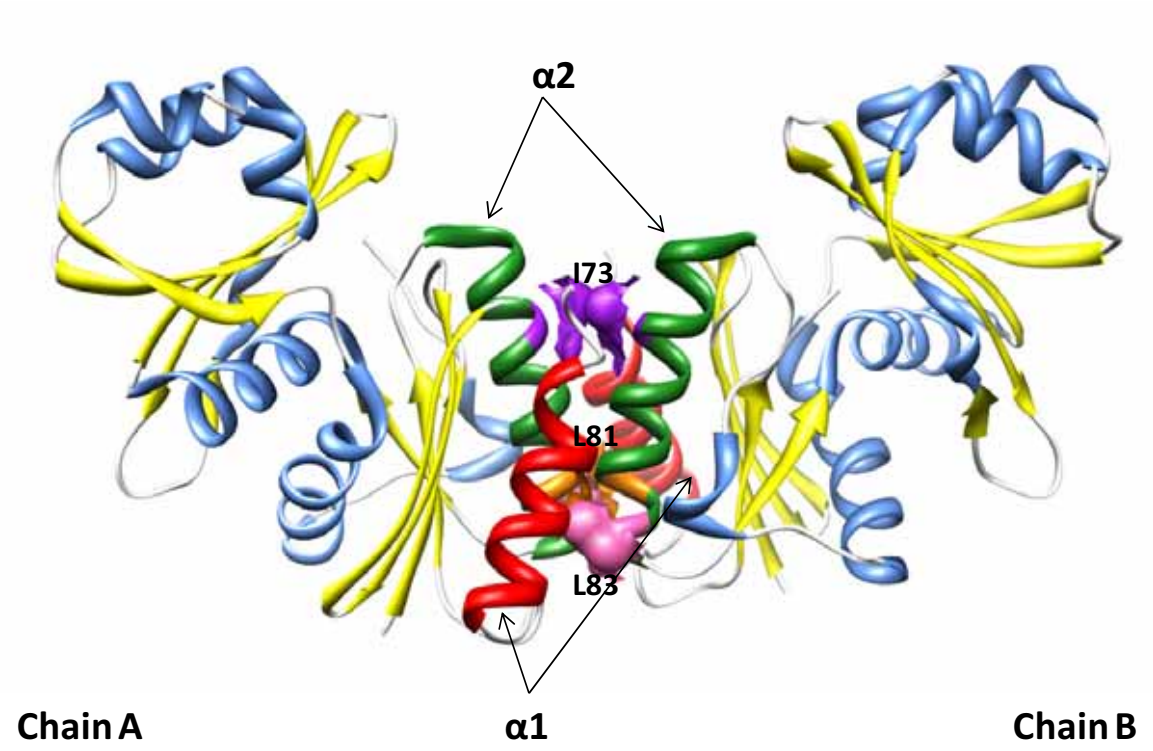

Figure 5.18: Potential interaction domains and amino acids in $YeaZ_{ST}$ dimers.

The structure of the *Salmonella* Typhimurium LT2 YeaZ dimer contains two chains (chains A and B) is shown together with potential interaction motifs in α 1 (red) and α 2 (green). The surface structure shows potential interacting amino acids I73, L81 and L83 (indicated in purple, orange and pink, respectively) on α 2. The equivalent amino acids on the $YeaZ_{Vp}$ are I75, L83 and F85. The image was generated from PBD data (PDB accession 2GEL) using Chimera software (Pettersen et al., 2004).

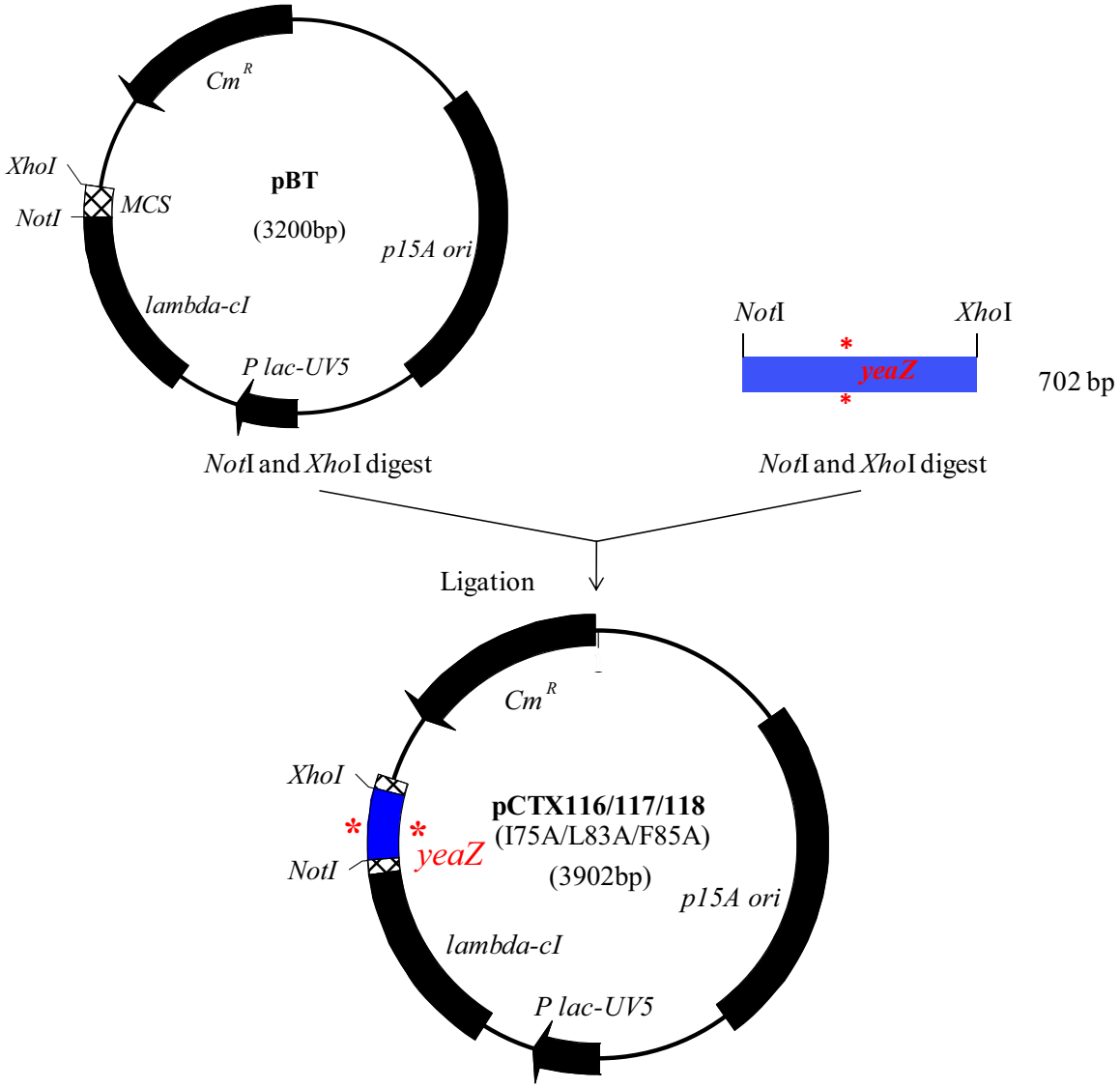

Figure 5.19: Construction of plasmids pCTX116, pCTX117 and pCTX118.

Three separate 702 bp *yeaZ*$_{Vp}$ fragments, each carrying mutations that create I75A, L83A and F85A amino acid substitutions, were PCR amplified from plasmid pCTX106 using overlap extension PCR. The *Not*I/*Xho*I digested *yeaZ*$_{Vp}$ fragments were ligated into *Not*I/*Xho*I digested pBT to create plasmids pCTX116, pCTX117 and pCTX118 (each carrying DNA encoding a I75A, L83A or F85A substitution). These plasmids were used for bacterial two-hybrid analysis.

Abbreviations: Cm^R, chloramphenciol resistance; *p15A ori*, p15A origin; *lambda*-cI, λ-cI gene; MCS, multiple cloning sites.

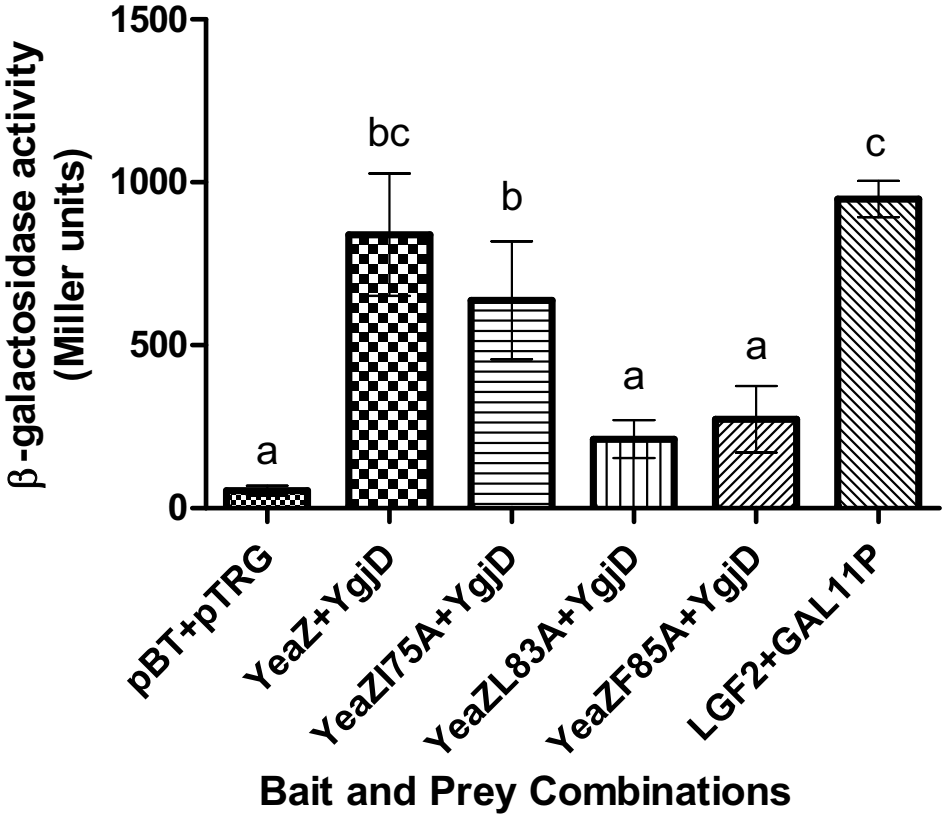

Figure 5.20: Interaction of $YeaZ_{Vp}$ mutants with $YgjD_{Vp}$.

Bacterial two-hybrid interaction analysis was carried out using each of the three $YeaZ_{Vp}$ I75A, L83A or F85A substitution mutants and $YgjD_{Vp}$. Interactions were tested using the β-galactosidase activity reporter assay for this two-hybrid system. The *ygjD*$_{Vp}$ gene was cloned into pTRG as a prey protein. The *yeaZ*$_{Vp}$ wild type and *yeaZ*$_{Vp}$ mutants were cloned into pBT as bait proteins. The negative control was empty vector pBT and pTRG. The positive controls used plasmids pBTLGF2 and pTRGGal11p. These construct pairs were used to transform *E. coli* strain KS1. Transformants were selected and used to inoculate LB medium containing with appropriate antibiotics. These cultures were assayed for β-galactosidase as a means of assessing the strength of interaction between bait and prey proteins. GraphPad prism was used to analyse data by performing a one way ANOVA with a Tukey-Kramer multiple comparison test to make pairwise comparisons of each data set. Data set with the same single letter label are not significantly different ($p>0.05$). Error bars represent standard error of the means; n= 5.

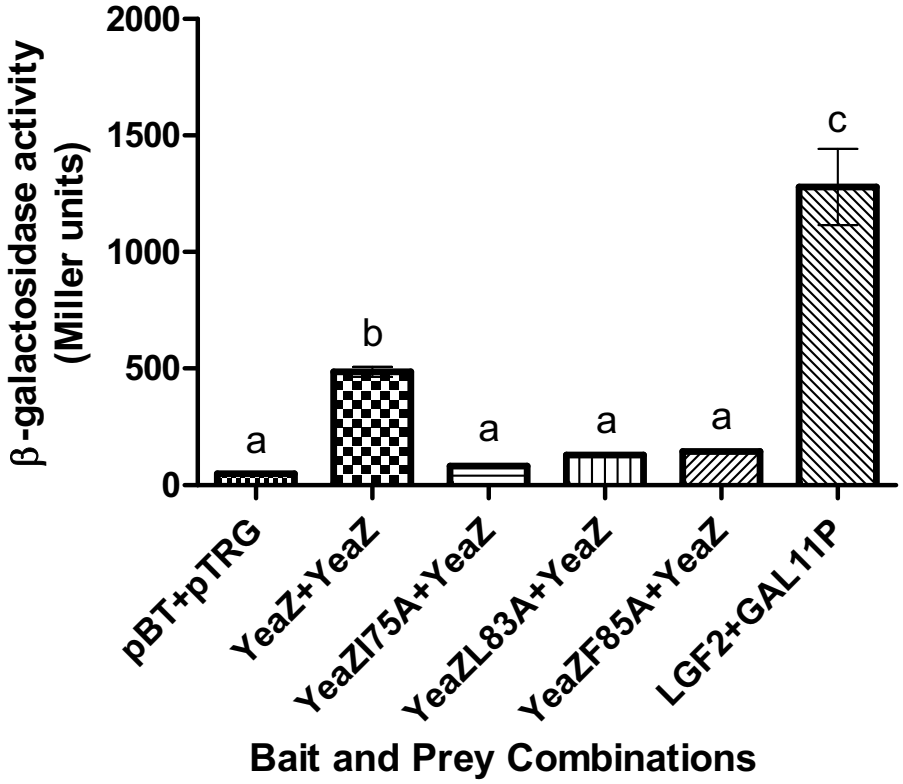

Figure 5.21: Interaction of I75A, L83A and F85A $YeaZ_{Vp}$ mutants with $YeaZ_{Vp}$.

Bacterial two-hybrid interaction analysis was carried out using $YeaZ_{Vp}$ I75A, L83A or F85A substitution mutants. Interactions were based on β-galactosidase activity assessed using the reporter assay for this two-hybrid system. The *yeaZ*$_{Vp}$ gene was cloned into pBT as bait. The I75A, L83A and F85A mutations were cloned into pTRG as prey. The negative control was empty vector pBT and pTRG. The positive control was pBTLGF2 and pTRGGal11p. The *E. coli* KS1 strain was cotransformed with pBT and pTRG plasmid derivatives. A single colony of transformation was picked and inoculated in LB medium applied with appropriate antibiotics and β-galactosidase assays were used to analysis the interaction activity by following the method of Miller (Miller, 1992). GraphPad prism was used to analyse data by performing a one way ANOVA with a Tukey-Kramer multiple comparison test to make pairwise comparisons of each data set. Data set with the same single letter label are not significantly different ($p>0.05$). Error bars represent standard error of the means; n= 5.

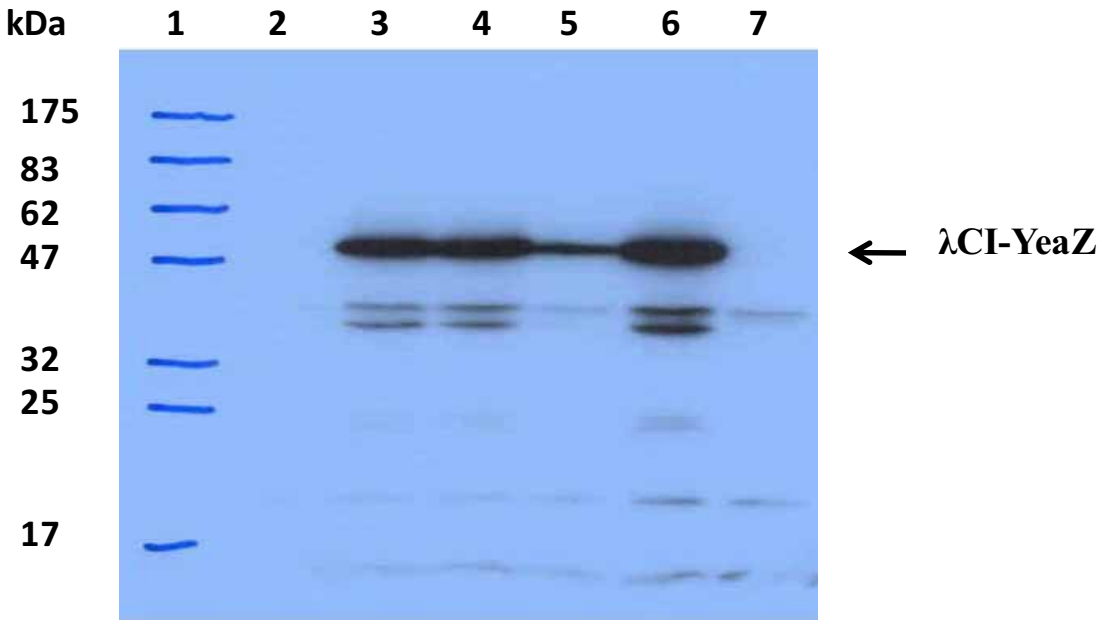

Figure 5.22: Western blot analysis of interacting $YeaZ_{Vp}$ and $YgjD_{Vp}$ protein.

Lanes are marked as below:

1. Prestained protein marker
2. Cell lysate from *E. coli* carrying pBT + pTRG (negative control)
3. Cell lysate from *E. coli* carrying pBT-$YeaZ_{Vp}$ + pTRG-$YgjD_{Vp}$ (wild type)
4. Cell lysate from *E. coli* carrying pBT-YeaZI75A + pTRG-$YgjD_{Vp}$ (mutant)
5. Cell lysate from *E. coli* carrying pBT-YeaZL83A + pTRG-$YgjD_{Vp}$ (mutant)
6. Cell lysate from *E. coli* carrying pBT-YeaZF85A + pTRG-$YgjD_{Vp}$ (mutant)
7. Cell lysate from *E. coli* carrying pBT-LGF2 + pTRG-GAL11p (positive control)

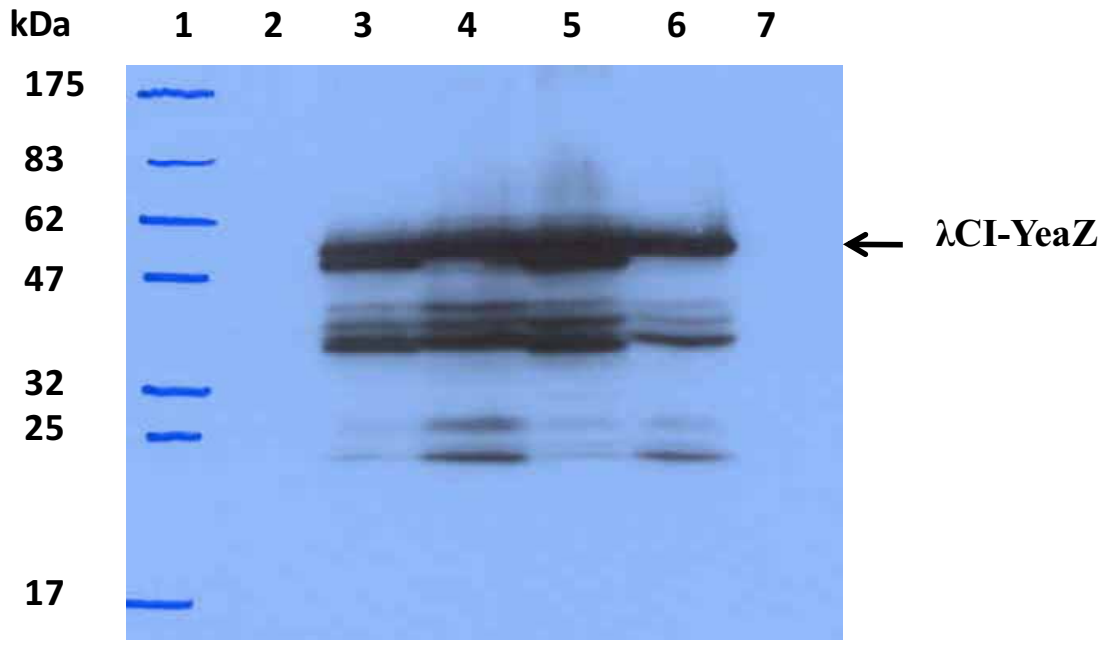

Figure 5.23: Western blot analysis of interacting $YeaZ_{Vp}$ mutants and $YeaZ_{Vp}$ wt proteins.

Lanes are marked as below:

1. Prestained protein marker
2. Cell lysate from *E. coli* carrying pBT+pTRG (negative control)
3. Cell lysate from *E. coli* carrying pBT-YeaZ+pTRG-$YeaZ_{Vp}$ (wild type)
4. Cell lysate from *E. coli* carrying pBT-YeaZI75A+pTRG-$YeaZ_{Vp}$ (mutant)
5. Cell lysate from *E. coli* carrying pBT-YeaZL83A+pTRG-$YeaZ_{Vp}$ (mutant)
6. Cell lysate from *E. coli* carrying pBT-YeaZF85A+pTRG-$YeaZ_{Vp}$ (mutant)
7. Cell lysate from *E. coli* carrying pBT-LGF2+pTRG-GAL11p (positive control)

Table 5.1: Protein mass spectrometry sequencing results for potential $YeaZ_{Vp}$ associated proteins.

Protein identification	Organism	Accession no.	Combined ion score	No. unique peptides	% seq. MS/MS	Predicted MW (kDa)
Outer membrane protein U	*V. parahaemolyticus*	OMPU_VIBPA	486/40	8	26	36.3
Protein recA	*V parahaemolyticus*	RECA_VIBPA	233/40	4	21	37.7
Outer membrane protein U	*V. vulnificus*	OMPU_VIBVU	226/40	2	6	36.7

Chapter 6: Conclusions

6.1 Introduction

V. parahaemolyticus is a G-ve bacterial pathogen, that is increasingly associated with disease caused by ingestion of raw, contaminated shellfish harvested from warmer seawater (>20°C) (Potasman et al., 2002). *V. parahaemolyticus* is widely distributed within marine and estuarine systems. Interestingly, there is a strong relationship exists between water temperature and *V. parahaemolyticus* levels. For example, elevated counts of *Vibrio* species associated with warmer seawater temperature in oysters that grown in this region of Australia (Madigan et al., 2007). Contamination of foods, normally eaten raw, presents a risk to public health that might be complicated by vibrios entering the VBNC state during refrigerated storage. Almost nothing is known about this outcome for contaminated foods, except that failure to enumerate these cells may lead to underestimation of risk of illness following consumption. Moreover, the potential for VBNC state bacteria to resuscitate following a temperature upshift may present additional risk. Thus VBNC state cells may make control of *V. parahaemolyticus* in seafood a significant challenge. Filling this information gap may assist the food industry to minimise the potential risk for consumption of contaminated seafood.

Recent studies of the VBNC state of other pathogens has reported that a secreted resuscitation promoting factor (Rpf or YeaZ) expressed by *Micrococcus luteus* cells can assist recovery of VBNC state *Micrococcus luteus, Salmonella* Typhimurium LT2 and *Salmonella* Oranienburg (Mukamolova et al., 1998). The protein encoded by the *yeaZ* gene of *Salmonella* Typhimurium LT2 shares 24.2% homology with *Micrococcus luteus* Rpf. Nevertheless, the $YeaZ_{ST}$ protein influenced rescuscitation of *Salmonella* Oranienburg cells from a VBNC state (Panutdaporn et al., 2006). What has not been recognized is a potential linkage between the $YeaZ_{Vp}$ protein and the VBNC state in *V. parahaemolyticus* NCTC 10884, nor is there any experimental evidence to establish that this gene is expressed. Recent interest in YeaZ and YeaZ related proteins (YjeE and YgjD) expressed by *E. coli* has indicated these are essential proteins required for bacterial viability. Moreover, it is now clear that these proteins are conserved across a wide range of prokaryotes. This unique

YeaZ/YgjD/YjeE network of essential proteins may also associate with the VBNC state in bacteria.

It is against this background that the principal aims of work described in this thesis was to (a) examine the influence of cell densities, salinity and pH on entry to, and exit from, the VBNC state by *V. parahaemolyticus* NCTC 10884, (b) analyse the effect of mutation of *yeaZ*$_{Vp}$ on establishment of the VBNC state and resuscitation, and (c) determine whether the protein-protein interactions reported for YeaZ are also conserved in YeaZ$_{Vp}$/YjeE$_{Vp}$/YgjD$_{Vp}$ of *V. parahaemolyticus* NCTC 10884.

6.2 Conclusions

The principal findings that have arisen from this study are as follows:

1. *V. parahaemolyticus* NCTC 10884 cells are able to enter VBNC state when suspended in ASW with incubation at 4°C. The finding that the rate of loss of culturability is dependent on the prevailing pH and salt concentration has not previously been established and indicates that the cell environment can have a significant impact on the rate of loss of culturability under low temperature conditions associated with establishment of the VBNC state.

2. A novel outcome of the work was the finding that the rate of loss of culturability during establishment of the VBNC state induction of *V. parahaemolyticus* NCTC 10884 occurred in a cell density dependent manner. Analysis of the kinetics of rate of loss of culturability under a variety of salt concentrations and suspending medium pH, confirmed that loss of culturability is dependent on cell suspension concentration. This finding indicated the establishment of a physiological state different to that of cell death where the death rate is independent of cell concentration.

3. As is the case for other types of bacteria, including other vibrios, low temperature and starvation induced VBNC state *V. parahaemolyticus* NCTC 10884 cells can be resuscitated by a temperature upshift. Importantly, high cell density suspensions of VBNC state cells could be resuscitated from the VBNC state, but not suspensions with cell densities of 10^5 cells mL^{-1} or less.

4. To examine the role of the resuscitation factor protein YeaZ on entry to and resuscitation from the VBNC state, a *yeaZ*$_{Vp}$ mutant was constructed. Significantly, this mutant was viable when cultured under normal laboratory conditions, but was unable to survive incubation under conditions that normally lead to the VBNC state. This finding is entirely novel. Indeed this is the first report of a *yeaZ* mutant that is not unconditionally lethal. However, what was most surprising was the fact that this mutant could not be resuscitated if cells were incubated in conditions used to induce the VBNC state. This result indicated that YeaZ and partner proteins may be implicated in survival of VBNC state cells and subsequent resuscitation by temperature upshift.

5. The morphology changes associated with establishment of the VBNC state in wild type *V. parahaemolyticus* NCTC 10884 were mimicked by introduction of a *yeaZ* mutation. This observation supports the contention that YeaZ is implicated in establishment of, and recovery from the VBNC state.

6. YeaZ$_{Vp}$ protein was shown to be either expressed *de novo*, or maintained by cells, throughout establishment of the VBNC state and during resuscitation. This finding was established for high density suspensions of cells by qRT-PCR and Western analysis. Whether this is the case for low density cells suspensions, has yet to be determined. Importantly however, immunofluorescence microscopy and Western analysis established the *ca.* 25 kDa YeaZ protein decorated the outer surface of *V. parahaemolyticus* NCTC 10884. Immunoprecipitation assays suggested that the exported YeaZ may be associated with the outer membrane protein OmpU, although how the cell exported YeaZ, and the significance of the interaction with OmpU have yet to be established.

7. In agreement with other published studies, YeaZ$_{Vp}$ has been shown to interact with other YeaZ$_{Vp}$ monomers as well as YgjD protein. This work supports other published research that implicates these proteins, together with YjeE, in a critical set of protein-protein interactions required for viability. Interaction between YeaZ and YgjD were established using two-hybrid systems together with experiments that showed these interactions occur natively in bacterial cells.

8. Analysis of the previously published *S.* Typhimurium LT2 YeaZ/YeaZ dimer structure identified amino acid residues located in α helix 1 and 2 that may be important for dimer formation. This analysis was extended to predict structure for *V. parahaemolyticus* NCTC 10884 YeaZ. The combination of site directed mutagenesis and bacterial two-hybrid analysis was then used to establish Leucine 83 and Phenylalanine 85 of $YeaZ_{Vp}$ protein are particularly important for protein-protein interactions between $YeaZ_{Vp}$ monomeric units. Given the remarkable N-terminal sequence and structure of YgjD to YeaZ, it is likely that the same amino acids are implicated in interaction between YeaZ and YgjD.

6.3 Significance and Future Work

Work presented in this thesis has pointed out that pathogen and environmental factors play a role in VBNC state induction and resuscitation by *V. parahaemolyticus* NCTC 10884. This work has also confirmed that adverse environmental condition compromise survival and resuscitation of VBNC state cells – optimum conditions for entry to and escape from the VBNC state are similar to optimum growth conditions for this organism. However, what is clear is that critical cell concentrations are required for VBNC state cells to survive and resuscitate to actively culturable forms. This finding is completely novel. This effect has probably escaped prior notice because almost all studies of the VBNC state have relied on high density preparations of VBNC state cells. The finding that recovery from the VBNC state is dependent on cell concentration suggested, for the first time, that dead cells present in high density suspensions may support the maintenance requirements of viable cells under conditions that promote establishment of the VBNC state.

Furthermore, the linkage between key viability proteins and the VBNC state represent a new aspect to the study of this intriguing phenomenon. The finding that *yeaZ* mutations significantly affect recovery from the VBNC state was a first clue that the YeaZ protein might be involved in molecular mechanisms responsible for establishment, maintenance and recovery from the VBNC state. In particular, the maintenance of cellular pools of YeaZ protein by cells undergoing loss of culturability, as well as cells during resuscitation, indicated that *yeaZ* is either maintained by the cell, or is subject to *de novo* synthesis. While this observation was demonstrated for high density cell populations, the same has not been

shown for low density populations of cells exposed to conditions that lead to establishment of the VBNC state and subsequent resuscitation. This in fact is an important deficiency of the work done. The implications are that if YeaZ levels cannot be maintained by cells in low density populations, then it is possible that this deficiency will affect the ability of these cells to recover from a VBNC state, as has been shown for the wild type and *yeaZ* mutant strains. In addition the data concerning the maintenance of cellular levels of YeaZ also needs more detailed analysis to confirm whether this protein is stably maintained or indeed expressed by VBNC state cells at low levels.

While the work done to demonstrate the interaction of $YeaZ_{Vp}$ with its partner protein $YgjD_{Vp}$ supports conclusions of other work on *S.* Typhimurium and *E. coli*, it also highlights that YeaZ protein-protein interactions may represent a fruitful target for small molecular weight inhibitors that could interfere with the YeaZ/YgjD/YjeE viability network. By identifying amino acid residues that are clearly implicated in protein-protein interactions, this work could act as a starting point for the molecular design of inhibitors that could be used to halt resuscitation of VBNC state pathogenic vibrios, or more broadly, other bacterial pathogens. These inhibitors need not necessarily lead to death of bacterial cells causing infections – reduction in the rate of growth may simply be all that is required to allow the immune system to recognize presence of pathogenic cells and mount an appropriate response. This is an approach that has been deployed to develop inhibitors based on virulence factors and inhibitors of signal transductions systems eg. two component regulatory systems (Escaich, 2008; Njoroge & Sperandio, 2009; Rasko & Sperandio, 2010; Reading et al., 2009; Ryan & Dow, 2011).

The combination of site directed mutagenesis and two-hybrid systems described in this thesis, represents a robust means to obtain a better understanding the involvement of proteins in enhancing the environmental adaptation of *V. parahaemolyticus* NCTC 10884. This project also provides insight into the survival strategies that *V. parahaemolyticus* NCTC 10884 might use to persist in the different ecological conditions. Therefore, future work should aim at fully characterizing the role of $YeaZ_{Vp}$, $YjeE_{Vp}$ and $YgjD_{Vp}$ proteins in the VBNC state of *V. parahaemolyticus* NCTC 10884.

Chapter 7: References

Abdullah, K.M., Lo, R.Y. and Mellors, A. (1991). Cloning, nucleotide sequence, and expression of the *Pasteurella haemolytica* A1 glycoprotease gene. *Journal of Bacteriology* **173**, 5597-5603.haemolyticus

Abe, A., Ohashi, E., Ren, H., Hayashi, T. and Endo, H. (2007). Isolation and characterization of a cold-induced nonculturable suppression mutant of *Vibrio vulnificus*. *Microbiology Research* **162**, 130-138.

Aiba, H., Adhya, S. and de Crombrugghe, B. (1981). Evidence for two functional *gal* promoters in intact *Escherichia coli* cells. *Journal of Biological Chemistry* **256**, 11905-11910.

Allali-Hassani, A., Campbell, T.L., Ho, A., Schertzer, J.W. and Brown, E.D. (2004). Probing the active site of YjeE: a vital *Escherichia coli* protein of unknown function. *Biochemical Journal* **384**, 577-584.

Anderson, M., Bollinger, D., Hagler, A., Hartwell, H., Rivers, B., Ward, K. and Steck, T. R. (2004). Viable but nonculturable bacteria are present in mouse and human urine specimens. *Journal of Clinical Microbiology* **42**, 753-758.

Anuchin, A.M., Mulyukin, A.L., Suzina, N.E., Duda, V.I., El-Registan, G.I. and Kaprelyants, A.S. (2009). Dormant forms of *Mycobacterium smegmatis* with distinct morphology. *Microbiology* **155**, 1071-1079.

Arias, C.R., Macián, M.C., Aznar, R., Garay, E. and Pujalte, M.J. (1999). Low incidence of *Vibrio vulnificus* among Vibrio isolates from sea water and shellfish of the western Mediterranean coast. *Journal of Applied Microbiology* **86**, 125-134.

Arigoni, F., Talabot, F., Peitsch, M. and other authors (1998). A genome-based approach for the identification of essential bacterial genes. *Nature Biotechnology* **16**, 851-856.

Asakura, H., Kawamoto, K., Haishima, Y., Igimi, S., Yamamoto, S. and Makino, S. (2008). Differential expression of the outer membrane protein W (OmpW) stress response in enterohemorrhagic *Escherichia coli* O157:H7 corresponds to the viable but non-culturable state. *Research in Microbiology* **159**, 709-717.

Asakura, P.N., Kawamoto K., Igimi S., Yamamoto S., Makino S. (2007). Proteomic characterization of enterohemorrhagic *Escherichia coli* O157:H7 in the oxidation-induced viable but non-culturable state. *Microbiology and Immunology* **51**, 875-881.

Aydin, I., Dimitropoulos, A., Chen, S.H., Thomas, C. and Roujeinikova, A. (2011). Purification, crystallization and preliminary X-ray crystallographic analysis of the putative *Vibrio parahaemolyticus* resuscitation-promoting factor YeaZ. *Acta crystallographica* Section F, Structural biology and crystallization communications **67**, 604-607.

Baba, T., Ara, T., Hasegawa, M. and other authors (2006). Construction of *Escherichia coli* K-12 in-frame, single-gene knockout mutants: the Keio collection. *Molecular Systems Biology* **2**, 1-11.

Baffone, W., Citterio, B., Vittoria, E., Casaroli, A., Campana, R., Falzano, L. and Donelli, G. (2003). Retention of virulence in viable but non-culturable halophilic *Vibrio* spp. *International Journal of Food Microbiology* **89**, 31-39.

Banin, E., Israely, T., Kushmaro, A., Loya, Y., Orr, E. and Rosenberg, E. (2000). Penetration of the coral-bleaching bacterium *Vibrio shiloi* into *Oculina patagonica*. *Applied and Environmental Microbiology* **66**, 3031-3036.

Barcina, I. and Arana, I. (2009). The viable but nonculturable phenotype: a crossroads in the life-cycle of non-differentiating bacteria? *Reviews in Environmental Science and Biotechnology* **8**, 245-255.

Barer, M.R. (1997). Viable but non-culturable and dormant bacteria: time to resolve an oxymoron and a misnomer? *Journal of Medical Microbiology* **46**, 629-631.

Baross, J.A., Liston, J. and Morita, R.Y. (1978). Incidence of *Vibrio parahaemolyticus* bacteriophages and other *Vibrio* bacteriophages in marine samples. *Applied and Environmental Microbiology* **36**, 492-499.

Bates, T.C. and Oliver, J.D. (2004). The viable but nonculturable state of Kanagawa positive and negative strains of *Vibrio parahaemolyticus*. *Journal of Microbiology* **42**, 74-79.

Bej, A.K., Patterson, D.P., Brasher, C.W., Vickery, M.C.L., Jones, D.D. and Kaysner, C.A. (1999). Detection of total and hemolysin-producing *Vibrio parahaemolyticus* in shellfish using multiplex PCR amplification of *tlh*, *tdh* and *trh*. *Journal of Microbiological Methods* **36**, 215-225.

Ben Abdallah, F., Ellafi, A., Lagha, R., Bakhrouf, A., Namane, A., Rousselle, J.C., Lenormand, P. and Kallel, H. (2010). Identification of outer membrane proteins of *Vibrio parahaemolyticus* and *Vibrio alginolyticus* altered in response to γ-irradiation or long-term starvation. *Research in Microbiology* **161**, 869-875.

Beumer, R.R., de Vries, J. and Rombouts, F.M. (1992). *Campylobacter jejuni* non-culturable coccoid cells. *International Journal of Food Microbiology* **15**, 153-163.

Biosca, E.G., Amaro, C., MarcoNoales, E. and Oliver, J.D. (1996). Effect of low temperature on starvation-survival of the eel pathogen *Vibrio vulnificus* biotype 2. *Applied and Environmental Microbiology* **62**, 450-455.

Bisgaard, M. and Kristensen, K.K. (1975). Isolation, characterization and public health aspects of *Vibrio cholerae* NAG isolated from a Danish duck farm. *Avian Pathology* **4**, 271-276.

Blomfield, I.C., Vaughan, V., Rest, R.F. and Eisenstein, B.I. (1991). Allelic exchange in *Escherichia coli* using the *Bacillus subtilis sacB* gene and a temperature-sensitive pSC101 replicon. *Molecular Microbiology* **5**, 1447-1457.

Bogosian, G. and Bourneuf, E.V. (2001). A matter of bacterial life and death. *European Molecular Biology Organization* **2**, 770-774.

Bradford, M.M. (1976). A rapid and sensitive method for the quantitation of microgram quantities of protein utilizing the principle of protein-dye binding. *Analytical Biochemistry* **72**, 248-254.

Bryan, P.J., Steffan, R.J., DePaola, A., Foster, J.W. and Bej, A.K. (1999). Adaptive response to cold temperatures in *Vibrio vulnificus*. *Current Microbiology* **38**, 168-175.

Buck, D.J. (1990). Isolation of *Candida albicans* and halophilic *Vibrio* spp. from aquatic birds in Connecticut and Florida. *Applied and Environmental Microbiology* **56**, 826-828.

Butland, G., Peregrin-Alvarez, J.M., Li, J. and other authors (2005). Interaction network containing conserved and essential protein complexes in *Escherichia coli*. *Nature* **433**, 531-537.

Campbell T.L., Ederer, C.S., Allali-Hassani, A. and E.D., B. (2007). Isolation of the *rstA* gene as a multicopy suppressor of YjeE, an essential ATPase of unknown function in *Escherichia coli*. *Journal of Bacteriology* **89**, 3318-3321.

Cappelier, J.M., Magras, C., Jouve, J. L. and Federighi, M. (1999). Recovery of viable but non-culturable *Campylobacter jejuni* cells in two animal models. *Food Microbiology* **16**, 375-383.

Carli, A.,L. Pane, L. Casareto, S. Bertone and Pruzzo, C. (1993). Occurrence of *Vibrio alginolyticus* in ligurian coast rock pools (Tyrrhenian Sea, Italy) and its association with the copepod *Tigriopus fulvus* (Fisher 1860). *Applied and Environmental Microbiology* **59**, 1960-1962.

Clark, C.A., R. Doyle, M.W. Heuzenroeder, and P.A. Manning. The construction of a counter-selective temperature sensitive suicide vector in *Legionella longbeachii*. Unpublished data. Department of Microbiology and Immunology, University of Adelaide.

Coallier, J., Prevost, M., Rompre, A. and Duchesne, D. (1994). The optimization and application of two direct viable count methods for bacteria in distributed drinking water. *Canadian Journal of Microbiology* **40**, 830-836.

Colwell, R.R., Brayton, P.R., Grimes, D.J., Roszak, D.B., Huq, S.A. and Palmer, L.M. (1985). Viable but Non-Culturable *Vibrio cholerae* and Related Pathogens in the Environment: Implications for Release of Genetically Engineered Microorganisms. *Nature Biotechnology* **3**, 817-820.

Colwell, R.R., Brayton, P., Herrington, D., Tall, B., Huq, A. and Levine, M.M. (1996). Viable but non-culturable *Vibrio cholerae* O1 revert to a cultivable state in the human intestine. *World Journal of Microbiology and Biotechnology* **12**, 28-31.

Colwell, R.R. (2000). Viable but nonculturable bacteria: a survival strategy. *Journal of Infection and Chemotherapy* **6**, 121–125.

Colwell, R.R. and Grimes, D.J. (2000). Nonculturable microorganisms in the environment. Washington, DC: ASM Press.

Comeau, A.M., Buenaventura, E. and Suttle, C.A. (2005). A persistent, productive, and seasonally dynamic Vibriophage population within Pacific oysters (*Crassostrea gigas*). *Applied and Environmental Microbiology* **71**, 5324-5331.

Comeau, A.M., Chan, A.M. and Suttle, C.A. (2006). Genetic richness of vibriophages isolated in a coastal environment. *Environmental Microbiology* **8**, 1164-1176.

Cook, D.W., Oleary P., Hunsucker, J.C., Sloan, E.M., Bowers, J.C., Blodgett, R.J. and DePaola A. (2002). *Vibrio vulnificus* and *Vibrio parahaemolyticus* in U.S. Retail Shell Oysters: A National Survey from June 1998 to July 1999. *Journal of Food Protection* **65**, 79-87.

Cook, K.L. and Bolster, C.H. (2007). Survival of *Campylobacter jejun*i and *Escherichia coli* in groundwater during prolonged starvation at low temperatures. *Journal of Applied Microbiology* **103**, 573-583.

Crawford, J.A., Kaper, J.B. and DiRita, V.J. (1998). Analysis of ToxR-dependent transcription activation of *ompU*, the gene encoding a major envelope protein in *Vibrio cholerae*. *Molecular Microbiology* **29**, 235-246.

Cunningham, E., O'Byrne, C. and Oliver, J.D. (2009). Effect of weak acids on Listeria monocytogenes survival: Evidence for a viable but nonculturable state in response to low pH. *Food Control* **20**, 1141-1144.

Del Campo, R., Russi, P., Mara, P., Mara, H., Peyrou, M., De León, I.P. and Gaggero, C. (2009). *Xanthomonas axonopodis pv. citri* enters the VBNC state after copper treatment and retains its virulence. *FEMS Microbiology Letters* **298**, 143-148.

Del Mar Lleò, M., Benedetti, D., Tafi, M.C., Signoretto, C. and Canepari, P. (2007). Inhibition of the resuscitation from the viable but non-culturable state in *Enterococcus faecalis*. *Environmental Microbiology* **9**, 2313-2320.

Demain, A.L., Davies, J.E. and Atlas, R.M. (1999). Manual of industrial microbiology and biotechnology, 2 edn. Washington D.C. American Society for Microbiology.

DePaola, A., Hopkins, J.T., Peeler, B.W. and McPhearson, R.M. (1990). Incidence of *Vibrio parahaemolyticus* in U.S. coastal waters and oysters. *Applied and Environmental Microbiology* **56**, 2299-2302.

DePaola, A., Capers, G.M. and Alexander, D. (1994). Densities of *Vibrio vulnificus* in the intestines of fish from the U.S. Gulf Coast. *Applied and Environmental Microbiology* **60**, 984-988.

DePaola, A., McLeroy, S. and McManus, G. (1997). Distribution of *Vibrio vulnificus* phage in oyster tissues and other estuarine habitats. *Applied and Environmental Microbiology* **63**, 2464-2467.

Domingue, G.J., Ghoniem, G.M., Bost, K.L., Fermin, C. and Human, L.G. (1995). Dormant microbes in interstitial cystitis. *Journal of Urology* **153**, 1321-1326.

Dove, S.L., Joung, J.K. and Hochschild, A. (1997). Activation of prokaryotic transcription through arbitrary protein-protein contacts. *Nature* **386**, 627-630.

Dove, S.L. and Hochschild, A. (2004). A bacterial two-hybrid system based on transcription activation. *Methods in Molecular Biology* **261**, 231-246.

Downey, M., Houlsworth, R., Maringele, L. and other authors (2006). A genome-wide screen identifies the evolutionarily conserved KEOPS complex as a telomere regulator. *Cell* **124**, 1155-1168.

Du, M., Chen, J., Zhang, X., Li, A. and Li, Y. (2007). Characterization and resuscitation of viable but nonculturable *Vibrio alginolyticus* VIB283. *Archives of Microbiology* **188**, 283-288.

Edwards, C. (2000). Problems posed by natural environments for monitoring microorganisms. *Molecular Biotechnology* **15**, 211-223-223.

Ehrlich, G.D., Veeh, R., Wang, X., Costerton, J.W., Hayes, J.D., Hu, F.Z., Daigle, B.J., Ehrlich, M.D. and Post, J.C. (2002). Mucosal biofilm formation on middle-ear mucosa in the chinchilla model of *otitis media*. *The Journal of the American Medical Association* **287**, 1710-1715.

Escaich, S. (2008). Antivirulence as a new antibacterial approach for chemotherapy. *Current Opinion in Chemical Biology* **12**, 400-408.

Federighi, M., Tholozan, J.L., Cappelier, J.M., Tissier, J. P. and Jouve., J.L. (1998). Evidence of non-coccoid viable but non-culturable *Campylobacter jejuni* cells in microcosm water by direct viable count, CTC-DAPI double staining, and scanning electron microscopy. *Food Microbiology* **15**, 539-550.

Fields, S. and Song, O. (1989). A novel genetic system to detect protein–protein interactions. *Nature* **340**, 245-246.

Freestone, P.P., Haigh, R.D., Williams, P.H. and Lyte, M. (1999). Stimulation of bacterial growth by heat-stable, norepinephrine-induced autoinducers. *FEMS Microbiology Letters* **172**, 53-60.

Gallagher, L.A., Ramage, E., Jacobs, M. A., Kaul, R., Brittnacher, M. and Manoil, C. (2007). A comprehensive transposon mutant library of *Francisella novicida*, a bioweapon surrogate. *Proceedings of the National Academy of Sciences of the United States of America* **104**, 1009-1014.

García, M. T., Jones, S., Pelaz, C., Millar, R.D. and Abu Kwaik, Y. (2007). *Acanthamoeba polyphaga* resuscitates viable non-culturable *Legionella pneumophila* after disinfection. *Environmental Microbiology* 9, 1267-1277.

Gardel, C. and Mekalanos, J.J. (1994). Regulation of cholera toxin by temperature, pH, and osmolarity. *Methods in Enzymology* **235**, 517-526.

Gauthier, M. (2000). Nonculturable microorganisms in the environment. Washington , D.C: ASM Press.

Ghezzi, J.I. and Steck, T.R. (1999). Induction of the viable but non-culturable condition in *Xanthomonas campestris pv. campestris* in liquid microcosms and sterile soil. *FEMS Microbiology Ecology* **30**, 203-208.

Giaever, G., Chu, A.M., Ni, L. and other authors (2002). Functional profiling of the *Saccharomyces cerevisiae* genome. *Nature* **418**, 387-391.

Glass, J.I., Assad-Garcia, N., Alperovich, N., Yooseph, S., Lewis, M.R., Maruf, M., Hutchison, C.A., Smith, H.O. and Venter, J.C. (2006). Essential genes of a minimal bacterium. *Proceedings of the National Academy of Sciences of the United States of America* **103**, 425-430.

Golemis, E.A., Serebriiskii, I., Finley, R.L., Kolonin, M.G., Gyuris, J. and Brent, R. (2001). Interaction trap/two-hybrid system to identify interacting proteins. Philadelphia: John Wiley and Sons, Inc.

González-Escalona, N., Fey, A., Höfle, M.G., Espejo, R.T. and Guzmán, C.A. (2006). Quantitative reverse transcription polymerase chain reaction analysis of *Vibrio cholerae* cells entering the viable but non-culturable state and starvation in response to cold shock. *Environmental Microbiology* **8**, 658-666.

Gourmelon, M., Cillard, J. and Pommepuy, M. (1994). Visble-light damage to *Escherichia coli* in seawater oxidative stress hypothesis. *Journal of Applied Bacteriology* **77**, 105-112.

Grey, B.E. and Steck, T.R. (2001). The viable but nonculturable state of *Ralstonia solanacearum* may be involved in long-term survival and plant infection. *Applied and Environmental Microbiology* **67**, 3866-3872.

Gupte, A. R., de Rezende, C.L. and Joseph, S.W. (2003). Induction and resuscitation of viable but nonculturable *Salmonella enterica* serovar Typhimurium DT104. *Applied and Environmental Microbiology* **69**, 6669-6675.

Hanahan, D. (1983). Studies on transformation of *Escherichia coli* with plasmids. *Journal of Molecular Biology* **166**, 557-580.

Handford, J. I., Ize, B., Buchanan, G., Butland, G.P., Greenblatt, J., Emili, A. and Palmer, T. (2009). Conserved network of proteins essential for bacterial viability. *Journal of Bacteriology* **191**, 4732-4749.

Heckman, K.L. and Pease, L.R. (2007). Gene splicing and mutagenesis by PCR-driven overlap extension. *Nature Protocols* **2**, 924-932.

Heidelberg, J.F., Heidelberg, K.B. and Colwell, R.R. (2002). Bacteria of the γ-subclass proteobacteria associated with zooplankton in Chesapeake Bay. *Applied and Environmental Microbiology* **68**, 5498-5507.

Hervio-Heath, D., Colwell, R.R., Derrien, A., Robert-Pillot, A., Fournier, J. M. and Pommepuy, M. (2002). Occurrence of pathogenic vibrios in coastal areas of France. *Journal of Applied Microbiology* **92**, 1123-1135.

Holtman, C.K., Pawlyk, A.C., Meadow, N., Roseman, S. and Pettigrew, D.W. (2001). IIA(Glc) allosteric control of *Escherichia coli* glycerol kinase: Binding site cooperative transitions and cation-promoted association by zinc(II). *Biochemistry* **40**, 14302-14308.

Honda, S, Goto, I., Minematsu, I., Ikeda, N., Asano, N., Ishibashi, M., Kinoshita, Y., Nishibuchi, N., Honda, T. and Miwatani, T. (1987). Gastroenteritis due to Kanagawa negative *Vibrio parahaemolyticus*. Lancet 1, 331-332.

Hood, M.A., Guckert, J.B., White, D.C. and Deck, F. (1986). Effect of nutrient deprivation on lipid, carbohydrate, DNA, RNA, and protein levels in *Vibrio cholerae*. *Applied and Environmental Microbiology* **52**, 788-793.

Hunt, A., Rawlins, J.P., Thomaides, H. B. and Errington, J. (2006). Functional analysis of 11 putative essential genes in *Bacillus subtilis*. *Microbiology* **152**, 2895-2907.

Huq, A., Small, E.B., West, P.A., Huq, M., Rahman, I.R. and Colwell, R.R. (1983). Ecological relationships between *Vibrio cholerae* and planktonic crustacean copepods. *Applied and Environmental Microbiology* **45**, 275-283.

International Commission on Microbiological Specifications for Foods (ICMSF). (1996). Edited by: Roberts, T.A., Baird-Parker, A.C. and Tompkin, R.B. Microorganisms in Foods 5. Blackie Academic and Professional, London, United Kingdom. ISBN: 041247350X.

Jeudy, S., Meike, S., Bruno, C., Richard, K. and Chantal, A. (2005). Preliminary crystallographic analysis of the *Escherichia coli* YeaZ protein using the anomalous signal of a gadolinium derivative. *Acta Crystallographica* Section F Structural Biology and Crystallization Communications **F61**, 848-851.

Jiang, S.C. and Paul, J.H. (1994). Seasonal and diel abundance of viruses and occurrence of lysogen bacterinogeny in the marine environment. *Marine Ecology-Progress Series* **104**, 163-172.

Jiang, X.P. and Chai, T.J. (1996). Survival of *Vibrio parahaemolyticus* at low temperatures under starvation conditions and subsequent resuscitation of viable, nonculturable cells. *Applied and Environmental Microbiology* **62**, 1300–1305.

Johnston, M.D. and Brown, M.H. (2002). An investigation into the changed physiological state of Vibrio bacteria as a survival mechanism in response to cold temperatures and studies on their sensitivity to heating and freezing. *Journal of Applied Microbiology* **92**, 1066-1077.

Jones, M.V., Herd, T.M. and Christie, H.J. (1989). Resistance of *Pseudomonas aeruginosa* to amphoteric and quaternary ammonium biocides. *Microbios* **58**, 49-61.

Joseph, S. W., Colwell, R.R. and Kaper, J.B. (1983). *Vibrio parahaemolyticus* and related halophilic vibrios. *Critical Reviews in Microbiology* **10**, 77-123.

Jung, C. R., Park, M. J. and Heo, M. S. (2005). Immunization with major outer membrane protein of *Vibrio vulnificus* elicits protective antibodies in a murine model. *Journal of Microbiology* **43**, 437-442.

Kabsch, W. and Sander, C. (1983). Dictionary of protein secondary structure: Pattern recognition of hydrogen-bonded and geometrical features. *Biopolymers* **22**, 2577-2637.

Kana, B.D., Gordhan, B.G., Downing, K.J. and other authors (2008). The resuscitation-promoting factors of *Mycobacterium tuberculosis* are required for virulence and resuscitation from dormancy but are collectively dispensable for growth *in vitro*. *Molecular Microbiology* **67**, 672-684.

Kaneko, T. and Colwell, R.R. (1974). Distribution of *Vibrio parahaemolyticus* and related organisms in the Atlantic Ocean off South Carolina and Georgia. *Applied Microbiology* **28**, 1009-1017.

Karimova, G., Pidoux, J., Ullmann, A. and Ladant, D. (1998). A bacterial two-hybrid system based on a reconstituted signal transduction pathway. *Proceedings of the National Academy of Science of the United States of America* **95**, 5752-5756.

Karandashova, I., Elanskaya, I., Marin, K., Vinnemeier, J. and Hagemann, M. (2002). Identification of genes essential for growth at high salt concentrations using salt-sensitive mutants of the cyanobacterium *Synechocystis* sp. strain PCC 6803. *Current Microbiology* **44**, 184-188.

Kaspar, C.W. and Tamplin, M.L. (1993). Effects of temperature and salinity on the survival of *Vibrio vulnificus* in seawater and shellfish. *Applied and Environmental Microbiology* **59**, 2425-2429.

Kaufman, G.E., Bej, A.K., Bowers, J. and DePaola, A. (2003). Oyster-to-oyster variability in levels of *Vibrio parahaemolyticus*. *Journal of Food Protection* **66**, 125-129.

Kaysner, C.A. and DePaola, A. (2001). Vibrio. In: Bacteriological Analytical Manual. 8th Edition. Chapter 9. Arlington, VA: U.S. Food and Drug Administration.

Kell, D.B., Kaprelyants, A.S., Weichart, D.H., Harwood, C.R. and Barer, M.R. (1998). Viability and activity in readily culturable bacteria: a review and discussion of the practical issues. *Antonie van Leeuwenhoek* **73**, 169-187.

Kelly, M.T. (1982). Effect of temperature and salinity on *Vibrio (Beneckea) vulnificus* occurrence in a Gulf Coast environment. *Applied and Environmental Microbiology* **44**, 820-824.

Kelly, M.T. and Stroh, E.M. (1988). Temporal relationship of *Vibrio parahaemolyticus* in patients and the environment. *Journal of Clinical Microbiology* **26**, 1754-1756.

Kisseleva-Romanova, E., Lopreiato, R., Baudin-Baillieu, A., Rousselle, J.C., Ilan, L., Hofmann, K., Namane, A., Mann, C. and Libri, D. (2006). Yeast homolog of a cancer-testis antigen defines a new transcription complex. *EMBO Journal* **25**, 3576-3585.

Knuth, K., Niesalla, H., Hueck, C.J. and Fuchs, T.M. (2004). Large-scale identification of essential *Salmonella* genes by trapping lethal insertions. *Molecular Microbiology* **51**, 1729-1744.

Kobayashi, K., Ehrlich, S. D., Albertini, A. and other authors (2003). Essential *Bacillus subtilis* genes. *Proceedings of the National Academy of Sciences of the United States of America* **100**, 4678-4683.

Koga, T., Toyoshima, S. and Kawata, T. (1982). Morphological varieties and host ranges of *Vibrio parahaemolyticus* bacteriophages isolated from seawater. *Applied and Environmental Microbiology* **44**, 466-470.

Lagarrigue, E., Maciver, S. K., Fattoum, A., Benyamin, Y. and Roustan, C. (2003). Co-operation of domain-binding and calcium-binding sites in the activation of gelsolin. European Journal of Biochemistry 270, 2236-2243.

Lee, J.V., Bashford, D.J., Donovan, T.J., Furniss, A.L. and West, P.A. (1982). The incidence of *Vibrio cholerae* in water, animals and birds in Kent, England. *The Journal of Applied Bacteriology* **52**, 281-291.

Lerner, C.G., Hajduk, P.J., Wagner, R. and other authors (2007). From bacterial genomes to novel antibacterial agents: discovery, characterization, and antibacterial activity of compounds that bind to HI0065 (YjeE) from *Haemophilus influenzae*. *Chemical Biology and Drug Design* **69**, 395-404.

Li, C.C., Crawford, J.A., DiRita, V.J. and Kaper, J.B. (2000). Molecular cloning and transcriptional regulation of *ompT*, a ToxR-repressed gene in *Vibrio cholerae*. *Molecular Microbiology* **35**, 189-203.

Liberati, N.T., Urbach, J.M., Miyata, S., Lee, D.G., Drenkard, E., Wu, G., Villanueva, J., Wei, T. and Ausubel, F.M. (2006). An ordered, nonredundant library of *Pseudomonas aeruginosa* strain PA14 transposon insertion mutants. *Proceedings of the National Academy of Sciences of the United States of America* **103**, 2833-2838.

Linder, K. and Oliver, J.D. (1989). Membrane fatty acid and virulence changes in the viable but nonculturable state of *Vibrio vulnificus*. *Applied and Environmental Microbiology* **55**, 2837-2842.

Livak, K.J. and Schmittgen, T.D. (2001). Analysis of relative gene expression data using real-time quantitative PCR and the 2-δδCT Method. *Methods* **25**, 402-408.

Maalej, S., Denis, M. and Dukan, S. (2004). Temperature and growth-phase effects on *Aeromonas hydrophila* survival in natural seawater microcosms: role of protein synthesis and nucleic acid content on viable but temporarily nonculturable response. *Microbiology* **150**, 181-187.

Madigan TL, L. K., Pointon AM, Thomas CJ (2007). A supply-chain assessment of marine Vibrios in Pacific oysters in South Australia: prevalence, quantification and public health risk. Project Report SIDF 2005/401. Fisheries Research and Development Corporation, Australia. ISBN: 978-0-7590-1399-5.

Magariños, B., Romalde, J.L., Barja, J.L. and Toranzo, A.E. (1994). Evidence of a dormant but infective state of the fish pathogen *Pasteurella piscicida* in seawater and sediment. *Applied and Environmental Microbiology* **60**, 180-186.

Makino, K., Oshima, K., Kurokawa, K. and other authors (2003). Genome sequence of *Vibrio parahaemolyticus*: a pathogenic mechanism distinct from that of *Vibrio cholerae*. *Lancet* **361**, 743-749.

Mårdén, P., Tunlid, A., Malmcrona-Friberg, K., Odham, G. and Kjelleberg, S. (1985). Physiological and morphological changes during short term starvation of marine bacterial isolates. *Archives of Microbiology* **142**, 326-332.

Mason, D.J., Power, E.G., Talsania, H., Phillips, I. and Gant, V.A. (1995). Antibacterial action of ciprofloxacin. *Antimicrobial Agents and Chemotherapy* **39**, 2752-2758.

Masuda, Y., Tajima, K. and Ezura, Y. (2004). Resuscitation of *Tenacibaculum* sp., the causative bacterium of spotting disease of sea urchin *Strongylocentroutus intermedius*, from the viable but non-culturable state. *Fisheries Science* **70**, 277-284.

McCarthy, S.A., DePaola, A., Cook, D.W., Kaysner, C.A. and Hill, W.E. (1999). Evaluation of alkaline phosphatase- and digoxigenin-labelled probes for detection of the thermolabile hemolysin (*tlh*) gene of *Vibrio parahaemolyticus*. *Letters in Applied Microbiology* **28**, 66-70.

McCutcheon, J.P. and Moran, N.A. (2007). Parallel genomic evolution and metabolic interdependence in an ancient symbiosis. *Proceedings of the National Academy of Sciences of the United States of America* **104**, 19392-19397.

McDougald, D., Rice, S.A., Weichart, D. and Kjelleberg, S. (1998). Nonculturability: adaptation or debilitation? *FEMS Microbiology Ecology* **25**, 1-9.

McGovern, V.P. and Oliver., J.D. (1995). Induction of cold responsive proteins in *Vibrio vulnificus*. *Journal of Bacteriology* **177**, 4131-4133.

McLaughlin, J. (1995). Manual of clinical microbiology, 6th edn. Washington D.C.: American society for microbiology.

McLaughlin, J.B., DePaola, A., Bopp, C.A. and other authors (2005). Outbreak of *Vibrio parahaemolyticus* gastroenteritis associated with Alaskan oysters. *The New England Journal of Medicine* **353**, 1463-1470.

Menard, R., Sansonetti, P. J. and Parsot, C. (1993). Nonpolar mutagenesis of the ipa genes defines IpaB, IpaC, and IpaD as effectors of *Shigella flexneri* entry into epithelial cells. *Journal of Bacteriology* **175**, 5899-5906.

Miller, J.H. (1972). Experiments in molecular genetics. Cold Spring Harbor Laboratory Press. New York.

Miller, J.H. (1992). A short course in bacterial genetics : a laboratory manual and handbook for *Escherichia coli* and related bacteria. Cold Spring Harbor Laboratory Press. New York.

Miller, V.L., Taylor, R.K. and Mekalanos, J.J. (1987). Cholera toxin transcriptional activator ToxR is a transmembrane DNA binding protein. *Cell* **48**, 271-279.

Miller, V.L. and Mekalanos, J.J. (1988). A novel suicide vector and its use in construction of insertion mutations: osmoregulation of outer membrane proteins and virulence determinants in *Vibrio cholerae* requires *toxR*. *Journal of Bacteriology* **170**, 2575-2583.

Minagawa, S., Ogasawara, H., Kato, A., Yamamoto, K., Eguchi, Y., Oshima, T., Mori, H., Ishihama, A. and Utsumi, R. (2003). Identification and molecular characterization of the Mg^{2+} stimulon of *Escherichia coli*. *Journal of Bacteriology* **185**, 3696-3702.

Miyasaka, J., Yahiro, S., Arahira, Y., Tokunaga, H., Katsuki, K. and Hara-Kudo, Y. (2006). Isolation of *Vibrio parahaemolyticus* and *Vibrio vulnificus* from wild aquatic birds in Japan. *Epidemiology and Infection* **134**, 780-785.

Morton, D. and Oliver., J.D. (1994). Induction of carbon starvation proteins in *Vibrio vulnificus*. *Applied and Environmental Microbiology* **60**, 3653-3659.

Motes, M.L., DePaola, A., Cook, D.W., Veazey, J.E., Hunsucker, J.C., Garthright, W.E., Blodgett, R.J. and Chirtel, S.J. (1998). Influence of Water Temperature and Salinity on *Vibrio vulnificus* in Northern Gulf and Atlantic Coast Oysters (*Crassostrea virginica*). *Applied and Environmental Microbiology* **64**, 1459-1465.

Msadek, T. (2009). Grasping at Shadows: Revealing the Elusive Nature of Essential Genes. *Journal of Bacteriology* **191**, 4701-4704.

Mukamolova, G.V., Kaprelyants, A.S., Young, D.I., Young, M. and Kell, D.B. (1998). A bacterial cytokine. *Proceedings of the National Academy of Sciences of the United States of America* **95**, 8916-8921.

Mukamolova, G.V., Turapov, O.A., Young, D.I., Kaprelyants, A.S., Kell, D.B. and Young, M. (2002). A family of autocrine growth factors in *Mycobacterium tuberculosis*. *Molecular Microbiology* **46**, 623-635.

Mulvey, M.A., Schilling, J.D. and Hultgren, S.J. (2001). Establishment of a persistent *Escherichia coli* reservoir during the acute phase of a bladder infection. *Infection and Immunity* **69**, 4572-4579.

Nair, G.B., Ramamurthy, T., Bhattacharya, S.K., Dutta, B., Takeda, Y. and Sack, D.A. (2007). Global dissemination of *Vibrio parahaemolyticus* serotype O3:K6 and its serovariants. *Clinical Microbiology Reviews* **20**, 39-48.

Nakabachi, A., Yamashita, A., Toh, H., Ishikawa, H., Dunbar, H. E., Moran, N. A. and Hattori, M. (2006). The 160-kilobase genome of the bacterial endosymbiont *Carsonella*. *Science* **314**, 267.

Nesin, M., Lupski, J. R., Svec, P. and Godson, G.N. (1987). Possible new genes as revealed by molecular analysis of a 5-kb *Escherichia coli* chromosomal region 5' to the *rpsU-dnaG-rpoD* macromolecular-synthesis operon. *Gene* **51**, 149-161.

Ng, A.P., Howe Fong, J., Sijin Nin, D., Hirpara, J.L., Asou, N., Chen, C.S., Pervaiz, S. and Khan, M. (2006). Cleavage of Misfolded Nuclear Receptor Corepressor Confers Resistance to Unfolded Protein Response–Induced Apoptosis. *Cancer Research* **66**, 9903-9912.

Nichols, C.E., Johnson, C., Lockyer, M., Charles, I.G., Lamb, H.K., Hawkins, A.R. and Stammers, D.K. (2006). Structural characterization of *Salmonella typhimurium* YeaZ, an M22 O-sialoglycoprotein endopeptidase homolog. *Proteins: Structure, Function, and Bioinformatics* **64**, 111-123.

Nilsson, L., Oliver, J.D. and Kjelleberg, S. (1991). Resuscitation of *Vibrio vulnificus* from the viable but nonculturable state. *Journal of Bacteriology* **173**, 5054-5059.

Nishibuchi, M., Taniguchi, T., Misawa, T., Khaeomanee-Iam, V., Honda, T. and Miwatani, T. (1989). Cloning and nucleotide sequence of the gene (*trh*) encoding the hemolysin related to the thermostable direct hemolysin of *Vibrio parahaemolyticus*. *Infection and Immunity* **57**, 2691-2697.

Nishibuchi, M. and Kaper, J.B. (1995). Thermostable direct hemolysin gene of *Vibrio parahaemolyticus*: a virulence gene acquired by a marine bacterium. *Infection and Immunity* **63**, 2093-2099.

Njoroge, J. and Sperandio, V. (2009). Jamming bacterial communication: new approaches for the treatment of infectious diseases. *EMBO Molecular Medicine* **1**, 201-210.

Nolan, T., Hands, R. E. and Bustin, S. A. (2006). Quantification of mRNA using real-time RT-PCR. *Nature Protocols* **1**, 1559-1582.

Nyström, T. (2001). Not quite dead enough: on bacterial life, culturability, senescence, and death. *Archives of Microbiology* **176**, 159-164.

Nyström, T. (2005). Bacterial senescence, programmed death, and premeditated sterility. *American Society for Microbiology News* **71**, 363-369.

O'Neill, K.R., Jones, S.H. and Grimes, D.J. (1992). Seasonal incidence of *Vibrio vulnificus* in the Great Bay estuary of New Hampshire and Maine. *Applied and Environmental Microbiology* **58**, 3257-3262.

Ogierman, M.A., Fallarino, A., Riess, T., Williams, S.G., Attridge, S.R. and Manning, P.A. (1997). Characterization of the *Vibrio cholerae* El Tor lipase operon *lipAB* and a protease gene downstream of the *hly* region. *Journal of Bacteriology* **179**, 7072-7080.

Oliver, J.D. (2000). Nonculturable microorganisms in the environment. Washington , D.C: ASM Press.

Oliver, J.D. (2005). Viable but nonculturable bacteria in food environments. Food-Borne Pathogens: Microbiology and Molecular Biology. Norfolk, UK: Caister Academic Press.

Oliver, J.D. and Colwell, R. R. (1973). Extractable lipids of gram-negative marine bacteria fatty acid composition. *International Journal of Systematic Bacteriology* **23**, 442-458.

Oliver, J.D., Warner, R.A. and Cleland, D.R. (1982). Distribution and ecology of *Vibrio vulnificus* and other lactose-fermenting marine vibrios in coastal waters of the southeastern United States. *Applied and Environmental Microbiology* **44**, 1404-1414.

Oliver, J.D. and Wanucha, D. (1989). Survial of *Vibrio vulnificus* at Reduced Temperatures and Elevated Nutrient. *Journal of Food Safety* **10**, 79-86.

Oliver, J.D., Nilsson, L. and Kjelleberg, S. (1991). Formation of nonculturable *Vibrio vulnificus* cells and its relationship to the starvation state. *Applied and Environmental Microbiology* **57**, 2640–2644.

Oliver, J.D. and Bockian, R. (1995). In vivo resuscitation, and virulence towards mice, of viable but nonculturable cells of *Vibrio vulnificus*. *Applied and Environmental Microbiology* **61**, 2620-2623.

Oliver, J.D., Hite, F., McDougald, D., Andon, N.L. and Simpson, L.M. (1995). Entry into, and resuscitation from, the viable but nonculturable state by *Vibrio vulnificus* in an estuarine environment. *Applied and Environmental Microbiology* **61**, 2624-2630.

Oliver, J.D. (2005b). The Viable but Nonculturable State in Bacteria. *Journal of Microbiology* **43**, 93-100.

Oliver, J.D. (2010). Recent findings on the viable but nonculturable state in pathogenic bacteria. *FEMS Microbiology Reviews* **34**, 415-425.

Ordax, M., Biosca, E.G., Wimalajeewa, S.C., López, M.M. and Marco-Noales, E. (2009). Survival of *Erwinia amylovora* in mature apple fruit calyces through the viable but nonculturable (VBNC) state. *Journal of Applied Microbiology* **107**, 106-116.

Pai, S.R., Actor, J.K., Sepulveda, E., Hunter, R.L. and Jagannath, C. (2000). Identification of viable and non-viable *Mycobacterium tuberculosis* in mouse organs by directed RT-PCR for antigen 85B mRNA. *Microbial Pathogenesis* **28**, 335-342.

Panutdaporn, N., Kawamoto, K., Asakura, H. and Makino, S.I. (2006). Resuscitation of the viable but non-culturable state of *Salmonella enterica* serovar Oranienburg by recombinant resuscitation-promoting factor derived from *Salmonella* Typhimurium strain LT2. *International Journal of Food Microbiology* **106**, 241-247.

Pelon, W., Siebeling, R.J., Simonson, J. and Luftig, R.B. (1995). Isolation of bacteriophage infectious for *Vibrio vulnificus*. *Current Microbiology* **30**, 331-336-336.

Pfeffer, C.S., Hite, M.F. and Oliver, J.D. (2003). Ecology of *Vibrio vulnificus* in estuarine waters of eastern North Carolina. *Applied and Environmental Microbiology* **69**, 3526-3531.

Pommepuy, M., Butin, M., Derrien, A., Gourmelon, M., Colwell, R.R. and Cormier, M. (1996). Retention of enteropathogenicity by viable but nonculturable *Escherichia coli* exposed to seawater and sunlight. *Applied and Environmental Microbiology* **62**, 4621-4626.

Porter, J., Edwards C. and Pickup R.W. (1995). Rapid assessment of physiological status in *Escherichia coli* using fluorescent probe. *Journal of Applied Bacteriology* **79**, 399-408.

Potasman, I., Paz, A. and Odeh, M. (2002). Infectious outbreaks associated with bivalve shellfish consumption: a worldwide perspective. *Clinical Infectious Diseases* **35**, 921-928.

Rahman, I., Shahamat, M., Kirchman, P. A., Russek-Cohen, E. and Colwell, R.R. (1994). Methionine uptake and cytopathogenicity of viable but nonculturable *Shigella dysenteriae* Type 1. *Applied and Environmental Microbiology* **60**, 3573-3578.

Rahman, I., Shahamat, M., Chowdhury, M.A.R. and Colwell, R.R. (1996). Potential virulence of viable but nonculturable *Shigella dysenteriae* Type 1. *Applied and Environmental Microbiology* **62**, 115–120.

Rajagopala, S., Yamamoto, N., Zweifel, A. and other authors (2010). The *Escherichia coli* K-12 ORFeome: a resource for comparative molecular microbiology. *BMC Genomics* **11**, 470.

Rasko, D.A. and Sperandio, V. (2010). Anti-virulence strategies to combat bacteria-mediated disease. *Nature Reviews Drug Discovery* **9**, 117-128.

Reading, N.C., Rasko, D. A., Torres, A.G. and Sperandio, V. (2009). The two-component system QseEF and the membrane protein QseG link adrenergic and stress sensing to bacterial pathogenesis. *Proceedings of the National Academy of Sciences of the United States of America* **106**, 5889-5894.

Reissbrodt, R., Rienaecker, I., Romanova, J. A., Freestone, P.P.E., Haigh, R.D., Lyte, A., Tschape, H. and Williams, P.H. (2002). Resuscitation of *Salmonella enterica* serovar Typhimurium and enterohemorrhagic *Escherichia coli* from the viable but nonculturable state by heat-stable enterobacterial autoinducer. *Applied and Environmental Microbiology* **68**, 4788-4794.

Reynolds, E.S. (1963). The use of lead citrate at high pH as an electron-opaque stain in electron microscopy. *Journal of Cell Biology* **17**, 208-212.

Rice, S.A., McDougald, D. and Kjelleberg, S. (2000). *Vibrio vulnificus* : a physiological and genetic approach to the viable but nonculturable response. Journal of Infection and Chemotherapy 6, 115-120.

Rivers, B. and Steck, T.R. (2001). Viable but nonculturable uropathogenic bacteria are present in the mouse urinary tract following urinary tract infection and antibiotic therapy. *Urological Research* **29**, 60-66.

Rowan, N.J. (2004). Viable but non-culturable forms of food and waterborne bacteria: *Quo Vadis*? *Trends in Food Science and Technology* **15**, 462-467.

Ryan, R.P. and Dow, J.M. (2011). Communication with a growing family: diffusible signal factor (DSF) signaling in bacteria. *Trends in Microbiology* **19**, 145-152.

Sakazaki R., Tamura, K., Kato T, Obara Y, Yamai S. (1968). Studies on the enteropathogenic, facultatively halophilic bacterium, *Vibrio parahaemolyticus*. 3. Enteropathogenicity. *Japanese Journal of Medical Science and Biology* **21**, 325-331.

Sardessai, Y.N. (2005). Viable but non-culturable bacteria: their impact on public health. *Current Science* **89**, 1650.

Sarkar, B.L., Kumar, R., De, S. P. and Pal, S.C. (1987). Hemolytic activity of and lethal toxin production by environmental strains of *Vibrio parahaemolyticus*. *Applied and Environmental Microbiology* **53**, 2696-2698.

Shinoda, S., Matsuoka, H., Tsuchie, T., Miyoshi, S.I., Yamamoto, S., Taniguchi, H. and Mizuguchi, Y. (1991). Purification and characterization of a lecithin-dependent haemolysin from *Escherichia coli* transformed by a *Vibrio parahaemolyticus* gene. *Journal of General Microbiology* **137**, 2705-2711.

Shleeva, M.O., Bagramyan, K., Telkov, M.V., Mukamolova, G.V., Young, M., Kell, D.B. and Kaprelyants, A.S. (2002). Formation and resuscitation of "non-culturable" cells of *Rhodococcus rhodochrous* and *Mycobacterium tuberculosis* in prolonged stationary phase. *Microbiology* **148**, 1581–1591.

Shleeva, M.O., Mukamolova, G.V., Young, M., Williams, H.D. and Kaprelyants, A.S. (2004). Formation of "Non- culturable" Cells of *Mycobacterium smegmatis* in stationary phase in response to growth under suboptimal conditions and their Rpf-mediated resuscitation. *Microbiology* **150**, 1687-1697.

Simonson, J. and Siebeling, R.J. (1986). Rapid serological identification of *Vibrio vulnificus* by anti-H coagglutination. *Applied and Environmental Microbiology* **52**, 1299-1304.

Sinton, L. (2006). Viable but non-culturable' bacteria – menace or myth? *New Zealand Water and Wastes Association Journal* **143**, 31-38.

Sperandio, V., Giron, J. A., Silveira, W.D. and Kaper, J.B. (1995). The OmpU outer membrane protein, a potential adherence factor of *Vibrio cholerae*. *Infection and Immunity* **63**, 4433-4438.

Sperandio, V., Torres, A.G., Jarvis, B., Nataro, J.P. and Kaper, J.B. (2003). Bacteria-host communication: The language of hormones. *Proceedings of the National Academy of Sciences of the United States of America* **100**, 8951-8956.

Steinert, M., Emody, L., Amann, R. and Hacker, J. (1997). Resuscitation of viable but nonculturable *Legionella pneumophila* Philadelphia JR32 by *Acanthamoeba castellanii*. *Applied and Environmental Microbiology* **63**, 2047-2053.

Sun, F., Chen, J., Zhong, L., Zhang, X., Wang, R., Guo, Q. and Dong, Y. (2008). Characterization and virulence retention of viable but nonculturable *Vibrio harveyi*. *FEMS Microbiology Ecology* **64**, 37-44.

Sussman, M., Loya, Y., Fine, M. and Rosenberg, E. (2003). The marine fireworm *Hermodice carunculata* is a winter reservoir and spring-summer vector for the coral-bleaching pathogen *Vibrio shiloi. Environmental Microbiology* **5**, 250-255.

Takeda, Y. (1983). Thermostable direct hemolysin of *Vibrio parahaemolyticus*. *Pharmacology and Therapeutics* **19**, 123-146.

Tamplin, M., Rodrick, G.E., Blake, N.J. and Cuba, T. (1982). Isolation and characterization of *Vibrio vulnificus* from two Florida estuaries. *Applied and Environmental Microbiology* **44**, 1466-1470.

Taniguchi, H., Ohta, H., Ogawa, M. and Mizuguchi, Y. (1985). Cloning and expression in *Escherichia coli* of *Vibrio parahaemolyticus* thermostable direct hemolysin and thermolabile hemolysin genes. *The Journal of Bacteriology* **162**, 510-515.

Taniguchi, H., Hirano, H., Kubomura, S., Higashi, K. and Mizuguchi, Y. (1986). Comparison of the nucleotide sequences of the genes for the thermostable direct hemolysin and the thermolabile hemolysin from *Vibrio parahaemolyticus*. *Microbial Pathogenesis* **1**, 425-432.

Taniguchi, H., Kubomura, S., Hirano, H., Mizue, K., Ogawa, M. and Mizuguchi, Y. (1990). Cloning and characterization of a gene encoding a new thermostable hemolysin from *Vibrio parahaemolyticus*. *FEMS Microbiology Letters* **67**, 339-345.

Tantillo, G.M., Fontanarosa, M., Di Pinto, A. and Musti, M. (2004). Updated perspectives on emerging vibrios associated with human infections. *Letters in Applied Microbiology* **39**, 117-126.

Tepedino, A. (1982). *Vibrio parahaemolyticus* in Long Island oysters. *Journal of Food Protection* **45**, 150-151.

Teplyakov, A., Obmolova, G., Tordova, M., Thanki, N., Bonander, N., Eisenstein, E., Howard, A.J. and Gilliland, G.L. (2002). Crystal structure of the YjeE protein from *Haemophilus influenzae*: A putative Atpase involved in cell wall synthesis. *Proteins: Structure, Function, and Bioinformatics* **48**, 220-226.

Thanassi, J.A., Hartman□Neumann, S.L., Dougherty, T.J., Dougherty, B.A. and Pucci, M.J. (2002). Identification of 113 conserved essential genes using a high□throughput gene disruption system in *Streptococcus pneumoniae. Nucleic Acids Research* **30**, 3152-3162.

Tomer, I., Ehud, B. and Eugene, R. (2001). Growth, differentiation and death of *Vibrio shiloi* in coral tissue as a function of seawater temperature. *Aquatic Microbial Ecology* **24**, 1-8.

Valérie, B., Michel, F., Eric, D., Florence, J. and Jean-Michel, C. (2002). Environmental and physico-chemical factors induce VBNC state in *Listeria monocytogenes*. *Veterinary Research* **33**, 359-370.

Vanoy, R.W., Tamplin, M.L. and Schwarz, J.R. (1992). Ecology of *Vibrio vulnificus* in Galveston Bay oysters, suspended particulate matter, sediment and seawater: detection

by monoclonal antibody - immunoassay - most probable number procedures. *Journal of Industrial Microbiology and Biotechnology* **9**, 219-223-223.

Wang, R.F. and Kushner, S.R. (1991). Construction of versatile low-copy-number vectors for cloning, sequencing and gene expression in *Escherichia coli*. *Gene* **100**, 195-199.

Watkins, W.D. and Cabelli, V.J. (1985). Effect of fecal pollution on *Vibrio parahaemolyticus* densities in an estuarine environment. *Applied and Environmental Microbiology* **49**, 1307-1313.

Weichart, D., Oliver, J.D. and Kjelleberg, S. (1992). Low temperature induced non-culturability and killing of *Vibrio vulnificus*. *FEMS Microbiology Letters* **100**, 205-210.

Weichart, D. and Kjelleberg, S. (1996). Stress resistance and recovery potential of culturable and viable but nonculturable cells of *Vibrio vulnificus*. *Microbiology* **142**, 845–853.

Whitaker, W.B., Parent, M.A., Naughton, L. M., Richards, G.P., Blumerman, S.L. and Boyd, E.F. (2010). Modulation of responses of *Vibrio parahaemolyticus* O3:K6 to pH and temperature stresses by growth at different salt concentrations. *Applied and Environmental Microbiology* **76**, 4720-4729.

Whitesides, M.D. and Oliver, J.D. (1997). Resuscitation of *Vibrio vulnificus* from the Viable but Nonculturable State. *Applied and Environmental Microbiology* **63**, 1002-1005.

Wolf, P.W. and Oliver, J.D. (1992). Temperature effects on the viable but non-culturable state of *Vibrio vulnificus*. *FEMS Microbiology Ecology* **101**, 33-39.

Wong, H.C., Peng, P.Y., Han, J.M., Chang, C.Y. and Lan, S.L. (1998). Effect of mild acid treatment on the survival, enteropathogenicity, and protein production in *Vibrio parahaemolyticus*. *Infection and Immunity* **66**, 3066-3071.

Wong, H.C. and Liu, S.H. (2008). Characterization of the low-salinity stress in *Vibrio vulnificus*. *Journal of Food Protection* **71**, 416-419.

Wong, H.C. and Wang, P. (2004). Induction of viable but nonculturable state in *Vibrio parahaemolyticus* and its susceptibility to environmental stresses. *Journal of Applied Microbiology* **96**, 359-366.

Wong, H.C., Shen, C.T., Chang, C.N., Lee, Y.S. and Oliver, J.D. (2004). Biochemical and virulence characterization of viable but nonculturable cells of *Vibrio parahaemolyticus*. *Journal of Food Protection* **67**, 2430-2435.

Wright, A.C., Hill, R.T., Johnson, J.A., Roghman, M.C., Colwell, R.R. and Morris, J.G., Jr. (1996). Distribution of *Vibrio vulnificus* in the Chesapeake Bay. *Applied and Environmental Microbiology* **62**, 717-724.

Xu, M., Iida, T., Yamamoto, K., Takarada, Y., Miwatani, T. and Honda, T. (1994a). Demonstration and characterization of simultaneous production of a thermostable direct hemolysin (TDH/I) and a TDH-related hemolysin (TRHx) by a clinically isolated *Vibrio parahaemolyticus* strain, TH3766. *Infection and Immunity* **62**, 166-171.

Xu, M., Yamamoto, K., Honda, T. and Ming, X. (1994b). Construction and characterization of an isogenic mutant of *Vibrio parahaemolyticus* having a deletion in the thermostable direct hemolysin-related hemolysin gene (*trh*). *Journal of Bacteriology* **176**, 4757-4760.

Xu, Q., McMullan, D., Jaroszewski, L. and other authors (2010). Structure of an essential bacterial protein YeaZ (TM0874) from *Thermotoga maritima* at 2.5A° resolution. *Acta Crystallographica* **F66**, 1230-1236.

Yamamoto, H. (2000). Viable but nonculturable state as a general phenomenon of non-spore-forming bacteria, and its modeling. *Journal of Infection and Chemotherapy* **6**, 112-114.

Yaron, S. and Matthews, K.R. (2002). A reverse transcriptase-polymerase chain reaction assay for detection of viable *Escherichia coli* O157:H7: investigation of specific target genes. *Journal of Applied Microbiology* **92**, 633-640.

Zalacain, M., Biswas, S., Ingraham, K.A. and other authors (2003). A global approach to identify novel broad-spectrum antibacterial targets among proteins of unknown function. *Journal of Molecular Microbiology and Biotechnology* **6**, 109-126.

Zheng, L., Yang, J., Landwehr, C., Fan, F. and Ji, Y. (2005). Identification of an essential glycoprotease in *Staphylococcus aureus. FEMS Microbiology Letters* **245**, 279-285.

Zuther, E., Schubert, H. and Hagemann, M. (1998). Mutation of a gene encoding a putative glycoprotease leads to reduced salt tolerance, altered pigmentation, and cyanophycin accumulation in the cyanobacterium *Synechocystis* sp. strain PCC 6803. *Journal of Bacteriology* **180**, 1715-1722.

Appendix A

Chemicals used in this study.

Chemical	Company
Acetic acid	BDH-AnalaR
Agarose	Progen
Ampicillin	Sigma
Bacto-agar	Difco
Bacto-tryptone	Difco
Bromophenol blue	Sigma
Coomassie brilliant blue	Sigma
Ethanol	BDH-AnalaR
Fluorescein-5-isothiocyanate (FITC)	Sigma
Glycerol	Sigma
Isopropyl-β-D-thiogalactopyranoside (IPTG)	Sigma
Methanol	BDH-AnalaR
NaCl	Sigma
NaOH	Sigma
Propan-2-ol (Isopropanol)	BDH-AnalaR
Restriction endonucleases	New England Biolabs
Skim milk powder	Diploma
Sodium dodecyl sulfate (SDS)	Sigma
T4 DNA Ligase	New England Biolabs
TEMED	Sigma
Triton X-100	Sigma
Tween-20	Sigma
X-Gal	Progen
Yeast extract	Difco
β-mercaptoethanol	Sigma

Appendix B

Buffers and Reagents used in this study.

Buffer	Composition
Agarose gel 1%	Agarose gel 1% (w/v) DNA grad agarose (Quantum Scientific) in 10× TAE buffer
Blocking solution	0.5% (w/v) skim milk in TBS
Bradford reagent	0.01% (w/v) Coomassie brilliant blue G-250, 5% (v/v) methanol, 8.5% (w/v) H_3PO_4
Coomassie blue	0.1% (w/v) Coomassie brilliant blue G-250, 30% (v/v) methanol, 10% (v/v) acetic acid
DNA loading dye	0.1% (w/v) Bromophenol blue, 20% (v/v) glycerol, 0.1 mg/ml
GTS buffer	144 $g.L^{-1}$ Tris, 1.44 $g.L^{-1}$ Glycine, 20% (v/v) Methanol
Co-IP elution buffer	50 mM Glycine pH 2.8
Protein destain solution	10% (v/v) methanol, 5% (v/v) acetic acid
PBS	8% (w/v) NaCl, 0.02% (w/v) KCl, 0.02% (w/v) KH_2PO_4, 0.115% (w/v) Na_2HPO_4
PBST	8% (w/v) NaCl, 0.02% (w/v) KCl, 0.02% (w/v) KH_2PO_4, 0.115% (w/v) Na_2HPO_4, 0.1% (v/v) Tween 20
Purification washing buffer	100mM Tris, 10mM imidazole (pH 7.5)
Purification elution buffer	100mM Tris, 50mM imidazole (pH 7.5)
SDS-PAGE loading buffer	0.05 M Tris (pH 6.8), 4% (w/v) SDS, 12% (v/v) glycerol, 2% (v/v) β-mercaptoethanol, 0.01% (w/v) Coomassie brilliant blue
TAE	40 mM Tris, 20 mM NaAc, 10 mM EDTA (pH 8.2)
TBS	20 mM Tris pH 7.4, 150 mM NaCl

TTBS	TBS, 0.1% (v/v) Tween 20
Western Blocking solution	TBS, 0.1% (v/v) Tween-20, 4% (w/v) skim milk
Western transfer solution	190 mM glycine, 25 mM Tris and 15% (v/v) methanol
X-Gal	20 $mg.mL^{-1}$ in DMF, stored at -20°C
Z buffer	6.5 mM $Na_2HPO_47H_2O$, 4 mM NaH_2PO4H_2O, 10 mM KCl, 0.75 mM $MgSO_47H_2O$, 0.27% (v/v) β-mercaptoethanol (pH7)

Appendix C

2-log DNA ladder used for agarose gel electrophoresis of DNA fragments.

Fragment	Size (bp)
1	10000
2	8000
3	6000
4	5000
5	4000
6	3000
7	2000
8	1500
9	1200
10	1000
11	900
12	800
13	700
14	600
15	500
16	400
17	300
18	200
19	100

Appendix D

Composition of SDS PAGE separating and stacking gels.

Components	Separating Gel 12.5%	Stacking Gel 4%
0.5M Tris-HCl	-	0.5 mL
1.5M Tris-HCl	2 mL	-
10% (w/v) SDS	80 µL	40 µL
Acrylamide/Bis (30% stock)	3.2 mL	0.68 mL
10% (w/v) ammonium persulfate	80 µL	40 µL
TEMED	3.2 µL	4 µL
Distilled water	2.64 mL	2.72 mL
Total Monomer	2	2

Appendix E

Protein markers used for SDS PAGE analysis.

Protein	Source	Molecular Weight(kDa)
MBP-β-galactosidase	*E. coli*	175
MBP-paramyos	*E. coli*	80
MBP-CBD	*E. coli*	58
CBD-*Mxe* Intein-2CBD	*E. coli*	46
CBD-*Mxe* Intein	*E. coli*	30
CBD-BmFKBP13	*E. coli*	25
Lysozyme	Chicken egg white	17
Aprotinin	Bovine lung	7

Appendix F

Mean $\ln(N/N_0)$ values (3 replicates) at 2.5% NaCl for an initial viable number of $N_0 = 1 \times 10^9$ (cells.mL^{-1}).

Days at 4°C	$\ln(N/N_0)$
0	0
4	0.081468
8	0.919034
12	-9.01906
16	-10.4555
20	-10.9845
24	-12.3088
28	-14.2565
32	-15.7999

Mean $\ln(N/N_0)$ values (3 replicates) at 2.5%NaCl for an initial viable number of $N_0 = 1 \times 10^7$ (cells.mL^{-1}).

day	$\ln(N/N_0)$
0	0
4	-4.26325
8	-5.36186
12	-7.52929
16	-10.2117

Mean ln(N/N_0) values (3 replicates) at 2.5%NaCl for an initial viable number of $N_0 = 1 \times 10^5$ (cells.mL^{-1}).

day	ln(N/N_0)
0	0
4	-4.78977

Summary fit of ln(N/N_0) versus days at4°C in 2.5%NaCl for each of initial viable cell numbers of $N_0 = 1 \times 10^9$, 1×10^7 and 1×10^5 (cells.mL^{-1}).

	Initial viable numbers N_0 (cells.mL^{-1})			
	1×10^9	1×10^7	1×10^5	1×10^3
slope	-0.517	-0.6563	-1.1974	
r^2	1	1		
t	**Ln(N/No)**			
0	0.000	0.000	0.000	
4	-2.068	-2.614	-4.7896	
8	-4.136	-5.228	-9.5792	
12	-6.204	-7.842	-14.3688	
16	-8.272	-10.456	-19.1584	
20	-10.34	-13.070	-23.9480	
24	-12.408	-15.684	-28.7376	
28	-14.476	-18.298	-33.5272	
32	-16.544	-20.912	-38.3168	

Appendix G

Mean ln(N/N$_0$) values (3 replicates) at 5% NaCl for an initial viable number of N$_0$ = 1 x 10^9 (cells.mL^{-1}).

day	ln(N/N$_0$)
0	0
4	-0.69591
8	-0.17217
12	-10.8807
16	-13.0894
20	-13.298
24	-14.9438
28	-16.2216
32	-18.5972

Mean ln(N/N$_0$) values (3 replicates) at 5% NaCl for an initial viable number of N$_0$ = 1 x 10^7 (cells.mL^{-1}).

day	ln(N/N$_0$)
0	0
4	-5.71085
8	-6.88384
12	-8.80764
16	-11.8898

Mean ln(N/N$_0$) values (3 replicates) at 5% NaCl for an initial viable number of N$_0$ = 1 x 10^7 (cells.mL^{-1}).

day	ln(N/N$_0$)
0	0
4	-3.47085

Summary fit of ln(N/N_0) versus day at 4°C in 5% NaCl for each of initial viable cell numbers of N_0 = 1 x 10^9,1 x 10^7 and 1 x 10^5 (cells.mL^{-1}).

	Initial viable numbers N_0 (cells.mL^{-1})			
	1 x 10^9	1 x 10^7	1 x 10^5	1 x 10^3
slope	-0.637	-0.6884	-0.8677	-
r^2	0.884	0.962	1-	-
t	**Ln(N/No)**			
0	0.0000	0.00000	0.0000	-
4	-2.5488	-2.75360	-3.4708	-
8	-5.0976	-5.50720	-6.9416	-
12	-7.6464	-8.26080	-10.4124	-
16	-10.1952	-11.01440	-13.8832	-
20	-12.7440	-13.76800	-17.354	-
24	-15.2928	-16.52160	-20.8248	-
28	-17.8416	-19.27520	-24.2956	-
32	-20.3904	-22.02880	-27.7664	-

Appendix H

Mean $\ln(N/N_0)$ values (3 replicates) at 10% NaCl for an initial viable number of $N_0 = 1 \times 10^9$ (cells.mL^{-1}).

day	$\ln(N/N_0)$
0	0
4	-7.6746
8	-11.8456
12	-18.434

Mean $\ln(N/N_0)$ values (3 replicates) at 10% NaCl for an initial viable number of $N_0 = 1 \times 10^7$ (cells.mL^{-1}).

day	$\ln(N/N_0)$
0	0
4	-10.3998

Mean $\ln(N/N_0)$ values (3 replicates) at 10% NaCl for an initial viable number of $N_0 = 1 \times 10^5$ (cells.mL^{-1}).

day	$\ln(N/N_0)$
0	0
4	-8.09257

Summary fit of ln(N/N_0) versus days at 4°C in 10% NaCl for each of initial viable cell numbers of N_0 = 1 x 10^9,1 x 10^7 and 1 x 10^5 (cells.mL^{-1}).

	Initial viable numbers N_0 (cells.mL^{-1})			
	1 x 10^9	1 x 10^7	1 x 10^5	1 x 10^3
slope	-1.548	-2.6	-2.008	
r^2	1	1	1	
t	**Ln(N/No)**			
0	0.0000	0.0000	0.000	
4	-6.1920	-10.4000	-8.092	
8	-12.3840	-20.8000	-16.184	
12	-18.5760	-31.2000	-24.276	
16	-24.7680	-41.6000	-32.368	
20	-30.9600	-52.0000	-40.460	
24	-37.1520	-62.4000	-48.552	
28	-43.3440	-72.8000	-56.644	
32	-49.5360	-83.2000	-64.736	

Appendix I

Mean $\ln(N/N_0)$ values (3 replicates) at pH 8 for an initial viable number of $N_0 = 1 \times 10^9$ (cells.mL^{-1}).

day	$\ln(N/N_0)$
0	0.03
4	-0.79
8	-2.54
12	-4.95
16	-4.71
20	-7.76
24	-9.52
28	-10.75
34	-13.82

Mean $\ln(N/N_0)$ values (3 replicates) at pH = 8 for an initial viable number of $N_0 = 1 \times 10^7$ (cells.mL^{-1}).

day	$\ln(N/N_0)$
0	0.00
4	-3.02
8	-7.29
12	-9.03
16	-9.88
20	-11.73
24	-12.62
28	-14.48

Mean ln(N/N_0) values (3 replicates) at pH = 8 for an initial viable number of $N_0 = 1 \times 10^5$ (cells.mL^{-1}).

day	ln(N/N_0)
0	0.00
4	-2.30
8	-6.74

Summary fit of ln(N/N_0) versus days at 4°C in pH = 8 for each of initial viable cell numbers of $N_0 = 1 \times 10^9$, 1×10^7 and 1×10^5 (cells.mL^{-1}).

	Initial viable numbers N_0 (cells.mL^{-1})			
	1×10^9	1×10^7	1×10^5	1×10^3
slope	-0.3865	-0.5714	-0.7893	
r^2	0.9794	0.9008	0.9607	
t	**Ln(N/No)**			
0	0.00	0.00	0.00	
4	-1.55	-2.29	-3.16	
8	-3.09	-4.57	-6.31	
12	-4.64	-6.86	-9.47	
16	-6.18	-9.14	-12.63	
20	-7.73	-11.43	-15.79	
24	-9.28	-13.71	-18.94	
28	-10.82	-16.00	-22.10	
34	-13.14	-19.43	-26.84	

Appendix J

Mean $\ln(N/N_0)$ values (3 replicates) at pH 9.5 for an initial viable number of $N_0 = 1 \times 10^9$ (cells.mL^{-1}).

day	$\ln(N/N_0)$
0	0.00
4	4.18
8	-15.45

Mean $\ln(N/N_0)$ values (3 replicates) at pH 9.5 for an initial viable number of $N_0 = 1 \times 10^7$ (cells.mL^{-1}).

day	$\ln(N/N_0)$
0	0
4	-7.01

Mean $\ln(N/N_0)$ values (3 replicates) at pH 9.5 for an initial viable number of $N_0 = 1 \times 10^5$ (cells.mL^{-1})

day	$\ln(N/N_0)$
0	0
4	-7.74

Summary fit of ln(N/N_0) versus day at4°C in pH 9.5 for each of initial viable cell numbers of $N_0 = 1 \times 10^9$, 1×10^7 and1×10^5 (cells.mL^{-1}).

	Initial viable numbers N_0 (cells.mL^{-1})			
	1×10^9	1×10^7	1×10^5	1×10^3
slope	-1.3356	-1.7543	-1.9347	-
r^2	0.4697	1.000	1.000	-
t	**Ln(N/No)**			
0	0.00	0.00	0.00	-
4	-5.34	-7.02	-7.74	-
8	-10.68	-14.03	-15.48	-
12	-16.03	-21.05	-23.22	-
16	-21.37	-28.07	-30.96	-
20	-26.71	-35.09	-38.69	-
24	-32.05	-42.10	-46.43	-
28	-37.40	-49.12	-54.17	-
34	-45.41	-59.65	-65.78	-

Appendix K

Mean $\ln(N/N_0)$ values (3 replicates) at pH 5 for an initial viable number of $N_0 = 1 \times 10^9$ (cells.mL^{-1}).

day	$\ln(N/N_0)$
0	0
4	1.36
8	-6.38
12	-10.3
16	-13.2
20	-18.4

Mean $\ln(N/N_0)$ values (3 replicates) at pH 5 for an initial viable number of $N_0 = 1 \times 10^7$ (cells.mL^{-1}).

day	$\ln(N/N_0)$
0	0
4	-6.91
8	-11.62

Mean $\ln(N/N_0)$ values (3 replicates) at pH 5 for an initial viable number of $N_0 = 1 \times 10^5$ (cells.mL^{-1}).

day	$\ln(N/N_0)$
0	0
4	-8.17

Summary fit of ln(N/N_0) versus days at 4°C in pH 5 for each of initial viable cell numbers of $N_0 = 1 \times 10^9$, 1×10^7 and 1×10^5 (cells.mL^{-1}).

	Initial viable numbers N_0 (cells.mL^{-1})			
	1×10^9	1×10^7	1×10^5	1×10^3
slope	-0.8503	-1.5072	-2.0422	-
r^2	0.9154	0.9851	1	-
t	**Ln(N/No)**			
0	0.00	0.00	0.00	-
4	-3.40	-6.03	-8.17	-
8	-6.80	-12.06	-16.34	-
12	-10.20	-18.09	-24.51	-
16	-13.60	-24.12	-32.68	-
20	-17.01	-30.14	-40.84	-
24	-20.41	-36.17	-49.01	-
28	-23.81	-42.20	-57.18	-
34	-28.91	-51.24	-69.43	-

Appendix L

Nucleotide sequence (5' – 3') for a 1561 bp region of *yeaZ* amplified and sequenced using M13F/M13R oligonucleotide pair. The introduced *Sph*I sites (GCATGC) are underlined.

```
   1 - TACGCCAGCTATTTAGGTGACACTATAGAATACTCAAGCTATGCATCCAACGCGTTGGGA - 60
   1 -   R  Q  L  F  R  *  H  Y  R  I  L  K  L  C  I  Q  R  V  G  S - 20

                                                          SphI
  61 - GCTCTCCCATATGGTCGACCTGCAGGCGGCCGCGAATTCACTAGTGATTGCATGCCTGAG - 120
  21 -   S  P  I  W  S  T  C  R  R  P  R  I  H  *  *  L  H  A  *  A - 40

 121 - CCAAACAGCCCAGGCTTAGCGGACAAATTGGTGAGAATGTTAGCGCCAGTCATTGAAGAA - 180
  41 -   K  Q  P  R  L  S  G  Q  I  G  E  N  V  S  A  S  H  *  R  K - 60

 181 - AATGACGGTCGTTGTTTCTTCTTATGTACTTCTCACAGCATGATGCGTGAGTTGGGAGAG - 240
  61 -   *  R  S  L  F  L  L  M  Y  F  S  Q  H  D  A  *  V  G  R  E - 80

 241 - AAGTTCCGTGAGGTGTTGGATCTTCCGGTTCTTATGCAAGGTGAAATGAGCAAGCAAAAG - 300
  81 -   V  P  *  G  V  G  S  S  G  S  Y  A  R  *  N  E  Q  A  K  D - 100

 301 - ACTCTTGCAGAGTTTATGGAGCTGGGTAACGCTTTGCTTGTGGCGACGGGGGCGTTTTGG - 360
 101 -   S  C  R  V  Y  G  A  G  *  R  F  A  C  G  D  G  G  V  L  G - 120

 361 - GAAGGGATCGATGTTAGAGGTGACGCACTGAGCTGTGTTATCATCGACAAATTGCCGTTT - 420
 121 -   R  D  R  C  *  R  *  R  T  E  L  C  Y  H  R  Q  I  A  V  Y - 140

 421 - ACTGCCCCGGATGATCCGCTGCTAAAAGCCCGAATTGAAGATTGTCGATTGCGTGGTGGT - 480
 141 -   C  P  G  *  S  A  A  K  S  P  N  *  R  L  S  I  A  W  W  * - 160

 481 - GAGCCGTTTGCTGAAGTGCAAATCCCCGATGCGGTGATCACTTTAAAGCAGGGCGTAGGG - 540
 161 -   A  V  C  *  S  A  N  P  R  C  G  D  H  F  K  A  G  R  R  A - 180

 541 - CGTTTGATTCGAGATCAGAAAGATCATGGTGCATTGATCATTTGTGACAATCGCCTTGTC - 600
 181 -   F  D  S  R  S  E  R  S  W  C  I  D  H  L  *  Q  S  P  C  H - 200

 601 - ACCCGTGACTATGGCGGCACGTTCCTTGGAAGCTTACCTCCTATCCCAAGAACACGAGAT - 660
 201 -   P  *  L  W  R  H  V  P  W  K  L  T  S  Y  P  K  N  T  R  F - 220

 661 - TTAGAACGTATCAAAGCGTTTCTTAAAGCAGAATAATTAGTCGCAGCCTGTGCTGTGATG - 720
 221 -   R  T  Y  Q  S  V  S  *  S  R  I  I  S  R  S  L  C  C  D  V - 240

 721 - TAACCAAATAAAATAGAGTTTTAGAGAGTTAAATGAGCGCAAAAATTCTTGCTATCGATA - 780
 241 -   T  K  *  N  R  V  L  E  S  *  M  S  A  K  I  L  A  I  D  T - 260

 781 - CCGCAACTGAAAACTGTTCAGTTGCACTACTGGTTAATGACCAAGTGATTTCACGCAGCG - 840
 261 -   A  T  E  N  C  S  V  A  L  L  V  N  D  Q  V  I  S  R  S  E - 280

 841 - AAGTGGCACCTCGTGACCACACGAAAAAAGTACTGCCAATGGTTGACGAAGTGCTGAAAG - 900
 281 -   V  A  P  R  D  H  T  K  K  V  L  P  M  V  D  E  V  L  K  E - 300

 901 - AAGCGGGTCTAACTCTACAAGACTTGGATGCACTAGCGTTTGGCCGTGGCCCTGGTAGCT - 960
 301 -   A  G  L  T  L  Q  D  L  D  A  L  A  F  G  R  G  P  G  S  F - 320

 961 - TTACTGGTGTTCGTATCGGTATTGGCATCGCTCAAGGCCTAGCATTTGGTGCAGAACTGC - 1020
 321 -   T  G  V  R  I  G  I  G  I  A  Q  G  L  A  F  G  A  E  L  P - 340

1021 - CGATGATTGGTGTTTCAACATTGGCTGCGATGGCACAAGCAAGCTACCGCCTGCATGGTG - 1080
 341 -   M  I  G  V  S  T  L  A  A  M  A  Q  A  S  Y  R  L  H  G  A - 360
```

```
1081 - CAACTGATGTCGCTGTAGCGATTGATGCGCGCATGAGCGAGGTTTACTGGGCACGTTATT - 1140
 361 -   T  D  V  A  V  A  I  D  A  R  M  S  E  V  Y  W  A  R  Y  S - 380

1141 - CTCGCCAAGAAAACGGCGAATGGATCGGTGTTGATGAAGAATGTGTGATTCCACCAGCTC - 1200
 381 -   R  Q  E  N  G  E  W  I  G  V  D  E  E  C  V  I  P  P  A  R - 400

1201 - GTTTGGCGGAAGAAGCACAAGCTGACTCTAAAACGTGGACAACAGCTGGTACAGGTTGGT - 1260
 401 -   L  A  E  E  A  Q  A  D  S  K  T  W  T  T  A  G  T  G  W  S - 420

1261 - CTGCATATCAAGAAGAACTGGCGGGCCTGCCGTTTAACACTGCAGACAGTGAGGTATTGT - 1320
 421 -   A  Y  Q  E  E  L  A  G  L  P  F  N  T  A  D  S  E  V  L  Y - 440

1321 - ACCCTGACTCACAAGACATTGTGATTTTAGCTAAGCAAGAACTAGAAAAAGGCAATACGG - 1380
 441 -   P  D  S  Q  D  I  V  I  L  A  K  Q  E  L  E  K  G  N  T  V - 460

1381 - TTCCTGTTGAAGAATCTAGCCCGGTTTACCTGCGTGATAACGTGACTTGGAAGAAGCTTC - 1440
 461 -   P  V  E  E  S  S  P  V  Y  L  R  D  N  V  T  W  K  K  L  P - 480

1441 - CAGGCCGCGAATAATTAGGAAAAAAATAAAGACGGGGCGGTAGCCCTGTCTTTTTATGGA - 1500
 481 -   G  R  E  *  L  G  K  K  *  R  R  G  G  S  P  V  F  L  W  S - 500

1501 - GCGTTATGGCGTCGATTAATGGTTTACCTCCTTCACTGATACCCGGTACCAACCGTACCA - 1560
 501 -   V  M  A  S  I  N  G  L  P  P  S  L  I  P  G  T  N  R  T  N - 520

1561 - ATAAAGTGGGTAAAAAAGGGCAGGTAAAGAAAGCTCAAAATAAGCAGTCCGTTGGTCAAC - 1620
 521 -   K  V  G  K  K  G  Q  V  K  K  A  Q  N  K  Q  S  V  G  Q  P - 540

                                                          SphI
1621 - CTTCAAAGGTGGCAAACGCAGTCGCGCATTCCATAAAACAAGTTGATGAGTCCCAAGCAT - 1680
 541 -   S  K  V  A  N  A  V  A  H  S  I  K  Q  V  D  E  S  Q  A  C - 560

1681 - GCAATCGAATTCCCGCGGCCGCCATGGCGGCCGGGAGCNTGCGACGTCGGGCCCANTCGC - 1740
 561 -   N  R  I  P  A  A  A  M  A  A  G  S  X  R  R  R  A  X  S  P - 580

1741 - CCTATAG - 1747
 581 -   Y  X  - 600
```

Appendix M

Nucleotide sequence (5' – 3') for a 1.9kbp region of *yeaZ:kan* amplified and sequenced using RPFmuSphIF/R1 oligonucleotide pair. The *Eco*RI and *Pst*I sites are underlined. The *aphA*3 gene (red text) is inserted and replaced the most part of $yeaZ_{Vp}$ gene.

```
   1 - GCATGCCTGAGCCAAACAGCCCAGGCTTAGCGGACAAATTGGTGAGAATGTTAGCGCCAG - 60
  61 - TCATTGAAGAAAATGACGGTCGTTGTTTCTTCTTATGTACTTCTCACAGCATGATGCGTG - 120
 121 - AGTTGGGAGAGAAGTTCCGTGAGGTGTTGGATCTTCCGGTTCTTATGCAAGGTGAAATGA - 180
 181 - GCAAGCAAAAGACTCTTGCAGAGTTTATGGAGCTGGGTAACGCTTTGCTTGTGGCGACGG - 240
 241 - GGGCGTTTTGGGAAGGGATCGATGTTAGAGGTGACGCACTGAGCTGTGTTATCATCGACA - 300
 301 - AATTGCCGTTTACTGCCCCGGATGATCCGCTGCTAAAAGCCCGAATTGAAGATTGTCGAT - 360
 361 - TGCGTGGTGGTGAGCCGTTTGCTGAAGTGCAAATCCCCGATGCGGTGATCACTTTAAAGC - 420
 421 - AGGGCGTAGGGCGTTTGATTCGAGATCAGAAAGATCATGGTGCATTGATCATTTGTGACA - 480
 481 - ATCGCCTTGTCACCCGTGACTATGGCGGCACGTTCCTTGGAAGCTTACCTCCTATCCCAA - 540
 541 - GAACACGAGATTTAGAACGTATCAAAGCGTTTCTTAAAGCAGAATAATTAGTCGCAGCCT - 600
                                                      EcoRI
 601 - GTGCTGTGATGTAACCAAATAAAATAGAGTTTTAGAGAGTTAAATGAGCGCAAAAATTCG - 660
 661 - AGCTCGGTACCCCGGGTGACTAACTAGGAGGAATAAATGGCTAAAATGAGAATATCACCG - 720
 721 - GAATTGAAAAAACTGATCGAAAAATACCGCTGCGTAAAAGATACGGAAGGAATGTCTCCT - 780
 781 - GCTAAGGTATATAAGCTGGTGGGAGAAAATGAAAACCTATATTTAAAAATGACGGACAGC - 840
 841 - CGGTATAAAGGGACCACCTATGATGTGGAACGGGAAAAGGACATGATGCTATGGCTGGAA - 900
 901 - GGAAAGCTGCCTGTTCCAAAGGTCCTGCACTTTGAACGGCATGATGGCTGGAGCAATCTG - 960
 961 - CTCATGAGTGAGGCCGATGGCGTCCTTTGCTCGGAAGAGTATGAAGATGAACAAAGCCCT - 1020
1021 - GAAAAGATTATCGAGCTGTATGCGGAGTGCATCAGGCTCTTTCACTCCATCGACATATCG - 1080
1081 - GATTGTCCCTATACGAATAGCTTAGACAGCCGCTTAGCCGAATTGGATTACTTACTGAAT - 1140
1141 - AACGATCTGGCCGATGTGGATTGCGAAAACTGGGAAGAAGACACTCCATTTAAAGATCCG - 1200
1201 - CGCGAGCTGTATGATTTTTTAAAGACGGAAAAGCCCGAAGAGGAACTTGTCTTTTCCCAC - 1260
1261 - GGCGACCTGGGAGACAGCAACATCTTTGTGAAAGATGGCAAAGTAAGTGGCTTTATTGAT - 1320
1321 - CTTGGGAGAAGCGGCAGGGCGGACAAGTGGTATGACATTGCCTTCTGCATCCGGTCGATC - 1380
1381 - AGGGAGGATATCGGGGAAGAACAGTATGTCGAGCTATTTTTTGACTTACTGGGGATCAAG - 1440
1441 - CCTGATTGGGAGAAAATAAAATATTATATTTTACTGGATGAATTGTTTTAGTACCTGGAG - 1500
                                                      PstI
1501 - GGAATAATGACCCGGGATCCTCTAGAGTCGACCTGCAGACAGTGAGGTATTGTACCCTGA - 1560
1561 - CTCACAAGACATTGTGATTTTAGCTAAGCAAGAACTAGAAAAAGGCAATACGGTTCCTGT - 1620
1621 - TGAAGAATCTAGCCCGGTTTACCTGCGTGATAACGTGACTTGGAAGAAGCTTCCAGGCCG - 1680
1681 - CGAATAATTAGGAAAAAAATAAAGACGGGGCGGTAGCCCTGTCTTTTTATGGAGCGTTAT - 1740
1741 - GGCGTCGATTAATGGTTTACCTCCTTCACTGATACCCGGTACCAACCGTACCAATAAAGT - 1800
1801 - GGGTAAAAAAGGGCAGGTAAAGAAAGCTCAAAATAAGCAGTCCGTTGGTCAACCTTCAAA - 1860
1861 - GGTGGCAAACGCAGTCGCGCATTCCATAAAACAAGTTGATGAGTCCCAAGCATGC      - 1915
```

Appendix N

Nucleotide sequence (5' – 3') for a 0.7 kbp region of *yeaZ* amplified and sequenced using T7F/R oligonucleotide pair. The introduced *Nde*I (CATATG) site and the *Xho*I (CTCGAG) are in bold text. Introduction of the *Xho*I site at the 3' end of the ORF resulted in an animo acid change from N → L (underlined). Translation of the His-Tag indicated in red text.

```
                      NdeI
  1 - TAAGAAGGAGATATACATATGAGCGCAAAAATTCTTGCTATCGATACCGCAACTGAAAAC - 60
  1 -                 M  S  A  K  I  L  A  I  D  T  A  T  E  N   - 20

 61 - TGTTCAGTTGCACTACTGGTTAATGACCAAGTGATTTCACGCAGCGAAGTGGCACCTCGT - 120
 21 - C  S  V  A  L  L  V  N  D  Q  V  I  S  R  S  E  V  A  P  R   - 40

121 - GACCACACGAAAAAAGTACTGCCAATGGTTGACGAAGTGCTGAAAGAAGCGGGTCTAACT - 180
 41 - D  H  T  K  K  V  L  P  M  V  D  E  V  L  K  E  A  G  L  T   - 60

181 - CTACAAGACTTGGATGCACTAGCGTTTGGCCGTGGCCCTGGTAGCTTTACTGGTGTTCGT - 240
 61 - L  Q  D  L  D  A  L  A  F  G  R  G  P  G  S  F  T  G  V  R   - 80

241 - ATCGGTATTGGCATCGCTCAAGGCCTAGCATTTGGTGCAGAACTGCCGATGATTGGTGTT - 300
 81 - I  G  I  G  I  A  Q  G  L  A  F  G  A  E  L  P  M  I  G  V   - 100

301 - TCAACATTGGCTGCGATGGCACAAGCAAGCTACCGCCTGCATGGTGCAACTGATGTCGCT - 360
101 - S  T  L  A  A  M  A  Q  A  S  Y  R  L  H  G  A  T  D  V  A   - 120

361 - GTAGCGATTGATGCGCGCATGAGCGAGGTTTACTGGGCACGTTATTCTCGCCAAGAAAAC - 420
121 - V  A  I  D  A  R  M  S  E  V  Y  W  A  R  Y  S  R  Q  E  N   - 140

421 - GGCGAATGGATCGGTGTTGATGAAGAATGTGTGATTCCACCAGCTCGTTTGGCGGAAGAA - 480
141 - G  E  W  I  G  V  D  E  E  C  V  I  P  P  A  R  L  A  E  E   - 160

481 - GCACAAGCTGACTCTAAAACGTGGACAACAGCTGGTACAGGTTGGTCTGCATATCAAGAA - 540
161 - A  Q  A  D  S  K  T  W  T  T  A  G  T  G  W  S  A  Y  Q  E   - 180

541 - GAACTGGCGGGCCTGCCGTTTAACACTGCAGACAGTGAGGTATTGTACCCTGACTCACAA - 600
181 - E  L  A  G  L  P  F  N  T  A  D  S  E  V  L  Y  P  D  S  Q   - 200

601 - GACATTGTGATTTTAGCTAAGCAAGAACTAGAAAAAGGCAATACGGTTCCTGTTGAAGAA - 660
201 - D  I  V  I  L  A  K  Q  E  L  E  K  G  N  T  V  P  V  E  E   - 220

                                                      XhoI
661 - TCTAGCCCGGTTTACCTGCGTGATAACGTGACTTGGAAGAAGCTTCCAGGCCTCGAGCAC - 720
221 - S  S  P  V  Y  L  R  D  N  V  T  W  K  K  L  P  G  L  E  H   - 240

721 - CACCACCACCACCACTGA - 738
241 - H  H  H  H  H  *   - 260
```

Appendix O

Nucleotide sequence (5' – 3') for a 0.7 kbp region of *yeaZ* amplified and sequenced using pBT 5'/3' oligonucleotide pair. The introduced *Not*I (GCGGCCGC) site and the *Xho*I (CTCGAG) site are bolded. The ORF of YeaZ (shown in red) is shown at the end of λ cI (green).

```
     End of λ cI   NotI
  1 - GAAGAGACGTTTGGCGCGGCCGCAATGAGCGCAAAAATTCTTGCTATCGATACCGCAACT - 60
  1 - E  E  T  F  G  A  A  A  M  S  A  K  I  L  A  I  D  T  A  T   - 20

 61 - GAAAACTGTTCAGTTGCACTACTGGTTAATGACCAAGTGATTTCACGCAGCGAAGTGGCA - 120
 21 - E  N  C  S  V  A  L  L  V  N  D  Q  V  I  S  R  S  E  V  A   - 40

121 - CCTCGTGACCACACGAAAAAAGTACTGCCAATGGTTGACGAAGTGCTGAAAGAAGCGGGT - 180
 41 - P  R  D  H  T  K  K  V  L  P  M  V  D  E  V  L  K  E  A  G   - 60

181 - CTAACTCTACAAGACTTGGATGCACTAGCGTTTGGCCGTGGCCCTGGTAGCTTTACTGGT - 240
 61 - L  T  L  Q  D  L  D  A  L  A  F  G  R  G  P  G  S  F  T  G   - 80

241 - GTTCGTATCGGTATTGGCATCGCTCAAGGCCTAGCATTTGGTGCAGAACTGCCGATGATT - 300
 81 - V  R  I  G  I  G  I  A  Q  G  L  A  F  G  A  E  L  P  M  I   - 100

301 - GGTGTTTCAACATTGGCTGCGATGGCACAAGCAAGCTACCGCCTGCATGGTGCAACTGAT - 360
101 - G  V  S  T  L  A  A  M  A  Q  A  S  Y  R  L  H  G  A  T  D   - 120

361 - GTCGCTGTAGCGATTGATGCGCGCATGAGCGAGGTTTACTGGGCACGTTATTCTCGCCAA - 420
121 - V  A  V  A  I  D  A  R  M  S  E  V  Y  W  A  R  Y  S  R  Q   - 140

421 - GAAAACGGCGAATGGATCGGTGTTGATGAAGAATGTGTGATTCCACCAGCTCGTTTGGCG - 480
141 - E  N  G  E  W  I  G  V  D  E  E  C  V  I  P  P  A  R  L  A   - 160

481 - GAAGAAGCACAAGCTGACTCTAAAACGTGGACAACAGCTGGTACAGGTTGGTCTGCATAT - 540
161 - E  E  A  Q  A  D  S  K  T  W  T  T  A  G  T  G  W  S  A  Y   - 180

541 - CAAGAAGAACTGGCGGGCCTGCCGTTTAACACTGCAGACAGTGAGGTATTGTACCCTGAC - 600
181 - Q  E  E  L  A  G  L  P  F  N  T  A  D  S  E  V  L  Y  P  D   - 200

601 - TCACAAGACATTGTGATTTTAGCTAAGCAAGAACTAGAAAAAGGCAATACGGTTCCTGTT - 660
201 - S  Q  D  I  V  I  L  A  K  Q  E  L  E  K  G  N  T  V  P  V   - 220
                                                                XhoI
661 - GAAGAATCTAGCCCGGTTTACCTGCGTGATAACGTGACTTGGAAGAAGCTTCCAGGCCTC - 720
221 - E  E  S  S  P  V  Y  L  R  D  N  V  T  W  K  K  L  P  G  L   - 240

721 - GAGTAATTA - 729
241 - E  *
```

Appendix P

Nucleotide sequence (5' – 3') for a 0.7 kbp region of *yeaZ* amplified and sequenced using pTRG 5'/3' oligonucleotide pair. The introduced *Not*I (GCGGCCGC) site and the *Xho*I (CTCGAG) site are in bold text. The ORF of YeaZ (red) is shown at the end of RNAPα (green).

```
      End of RNAPα      NotI
  1 - AAACCAGAGGCGGCCGGATCCGCGGCCGCAATGAGCGCAAAAATTCTTGCTATCGATACC - 60
  1 - K  P  E  A  A  G  S  A  A  A  M  S  A  K  I  L  A  I  D  T   - 20

 61 - GCAACTGAAAACTGTTCAGTTGCACTACTGGTTAATGACCAAGTGATTTCACGCAGCGAA - 120
 21 - A  T  E  N  C  S  V  A  L  L  V  N  D  Q  V  I  S  R  S  E   - 40

121 - GTGGCACCTCGTGACCACACGAAAAAAGTACTGCCAATGGTTGACGAAGTGCTGAAAGAA - 180
 41 - V  A  P  R  D  H  T  K  K  V  L  P  M  V  D  E  V  L  K  E   - 60

181 - GCGGGTCTAACTCTACAAGACTTGGATGCACTAGCGTTTGGCCGTGGCCCTGGTAGCTTT - 240
 61 - A  G  L  T  L  Q  D  L  D  A  L  A  F  G  R  G  P  G  S  F   - 80

241 - ACTGGTGTTCGTATCGGTATTGGCATCGCTCAAGGCCTAGCATTTGGTGCAGAACTGCCG - 300
 81 - T  G  V  R  I  G  I  G  I  A  Q  G  L  A  F  G  A  E  L  P   - 100

301 - ATGATTGGTGTTTCAACATTGGCTGCGATGGCACAAGCAAGCTACCGCCTGCATGGTGCA - 360
101 - M  I  G  V  S  T  L  A  A  M  A  Q  A  S  Y  R  L  H  G  A   - 120

361 - ACTGATGTCGCTGTAGCGATTGATGCGCGCATGAGCGAGGTTTACTGGGCACGTTATTCT - 420
121 - T  D  V  A  V  A  I  D  A  R  M  S  E  V  Y  W  A  R  Y  S   - 140

421 - CGCCAAGAAAACGGCGAATGGATCGGTGTTGATGAAGAATGTGTGATTCCACCAGCTCGT - 480
141 - R  Q  E  N  G  E  W  I  G  V  D  E  E  C  V  I  P  P  A  R   - 160

481 - TTGGCGGAAGAAGCACAAGCTGACTCTAAAACGTGGACAACAGCTGGTACAGGTTGGTCT - 540
161 - L  A  E  E  A  Q  A  D  S  K  T  W  T  T  A  G  T  G  W  S   - 180

541 - GCATATCAAGAAGAACTGGCGGGCCTGCCGTTTAACACTGCAGACAGTGAGGTATTGTAC - 600
181 - A  Y  Q  E  E  L  A  G  L  P  F  N  T  A  D  S  E  V  L  Y   - 200

601 - CCTGACTCACAAGACATTGTGATTTTAGCTAAGCAAGAACTAGAAAAAGGCAATACGGTT - 660
201 - P  D  S  Q  D  I  V  I  L  A  K  Q  E  L  E  K  G  N  T  V   - 220

661 - CCTGTTGAAGAATCTAGCCCGGTTTACCTGCGTGATAACGTGACTTGGAAGAAGCTTCCA - 720
221 - P  V  E  E  S  S  P  V  Y  L  R  D  N  V  T  W  K  K  L  P   - 240
          XhoI
721 - GGCCTCGAGTAATTA - 735
241 - G  L  E  *
```

Appendix Q

Nucleotide sequence (5' – 3') for a 0.45 kbp region of *yjeE* amplified and sequenced using pTRG 5'/3' oligonucleotide pair. The introduced *Not*I (GCGGCCGC) site and the *Xho*I (CTCGAG) site are indicated in bold text. The ORF of YjeE (red) is shown at the end of RNAPα (green).

```
      End of RNAPα      NotI
  1 - AAACCAGAGGCGGCCGGATCCGCGGCCGCAATGAGCACGAAACAATTTACTTTAAAAGAT - 60
  1 - K  P  E  A  A  G  S  A  A  A  M  S  T  K  Q  F  T  L  K  D  - 20

 61 - GAGCAAGAAACGGTAGCACTGGGCACCGAGCTGGCTCAACTTTGTTCTCAACAAACCACT - 120
 21 - E  Q  E  T  V  A  L  G  T  E  L  A  Q  L  C  S  Q  Q  T  T  - 40

121 - ATTTATCTGCATGGTGATTTAGGTGCAGGTAAAACAACCTTCAGTCGTGGTTTTGTCCGT - 180
 41 - I  Y  L  H  G  D  L  G  A  G  K  T  T  F  S  R  G  F  V  R  - 60

181 - GCTCTTGGGCATCAAGGAAACGTGAAAAGTCCGACTTATACGCTTGTCGAACCTTACCAA - 240
 61 - A  L  G  H  Q  G  N  V  K  S  P  T  Y  T  L  V  E  P  Y  Q  - 80

241 - TTAGATAAGTGGCAGGTTTACCACTTTGATCTTTACCGATTGGCAGATCCTGAAGAATTG - 300
 81 - L  D  K  W  Q  V  Y  H  F  D  L  Y  R  L  A  D  P  E  E  L  - 100

301 - GAATTCATGGGGATCCGAGACTACTTCACAGATGATGCGATCTGCTTGGTTGAATGGCCT - 360
101 - E  F  M  G  I  R  D  Y  F  T  D  D  A  I  C  L  V  E  W  P  - 120

361 - GAAAAAGGGCAAGGATTGCTGCCACAACCAGATTTAGATGTAGAAATTCGTTATCAAGGT - 420
121 - E  K  G  Q  G  L  L  P  Q  P  D  L  D  V  E  I  R  Y  Q  G  - 140

421 - GAGCAACGCGTCGCTGAGATAACGGCGAACAATGATTACGGTGTGCAGTTACTCAGTCGA - 480
141 - E  Q  R  V  A  E  I  T  A  N  N  D  Y  G  V  Q  L  L  S  R  - 160
          XhoI
481 - TTGGAGCTCGAGTAATTA - 498
161 - L  E  L  E  *      - 180
```

Appendix R

Nucleotide sequence (5’ – 3’) for a 1.017 kbp region of *ygjD* amplified and sequenced using pTRG 5’/3’ oligonucleotide pair. The introduced *Not*I (GCGGCCGC) and *Xho*I (CTCGAG) sites are shown as bold text. The ORF of YgjD (red) is shown at the end of RNAPα (green).

```
      End of RNAPα    NotI
  1 - AAACCAGAGGCGGCCGGATCCGCGGCCGCAATGCGCATTATTGGTATCGAAACCTCTTGT - 60
  1 - K  P  E  A  A  G  S  A  A  A  M  R  I  I  G  I  E  T  S  C   - 20

 61 - GACGAGACAGGAATCGCGATTTACGACGATGAAAAAGGCCTGTTGGCGCACAAGCTTTAC - 120
 21 - D  E  T  G  I  A  I  Y  D  D  E  K  G  L  L  A  H  K  L  Y   - 40

121 - AGCCAAGTAAAACTTCACGCGGATTACGGCGGCGTGGTGCCAGAGTTGGCTTCACGTGAC - 180
 41 - S  Q  V  K  L  H  A  D  Y  G  G  V  V  P  E  L  A  S  R  D   - 60

181 - CATGTAAAGAAAACCATTCCTCTTATTAAAGAGGCACTAAAAGAAGCAAACTTAACATCC - 240
 61 - H  V  K  K  T  I  P  L  I  K  E  A  L  K  E  A  N  L  T  S   - 80

241 - CAAGACATCGACGGCGTGGCTTACACGGCCGGTCCTGGTTTGGTTGGTGCTTTGCTAGTG - 300
 81 - Q  D  I  D  G  V  A  Y  T  A  G  P  G  L  V  G  A  L  L  V   - 100

301 - GGTGCAACCATCGGTCGCAGTATTGCTTACGCATGGGGTGTTCCTGCTGTTCCTGTTCAT - 360
101 - G  A  T  I  G  R  S  I  A  Y  A  W  G  V  P  A  V  P  V  H   - 120

361 - CATATGGAAGGTCATTTACTTGCGCCAATGCTAGAAGACAACCCACCACCATTCCCATTT - 420
121 - H  M  E  G  H  L  L  A  P  M  L  E  D  N  P  P  P  F  P  F   - 140

421 - GTGGCGGTGTTGGTTTCTGGCGGTCACTCGATGATGGTGGAAGTAAAAGGCATTGGTGAA - 480
141 - V  A  V  L  V  S  G  G  H  S  M  M  V  E  V  K  G  I  G  E   - 160

481 - TACAAGATTCTAGGCGAATCCATTGATGATGCAGCCGGTGAAGCATTTGATAAGACGGCT - 540
161 - Y  K  I  L  G  E  S  I  D  D  A  A  G  E  A  F  D  K  T  A   - 180

541 - AAGCTGATGGGGTTAGATTACCCAGGCGGTCCTCTGTTATCCAAGCTAGCAGAGAAAGGT - 600
181 - K  L  M  G  L  D  Y  P  G  G  P  L  L  S  K  L  A  E  K  G   - 200

601 - ACTCCGGGTCGCTTTAAGTTCCCACGACCAATGACCAATGTGCCGGGTTTGGATATGAGT - 660
201 - T  P  G  R  F  K  F  P  R  P  M  T  N  V  P  G  L  D  M  S   - 220

661 - TTCTCTGGTTTGAAAACCTTCACGGCAAACACGATTGCAGCGAATGGCGATGACGAGCAG - 720
221 - F  S  G  L  K  T  F  T  A  N  T  I  A  A  N  G  D  D  E  Q   - 240

721 - ACTCGTGCTGATATTGCGTACGCTTTTGAAGAAGCCGTGTGTGCAACGTTGGCAATTAAA - 780
241 - T  R  A  D  I  A  Y  A  F  E  E  A  V  C  A  T  L  A  I  K   - 260

781 - TGTAAGCGTGCATTAGAGCAAACCGGTATGAAGCGCATCGTTATTGCTGGTGGTGTAAGT - 840
261 - C  K  R  A  L  E  Q  T  G  M  K  R  I  V  I  A  G  G  V  S   - 280

841 - GCGAACCGCCGCTTGCGTGCAGAGCTTGAGAAGCTTGCGAAGAAAATCGGTGGTGAAGTG - 900
281 - A  N  R  R  L  R  A  E  L  E  K  L  A  K  K  I  G  G  E  V   - 300
```

```
 901 - TATTACCCACGTACCGAGTTCTGTACTGACAACGGTGCAATGATTGCGTATGCGGGTATG - 960
 301 - Y  Y  P  R  T  E  F  C  T  D  N  G  A  M  I  A  Y  A  G  M   - 320

 961 - CAACGTTTGAAGAACGGTGAAGTCGCAGATATGTCGGTGGAAGCGCGTCCGCGCTGGCCA - 1020
 321 - Q  R  L  K  N  G  E  V  A  D  M  S  V  E  A  R  P  R  W  P   - 340
                        XhoI
1021 - ATTGACCAGCTAACGCCACTCGAGTAATTA - 1050
 341 - I  D  Q  L  T  P  L  E  *
```

Appendix S

Nucleotide sequence (5' – 3') for a 0.7 kbp region of *yeaZ* amplified and sequenced using pLexA 5' oligonucleotide pair. The introduced *Eco*RI (GAATTC) *Xho*I (CTCGAG) sites are indicated as bold text. The ORF of YeaZ (red) is shown at the end of DNA-BD (green).

```
      End of DNA-BD   EcoRI
  1 - ATTCGCAACGGCGACTGGCTGGAATTCATGAGCGCAAAAATTCTTGCTATCGATACCGCA - 60
  1 - I  R  N  G  D  W  L  E  F  M  S  A  K  I  L  A  I  D  T  A   - 20

 61 - ACTGAAAACTGTTCAGTTGCACTACTGGTTAATGACCAAGTGATTTCACGCAGCGAAGTG - 120
 21 - T  E  N  C  S  V  A  L  L  V  N  D  Q  V  I  S  R  S  E  V   - 40

121 - GCACCTCGTGACCACACGAAAAAAGTACTGCCAATGGTTGACGAAGTGCTGAAAGAAGCG - 180
 41 - A  P  R  D  H  T  K  K  V  L  P  M  V  D  E  V  L  K  E  A   - 60

181 - GGTCTAACTCTACAAGACTTGGATGCACTAGCGTTTGGCCGTGGCCCTGGTAGCTTTACT - 240
 61 - G  L  T  L  Q  D  L  D  A  L  A  F  G  R  G  P  G  S  F  T   - 80

241 - GGTGTTCGTATCGGTATTGGCATCGCTCAAGGCCTAGCATTTGGTGCAGAACTGCCGATG - 300
 81 - G  V  R  I  G  I  G  I  A  Q  G  L  A  F  G  A  E  L  P  M   - 100

301 - ATTGGTGTTTCAACATTGGCTGCGATGGCACAAGCAAGCTACCGCCTGCATGGTGCAACT - 360
101 - I  G  V  S  T  L  A  A  M  A  Q  A  S  Y  R  L  H  G  A  T   - 120

361 - GATGTCGCTGTAGCGATTGATGCGCGCATGAGCGAGGTTTACTGGGCACGTTATTCTCGC - 420
121 - D  V  A  V  A  I  D  A  R  M  S  E  V  Y  W  A  R  Y  S  R   - 140

421 - CAAGAAAACGGCGAATGGATCGGTGTTGATGAAGAATGTGTGATTCCACCAGCTCGTTTG - 480
141 - Q  E  N  G  E  W  I  G  V  D  E  E  C  V  I  P  P  A  R  L   - 160

481 - GCGGAAGAAGCACAAGCTGACTCTAAAACGTGGACAACAGCTGGTACAGGTTGGTCTGCA - 540
161 - A  E  E  A  Q  A  D  S  K  T  W  T  T  A  G  T  G  W  S  A   - 180

541 - TATCAAGAAGAACTGGCGGGCCTGCCGTTTAACACTGCAGACAGTGAGGTATTGTACCCT - 600
181 - Y  Q  E  E  L  A  G  L  P  F  N  T  A  D  S  E  V  L  Y  P   - 200

601 - GACTCACAAGACATTGTGATTTTAGCTAAGCAAGAACTAGAAAAAGGCAATACGGTTCCT - 660
201 - D  S  Q  D  I  V  I  L  A  K  Q  E  L  E  K  G  N  T  V  P   - 220

661 - GTTGAAGAATCTAGCCCGGTTTACCTGCGTGATAACGTGACTTGGAAGAAGCTTCCAGGC - 720
221 - V  E  E  S  S  P  V  Y  L  R  D  N  V  T  W  K  K  L  P  G   - 240
      XhoI
721 - CTCGAGTCGACCTGCAGCCAAGCTAATTCCGGGCGAATTTCTTATGATTTATGA - 774
241 - L  E  S  T  C  S  Q  A  N  S  G  R  I  S  Y  D  L  *   - 260
```

Appendix T

Nucleotide sequence (5' – 3') for a 0.45 kbp region of *yjeE* amplified and sequenced using pB42AD 5' oligonucleotide pair. The introduced *Xho*I (CTCGAG) and *Xho*I (CTCGAG) sites are indicated in bold text. The ORF of YjeE (red) is shown at the end of active domain AD (green).

```
      End of AD                    XhoI
   1 - CCAGATTATGCCTCTCCCGAATTCGGCCGACTCGAGATGAGCACGAAACAATTTACTTTA - 60
   1 - P  D  Y  A  S  P  E  F  G  R  L  E  M  S  T  K  Q  F  T  L   - 20

  61 - AAAGATGAGCAAGAAACGGTAGCACTGGGCACCGAGCTGGCTCAACTTTGTTCTCAACAA - 120
  21 - K  D  E  Q  E  T  V  A  L  G  T  E  L  A  Q  L  C  S  Q  Q   - 40

 121 - ACCACTATTTATCTGCATGGTGATTTAGGTGCAGGTAAAACAACCTTCAGTCGTGGTTTT - 180
  41 - T  T  I  Y  L  H  G  D  L  G  A  G  K  T  T  F  S  R  G  F   - 60

 181 - GTCCGTGCTCTTGGGCATCAAGGAAACGTGAAAAGTCCGACTTATACGCTTGTCGAACCT - 240
  61 - V  R  A  L  G  H  Q  G  N  V  K  S  P  T  Y  T  L  V  E  P   - 80

 241 - TACCAATTAGATAAGTGGCAGGTTTACCACTTTGATCTTTACCGATTGGCAGATCCTGAA - 300
  81 - Y  Q  L  D  K  W  Q  V  Y  H  F  D  L  Y  R  L  A  D  P  E   - 100

 301 - GAATTGGAATTCATGGGGATCCGAGACTACTTCACAGATGATGCGATCTGCTTGGTTGAA - 360
 101 - E  L  E  F  M  G  I  R  D  Y  F  T  D  D  A  I  C  L  V  E   - 120

 361 - TGGCCTGAAAAAGGGCAAGGATTGCTGCCACAACCAGATTTAGATGTAGAAATTCGTTAT - 420
 121 - W  P  E  K  G  Q  G  L  L  P  Q  P  D  L  D  V  E  I  R  Y   - 140

 421 - CAAGGTGAGCAACGCGTCGCTGAGATAACGGCGAACAATGATTACGGTGTGCAGTTACTC - 480
 141 - Q  G  E  Q  R  V  A  E  I  T  A  N  N  D  Y  G  V  Q  L  L   - 160
            XhoI
 481 - AGTCGATTGGAGCTCGAGAAGCTTTGGACTTCTTCGCCAGAGGTTTCAAGTCTCCAATCA - 540
 161 - S  R  L  E  L  E  K  L  W  T  S  S  P  E  V  S  S  L  Q  S   - 180

 541 - AGGTTGTCGGCTTGTCTACCTTGCCAGAAATTTACGAAAAGATGGAAAAGGGTCAAATCG - 600
 181 - R  L  S  A  C  L  P  C  Q  K  F  T  K  R  W  K  R  V  K  S   - 200

 601 - TTGGTAGATACGTTGTTGTTGACACTTCTAAATAAGCGAATTTCTTATGATTTATGA - 657
 201 - L  V  D  T  L  L  L  T  L  L  N  K  R  I  S  Y  D  L  *   - 220
```

Appendix U

Nucleotide sequence (5' – 3') for a 1.017 kbp region of *ygjD* amplified and sequenced using pB42AD 5' oligonucleotide pair. The introduced *Eco*RI (GAATTC) and *Xho*I (CTCGAG) sites are indicated in bold text. The ORF of YgjD (red)is shown at the end of active domain AD (green).

End of AD ***Eco*RI**

```
  1 - CCAGATTATGCCTCTCCCGAATTCATGCGCATTATTGGTATCGAAACCTCTTGTGACGAG - 60
  1 - P  D  Y  A  S  P  E  F  M  R  I  I  G  I  E  T  S  C  D  E   - 20

 61 - ACAGGAATCGCGATTTACGACGATGAAAAAGGCCTGTTGGCGCACAAGCTTTACAGCCAA - 120
 21 - T  G  I  A  I  Y  D  D  E  K  G  L  L  A  H  K  L  Y  S  Q   - 40

121 - GTAAAACTTCACGCGGATTACGGCGGCGTGGTGCCAGAGTTGGCTTCACGTGACCATGTA - 180
 41 - V  K  L  H  A  D  Y  G  G  V  V  P  E  L  A  S  R  D  H  V   - 60

181 - AAGAAAACCATTCCTCTTATTAAAGAGGCACTAAAAGAAGCAAACTTAACATCCCAAGAC - 240
 61 - K  K  T  I  P  L  I  K  E  A  L  K  E  A  N  L  T  S  Q  D   - 80

241 - ATCGACGGCGTGGCTTACACGGCCGGTCCTGGTTTGGTTGGTGCTTTGCTAGTGGGTGCA - 300
 81 - I  D  G  V  A  Y  T  A  G  P  G  L  V  G  A  L  L  V  G  A   - 100

301 - ACCATCGGTCGCAGTATTGCTTACGCATGGGGTGTTCCTGCTGTTCCTGTTCATCATATG - 360
101 - T  I  G  R  S  I  A  Y  A  W  G  V  P  A  V  P  V  H  H  M   - 120

361 - GAAGGTCATTTACTTGCGCCAATGCTAGAAGACAACCCACCACCATTCCCATTTGTGGCG - 420
121 - E  G  H  L  L  A  P  M  L  E  D  N  P  P  P  F  P  F  V  A   - 140

421 - GTGTTGGTTTCTGGCGGTCACTCGATGATGGTGGAAGTAAAAGGCATTGGTGAATACAAG - 480
141 - V  L  V  S  G  G  H  S  M  M  V  E  V  K  G  I  G  E  Y  K   - 160

481 - ATTCTAGGCGAATCCATTGATGATGCAGCCGGTGAAGCATTTGATAAGACGGCTAAGCTG - 540
161 - I  L  G  E  S  I  D  D  A  A  G  E  A  F  D  K  T  A  K  L   - 180

541 - ATGGGGTTAGATTACCCAGGCGGTCCTCTGTTATCCAAGCTAGCAGAGAAAGGTACTCCG - 600
181 - M  G  L  D  Y  P  G  G  P  L  L  S  K  L  A  E  K  G  T  P   - 200

601 - GGTCGCTTTAAGTTCCCACGACCAATGACCAATGTGCCGGGTTTGGATATGAGTTTCTCT - 660
201 - G  R  F  K  F  P  R  P  M  T  N  V  P  G  L  D  M  S  F  S   - 220

661 - GGTTTGAAAACCTTCACGGCAAACACGATTGCAGCGAATGGCGATGACGAGCAGACTCGT - 720
221 - G  L  K  T  F  T  A  N  T  I  A  A  N  G  D  D  E  Q  T  R   - 240

721 - GCTGATATTGCGTACGCTTTTGAAGAAGCCGTGTGTGCAACGTTGGCAATTAAATGTAAG - 780
241 - A  D  I  A  Y  A  F  E  E  A  V  C  A  T  L  A  I  K  C  K   - 260

781 - CGTGCATTAGAGCAAACCGGTATGAAGCGCATCGTTATTGCTGGTGGTGTAAGTGCGAAC - 840
261 - R  A  L  E  Q  T  G  M  K  R  I  V  I  A  G  G  V  S  A  N   - 280
```

```
 841 - CGCCGCTTGCGTGCAGAGCTTGAGAAGCTTGCGAAGAAAATCGGTGGTGAAGTGTATTAC - 900
 281 - R  R  L  R  A  E  L  E  K  L  A  K  K  I  G  G  E  V  Y  Y   - 300

 901 - CCACGTACCGAGTTCTGTACTGACAACGGTGCAATGATTGCGTATGCGGGTATGCAACGT - 960
 301 - P  R  T  E  F  C  T  D  N  G  A  M  I  A  Y  A  G  M  Q  R   - 320

 961 - TTGAAGAACGGTGAAGTCGCAGATATGTCGGTGGAAGCGCGTCCGCGCTGGCCAATTGAC - 1020
 321 - L  K  N  G  E  V  A  D  M  S  V  E  A  R  P  R  W  P  I  D   - 340
                    XhoI
1021 - CAGCTAACGCCACTCGAGAAGCTTTGGACTTCTTCGCCAGAGGTTTCAAGTCTCCAATCA - 1080
 341 - Q  L  T  P  L  E  K  L  W  T  S  S  P  E  V  S  S  L  Q  S   - 360

1081 - AGGTTGTCGGCTTGTCTACCTTGCCAGAAATTTACGAAAAGATGGAAAAGGGTCAAATCG - 1140
 361 - R  L  S  A  C  L  P  C  Q  K  F  T  K  R  W  K  R  V  K  S   - 380

1141 - TTGGTAGATACGTTGTTGTTGACACTTCTAAATAAGCGAATTTCTTATGATTTATGA - 1197
 381 - L  V  D  T  L  L  L  T  L  L  N  K  R  I  S  Y  D  L  *   - 400
```

Appendix V

Introduction of point mutation sites into *yeaZ*$_{Vp}$ using overlap extension PCR.

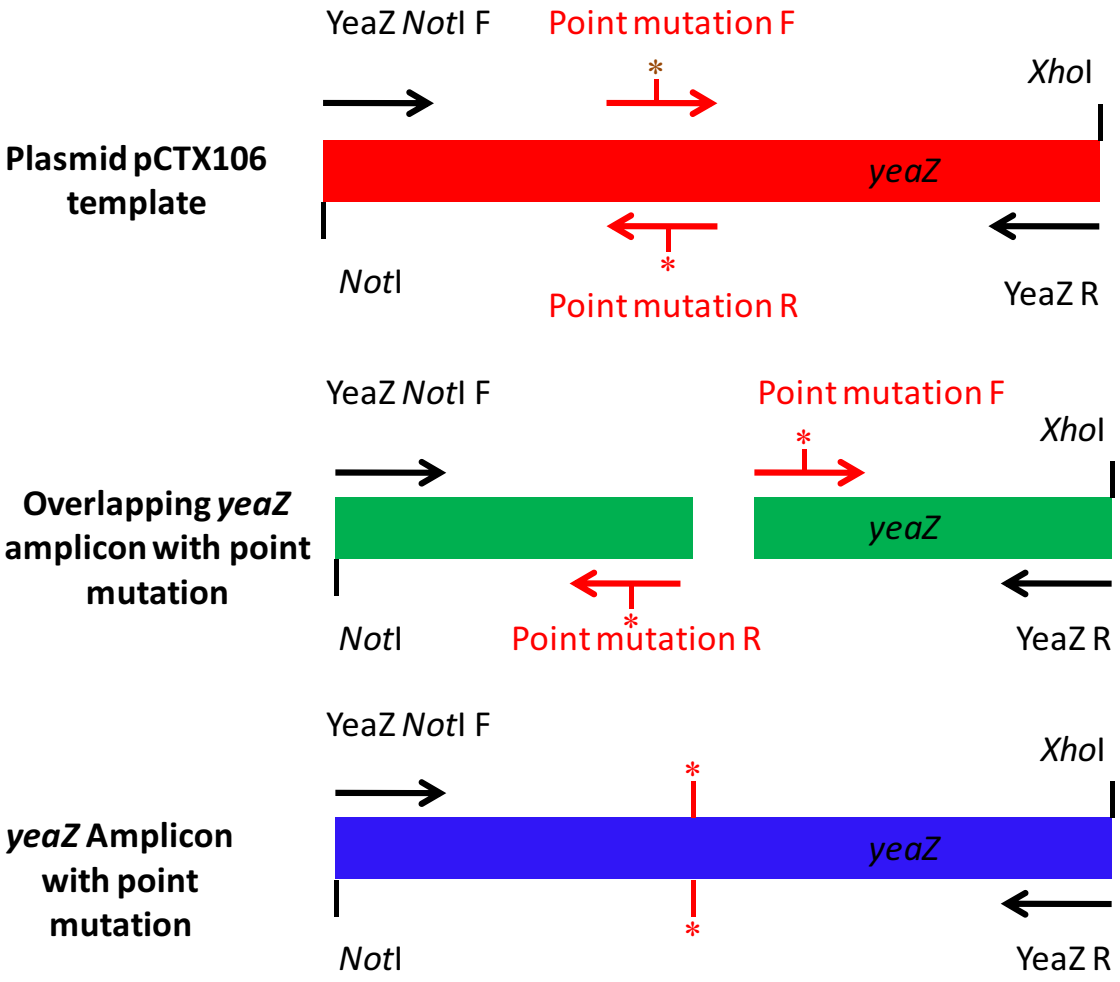

Appendix W

DNA sequencing of yeaZ mutants showed in electropherogram data. Codons for I75A (A), L83A (B) and F85A (C) residues are boxed.

(A) I75A

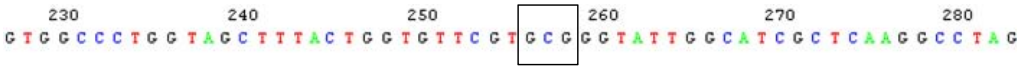

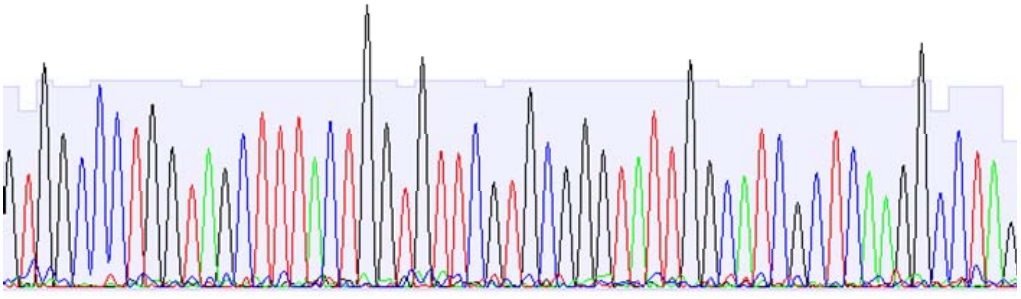

(B)L83A

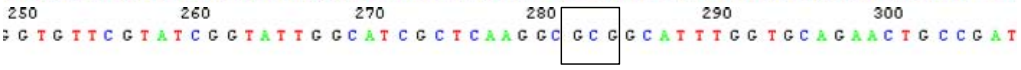

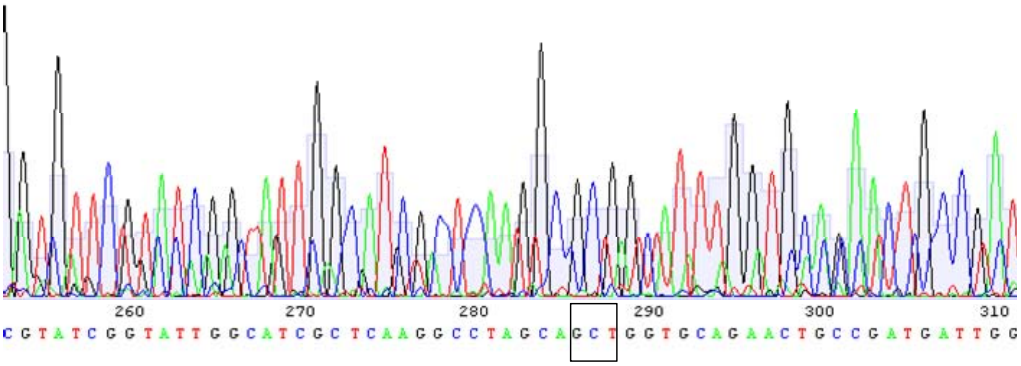

(C)F85A

